Title
Dissipative and Spin Effects in Classical Gravity from Quantum Scattering Amplitudes

ISBN
9798265454270

Author
Gatica, Juan Pablo

Publication Date
2025-12-02

Peer reviewed|Thesis/dissertation

UNIVERSITY OF CALIFORNIA
Los Angeles

Dissipative and Spin Effects in Classical Gravity from Quantum Scattering Amplitudes

A dissertation submitted in partial satisfaction
of the requirements for the degree
Doctor of Philosophy in Physics

by

Juan Pablo Gatica

2025

ABSTRACT OF THE DISSERTATION

Dissipative and Spin Effects in Classical Gravity
from
Quantum Scattering Amplitudes

by

Juan Pablo Gatica
Doctor of Philosophy in Physics
University of California, Los Angeles, 2025
Professor Zvi Bern, Chair

Quantum scattering amplitudes have proven to be a powerful tool in high-precision calculations of classical gravity; especially in the dynamics of gravitational waves. By considering a hierarchy of relevant length scales, extracting the classical limit of black hole scattering from the quantum field theory approach has successfully pushed the Post-Minkowskian expansion further and faster than ever. In this work, we will continue this program while focusing on dissipative and spin effects. We will also explore these effects for the case of general spinning bodies, reducing to the special case of black holes for comparisons. In Chapter 1, we calculate radiative corrections to classical two-body scattering in electrodynamics using the Kosower-Maybee-O'Connell (KMOC) formalism and Eikonal phase while comparing to traditional equations of motions techniques. Electrodynamics has long been an insightful toy model for gravity; the results of Chapter 1 helped inform the interpretation of high-energy limit divergences that persist in spite of considering non-conservative effects. In Chapter 2, we introduce spin by considering higher spin fields as an effective field theory (EFT) and

calculate a formula directly relating the impulse and spin kick to the Eikonal phase. We limit ourselves to linear-in-spin corrections in order to better understand how the inclusion of spin complicates the calculation of scattering observables using the KMOC formalism. In Chapter 3, we generalize the linear-in-spin calculation to all orders in spin by only considering general properties of higher spin fields. In this more general case, we derive a formula relating observables to operators acting on the Eikonal phase valid to all orders in spin. We also observe interesting similarities between the impulse and spin kick calculations. For the both the linear-in-spin and all-orders-in-spin cases, we verified our derivation by comparing to known results from the worldline formalism and the stationary phase approximation. In Chapter 4, we consider spin-transition and absorptive effects in tandem. We account for spin transition and absorption by coupling fields of different spins and masses to massless scalars, photons and gravitons, creating a series of non-minimal couplings in our EFT Lagrangian. We then use KMOC and Källen-Lehman propagators to calculate the absorptive impulse of various spin-transition channels. We observe an interesting symmetry and suppression, which we call Floor-Ceiling Symmetry and No-Floor suppression. We also observe that spin universality is maintained. We include an appendix to supplement arguments in the body of the Chapters that would otherwise obscure the main goal findings of the Chapters.

The dissertation of Juan Pablo Gatica is approved.

Graciela B. Gelmini

Michael Gutperle

Mikhail Pil Solon

Zvi Bern, Committee Chair

University of California, Los Angeles

2025

... to my mother, Maria Haydee Cuevas Chacon."*Esto no te pueden quitar.*"

TABLE OF CONTENTS

LIST OF FIGURES

LIST OF TABLES

ACKNOWLEDGMENTS

This dissertation includes material that is based upon work supported by the U.S. Department of Energy under Award Number DE-SC0009937. Any opinions, findings, and conclusions or recommendations expressed in this material are those of the authors(s) and do not necessarily reflect the views of the National Science Foundation. This work was also supported in part by the Mani L. Bhaumik Institute for Theoretical Physics.

I acknowledge the results presented in this thesis are based upon published works with additional co-authors, and are reprinted here with permission when required. Chapter 1 is a version of Z. Bern, J.P. Gatica, E. Herrmann, A. Luna, M. Zeng, "QED as a toy model for higher-order effects in classical gravitational scattering." Journal of High Energy Physics (JHEP) 08 (2022) 131; arxiv: 2112.12243. Thank you to Clifford Cheung, Michael Ruf, and Mikhail Solon for very enlightening discussions. We also thank Alessandra Buonanno, Justin Vines, Jan Steinhoff, and Muddu Saketh for very helpful discussions and for sharing their results prior to publication, where the scattering angle is derived from the classical equations of motion. We thank Julio Parra-Martinez for discussions and comments on the manuscript.

Chapter 2 is a version of J.P. Gatica, "The Eikonal Phase and Spinning Observables." arxiv: 2312.04680. Thank you to Zvi Bern, Callum Jones, Lukas Lindwasser, Richard Myers, and Trevor Scheopner for numerous insightful discussions and helpful guidance throughout this work. We also thank Rafael Aoude for informative discussions on spin coherent states. We thank Zvi Bern, Dimitrios Kosmopoulos, Andres Luna, Radu Roiban, Trevor Scheopner, Fei Teng, and Justin Vines for sharing their results, which we used to verify our calculations.

Chapter 3 is a version of J.P. Gatica, "Spinning Observables from Field Theory." Submitted to JHEP; arxiv: 2312.04680. Thanks to Zvi Bern, Andres Luna, Trevor Scheopner, Callum Jones, Michael Ruf, Richard Myers, Justin Vines, Fei Teng, Giulia Isabella, and Rafael Aoude for useful discussions that were paramount to this work.

Chapter 4 is a version of J.P. Gatica, C. Jones, "Classical Spin Transitions and Absorptive

Scattering." Submitted to JHEP; arxiv: 2511.19601

On a more personal note – I would like to thank my thesis advisor Zvi Bern for taking me on as a PhD student and giving me the opportunity pursue this research. Without your guidance and mentorship I could never have done the work that led up to this.

I would like to thank Briley Lewis for her belief and support in me. We have known each other for over a decade and have seen each other change and grow throughout the years; to think you still are in my life is one of those gifts the universe saw fit to give me.

I'd like to acknowledge the close friends I've made while in graduate school. As important as it is to work as hard as you can, it would have been impossible to complete this degree without taking a break to enjoy life now and again. So to Hassan Farhat, Ada Morral, and Antonet Prado; the last few years would have been so different and near impossible without you.

I'd to acknowledge the people I've gotten to know over the years in seminars, conferences and journal clubs in the amplitudes community. It was a pleasure getting to know you all and to be around such brilliant people. In particular I'd like to thank Trevor Schoepner, Richard Myers, Anna Wolz, Giulia Isabella, Miguel Correia, Lucille Cangemi, Lara Bohenblust, Taro Valentin, Umut Oktem, Shruti Paranjape, Rafael Aoude, Paolo Pichini, Calvin Chen, Dimitrios Kosmopoulos, Nick Geiser, Alfredo Guevara, Justin Vines; discussing physics with you all felt the same as catching up with a friend.

I'd like to thank my unofficial mentors, people who, in their own way, helped shape the I way approached research and helped smooth those unavoidable speed bumps in research project. Thank you to Callum Jones, Andres Luna, Enrico Herrmann, Michael Ruf.

I would like to acknowledge the APS Bridge program at UCLA. You gave me the chance to pursue my interests and saw potential in me that I would never have realized without your aid. So thank you to Smadar Naoz, Josh Samani, Zhongbo Kang; making physics a more inclusive space is such an important pursuit and I am glad you have continued to fight for it.

To Kristian Barajas, Rory Bentley, Sohpie Crisp, Robert Dorst, Noah Miller, Jessica Pilgram, Caroline Riley; the pandemic and graduate school would have been absolutely unbearable without you all. From Bundy to Beverly Hills, it was a pleasure to live and breathe the same air as you day in and day out of lockdown. The adventures we have had I will also never forget; scaling mountains, climbing Half Dome, skiing the Sierras and backpacking all over the place are memories I will treasure eternally. Also a better Dungeons and Dragons team one can never find.

I would like to thank my lifelong friends from college who I have kept up with over the years. Richard Arends, Cesar Chabla-Sarmiento, Sean Jung, Martin Liberman, Joan Martinez, Brandon Moyer, Alexander Swanson, Cesar Trujillo; without your friendship college would have been so much less enjoyable and grad school near impossible.

I would like to thank my union UAW local 4811. Your dedication to caring for our needs as teaching assistants and graduate student researchers makes it possible for the high quality research and work that we bring to the university.

A mi familia en Huechun Bajo y Santiago, Chile. Aunque no nos vemos mucho como antes, siempre siento tu apoyo y amor. Yo tengo ningun dudo que ustedes son un gran parte en los experiencias, lecciones, y etica que ha hecho posible este trabajo. Gracias a ustedes Tio Alvaro , Tia Erika , Nacho, Ana Karen , Tia Maria Salome, Francisca, Tio Carlo Alfredo, Tia Kenna, Karla, Tia Marta, Tio Vito, Tio Ricardo, Hector, y Tia Soledad.

I would like to thank my sisters, nephews, and nieces. Veronica, Paz, Nicolas, Gustavo, Carolina, and Paulina; holidays, reunions, and special moments with you were always the mental recharge I needed to finish graduate school. I am so thankful for your support and love.

I would like to thank the teachers and communities I had while growing up in Miami. Vivian Jauma Ventura, Besnik Hashani, Alan Hudson, the Greater Miami Youth Symphony, Mr. Cloutier, Dr. Alvarado: thank you so much for your mentorship and care in those early years.

I would like to thank Andy Medina, Martin Gonzalez, Nicholas Verrire and their families for being there then and now, always happy to say hello, reconnect, support each other and to never let each other forget that we are here for each other always; thank you.

I would like to thank my mentors from my undergraduate days at Columbia University. Jeremy Dodd, Emlyn Hughes, Giulia Lanza, and Rachel Rosen; in one or another you all nurtured me into a curious physicist.

I would like to thank George Bricker and Jorge Muniz: that trip at the beach was the beginning of it all making sense.

I would like to thank those who couldn't make it to this moment. Papa, Abuelita Romelia, Abuelita Ortenzia, Tia Gloria, Thomas: I do not know how you helped along the way, but this is what we built together.

I would like to thank the projects that never got finished. You taught me many lessons including patience, organization, how to let go and knowing when you should.

To my foundational trinity: Mama, Tio Eduardo, and Tia Analilia. You three are my rock, the base of my life. You are my first teachers, my first mentors. These words and any I may ever write came from your patience, care, and love. Mama, I could never ask for a better start in life than the one you worked so hard to give me. Tio and Tia, there were times where it was just the four of us, and looking back that was more than enough; in fact, it was and is everything to me. "I love you" and "thank you" are words that scarcely describe my joy and gratitude for you being my family, I just hope you know that you mean the Earth, the Moon, the stars, and more to me.

VITA

2014 – 2018 B.A. in Physics, Columbia University.

2018 – 2020 M.Sc. in Physics , University of California, Los Angeles.

2018 – 2025 Ph.D. candidate in Physics, University of California, Los Angeles.

Awards

2018 Eugene V. Cota-Robles Fellowship

2018 Physics Division Fellowship, UCLA.

2020 Bhaumik Institute Summer Research Fellowship, UCLA.

PUBLICATIONS

Juan Pablo Gatica, Callum Jones, "Classical Spin Transitions and Absorptive Scattering." Submitted to JHEP; arxiv: 2511.19601

Juan Pablo Gatica, "Spinning Observables from Field Theory." Submitted to JHEP; arxiv: 2312.04680

Juan Pablo Gatica, "The Eikonal Phase and Spinning Observables." arxiv: 2312.04680

Zvi, Bern, Juan Pablo Gatica, Enrico Herrmann, Andres Luna, Mao Zeng, “QED as a toy model for higher-order effects in classical gravitational scattering.” Journal of High Energy Physics (JHEP) 08 (2022) 131; arxiv: 2112.12243

CHAPTER 1

Scalar QED as a Toy Model for Higher-Order Effects in Classical Gravitational Scattering

1.1 Introduction

The landmark detection of gravitational waves [1, 2] has opened a remarkable new window into the Universe that promises major new advances into black holes, neutron stars, and perhaps even provides new insights into fundamental physics. The recent experimental progress has inspired efforts to develop new theoretical tools for predicting gravitational-wave signals that meet the precision challenges of current and future detectors [3–6]. A variety of complementary tools are being used, including the effective one-body (EOB) formalism [7], numerical relativity [8–10], the self-force formalism [11, 12], as well as perturbative methods such as the post-Newtonian (PN) expansion [13, 14], the effective field theory (EFT) known as nonrelativistic general relativity (NRGR) [15–26], as well as the post-Minkowskian (PM) expansion [27–45] and the observables based method originally devised by Kosower, Maybee, and O'Connell [39, 40, 46–51]. Information from various approaches can be combined into state-of-the-art results and provide nontrivial cross-checks, see e.g. Refs. [42, 52–66].

The post-Minkowskian approach is a weak-field expansion in Newton's constant, G, and has risen in prominence in recent years. It has the advantage of maintaining Lorentz invariance and gives results with exact relativistic velocity dependence. The scattering amplitude framework for post-Minkowskian calculations [37–39, 41, 42, 48, 67] naturally meshes with this covariant approach. Calculations of scattering amplitudes have advanced enormously, making this a natural framework for state-of-the-art post-Minkowskian calculations. The modern amplitude tools include the unitarity method [68–70] which constructs loop-level scattering amplitude integrands from lower-order gauge-invariant on-shell data, as well as the double copy which relates gauge and gravity theories [71–75]. Furthermore, amplitude methods also incorporate powerful integration procedures [76], originally developed for particle-collider physics applications, such as integration by parts (IBP) [77–79], differential equations [80–85], and reverse unitarity [86–89].

Combining techniques based on scattering amplitudes with those of effective field theory (EFT), two-body effective Hamiltonians have been derived in Refs. [38, 41, 42, 67] that straightforwardly determine the conservative classical dynamics of bound orbits via their equations of motion, whenever nonlocalities associated with the tail effect [90–95] are absent. Such Hamiltonians can be imported into the EOB framework [35, 43] used by LIGO for constructing gravitational-wave templates. One can alternatively obtain bound-state physical observables from the ones of hyperbolic scattering processes via appropriate analytic continuation [96–99]. Cases involving the tail effect are more subtle [100, 101].

Scattering amplitudes are the natural realm to describe the hyperbolic motion of classical objects from the asymptotic past to the asymptotic future. This idea has been implemented in the work by Kosower, Maybee, and O'Connell (KMOC) [39] whose approach allows us to extract classical observables directly from scattering amplitudes and what are essentially unitarity cuts. Alternatively, in the classical limit, appropriately defined finite parts of the scattering amplitudes can be directly connected to the scattering angle or the isotropic gauge two-body Hamiltonian [42, 96]. The scattering amplitude can also be interpreted directly in terms of the radial action [59, 102, 103]. A related but distinct approach based on the eikonal phase [104] (for more recent examples see e.g. Refs. [49, 105–108] [49, 50, 105–109]) provides a natural way to extract the classical scattering angle from amplitudes. In this chapter we will use a variety of these approaches to extract classical observables in both the conservative and radiative sectors.

The usefulness of the scattering amplitude framework has been demonstrated through the first construction of the conservative two-body Hamiltonian at $\mathcal{O}(G^3)$ [41, 42] whose various aspect are confirmed in multiple studies [52–55, 63], as well as new results at $O(G^4)$ [59, 62]; see also Refs. [65, 66, 110] . There have also been a variety of new results for spin [111–126] [111–127] , tidal effects [128–137], and waveforms [48].

In carrying out such calculations, it is useful to analyze simpler models compared to Einstein gravity that eliminate unnecessary complications. As a recent example, the authors of Ref. [138] analyzed $\mathcal{N}=8$ supergravity to demonstrate the cancellation of mass singularities between conservative and radiative contributions to the classical scattering angle, leading to a complete resolution [139]. Likewise, gauge theory, especially electrodynamics, served as a toy model for gravity in the context of two-body dynamics for many decades [33, 140] [33, 39, 50, 99, 140] . While being a linear theory, it captures some of the technical difficulties encountered with general relativity (GR) at high orders of perturbation theory. Another reason for studying corresponding quantities in gauge theories, especially in non-abelian cases, is the double-copy relation between gauge and gravity theories [71–73].

Recently, the conservative and radiative dynamics in classical relativistic scattering was obtained by Saketh, Vines, Steinhoff, and Buonanno in scalar electrodynamics to the sixth order in the charges or the third order in the fine-structure constant [99]. This was accomplished by the direct iteration of the equations of motion. Here, we compare to these results using scattering amplitudes based approaches, finding full agreement. Using amplitude methods, we evaluate the angle including radiative effects in three distinct ways. First, we use the Kosower-Maybee-O'Connell formalism to obtain the impulse on two massive charged scalar particles scattering at large impact parameter b from which we extract the scattering angle. As an alternative, we extract the eikonal phase from the scattering amplitude which allows us to determine the scattering angle. Finally, using recent observations on the connection of the scattering amplitude in the classical limit to the radial action [59] (see also [102]), we present a simple prescription for extracting from the scattering amplitude a radial action that determines the scattering angle, including radiative effects. Although the system is not conservative (we include radiation reaction effects in the scattering angle), we find that the scattering angle obtained by differentiating this generalized radial action matches the previous results. All three of these approaches for extracting the classical scattering angle match, and agree with the result from the classical approach of Ref. [99].

As previously discussed in Ref. [99], in electromagnetism we encounter a mass singularity in the scattering angle, which does not cancel between potential and radiative contributions, as it does in the corresponding $\mathcal{O}(G^3)$ calculation in gravity [138, 139]. In fact, the singularity is power divergent for $m \to 0$, similar to the situation in the conservative sector of gravity at $\mathcal{O}(G^4)$ [59, 62]. From our perspective, we interpret this singularity as a breakdown of the classical expansion which requires $m^2|b|^2 \gg 1$. Another interesting feature of the amplitudes based approaches is that the Abraham-Lorentz-Dirac (ALD) force [141–143] that appears in more tradiational methods [33] is automatically built in and does not require any special treatment [39].

For the conservative sector, we also extracted a two-body Hamiltonian valid through the sixth order in the charges analogous to the $\mathcal{O}(G^3)$ isotropic-gauge Hamiltonian of the gravitational case. This is obtained from the mapping between infrared-finite parts of the amplitude to the coefficients in the two-body potential [42, 96]. As for any standard Hamiltonian it can be directly applied to the bound state case.

The chapter is organized as follows. In Section 1.2 we briefly review the methods used here. Then in Section 1.3 we evaluate the conservative contributions to the two-particle scattering through the sixth order in the charges. In Section 1.4 we include radiative corrections to the scattering angle and impulse and also compute the radiated momentum. We give our conclusions in Section 1.5. All our results are available in computer-readable form in the ancillary file attached to this article.

1.2 Review of Methods

The present section briefly summarizes and reviews the main technical ingredients that are required to obtain classical scattering observables in (scalar) QED up to two-loop order ($\mathcal{O}(\alpha^3)$ where $\alpha = e^2/4\pi$), corresponding to the sixth order in the charges, from various scattering amplitude based frameworks. Readers only interested in the final results may skip this section on a first reading. The remainder of this section is structured as follows: We first review the kinematic parametrization tailored towards the classical expansion of quantum scattering amplitudes in Subsection 1.2.1, before outlining the generalized unitarity framework to determine the amplitude integrands in Subsection 1.2.2. In Subsection 1.2.3, we telegraphically sketch the applicability of modern collider-physics based integration tools to compute precision-level classical observables with the help of integration-by-parts reduction to a minimal set of master integrals and their evaluation by differential equation methods. Subsection 1.2.4 introduces a new concept that allows us to define a radial action in the presence of soft-region radiation effects. In particular, we find an efficient computational scheme that allows us to compute the *soft radial action* by a well-motivated modification of the boundary conditions for the soft-region master integrals. Finally, in Subsection 1.2.5, we briefly summarize the Kosower, Maybee, and O'Connell (KMOC) formalism which allows us to extract the classical electromagnetic impulse, the radiated momentum, and the classical scattering angle up to $\mathcal{O}(\alpha^3)$.

1.2.1 Classical limit of quantum scattering amplitudes–soft and potential region

We compute classical observables for the relativistic scattering of two point-charges, in what might be called the "post-Lorentzian" (PL) expansion. This regime is in direct correspondence to the post-Minkowskian expansion in gravity.

The relevant length scales, summarized in Table 1.1, are the Compton wavelength λ_c, related to Planck's constant $\hbar$ and the particle mass scale m, the typical classical particle

	GR	QED
quantum:	$\lambda_c \sim \frac{\hbar}{m}$	$\lambda_c \sim \frac{\hbar}{m}$
classical particle size:	$r_S = Gm$	$r_Q = \frac{e^2 q_i^2}{4\pi\, m}$
particle separation:	b	b

Table 1.1: Comparison between relevant length scales in the post-Minkowskian (PM) expansion in GR and the post-Lorentzian (PL) regime in (scalar) QED in units where $c = 1$ and the fundamental charge e is measured in units where $\epsilon_0 = 1$.

size r_S or r_Q (Schwarzschild radius or classical charge radius), as well as the inter-particle separation b. The classical PM expansion corresponds to the following hierarchy of scales: $\lambda_c \ll r_S \ll b$, and similarly $\lambda_c \ll r_Q \ll b$ in the PL case. The classical limit posits that the individual particle size is much bigger than the Compton wavelength and forces us into a regime of large charges: $r_S/\lambda_c \gg 1 \leftrightarrow G\ m^2/\hbar \gg 1$, or $r_Q/\lambda_c \gg 1 \leftrightarrow e^2 q_i^2/\hbar \gg 1$, where q_i is the electric charge of the classical object in units of e. The large (macroscopic) charge regime makes intuitive sense from the point of view that classical physics should arise from the quantum theory in the limit of large quantum numbers. This seems to suggest that we are outside the traditional range of validity of perturbation theory. This, however, is a premature conclusion, because the PM or PL regime amounts to an expansion in terms of the small ratio $r_S/b \ll 1$ or $r_Q/b \ll 1$ which leads to a well-defined perturbative expansion. For an especially nice discussion of the relevant scales in the gravitational context, see e.g. Ref. [144].

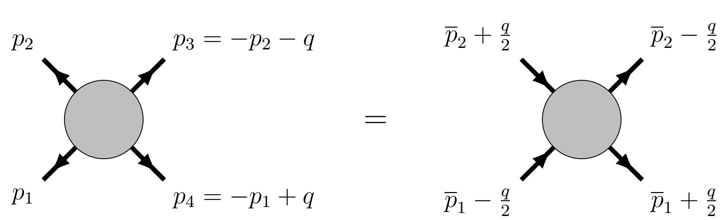

Figure 1.1: Parametrization of external kinematics.

In order to simplify our discussion, we focus on the scattering of spinless, structureless objects described by massive scalar fields. In the PL approximation, the above hierarchy of scales is converted into momentum space as follows: it is assumed that the masses of the scalars are very heavy and that the momentum transfer $|q| \sim 1/|b|$ is small in the classical limit, $(-q^2) \ll m_i^2$, in complete analogy to gravitational scattering. In order to extract classical physics, we utilize special kinematic variables that facilitate the classical $\hbar \to 0$ or equivalently *soft* (small $|q|$) expansion[1] in the context of the method of regions [145]. These variables have previously appeared in e.g. Ref. [76] and are summarized in Fig. 1.1,

$$p_1 = -\left(\overline{p}_1 - \frac{q}{2}\right)\,,\; p_2 = -\left(\overline{p}_2 + \frac{q}{2}\right)\,,\; p_3 = \left(\overline{p}_2 - \frac{q}{2}\right)\,,\; p_4 = \left(\overline{p}_1 + \frac{q}{2}\right)\,. \tag{1.1}$$

The new vectors $\overline{p}_i$ are orthogonal to the momentum transfer q, $\overline{p}_i \cdot q = 0$, which directly follows from the on-shell conditions $p_1^2 = p_4^2 = m_1^2$ and $p_2^2 = p_3^2 = m_2^2$. For later convenience, we also introduce 'soft-masses' $\overline{m}_i$ defined by

$$\overline{m}_i^2 = \overline{p}_i^2 = m_i^2 - \frac{q^2}{4} \quad \to \quad \overline{m}_i = m_i + \frac{(-q^2)}{8m_i} + \mathcal{O}(q^4)\,. \tag{1.2}$$

Notably, in the specialized barred variables, $s{=}(\overline{p}_1 + \overline{p}_2)^2{=}(p_1 + p_2)^2$ the physical scattering region $s{>}(m_1 + m_2)^2$, $q^2{<}0$ remains the same. Following earlier conventions [76], we define the soft four-velocities of the two black holes $u_i^\mu = \overline{p}_i^\mu / |\overline{p}_i|$, such that $u_i^2 = 1$, and

$$y \equiv u_1 \cdot u_2 = \frac{1 + x^2}{2x} = \sigma - (-q^2)\frac{(m_1^2{+}m_2^2)\,\sigma + 2m_1 m_2}{8\,m_1^2 m_2^2} + \mathcal{O}(q^4)\,. \tag{1.3}$$

For physical scattering in the s-channel we have $y > 1$. Often, it will prove advantageous to change variables to x in the range $0 < x < 1$ in order to rationalize the naturally appearing square-root $\sqrt{y^2 - 1} = \frac{1-x^2}{2x}$.

Note that the soft velocities u_i coincide with the classical four velocities of the massive scalars only up to corrections of $\mathcal{O}(q)$. The KMOC setup directly targets physical observables where this difference is immaterial. However, for the eikonal computations, the $\mathcal{O}(q)$

[1] From now on, we work in natural units and set $\hbar = 1$ unless stated otherwise.

corrections do matter and one has to carefully track them. In the classical limit (without restricting to the conservative sector), we are interested in the soft expansion of loop amplitudes with the hierarchy of scales given by $|\ell| \sim |q| \ll |\bar{p}_i|, m, \sqrt{s}$. Here, ℓ schematically represents arbitrary combinations of photon momenta of the form $(\ell_1, \ell_2, \ell_1 \pm \ell_2, \ldots)$ and typical photon propagators take the form $\frac{1}{\ell^2}$, $\frac{1}{(\ell-q)^2}$. These have a homogeneous $|q|$-scaling and do not require any further expansions. Distinctly, matter propagators do have a non-trivial $|q|$ expansion expressed via dimensionless velocity variables u_i

$$\frac{1}{(\ell - p_i)^2 - m_i^2} = \frac{1}{\ell^2 - 2\,\ell \cdot p_i} = \frac{1}{2u_i \cdot \ell}\,\frac{1}{m_i} - \frac{\ell^2 \mp \ell \cdot q}{(2u_i \cdot \ell)^2}\,\frac{1}{m_i^2} + \cdots . \tag{1.4}$$

Each order in the expansion is homogeneous in $|q|$ and the mass dependence factorizes. The matter propagators effectively "eikonalize" and the soft expansion to higher orders in $|q|$ can lead to raised propagator powers.

To focus on conservative dynamics one would perform a further expansion where the temporal part of any photon line is suppressed by an additional power of the formally small velocity v, related to $y \approx \sigma = \frac{1}{\sqrt{1-v^2}}$ to signal instantaneous interactions. These *potential region* expansions have been described in great detail elsewhere [41, 42, 76] and we refrain from repeating them here for the sake of brevity.

1.2.2 Generalized Unitarity and scalar QED scattering amplitudes up to $\mathcal{O}(\alpha^3)$

As we are going to review in the following subsections, a number of novel approaches to the classical two-body problem in gravity and electromagnetism involve the (classical limit of) quantum scattering amplitudes. These enter either in the EFT matching calculation to a classical two-body potential, in the eikonal approach to classical scattering, or in the KMOC framework that expresses classical physical observables (e.g. the impulse or the radiate momentum) in terms of scattering amplitudes and weighted cross-section-like objects. Therefore, it is crucial to have at our disposal compact expressions for the relevant (classical parts) of the higher-loop scattering amplitudes in the theories under consideration. Recent years have seen enormous advances in our ability to obtain analytic results for quantum scattering amplitudes via modern on-shell methods. On one hand, this progress enhanced our ability to compute phenomenologically relevant collider physics processes in quantum chromodynamics (QCD) and the Standard Model. On the other hand, in simplified toy theories such as maximally supersymmetric Yang-Mills theory or in supersymmetric gravity theories, similar computations were crucial to shed light on a number of impressive theoretical insights into the deeper structures of quantum field theory. A chief ingredient in many of these calculations is an efficient way to obtain a scattering amplitude *integrand*, i.e. an expression of the amplitude before loop integration. Generalized unitarity [68–70] is based on the factorization of amplitudes into simpler gauge-invariant on-shell building blocks which allows to export the simplicity of tree-amplitudes to loop-calculations. In the context of classical gravitational dynamics, these methods have been recently used [47] to obtain the radiated momentum and the impulse at $\mathcal{O}(G^3)$ in general relativity from the KMOC setup and from eikonal considerations [144]. Since these methods have been comprehensively documented elsewhere in the context of general relativity [41, 42, 47, 76], we are only giving a telegraphic account of the main ingredients of our QED calculation.

1.2.2.1 Tree-level amplitudes in scalar QED

The main building blocks in the derivation of loop integrands via generalized unitarity are on-shell tree-level amplitudes out of which unitarity cuts are built. Later, these products of tree-level amplitudes are compared to the unitarity cuts of a putative ansatz of Feynman-like loop integrals in order to fix the free coefficients in the ansatz by solving a linear system of equations. We are interested in the scattering of two massive charged scalars in scalar QED that have charges $eq_{1,2}$ and masses $m_{1,2}$, respectively and interact via the exchange of $U(1)$ gauge bosons, i.e. photons. The Lagrangian for the system is

$$\mathcal{L} = -\frac{1}{4}F_{\mu\nu}F^{\mu\nu} + \sum_{i=1}^{2}\Big[(D_\mu\phi_i)^\dagger(D^\mu\phi_i) - m_i^2\phi_i^\dagger\phi_i\Big]\,, \tag{1.5}$$

where the covariant derivative $D^\mu = \partial^\mu - \mathrm{i}\, e\, q_i\, A^\mu$ contains the photon field $A^\mu(x)$ and the appropriate electric charge q_i (in multiples of the fundamental charge[2] e) of the scalar ϕ_i. The $U(1)$ field strength is $F_{\mu\nu} = \partial_\mu A_\nu - \partial_\nu A_\mu$.

The basic input is the three-point coupling between the scalars and a photon in an all-outgoing convention for the particle momenta

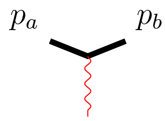

$$= -\mathrm{i}\, e\, q_i (p_a - p_b)^\mu\,, \tag{1.6}$$

from which we can build the tree-level scattering amplitude between the two charged scalars due to photon exchange

$$\mathcal{A}_4^{\text{tree}}(p_1, p_2, p_3, p_4) =$$

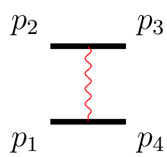

$$= -\frac{4e^2\, q_1 q_2\, \overline{m}_1 \overline{m}_2\, y}{-q^2}\,, \tag{1.7}$$

written in terms of the soft-kinematics of Eq. (1.1). For higher-order calculations, we also require the Compton amplitude for the tree-level scattering of two scalars with two photons

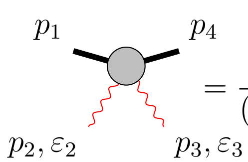

$$\begin{aligned} &= \frac{-2e^2 q_i^2}{(2p_1\cdot p_2)(2p_1\cdot p_3)}\Big[2p_1{\cdot}F_2{\cdot}F_3{\cdot}p_4 + 2p_1{\cdot}F_3{\cdot}F_2{\cdot}p_4 + \frac{1}{2}(p_1{+}p_4)^2 F_2{\cdot}F_3\Big] \\ &= -2e^2 q_i^2\Big[\varepsilon_2\cdot\varepsilon_3 - \frac{\varepsilon_2\cdot p_1(\varepsilon_3\cdot p_1 + \varepsilon_3\cdot p_2)}{p_1\cdot p_2} - \frac{\varepsilon_3\cdot p_1(\varepsilon_2\cdot p_1 + \varepsilon_2\cdot p_2)}{p_1\cdot p_3}\Big]\,, \end{aligned} \tag{1.8}$$

where we have introduced the linearized field-strengths $F_i^{\mu\nu} = \varepsilon_i^\mu p_i^\nu - \varepsilon_i^\nu p_i^\mu$. From the first line of Eq. (1.8) it is clear that we have expressed the amplitude in terms of gauge-invariant building blocks that manifestly vanish when $\varepsilon_i \to p_i$, so that physical state sums that appear in the cut sewing procedure of generalized unitarity can be performed by the simple substitution (see the discussion in Ref. [146])

$$\sum_\lambda \varepsilon_{i,\lambda}^{*\mu}(k)\varepsilon_{i,\lambda}^{\nu}(-k) \to \eta^{\mu\nu}\,, \tag{1.9}$$

[2]In the following, we often trade the square of elementary charges for the coupling constant $\alpha = e^2/(4\pi)$.

where λ denotes the physical polarizations. To get to the compact expression on the second line of Eq. (1.8), we have used momentum conservation to eliminate p_4 and the transversality condition $\varepsilon_i \cdot p_i = 0$ of the polarization vectors.

For the two-loop computation, we also require the amplitude between three photons and two massive scalars

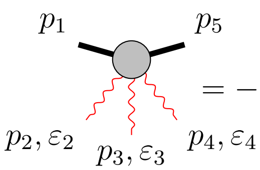

$$= -2ie^3 q_i^3 \Bigg[\frac{(\varepsilon_3\cdot\varepsilon_4)(p_1\cdot F_2\cdot p_5)}{(p_1\cdot p_2)(p_2\cdot p_5)} - \frac{\varepsilon_2\cdot p_1}{p_1\cdot p_2}\left[\frac{(\varepsilon_3\cdot p_5)\,\varepsilon_4\cdot(p_3+p_5)}{p_3\cdot p_5} + \frac{(\varepsilon_4\cdot p_5)\,\varepsilon_3\cdot(p_4+p_5)}{p_4\cdot p_5}\right] + (2\leftrightarrow 3) + (2\leftrightarrow 4) \Bigg]. \tag{1.10}$$

One can check that the representation of the amplitude satisfies generalized gauge invariance [146] for each of the photon lines. This property is defined to be that longitudinal states automatically decouple without the need to impose physical state conditions on other legs. The net effect is that state sums simplify as described in Eq. (1.9).

1.2.2.2 One-loop integrand in scalar QED

Equipped with the tree-level building blocks, we follow the generalized-unitarity framework [68–70] to write an ansatz of Feynman-like graphs with associated numerators dictated by the power-counting of scalar QED. At one loop, we can write the full integrand in terms of box, triangle, and bubble topologies. However, sometimes it is convenient to re-absorb contributions from topologies with fewer propagators ('contact terms') into the definition of the box numerator by multiplying the contact terms by appropriate powers of inverse propagators D_i.

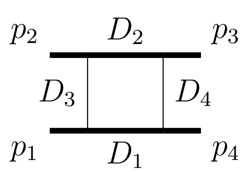

$$= \int \frac{d^D\ell}{(2\pi)^D} \frac{1}{D_1 D_2 D_3 D_4} \tag{1.11}$$

where the inverse propagators D_i are

$$D_1 = (\ell - p_1)^2 - m_1^2\,,\ D_2 = (\ell + p_2)^2 - m_2^2\,,\ D_3 = \ell^2\,,\ D_4 = (\ell - q)^2\,. \tag{1.12}$$

We employ the graphical notation in which thin lines denote massless propagators and thick lines denote the propagators of the massive particles. (We do not graphically distinguish particles of mass m_1 and m_2 that are always associated to the external momenta p_1, p_4 and p_2, p_3, respectively.) As has been advocated in e.g. Ref. [147], it is advantageous to directly express the numerator ansatz in terms of a basis of inverse propagators and irreducible elements (absent at one-loop). The power-counting of scalar QED dictates, that the numerator of the box integral should have a mass-scaling like $(p_i \cdot p_j)^2$. To build the ansatz, we write the numerator in terms of the following external Lorentz-products

$$\{p_1^2, p_2^2, s, -q^2\} \cup \{D_1, D_2, D_3, D_4\}\,. \tag{1.13}$$

From the power-counting of QED discussed above, we know that our numerator ansatz is quadratic in the variables of Eq. (1.13), so that

$$n_{\text{box}}^{\text{ansatz}} = a_1 (p_1^2)^2 + \cdots + a_{63} D_3 D_4 + a_{64} D_4^2\,. \tag{1.14}$$

Every numerator basis element that is proportional to one of the inverse propagators D_i corresponds to a contact term, so that we do not have to list these topologies separately. In a first step, we impose diagram symmetries of the scalar graph in Eq. (1.11) which reduces the number of unknown coefficients a_i and ensures that we only have to determine the numerator for this single graph.

In order to find the desired integrand, we subsequently compare the cut of the ansatz against the field theory result as determined by the product of tree-level amplitudes summed over the exchanged on-shell states that can cross the cut. Since we are interested in the classical, long-range interactions between the heavy scalar particles mediated by photon exchange, we never need to consider contact (i.e. short distance) interactions between the scalars. In order to obtain the relevant classical and quantum terms (required for the two-loop eikonal calculation in sections 1.3.2, 1.4.2) of the one-loop amplitude, it suffices to match the two-particle bubble-cut

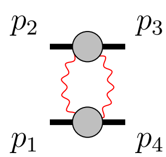

. (1.15)

Matching the above field theory cut (i.e. the product of two Compton amplitudes of Eq. (1.8)) with our basis ansatz requires relabeling the basic box integrand of Eq. (1.11) with the associated numerator (1.14). Solving the cut equations and dropping all terms proportional to inverse propagators that correspond to pinches of photon lines (which would correspond to short-distance contact interactions that are irrelevant for the classical physics of interest), we find

$$n_{\text{box}} = -4e^4 q_1^2 q_2^2 \left(4(p_1 \cdot p_2)^2 - p_2^2\, D_1 - p_1^2\, D_2 - (D_1^2 + D_2^2) + \frac{1}{4}(D_s - 2) D_1 D_2 \right) . \tag{1.16}$$

The terms proportional to $D_1 D_2$ correspond to a bubble integral that is only relevant for the quantum subtraction for the two-loop eikonal analysis. The triangle topologies are included through the numerators proportional to D_1 and D_2, respectively. The result (1.16) is written in terms of the state-counting parameter $D_s = \eta^{\mu}{}_{\mu}$ and we will work in the scheme where we set $D_s = 4$ and write the one-loop amplitude as a sum of a box and cross-box,

$\mathcal{A}_4^{(1)}(p_1, p_2, p_3, p_4) = n_{\text{box}}$ 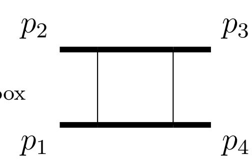

$+ \; n_{\text{x-box}}$ 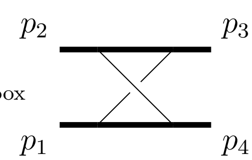

, (1.17)

where the numerator for the second box, $n_{\text{x-box}}$, is obtained from Eq. (1.16) by crossing $p_1 \leftrightarrow p_4$ and (the immaterial) $q_1 \to -q_1$.

1.2.2.3 Two-loop integrand in scalar QED

At two-loops, the cut construction proceeds in a fashion similar to the previous one-loop analysis. We start from the relevant graphs with cubic vertices, summarized in Fig. 1.2

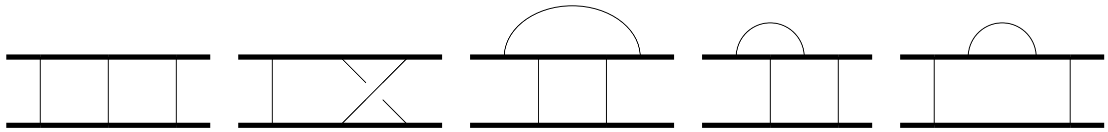

Figure 1.2: Diagrams with cubic vertices relevant for classical $\mathcal{O}(\alpha^3)$ observables in scalar QED. The first two graphs appear in the conservative sector and the three "mushroom" graphs are only relevant for radiative effects. The diagrams split into different gauge-invariant subsectors. The III and IX graphs (corresponding to the first two diagrams) are proportional to $q_1^3 q_2^3$, whereas the mushroom graphs are proportional to $q_1^2 q_2^4$ (and $q_1^4 q_2^2$ for the flipped graphs not explicitly drawn).

and write down a numerator ansatz for each diagram consistent with QED power counting: each trivalent vertex is associated with one power of momentum in the numerator. We then impose the diagram symmetries of the graphs on the respective numerator ansatz. To determine the pieces of the scalar QED two-loop amplitudes relevant for classical physics, both in the eikonal and KMOC approach, we fix the numerators by matching against the spanning sets of cuts depicted in Fig. 1.3 built out of products of the tree-level amplitudes from section 1.2.2.1.

1.2.3 Soft and potential region expansion, IBP, and differential equations

With the relevant one- and two-loop integrands at hand, we directly follow similar computations that have been performed in the gravitational setting [41, 42, 46, 47, 76]. In particular, we expand the scalar QED integrands of Subsection 1.2.2 in either the soft or potential region. We take advantage of the technology developed in Refs. [47, 76] and import the explicit

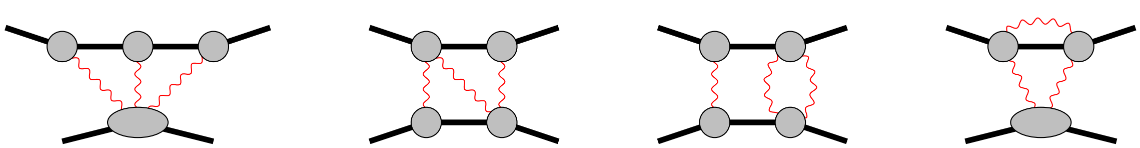

Figure 1.3: Spanning set of unitarity cuts relevant for the classical dynamics at $\mathcal{O}(\alpha^3)$.

values of all soft master integrals supplied in the ancillary files of Ref. [47] (for an alternative computation of the soft master integrals, see Ref. [144]). We will not review these steps in any detail and refer the interested reader to the original references. Briefly, there are two main steps involved in order to obtain integrated results. The first is to start from the initial integrands and expand them in small $|q|$ which leaves graviton propagators unaffected and linearizes (eikonalizes) all matter propagators. This step is related to the kinematic discussion in Subsection 1.2.1. To obtain conservative physics (i.e. the potential region in the language of the method of regions [145]), one further expands the propagators in a formal small velocity parameter v, where the graviton energy component is suppressed by an extra factor of v compared to the spatial components. This signals instantaneous interactions in the Fourier-conjugate time domain. In either case, upon expanding the integrand in the desired kinematic region of interest, one subsequently reduces all resulting integrals to a basic set of so-called master integrals. One can then solve for the values of the remaining master integrals using modern differential equation methods [80–85]. For the KMOC setup, besides the virtual two-loop integrals, one also needs to have access to certain cut-integrals whose computation was significantly simplified using reverse unitarity [86–88]—a well-known tool from collider physics computations (see e.g. Ref. [89]). In this work, we leverage the fact that all relevant integrals have been computed to the order required for our work and we essentially re-use the integration pipeline that already has been successfully implemented for GR both in the soft [46, 47] and potential region [41, 42, 76].

1.2.4 Soft radial action and master integral subtraction of classically divergent terms

In the discussion so far, we mainly focused on the computation of scattering amplitudes in the so-called *soft region* where we only assume that the momentum transfer $-q^2 \ll m_i^2$, s is much smaller than the masses or the energy of the scattering process. As we will explain in most of the remainder of our work, these amplitudes then enter either the eikonal formalism or the

KMOC framework in order to extract the relevant classical observables from the scattering amplitudes (or certain combinations of scattering amplitudes). Crucially, inherent in both the eikonal or the KMOC formalism is the fact that amplitudes not only have classical contributions but, at higher orders in perturbation theory, also involve classically divergent ('super-classical') terms that are more singular and have to cancel for classically well-defined observables.[3] In light of this discussion, one might wonder, whether or not there exists a formalism that directly targets the classical terms directly, without the need to compute the classically divergent terms directly and avoid problems at higher perturbative order of the form $\hbar/\hbar$ where the classically divergent terms interfere with quantum contributions to yield a naively classical result. In the conservative sector, [59] advocated for an EFT based approach with a particular subtraction scheme of classical iterations that allowed the definition and computation of the *radial action* I_r directly from the relation (Eq. (2) of Ref. [59])

$$\mathrm{i}\,\mathcal{A}(\mathbf{q}) = \int_J \left[e^{\mathrm{i}\, I_r(J)} - 1\right] \,, \tag{1.18}$$

which looks very similar to the eikonal exponentiation, but differs in important details [59].

As is well-known from classical physics, see e.g. Ref. [148], the radial action is an important quantity, associated with the classical Hamilton-Jacobi equation for the system, from which to extract relevant classical observables. (See e.g. recent work in the probe-limit [103].) Subsequently, the authors of Ref. [102] argued for a related exponential representation of the S-matrix, $S = e^{\mathrm{i}\,\hat{N}}$, where one calculates its phase, $\hat{N}$, from which one can extract classical observables (including radiation) due to a relation to the WKB approximation. This has been assembled into a computational framework in Ref. [149] where the radial action has been tied to certain *velocity cuts* (see also Ref. [150] for related work).

[3] Similar statements also hold in the EFT matching approach for the conservative two-body problem where classically divergent terms correspond to iterations of lower-order potentials, see e.g. Ref. [59] and references therein.

Similarly to the eikonal approach, the radial action $I_r(J)$ (and also the phase of the S-matrix $\hat{N}$) has a perturbative expansion $I_r(J) = I_r^{(0)}(J) + I_r^{(1)}(J) + I_r^{(2)}(J) + \cdots$ which leads to classical iterations from expanding the exponential to higher orders in the small coupling constant. In this section, we describe an approach to calculate the classical radial action at a given loop order $I_r^{(L)}(J)$ without the need of explicit classically divergent subtractions. Our new setup is closest in philosophy to that of Ref. [59]. In particular, we are going to find a prescription that is implemented at the level of boundary conditions for soft master integrals which manifestly eliminates classically divergent contributions, and allows us to define a soft radial action. By explicit calculation, we show that our prescription works up to two-loop order. Its study to higher orders in perturbation theory is an interesting open problem left to future work.

Formally, the perturbative expansion of Eq. (1.18) to a given loop-order L still entails the subtraction of nontrivial exponentiation terms involving two or more lower-order *iterations* $I_r^{(L'<L)}$ to isolate $I_r^{(L)}$ itself. The aforementioned reference [59] writes such iterations as $(D-1)$-dimensional integrals with linearized propagators. Meanwhile, the boundary conditions for soft master integrals near the static limit, when considering only the potential region, are also given by $(D-1)$-dimensional integrals where the "divergent" part involves linearized propagators [76]. Therefore, our strategy is to drop integrals with linearized propagators from the boundary conditions and solving the differential equations for the soft integrals subject to the modified "finite" boundary conditions.

The set of diagram topologies for master integrals related to the above "iterations" is shown in Fig. 1.4. It turns out that only the first graph in Fig. 1.4, called the III diagram, is relevant for the classically divergent terms in the real part of the two-loop amplitude. In the notation of Eq. (4.70) of [76], the top-level soft master integral for the III diagram is

$$f_{\mathrm{III},7} = \epsilon^4 (y^2 - 1)(-q^2) G_{1,1,1,1,1,1,1,0,0}\,, \tag{1.19}$$

where $G_{1,1,1,1,1,1,1,0,0}$ is the scalar double-box integral with a unit numerator, multiplied by additional prefactors are included. In the Euclidean region we have $-1 < x < 0$, and

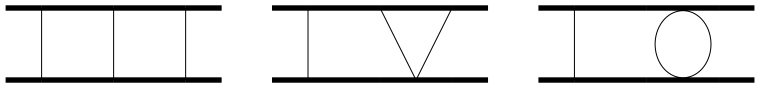

Figure 1.4: Master integral topologies related to iteration of radial action or EFT potential, responsible for classically divergent terms in the amplitude. The IX diagram corresponding to the second one in Fig. 1.2 does not appear since it is not divergent in the potential region, so receives no subtraction in a conservative calculation. The subtraction in the soft region is designed to be identical to the subtraction in the potential region—this works as long as we restrict to the real part where the only divergences comes from $\mathcal{A}^3_{\text{tree}}$.

$y = (1+x^2)/(2x) < -1$, with the value of the master integral given in Ref. [76] as

$$f_{\text{III},7} = -\frac{1}{2}\epsilon^2 \log^2(-x) + \frac{1}{12}\epsilon^3 \big[-24\text{Li}_3(x) - 24\text{Li}_3(-x) + 12\text{Li}_2(x)\log(-x) + 12\text{Li}_2(-x)\log(-x) + 2\log^3(-x) + \pi^2 \log(-x) + 6\zeta_3 \big] + \mathcal{O}(\epsilon^4) \,. \tag{1.20}$$

By analytic continuation, the value of integral in the Lorentzian region $0 < x < 1$, $y > 1$ is obtained from the above formula with an infinitesimal positive imaginary part given to y, or an infinitesimal negative imaginary part given to x,

$$f_{\text{III},7} = -\frac{1}{2}\epsilon^2 \left[\log(x) + i\pi\right]^2 + \mathcal{O}(\epsilon^3) \,, \tag{1.21}$$

where we omitted the analytic continuation result at $\mathcal{O}(\epsilon^3)$ which is needed for calculating the amplitude but not relevant for the discussion here.

When evaluated in the potential region, the integral cannot be analytically continued between positive and negative values of x, and we directly give the value of the integral for the Lorentzian region $0 < x < 1$, $y = (1+x^2)/(2x) > 1$,

$$f^{(\text{p})}_{\text{III},7} = \frac{\epsilon^2 \pi^2}{2} + 0 \cdot \epsilon^3 + \mathcal{O}(\epsilon^4) \,. \tag{1.22}$$

Compared with Eq. (1.21), in the $\mathcal{O}(\epsilon^2)$ term only the π^2 part survives, and the $\mathcal{O}(\epsilon^3)$ term has become genuinely zero, and not an omission.

There are 7 pure master integrals for the soft-expanded III diagram in the even-in-$|q|$ sector. In the potential region, the boundary condition near the static limit $y = 1$ is given in terms of $(3-2\epsilon)$-dimensional integrals in Eqs. (A.9)-(A.11) of Ref. [76]. In particular, for the top-level master integral near the static limit,

$$f^{(p)}_{\mathrm{III},7}\big|_{y=1} = \pi\epsilon^4(-q^2)\int \frac{\mathrm{d}^{D-1}\boldsymbol{\ell}_1 \mathrm{d}^{D-1}\boldsymbol{\ell}_2 \left(e^{\gamma_E \epsilon}\right)^2}{(\mathrm{i}\pi^{(D-1)/2})^2\, \boldsymbol{\ell}_1^2 \boldsymbol{\ell}_2^2 (\boldsymbol{\ell}_1 + \boldsymbol{\ell}_2 - \boldsymbol{q})^2 (2\ell_1^z)(-2\ell_2^z)}\,, \tag{1.23}$$

which is precisely of the form of a $(D-1)$-dimensional integral involving linearized propagators. The superscript (p) in the equation above indicates that only the potential region is considered. Now we implement a subtraction scheme similar to the 4PM potential-region calculation, by dropping $(3-2\epsilon)$-dimensional integrals involving linearized propagators arising from iterations of lower-loop potentials. This is equivalent to keeping Eqs. (A.9) and (A.10) in the reference while changing the RHS of Eq. (A.11), reproduced in Eq. (1.23), to zero. Solving differential equations with the altered boundary conditions, Eq. (1.22) becomes

$$f^{(\mathrm{p}),\mathrm{subtracted}}_{\mathrm{III},7} = 0\cdot\epsilon^2 + 0\cdot\epsilon^3 + \mathcal{O}(\epsilon^4)\,, \tag{1.24}$$

i.e. vanishes until $\mathcal{O}(\epsilon^4)$, which is beyond the order of ϵ needed in the classical calculation.

The boundary values for the master integrals in the soft region are decomposed into the sum of their values in the potential region and their soft-region corrections. We perform the same subtraction for the potential-region part, while keeping the soft-region corrections unchanged. Since the solutions to the homogeneous system of differential equations have multi-linear dependence on the boundary conditions, we have

$$f^{\mathrm{subtracted}}_{\mathrm{III},7} = f_{\mathrm{III},7} + \left(f^{(\mathrm{p}),\mathrm{subtracted}}_{\mathrm{III},7} - f^{(p)}_{\mathrm{III},7}\right)\,. \tag{1.25}$$

Explicitly,

$$f^{\mathrm{subtracted}}_{\mathrm{III},7} = -\frac{1}{2}\epsilon^2\left[\log(x)^2 + 2i\pi\log(x)\right] + \mathcal{O}(\epsilon^3)\,, \tag{1.26}$$

where in the $\mathcal{O}(\epsilon^2)$ term, the π^2 part has been removed, and the omitted $\mathcal{O}(\epsilon^3)$ term (also needed for assembling the amplitude) is completely unchanged.

If we calculate the two-loop amplitude in the soft expansion using the subtracted value Eq. (1.26) for the top-level III master integral and unsubtracted original results for all other master integrals, the real part of the result directly gives the radial action after Fourier transform.

1.2.5 KMOC framework for classical conservative and radiative observables

In this part of our review, we schematically recall aspects of the KMOC framework [39] as presented in Ref. [47]. We only introduce the relevant final formulae. For further details, the interested reader is encouraged to consult Refs. [39] or [47] directly.

In the KMOC [39] approach one first sets up a quantum mechanical Gedanken experiment for the scattering of two wavepackets representing massive particles from which the classical limit is carefully taken in order to extract the classical observables of interest. In the quantum setup, we can measure the change of some observable ΔO (corresponding to some quantum operator $\mathbb{O}$) following the time-evolution of states from the asymptotic past to the asymptotic future. In the asymptotic past, the wavepackets are represented by $|\text{in}\rangle$, an *in* quantum state constructed from the superposition of two-particle momentum eigenstates $|p_1, p_2\rangle_{\text{in}}$ with wavefunctions $\phi_i(p_i)$. For the case of interest to us, these states are well separated by an impact parameter b^μ [4]

$$|\text{in}\rangle = \int \mathrm{d}\Phi_2(p_1, p_2)\, \phi_1(p_1)\phi_2(p_2) e^{\mathrm{i}\, b\cdot p_1/\hbar}\, |p_1, p_2\rangle_{\text{in}}\,. \tag{1.27}$$

Such an *in* state will evolve to an *out* state in the asymptotic future, $|\text{out}\rangle$, that might contain additional particles created during the interaction. ΔO is obtained by evaluating the difference of the expectation value of $\mathbb{O}$ between *in* and *out* states

$$\Delta O = \langle \text{out}|\mathbb{O}|\text{out}\rangle - \langle \text{in}|\mathbb{O}|\text{in}\rangle\,. \tag{1.28}$$

In quantum mechanics, the *out* states are related to the *in* states by the time evolution

[4] The impact parameter b^μ is distinct from the eikonal impact parameter b_e that will appear later.

operator, i.e. the S-matrix: $|\text{out}\rangle = S|\text{in}\rangle$ and we can write

$$\Delta O = \mathrm{i} \int \mathrm{d}\Phi_4(p_1, \cdots, p_4)\, \phi_1(p_1)\phi_2(p_2)\phi_2^*(p_3)\phi_1^*(p_4)\, \hat{\delta}^{(D)}(\textstyle\sum_i p_i)\, e^{\mathrm{i}\, b\cdot(p_1+p_4)/\hbar}\, \mathcal{I}_O\,, \tag{1.29}$$

where we follow the same conventions as Ref. [47] for the phase-space $d\Phi_n$ and $\hat{\delta}$ factors. The kernel $\mathcal{I}_O$ is related to the matrix elements via

$$\widetilde{\mathcal{I}}_O \equiv \widehat{\delta}^{(D)}(\textstyle\sum p_i)\, \mathcal{I}_O = -\mathrm{i}\, \langle p_4, p_3|S^\dagger[\mathbb{O}, S]|p_1, p_2\rangle\,. \tag{1.30}$$

To arrive at this expression, we have used the unitarity of the S-matrix, $S^\dagger S = 1$. Following [39], $\widetilde{\mathcal{I}}_O$ can be related to scattering amplitudes by writing $S = 1 + \mathrm{i}T$ such that

$$\widetilde{\mathcal{I}}_O = \widetilde{\mathcal{I}}_{O,\,\mathrm{v}} + \widetilde{\mathcal{I}}_{O,\,\mathrm{r}} = \langle p_4, p_3|[\mathbb{O}, T]|p_1, p_2\rangle - i\, \langle p_4, p_3|T^\dagger[\mathbb{O}, T]|p_1, p_2\rangle\,. \tag{1.31}$$

We conveniently separated the kernel $\widetilde{\mathcal{I}}_O$ into two contributions $\widetilde{\mathcal{I}}_{O,\mathrm{v}}$ and $\widetilde{\mathcal{I}}_{O,\,\mathrm{r}}$, that we preemptively call *virtual* and *real*, respectively. This nomenclature becomes apparent when one evaluates the expectation values: The *virtual* part of the result is

$$\mathcal{I}_{O,\,\mathrm{v}} = \Delta\mathbb{O}\big[\mathcal{A}(p_1, p_2, p_3, p_4)\big] = \Delta\mathbb{O}$$

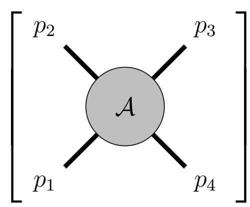

, (1.32)

where $\Delta\mathbb{O}$ acts on the scattering amplitude $\mathcal{A}$. In the *real* kernel

$$\mathcal{I}_{O,\,\mathrm{r}} = -\mathrm{i} \sum_X \int \mathrm{d}\widetilde{\Phi}_{2+|X|}\ \Delta\mathbb{O}$$

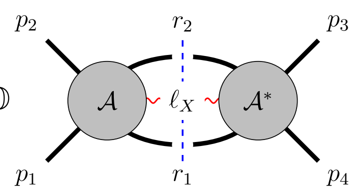

, (1.33)

$\Delta\mathbb{O}$ only acts on the amplitude on the left of the unitarity cut which was introduced by the insertion of a complete sum over states in Eq. (1.31).

While the KMOC formalism can be applied fully quantum mechanically, we are interested in *classical* observables. The classical limit corresponds to the regime where the Compton wavelength of the external particles is the smallest length scale in the problem. KMOC carefully analyze this limit with the net result that all computations ultimately reduce to those of simple plane-wave scattering. In the classical limit, the wavepackets sharply peak about their classical values of the momenta which leads to the appearance of on-shell delta functions and one arrives at a compact expression for the classical change of the observable O in terms of the (asymptotic) impact parameter b^μ, conjugate to the small momentum transfer $q^\mu = p_1^\mu + p_4^\mu \sim \mathcal{O}(\hbar)$,

$$\Delta O = \mathrm{i} \int \hat{\mathrm{d}}^D q \, \hat{\delta}(-2p_1 \cdot q) \, \hat{\delta}(2p_2 \cdot q) e^{\mathrm{i}b \cdot q} \, (\mathcal{I}_{O,\mathrm{v}} + \mathcal{I}_{O,\mathrm{r}}) \ . \tag{1.34}$$

The KMOC analysis suggests that we ought to focus on kinematic regions where the massive particle momenta p_i are large and scale like $\mathcal{O}(1)$ in the classical counting and the four-momentum transfer q, as well as graviton loop variables that we will denote by ℓ_i below, scale like $\mathcal{O}(\hbar)$. In the effective field theory context, employing terminology from the "method of regions" [145], the classical $\hbar$ expansion is therefore equivalent to the so-called soft expansion.

Furthermore, we also expand scattering amplitudes in the coupling e or equivalently α

$$\mathcal{A} = \mathcal{A}^{(0)} + \mathcal{A}^{(1)} + \mathcal{A}^{(2)} + \cdots = $$

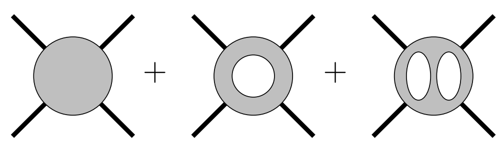

$$+ \cdots \ , \tag{1.35}$$

where the L-loop amplitude is $\mathcal{O}(\alpha^{L+1})$. The observables (and kernels) have analogous expansions

$$\Delta O = \Delta O^{(0)} + \Delta O^{(1)} + \Delta O^{(2)} + \cdots \ , \tag{1.36}$$

$$\mathcal{I}_O = \mathcal{I}_O^{(0)} + \mathcal{I}_O^{(1)} + \mathcal{I}_O^{(2)} + \cdots \ . \tag{1.37}$$

1.2.5.1 Electromagnetic Impulse

In this work, we discuss two observables relevant to classical electrodynamic scattering. The first is the impulse, Δp_i^μ, which is defined as the total change in momentum of one of the particles during the collision. In the KMOC setup this is encoded by the appropriate quantum momentum operator $\mathbb{P}_i$, which is measured asymptotically far from the collision region as follows

$$\Delta p_1^\mu = \langle \text{in}|S^\dagger \mathbb{P}_1^\mu S|\text{in}\rangle - \langle \text{in}|\mathbb{P}_1^\mu|\text{in}\rangle \, . \tag{1.38}$$

As summarized above, in the classical limit, this is simply a Fourier transform of the impulse kernel $\mathcal{I}_{p_1}^\mu$ from momentum transfer q to impact-parameter space b

$$\Delta p_1^\mu = \mathrm{i} \int \hat{\mathrm{d}}^D q \, \hat{\delta}(-2p_1 \cdot q) \, \hat{\delta}(2p_2 \cdot q) \, e^{\mathrm{i}b\cdot q} \, \mathcal{I}_{p_1}^\mu \, , \tag{1.39}$$

which is separated into virtual and real contributions, given in terms of the amplitude as

$$\mathcal{I}_{p_1,\mathrm{v}} = q^\mu$$

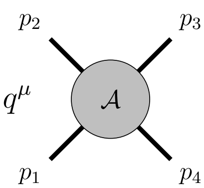

$$, \quad \mathcal{I}_{p_1,\mathrm{r}} = -\mathrm{i} \sum_X \int \mathrm{d}\widetilde{\Phi}_{2+|X|} \; \ell_1^\mu$$

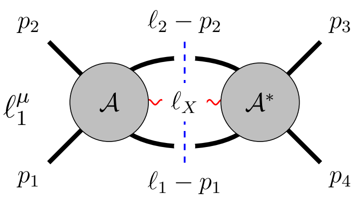

$$, \tag{1.40}$$

where the numerator insertions q^μ and ℓ_1 arise from the measurement function $\Delta\mathbb{P}_1^\mu$ acting on the respective amplitudes, which extracts the momentum change of particle 1. Note that relative to Eq. (1.33), we have changed variables in the real contribution by shifting the massive intermediate momenta $r_i = -p_i + \ell_i$, so that all ℓ_i are small, $\mathcal{O}(\hbar)$, in the classical expansion. The impulse on particle 2 can be obtained by simple relabelling.

In the following, we often decompose the total impulse into its transverse, $\Delta p_\perp$, and longitudinal, Δp_u, components

$$\Delta p^\mu = \Delta p_\perp^\mu + \Delta p_u^\mu \, , \tag{1.41}$$

where $u_i{\cdot}\Delta p_\perp{=}0$ and $q{\cdot}\Delta p_u{=}0$. The respective kernels get decomposed in a similar fashion

$$\mathcal{I}_{p_1}^\mu = \mathcal{I}_\perp \, q^\mu + \sum_{i=1,2} \mathcal{I}_{u_i} \, \check{u}_i^\mu \, . \tag{1.42}$$

We define *dual* four-velocities,

$$\check{u}_1^\mu = \frac{y u_2^\mu - u_1^\mu}{y^2 - 1}, \qquad \check{u}_2^\mu = \frac{y u_1^\mu - u_2^\mu}{y^2 - 1} \, , \tag{1.43}$$

which satisfy $u_i \cdot \check{u}_j = \delta_{ij}$ and remain orthogonal to the momentum transfer q. Decomposing the loop momentum dependent impulse numerator

$$\ell_1^\mu = \frac{\ell_1 \cdot q}{q^2} q^\mu + (\ell_1 \cdot u_1)\, \check{u}_1^\mu + (\ell_1 \cdot u_2)\, \check{u}_2^\mu \,, \tag{1.44}$$

exposes that only the transverse part of the impulse has a *virtual* contribution

$$\mathcal{I}_\perp =$$

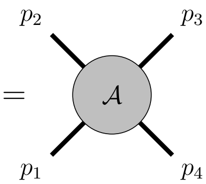

$$- \ \mathrm{i} \sum_X \int \mathrm{d}\widetilde{\Phi}_{2+|X|} \ \frac{\ell_1 \cdot q}{q^2}$$

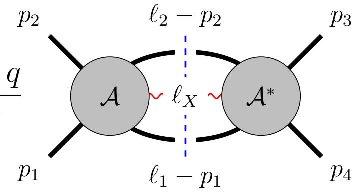

$$, \tag{1.45}$$

whereas the longitudinal part *only* receives contributions from the unitarity cut terms

$$\mathcal{I}_{u_i} = -\,\mathrm{i} \sum_X \int \mathrm{d}\widetilde{\Phi}_{2+|X|} \ \ell_1 \cdot u_i$$

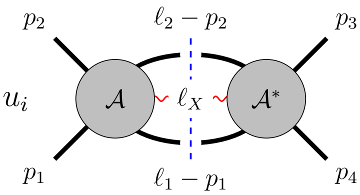

$$. \tag{1.46}$$

Loop amplitudes generically have real and imaginary parts, so one might wonder how all classical observables end up real-valued, and how various terms in the KMOC setup combine to serve this purpose. Keeping track of factors of 'i', it turns out that the transverse KMOC kernels need to be purely real to yield a real result after the final Fourier transform (Eq. (1.34)), whereas the longitudinal kernels are purely imaginary. The reality properties of various quantities has been argued abstractly in terms of unitarity cutting rules in Ref. [47] that later appeared in a slightly different context in Ref. [102]. Indeed, it will serve as a non-trivial check of our computation, that all imaginary contributions to the classical observables cancel.

1.2.5.2 Radiated momentum

Another observable of interest is the total radiated momentum ΔR^μ carried away in the form of electromagnetic waves during the scattering of two heavy charged objects. This observable is defined by measuring the momentum operator $\mathbb{R}^\mu$ of the emitted *messenger particles*, here photons. As explained in Ref. [39], this observable only receives *real* contributions and its respective kernel is

$$\mathcal{I}^{\mu}_{R,\mathrm{r}} = -\mathrm{i}\sum_{X}\int \mathrm{d}\widetilde{\Phi}_{2+X}\ \ell_X^{\mu} \tag{1.47}$$

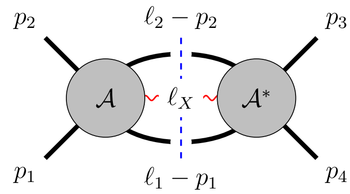

Like Eqs. (1.39) and (1.40), Eq. (1.47) is valid beyond perturbation theory, however, for explicit calculations we expand it perturbatively in α. The first contribution to ΔR^{μ} (obtained from Eq. (1.47) by performing the Fourier transform to impact-parameter space (1.34)) arises at $\mathcal{O}(\alpha^3)$. This can be understood from the fact that Bremsstrahlung of finite energy photons only arises once one heavy charged particle is slightly deflected due to its electromagnetic interaction with the other massive charged object.

The impulse and radiated momentum are not completely independent observables. As already pointed out in Ref. [39], their relation goes to the heart of one of the difficulties in traditional approaches to classical field theory with point sources. Two particles that scatter in e.g. classical electrodynamics exchange momentum via their interaction with the electromagnetic field. In the classical context, this is described by the Lorentz force. However, the energy or the momentum lost by the point particles to radiation is not accounted for by the Lorentz force. In the classical setup, momentum conservation is restored by including the additional Abraham–Lorentz–Dirac (ALD) force [141–143, 151] and e.g. Refs. [152–154] for some recent treatments. In the classical context, the inclusion of the ALD force term is associated with its own problems. In particular, it leads to issues of runaway solutions and causality violations in the description of point charges in classical EM. In contrast, in the quantum-mechanical description of charged-particle scattering these issues are absent and we will see that our results for the classical two-body dynamics in electrodynamics will conserve energy and momentum automatically. For more discussions on this point, see Sections 3.5 and 5.4 of Ref. [39] for a KMOC integrand level discussion of this point. The main conclusion of their analysis is that the ALD radiation reaction is automatically included in the KMOC setup via the cut-contribution where an on-shell radiation photon is exchanged. This contribution first appears at two-loop order, or $\mathcal{O}(\alpha^3)$ and was compared to the classical ALD force computation in Section 6.3 of Ref. [39]. Our agreement below with the $\mathcal{O}(\alpha^3)$ scattering angle computed using the ALD force [99] explicitly affirms these conclusions.

1.3 Conservative dynamics at $\mathcal{O}(\alpha^3)$

1.3.1 Conservative scattering amplitudes

In this section we give the results for the tree level, one-loop and two-loop scattering amplitudes in scalar QED in the conservative sector. We combine the integrands derived in section 1.2.2 with the integration techniques sketched in section 1.2.3. A detailed account of the potential region integrals is found in Refs. [41, 42, 76]. All potential region L-loop amplitudes will henceforth be denoted by $\mathcal{A}^{(L)}_{4,(p)}$.

The tree-level amplitude can be obtained from Eq. (1.7) by switching from the soft variables y, and $\overline{m}_1$ to σ and m_i via the relations from Subsection 1.2.1

$$\mathcal{A}^{(0)}_{4,(p)} = -(4\pi\alpha\, q_1 q_2)\frac{4m_1 m_2 \sigma}{-q^2}\,, \tag{1.48}$$

where we use the charge normalization $\alpha = e^2/4\pi$ and denote the multiple of the elementary charge e of the massive objects by q_i.

The conservative one-loop amplitude can be obtained from the integrand in Eq. (1.17) by taking the small-q expansion of the covariant integrand. Upon reducing the q-expanded integrals to a basis of master integrals, it is given in terms of the sum of the box and crossed box integrals, as well as two triangle integrals evaluated in the potential region. (Bubble integrals are zero in the potential region.)

$$\mathcal{A}^{(1)}_{4,(p)} = -\mathrm{i}c_{\mathrm{II}}\left(I^{(p)}_{\mathrm{II}} + I^{(p)}_{\mathrm{X}}\right) - \mathrm{i}c_{\triangleleft}\, I^{(p)}_{\triangleleft} - \mathrm{i}c_{\triangleright}\, I^{(p)}_{\triangleright}. \tag{1.49}$$

The coefficients are

$$c_{\mathrm{II}} = (16\pi\,\alpha q_1 q_2\, m_1 m_2 \sigma)^2\,, \quad c_{\triangleleft} = -\frac{1}{2}(16\pi\,\alpha q_1 q_2\, m_1)^2\,, \quad c_{\triangleright} = -\frac{1}{2}(16\pi\,\alpha q_1 q_2\, m_2)^2\,. \tag{1.50}$$

Inserting the explicit values of the integrals in the potential region (see e.g. Ref. [76]) yields

$$\begin{aligned}
\mathcal{A}^{(1)}_{4,(p)} = (4\pi\alpha\, q_1 q_2)^2 \frac{1}{(4\pi)^2}\left(\frac{-q^2}{\bar{\mu}^2}\right)^{-\epsilon} \Bigg\{ & \frac{1}{(-q^2)}\frac{\mathrm{i}\pi(\sigma^2 m_1 m_2)}{2\sqrt{\sigma^2-1}}\frac{e^{\epsilon\gamma_E}\Gamma(-\epsilon)^2\Gamma(1+\epsilon)}{\Gamma(-2\epsilon)} \\
& + 8\frac{1}{\sqrt{-q^2}}\sqrt{\pi}(m_1+m_2)\frac{e^{\epsilon\gamma_E}\Gamma\left(\frac{1}{2}-\epsilon\right)^2\Gamma\left(\epsilon+\frac{1}{2}\right)}{2\Gamma(1-2\epsilon)} \\
& - \epsilon\frac{1}{\sqrt{-q^2}}\frac{\sqrt{\pi}(m_1+m_2)}{(\sigma^2-1)}\frac{e^{\epsilon\gamma_E}\Gamma\left(\frac{1}{2}-\epsilon\right)^2\Gamma\left(\epsilon+\frac{1}{2}\right)}{\Gamma(1-2\epsilon)} \\
& - \epsilon\frac{\mathrm{i}\pi\left(m_1^2+m_2^2+2m_1 m_2\sigma\right)}{8m_1 m_2\left(\sigma^2-1\right)^{3/2}}\frac{e^{\epsilon\gamma_E}\Gamma(-\epsilon)^2\Gamma(1+\epsilon)}{\Gamma(-2\epsilon)}\Bigg\} + \ldots\,,
\end{aligned} \tag{1.51}$$

where $\bar{\mu}^2 = 4\pi e^{-\gamma_E}\mu^2$, while μ and γ_E are the dimensional regularization scale, and the Euler-Mascheroni constant, respectively. The ellipsis stand for terms with polynomial (including constant) dependence on q^2, with or without poles in ϵ. Such terms give rise to contact interactions after Fourier transform to impact-parameter space, and are irrelevant for long-range classical physics.

Finally, the two-loop amplitude in the potential region is given by

$$\begin{aligned}
\mathcal{A}^{(2)}_{4,(p)} = (4\pi\alpha\, q_1 q_2)^3 \left(\frac{\mathrm{i}}{(4\pi)^2}\right)^2 \left(\frac{-q^2}{\bar{\mu}^2}\right)^{-2\epsilon} \Bigg\{ & -\frac{1}{(-q^2)}\frac{32\pi^2 m^2 \nu\,\sigma^3}{(\sigma^2-1)}\left[\frac{1}{\epsilon^2}-\frac{\pi^2}{6}\right] \\
& + \frac{1}{\sqrt{-q^2}}\frac{16\mathrm{i}\pi\, m}{(\sigma^2-1)^{1/2}}\left[\frac{1}{\epsilon}-2\log(2)-\frac{4\sigma^3}{\sigma^2-1}+\mathcal{O}(\epsilon)\right] \\
& + \frac{8\pi^2}{\epsilon}\left[\frac{2\nu(1-\sigma^2-\sigma^4)+(1-2\nu)(\sigma-2\sigma^3)}{\nu(\sigma^2-1)^2}+\mathcal{O}(\epsilon)\right]\Bigg\} + \ldots
\end{aligned} \tag{1.52}$$

where we have used the total mass, m, and symmetric mass ratio, ν,

$$m = m_1 + m_2\,, \quad \nu = \frac{m_1 m_2}{(m_1+m_2)^2}\,. \tag{1.53}$$

1.3.2 Eikonal approach to classical conservative scattering

Armed with the conservative amplitude through two loops, we may compute the eikonal phase. Traditionally, one Fourier transforms the amplitudes to impact-parameter space in order to extract the eikonal phase. Here, following Ref. [76], we instead use the eikonal exponentiation directly in momentum space. This comes at the cost of products in impact-parameter space becoming convolutions in momentum space. However, all needed convolutions have already been evaluated in Ref. [76]. We summarize the result of our calculation of the eikonal phase (Our convention for eikonal phase differs by a factor of 2 from that of [76] and is consistent with the definition of the eikonal in the soft region of section 1.4.2.)

$$2\delta^{(0)}_{(p)}(\sigma, \boldsymbol{q}_\perp) = -(4\pi\alpha\, q_1 q_2) 4 m_1 m_2 \sigma \frac{1}{\boldsymbol{q}_\perp^2}\,, \tag{1.54}$$

$$2\delta^{(1)}_{(p)}(\sigma, \boldsymbol{q}_\perp) = (4\pi\alpha\, q_1 q_2)^2 \frac{(m_1+m_2)}{4} \frac{1}{|\boldsymbol{q}_\perp|}\,, \tag{1.55}$$

$$2\delta^{(2)}_{(p)}(\sigma, \boldsymbol{q}_\perp) = (4\pi\alpha\, q_1 q_2)^3 \frac{2\nu + (1-2\nu)\sigma}{16(\sigma^2-1)\nu} \log(\boldsymbol{q}_\perp^2)\,, \tag{1.56}$$

where we use the $D-2$-dimensional spacelike vector, $\boldsymbol{q}_\perp$, transverse to the scattering plane, satisfying $\boldsymbol{q}_\perp^2 = -q^2$. Finally, we can perform the Fourier transform to obtain the more familiar eikonal phase in impact-parameter space

$$\delta(\sigma, \boldsymbol{b}_\mathrm{e}) = \frac{1}{4 m_1 m_2 \sqrt{\sigma^2-1}} \int \frac{\mathrm{d}^{D-2}\boldsymbol{q}_\perp}{(2\pi)^{D-2}}\, e^{\mathrm{i}\boldsymbol{b}_\mathrm{e}\cdot\boldsymbol{q}_\perp}\, \delta(\sigma, \boldsymbol{q}_\perp)\,, \tag{1.57}$$

with the result

$$2\delta^{(0)}_{(p)}(\sigma, \boldsymbol{b}_\mathrm{e}) = (4\pi\alpha\, q_1 q_2) \frac{\sigma}{4\pi\sqrt{\sigma^2-1}} \log(\boldsymbol{b}_\mathrm{e}^2)\,, \tag{1.58}$$

$$2\delta^{(1)}_{(p)}(\sigma, \boldsymbol{b}_\mathrm{e}) = (4\pi\alpha\, q_1 q_2)^2 \frac{1}{32\pi m \nu \sqrt{\sigma^2-1}} \frac{1}{|\boldsymbol{b}_\mathrm{e}|}\,, \tag{1.59}$$

$$2\delta^{(2)}_{(p)}(\sigma, \boldsymbol{b}_\mathrm{e}) = -(4\pi\alpha\, q_1 q_2)^3 \frac{(2\nu + (1-2\nu)\sigma)}{64\pi^3 m^2 \nu^2 \sqrt{\sigma^2-1}} \frac{1}{\boldsymbol{b}_\mathrm{e}^2}\,, \tag{1.60}$$

where we have dropped terms that do not contribute to the classical scattering angle. As discussed below (see Eq. (1.70)), the eikonal imapact parameter $\boldsymbol{b}_\mathrm{e}$ is distinct from the geometric impact parameter $\boldsymbol{b}$.

1.3.3 Conservative eikonal phase, scattering angle, and two-body Hamiltonian

The stationary phase approximation of the Fourier transform of the exponentiated impact-parameter amplitude back to momentum space

$$\mathcal{A}(\sigma,-q^2) = \int d^{D-2}\boldsymbol{b}_{\rm e} \left(e^{2{\rm i}\delta(\sigma,\boldsymbol{b}_{\rm e})} - 1\right) e^{-{\rm i}\,\boldsymbol{q}\cdot\boldsymbol{b}_{\rm e}} \tag{1.61}$$

yields the relation

$$\boldsymbol{q} = -\frac{\partial}{\partial \boldsymbol{b}_{\rm e}} 2\delta(\sigma,\boldsymbol{b}_{\rm e})\,. \tag{1.62}$$

The magnitude of $\boldsymbol{q}$ is related to the scattering angle χ and the magnitude of the three-momentum $\boldsymbol{p}$ in the center-of-mass frame by

$$|\boldsymbol{q}| = 2|\boldsymbol{p}|\sin\frac{\chi}{2}\,. \tag{1.63}$$

From this, we may now calculate the gravitational scattering angle from the eikonal phase using the formula

$$\sin\frac{\chi}{2} = -\frac{1}{2|\boldsymbol{p}|}\frac{\partial}{\partial|\boldsymbol{b}_{\rm e}|} 2\delta(\sigma,\boldsymbol{b}_{\rm e})\,. \tag{1.64}$$

where in terms of the center of mass energy $E=\sqrt{s}$ and/or σ

$$p_\infty \equiv |\boldsymbol{p}| = \frac{m_1 m_2\sqrt{\sigma^2-1}}{E} = \frac{m_1 m_2\sqrt{\sigma^2-1}}{\sqrt{m_1^2+m_2^2+2m_1m_2\sigma}} = \frac{m\nu\sqrt{\sigma^2-1}}{\sqrt{1+2\nu(\sigma-1)}}\,. \tag{1.65}$$

Using this formula we find the following result for the scattering angle

$$\chi^{(0)}_{(p)} = -\frac{\alpha\, q_1 q_2}{|\boldsymbol{b}_e|}\frac{2\sigma}{|\boldsymbol{p}|\sqrt{\sigma^2-1}}\,, \tag{1.66}$$

$$\chi^{(1)}_{(p)} = \frac{(\alpha\, q_1 q_2)^2}{|\boldsymbol{b}_e|^2}\frac{1}{2|\boldsymbol{p}|m\nu\sqrt{\sigma^2-1}}\,, \tag{1.67}$$

$$\chi^{(2)}_{(p)} = -\frac{(\alpha\, q_1 q_2)^3}{|\boldsymbol{b}_e|^3}\left[\frac{\sigma^3}{3|\boldsymbol{p}|^3(\sigma^2-1)^{3/2}} + \frac{2\,(2\nu+(1-2\nu)\sigma)}{|\boldsymbol{p}|m^2\nu^2\sqrt{\sigma^2-1}}\right]\,. \tag{1.68}$$

Comparing the result in Eqs. (1.66)-(1.67), we find agreement (up to conventions) with Westpfahl [33]. It is useful to write the formulae in terms of the angular momentum, J, as defined via

$$J = |\boldsymbol{b}\times\boldsymbol{p}| = |\boldsymbol{b}||\boldsymbol{p}|\,, \tag{1.69}$$

where $\boldsymbol{b}$ is the asymptotic impact parameter perpendicular to the incoming center of mass momentum $\boldsymbol{p}$. As noted earlier, this is not the impact parameter, $\boldsymbol{b}_{\rm e}$, relevant to the eikonal phase and pointing in the direction of the momentum transfer $\boldsymbol{q}$. The magnitude of $\boldsymbol{b}$ and $\boldsymbol{b}_{\rm e}$ are then related by

$$|\boldsymbol{b}| = |\boldsymbol{b}_{\rm e}| \cos\frac{\chi}{2}\,, \tag{1.70}$$

so that the angular momentum is

$$J = |\boldsymbol{b}_{\rm e}||\boldsymbol{p}| \cos\frac{\chi}{2}\,. \tag{1.71}$$

This difference is unimportant at leading orders, and it will only matter at order J^{-3}. Using the relation (1.71) we find the scattering angle in terms of the angular momentum

$$\begin{aligned}
\chi^{(0)}_{(p)} &= -\frac{\alpha\, q_1 q_2}{J}\frac{2\sigma}{\sqrt{\sigma^2-1}}\,,\\
\chi^{(1)}_{(p)} &= \frac{(\alpha\, q_1 q_2)^2}{J^2}\frac{\pi}{2\sqrt{1+2\nu(\sigma-1)}},\\
\chi^{(2)}_{(p)} &= \frac{(\alpha\, q_1 q_2)^3}{J^3}\frac{4\nu(3-3\sigma^2+\sigma^4)+(1-2\nu)(6\sigma-4\sigma^3)}{3(1+2\nu(\sigma-1))(\sigma^2-1)^{3/2}}\,.
\end{aligned} \tag{1.72}$$

One can write the conservative Hamiltonian for a system of two spinless charges in an expansion in powers of the electromagnetic coupling as

$$\begin{aligned}
H(\boldsymbol{r}^2,\boldsymbol{p}^2) =& \sqrt{\boldsymbol{p}^2+m_1^2}+\sqrt{\boldsymbol{p}^2+m_2^2}\\
&+c_1(\boldsymbol{p}^2)\frac{\tilde\alpha}{|\boldsymbol{r}|}+c_2(\boldsymbol{p}^2)\left(\frac{\tilde\alpha}{|\boldsymbol{r}|}\right)^2+c_3(\boldsymbol{p}^2)\left(\frac{\tilde\alpha}{|\boldsymbol{r}|}\right)^3+\dots\,,
\end{aligned} \tag{1.73}$$

where $\tilde\alpha$=$4\pi\alpha q_1 q_2$ and the $c_i(\boldsymbol{p}^2)$ are yet to be determined coefficients. Such a Hamiltonian was used in Ref. [42], to obtain a related expansion of the classical scattering angle

$$\chi = \frac{P_1}{p_\infty}\left(\frac{\tilde\alpha}{J}\right)+\frac{\pi}{2}P_2\left(\frac{\tilde\alpha}{J}\right)^2-\frac{P_1^3-12p_\infty^2P_1P_2-24p_\infty^4P_3}{12p_\infty^3}\left(\frac{\tilde\alpha}{J}\right)^3+\mathcal{O}\left((\tilde\alpha/J)^4\right)\,, \tag{1.74}$$

where p_∞ was defined in Eq. (1.65). The P_i coefficients in the scattering angle are the natural expansion coefficients for the radial momentum $p_r^2(r)$ (see Sec. 11 of [42] for details in the context of GR), but are also related to the c_i coefficients in the Hamiltonian via [42]

$$P_1 = -2E\xi\,\bar{c}_1\,, \tag{1.75}$$

$$P_2 = -2E\xi\,\bar{c}_2 + (1-3\xi)\,\bar{c}_1^2 + 4E^2\xi^2\,\bar{c}_1\bar{c}_1'\,, \tag{1.76}$$

$$\begin{aligned} P_3 = &-2E\xi\bar{c}_3 + 2(1-3\xi)\bar{c}_1\bar{c}_2 - 4E^3\xi^3\bar{c}_1\left(2\bar{c}_1'^2 + \bar{c}_1\bar{c}_1''\right) + 4E^2\xi^2\left(\bar{c}_2\bar{c}_1' + \bar{c}_1\bar{c}_2'\right) \\ &- 6E(1-3\xi)\xi\bar{c}_1^2\bar{c}_1' + \frac{(1-4\xi)\bar{c}_1^3}{E}\,, \end{aligned} \tag{1.77}$$

where $\bar{c}_i{\equiv}c_i(p_\infty^2)$, primes denote derivatives with respect to the argument, $E{=}E_1{+}E_2 = m\sqrt{1{+}2\nu(\sigma{-}1)}$ and $\xi{=}E_1E_2/E^2{=}\frac{\nu\left(\nu(\sigma-1)^2+\sigma\right)}{(1+2\nu(\sigma-1))^2}$. Conversely, one may start from our scattering angles in Eq. (1.72), deduce the P_i coefficients in Eq. (1.74) up to $\mathcal{O}(\alpha^3)$

$$P_1 = -\frac{2m\,\nu\,\sigma}{(4\pi)\,\Gamma}\,, \qquad P_2 = \frac{1}{(4\pi)^2}\frac{1}{\Gamma}\,, \qquad P_3 = \frac{(\Gamma{-}1)\sigma + 2\nu(\sigma{-}1)}{(4\pi)^3\,\Gamma\,m\,\nu\,(\sigma^2-1)}\,, \tag{1.78}$$

where we have defined $\Gamma = E/m = \sqrt{1+2\nu(\sigma{-}1)}$. Relatedly, the coefficients in the expansion of the scattering angle can also be expressed via suitably defined finite parts of scattering amplitudes (see discussion around Eq. (12) of [41]) in terms of slightly rescaled coefficients $\tilde{d}_i$ which differ from P_i by powers of p_∞, $\tilde{d}_i = p_\infty^{i-2}\,P_i$:[5]

$$\chi = \tilde{d}_1\left(\frac{\tilde{\alpha}}{J}\right) + \frac{\pi}{2}\tilde{d}_2\left(\frac{\tilde{\alpha}}{J}\right)^2 - \left(\frac{\tilde{d}_1^3}{12} - \tilde{d}_1\,\tilde{d}_2 + 2\tilde{d}_3\right)\left(\frac{\tilde{\alpha}}{J}\right)^3 + \mathcal{O}\big((\tilde{\alpha}/J)^4\big)\,, \tag{1.79}$$

where the coefficients now read

$$\tilde{d}_1 = -\frac{2\sigma}{(4\pi)\sqrt{\sigma^2-1}}\,, \qquad \tilde{d}_2 = \frac{1}{(4\pi)^2\,\Gamma}\,, \qquad \tilde{d}_3 = \frac{(\Gamma{-}1)(1+\Gamma+\sigma)}{(4\pi)^3\Gamma^2\sqrt{\sigma^2-1}}\,. \tag{1.80}$$

An interesting feature is that two-loop function $\tilde{d}_3$ vanishes in the test mass limit $\nu{\to}0$ ($\Gamma{\to}1$), i.e. $\tilde{d}_3 \overset{\nu\to 0}{\longrightarrow} 0$. This is due to the fact that $\Gamma{-}1$ starts at $\mathcal{O}(\nu)$ in the test mass expansion. Crucially, $\tilde{d}_3 = 0$ implies that the $\mathcal{O}(\alpha^3)$ test-body Hamiltonian is fully determined by lower-loop information. In fact, in the test-body limit, the scattering angle is computable exactly

[5] We use $\tilde{d}_i$ rather than d_i to signal slight normalization differences by factors of π and the coupling constant compared to [41].

to all orders in the coupling (see e.g. Ref. [103][6] and references therein)

$$
\begin{aligned}
\chi_{\text{test}} &= \frac{J}{\sqrt{J^2-(\alpha q_1 q_2)^2}}\left(\pi + 2\arctan\left[\frac{-(\alpha q_1 q_2)}{\beta\sqrt{J^2-(\alpha q_1 q_2)^2}}\right]\right) - \pi\,, \\
&= -\frac{2\alpha q_1 q_2}{\beta J} + \frac{\pi\alpha^2 q_1^2 q_2^2}{2J^2} - \frac{2\alpha^3\left(3\beta^2-1\right)q_1^3 q_2^3}{3\beta^3 J^3} + \frac{3\pi\alpha^4 q_1^4 q_2^4}{8J^4} + \mathcal{O}(\alpha^5)\,,
\end{aligned}
\tag{1.81}
$$

where $\beta = \sqrt{\sigma^2-1}/\sigma$ is the velocity. With the test-body angle available to all orders in the coupling constant, we can investigate the angle relation of Eq. (1.74) for the P_i to higher orders in perturbation theory. At $\mathcal{O}(\alpha^4)$, we would find (see Eq. (11.25) of [42])

$$
\begin{aligned}
\chi &= (1.74) + \frac{3\pi}{8}\left(P_2^2 + 2P_1P_3 + 2p_\infty^2 P_4\right)\left(\frac{\tilde{\alpha}}{J}\right)^4 + \mathcal{O}\big((\tilde{\alpha}/J)^5\big)\,, \\
&= (1.79) + \frac{3\pi}{8}\left(\tilde{d}_2^2 + 2\tilde{d}_1\tilde{d}_3 + 2\tilde{d}_4\right)\left(\frac{\tilde{\alpha}}{J}\right)^4 + \mathcal{O}\big((\tilde{\alpha}/J)^5\big)
\end{aligned}
\tag{1.82}
$$

Comparing the explicit angle in the test-body limit (1.81) to the expansion in Eq. (1.82), we see that $\tilde{d}_3 = \tilde{d}_4 = 0$. Indeed, all $\tilde{d}_{i>2} = 0$ vanish in the test-body limit which in turn implies that the higher Hamiltonian coefficients $c_{i>2}$ are equally determined by at most one-loop data. In light of this discussion, the reason there is a simple closed form solution for the scattering angle is connected to the simplicity of the test mass Hamiltonian.

For the sake of completeness, we also tabulate the c_i coefficients in the Hamiltonian or general mass dependence up to $\mathcal{O}(\alpha^3)$. This yields

$$
c_1 = \frac{1}{4\pi(2\Gamma^2\xi^2)}(2\Gamma^2\xi^2\tilde{\nu})\,, \tag{1.83}
$$

$$
c_2 = \frac{1}{(4\pi)^2 m(2\Gamma^2\xi^2)}\left(-\xi + 2\Gamma\xi\tilde{\nu} - \Gamma\xi(1-\xi)\tilde{\nu}^2\right)\,, \tag{1.84}
$$

$$
\begin{aligned}
c_3 = \frac{1}{(4\pi)^3 m^2(2\Gamma^2\xi^2)}\Bigg\{&\frac{\sigma^2}{1-\sigma^2}\left(\frac{\Gamma-1}{\Gamma}\right)\frac{1}{\tilde{\nu}} - \frac{1+\sigma+2\Gamma\xi}{(1+\sigma)\Gamma} \\
&+\frac{2\Gamma+1-\xi}{\Gamma}\tilde{\nu} - (3-4\xi)\tilde{\nu}^2 + (1-2\xi)\tilde{\nu}^3\Bigg\}\,,
\end{aligned}
\tag{1.85}
$$

where $\tilde{\nu} = \frac{\sigma\nu}{\Gamma^2\xi} = \frac{\sigma(1+2\nu(\sigma-1))}{\nu(\sigma-1)^2+\sigma}$.

[6] In comparison to Ref. [103], our scattering angle is defined to go to zero in the absence of interactions ($\alpha\to 0$) which explains the additional $-\pi$. Our conventions for the charges lead to an additional sign in the argument of the arctan.

1.3.4 Conservative impulse and scattering angle via KMOC

Besides extracting the classical observables via the eikonal approach discussed in Sec. 1.3.2 or in terms of a classical Hamiltonian (see Sec. 1.3.3), we have also computed the conservative electromagnetic impulse within the KMOC framework, generally discussed in Sec. 1.2.5. In the conservative setting, energy is conserved in the scattering process, so that there is no radiated momentum or energy loss to consider. In terms of the method of regions, this is encoded in the fact that all photons are purely potential and can never go on-shell, so that the radiation cuts in Eq. (1.47) are always absent. Likewise, for the impulse, we only have to consider elastic processes without exchanged messenger particles in the *real* contribution in Eq. (1.40).

Due to energy conservation in the conservative sector, it suffices to determine the transverse impulse only and the longitudinal part is completely determined by the on-shell conditions and momentum conservation of the process

$$(p_i + \Delta p_i)^2 = p_i^2 \qquad \Delta p_1 + \Delta p_2 = 0\,. \tag{1.86}$$

Employing generalized unitarity, we constructed the relevant conservative integrand to extract the transverse impulse kernel from Eq. (1.45) where only the first two diagrams of Fig. (1.2) are relevant at $\mathcal{O}(\alpha^3)$. Using the same integration and assembly pipeline that has already produced the conservative gravitational results in Ref. [47] together with the potential region values of the master integrals from Ref. [76], we obtain the transverse impulse on particle 1 at two loops[7]

$$\Delta p_{1,\perp}^{\mu,\text{cons.}} = (\alpha q_1 q_2)^3 \frac{2\left(2m_1 m_2\left(\sigma^4 - \sigma^2 + 1\right) + (m_1^2 + m_2^2)\sigma\right)}{m_1^2 m_2^2\left(\sigma^2 - 1\right)^{5/2}} \frac{b^\mu}{|b|^4}\,. \tag{1.87}$$

The conservative longitudinal impulse at $\mathcal{O}(\alpha^3)$ is

$$\Delta p_{1,u}^{\mu,\text{cons.}} = (\alpha q_1 q_2)^3 \frac{\pi\left(m_1 + m_2\right)\sigma}{m_1 m_2\,|b|^3\left(\sigma^2 - 1\right)} \left(\frac{\check{u}_2^\mu}{m_2} - \frac{\check{u}_1^\mu}{m_1}\right)\,. \tag{1.88}$$

[7] We drop the explicit label of the perturbative order of the observable (see Eq. (1.36)) for brevity. The same information is encoded in the order of α.

Both the longitudinal and transverse impulse agree with the ones obtained from the scattering angles (1.72) and the help of the parametrization of the impulse in terms of the conservative scattering angle of appendix B in Ref. [47]. We also agree with the recent computation of the impulse obtained by solving classical equations of motion [99].

In comparing to the gravitational result [47], in electrodynamics there is no $\operatorname{arcsinh}\sqrt{\frac{\sigma-1}{2}}$ high-energy singularity in the transverse impulse, which also renders this feature absent from the scattering angle. At high energies, i.e. large $\sigma \gg 1$, and fixed impact parameter b, the leading large sigma behavior of the transverse and longitudinal impulse scale like $1/\sigma$ and $1/\sigma^2$ respectively. (For the longitudinal impulse, one has to take the definition of the $\check{u}_i \overset{\sigma\gg 1}{\sim} 1/\sigma$ in Eq. (1.43) into account.)

1.4 Radiative dynamics at $\mathcal{O}(\alpha^3)$

1.4.1 Radiative scattering amplitudes

In this section we give the results for the scattering amplitudes in the soft region that includes radiation effects by combining the integrands from section 1.2.2 with the integration techniques sketched in section 1.2.3. Detailed results of all soft-region integrals can be found in Ref. [47]. The tree-level amplitude remains

$$\mathcal{A}_4^{(0)}(p_1,p_2,p_3,p_4) =$$

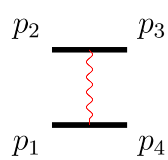

$$= -(4\pi\alpha\, q_1 q_2)\frac{4m_1 m_2\,\sigma}{-q^2}\,, \tag{1.89}$$

The one-loop amplitude in the soft region is

$$\begin{aligned}\mathcal{A}_4^{(1)}(p_1,p_2,p_3,p_4) =&(4\pi\alpha\, q_1 q_2)^2\left[\mathrm{i}\left(\frac{1}{4\pi}\right)^{2-\epsilon}\frac{e^{-\gamma\epsilon}}{(-q^2)^\epsilon}\right]\Bigg[\frac{4\pi^2 m_1 m_2\,(z^2+1)^2\, e^{\gamma\epsilon}\csc(\pi\epsilon)\Gamma(-\epsilon)}{(-q^2)z\,(z^2-1)\,\Gamma(-2\epsilon)}\\ &+\frac{\mathrm{i}\pi^2\,(m_1+m_2)\,4^{\epsilon+1}e^{\gamma\epsilon}\left(4\,(z^2+1)^2\,\epsilon-(z^2-1)^2\right)\sec(\pi\epsilon)}{\sqrt{-q^2}\,(z^2-1)^2\,\Gamma(1-\epsilon)}\\ &+\frac{\pi^{3/2}2^{2\epsilon+1}e^{\gamma\epsilon}\csc(\pi\epsilon)}{\Gamma\left(\frac{3}{2}-\epsilon\right)m_1 m_2\,(z^2-1)^3}\; f(z,\epsilon)+\mathcal{O}(|q|)\Bigg]\,,\end{aligned} \tag{1.90}$$

where γ is the Euler-Mascharoni constant and

$$\begin{aligned}f(z,\epsilon)=&\Big[2\pi\left(m_1^2+m_2^2\right)z\left(z^2+1\right)^2\epsilon(2\epsilon-1)+m_1 m_2\Big\{4\left(z^2+1\right)^2\left((\pi+2i)z^2-2i+\pi\right)\epsilon^2\\ &-2\left(\pi\left(z^2+1\right)^3+2i\left(z^2-1\right)^3\right)\epsilon+2i(z^2+1)(2\epsilon-1)\left(2\left(z^2+1\right)^2\epsilon-z^4+6z^2-1\right)\log(z)\\ &-i\left(z^6+5z^4-5z^2-1\right)\Big\}\Big]\,,\end{aligned} \tag{1.91}$$

is written in terms of z, related to $\sigma=\frac{1+z^2}{2z}$ in order to rationalize square roots such as $\sqrt{\sigma^2-1}=\frac{1-z^2}{2z}$. When converting the computations in terms of the soft-variables y, x, $\overline{m}_i$ to the original masses m_i and σ, z, one has to be careful to take into account subleading $\mathcal{O}(q^2)$ terms in the conversion in order to obtain the correct expression for the one-loop quantum piece.

The relevant parts of the two-loop amplitude are

$$\frac{\mathcal{A}_4^{(2)}(p_1,p_2,p_3,p_4)}{(4\pi\alpha)^3}=\left[\mathrm{i}\left(\frac{1}{4\pi}\right)^{2-\epsilon}\frac{e^{-\gamma\epsilon}}{(-q^2)^\epsilon}\right]^2\left[\frac{a^{(2)}_{-1,-2}}{(-q^2)\,\epsilon^2}+\frac{a^{(2)}_{-1,-1}}{(-q^2)\,\epsilon}+\frac{a^{(2)}_{-\frac{1}{2},-1}}{\sqrt{-q^2}\,\epsilon}+\frac{a^{(2)}_{0,-2}}{\epsilon^2}+\frac{a^{(2)}_{0,-1}}{\epsilon}\right], \tag{1.92}$$

where the two-loop amplitude coefficients $a^{(2)}_{i,j}$ are labeled by the order in the q and ϵ expansion. In principle, we also have access to higher-order terms in the ϵ and q expansion, but they do not play a role for the purpose of our discussion here. The expression for the classical term $a^{(2)}_{0,-1}$ is rather lengthy, so we do not display it here. (We supply all expressions in computer readable form as an ancillary file.) The classical term $a^{(2)}_{0,-1}$ contains contributions from both the charge sector proportional to $q_1^3 q_2^3$ as well as from the mushroom topologies

$q_i^4 q_j^2$. In contrast, the classically divergent terms as well as the $1/\epsilon^2$ coefficient of the classical piece are entirely within the $q_1^3 q_2^3$ sub-sector,

$$a^{(2)}_{-1,-2} = -(q_1 q_2)^3 \frac{16\pi^2 m_1 m_2 \left(z^2+1\right)^3}{z\left(z^2-1\right)^2}\,, \qquad a^{(2)}_{-1,-1} = 0\,, \tag{1.93}$$

$$a^{(2)}_{-\frac{1}{2},-1} = (q_1 q_2)^3 \frac{16\mathrm{i}\pi^3 (m_1+m_2)\left(z^2+1\right)}{\left(z^2-1\right)}\,, \tag{1.94}$$

$$a^{(2)}_{0,-2} = (q_1 q_2)^3 \frac{8\mathrm{i}\pi\left(z^2+1\right)\left(3z^6+7z^4-7z^2-3+2\left(z^6-9z^4-9z^2+1\right)\log(z)\right)}{\left(z^2-1\right)^4}\,. \tag{1.95}$$

Again, all results are written in the terms of the z variable that rationalizes $\sqrt{\sigma^2-1}$.

1.4.2 Eikonal approach to classical scattering including radiation effects

In a first implementation of radiative effects in scalar QED at $\mathcal{O}(\alpha^3)$, we follow the eikonal approach that has been successfully used in Ref. [144] to extract the classical scattering angle in gravity. The steps in their derivation are independent of the theory under consideration as long as they admit a suitable classical limit. It is therefore natural to expect that we can follow Sec. 2.2 of Ref. [144] for scalar QED. As we will show, this expectation is indeed correct. Since the physical intuition behind the eikonal approach has already been discussed extensively by Di Vecchia et al. [144], we restrict ourselves to only the most important formulae. At the heart of the eikonal approach is the expected exponentiation of certain parts of the scattering amplitude in impact-parameter space

$$1 + i\widetilde{\mathcal{A}}(s,b_e) = \big(1 + 2i\Delta(s,b_e)\big)e^{2i\delta(s,b_e)}\,, \tag{1.96}$$

where $\delta(s,b_e)$ is the classical eikonal phase and $\Delta(s,b_e)$ is a quantum remainder that starts with one-loop contributions. (We follow the notation of Ref. [144] but keep in mind that we express s in terms of σ or z.) Let us note, that it is a priori unclear what part of the amplitude exponentiates beyond leading order. In the conservative sector discussed in Sec. 1.3.2, there is an good argument based on elastic unitarity, that the amplitude (including quantum terms) exponentiates. Here, we follow the prescription of Ref. [144] that exponentiate strictly classical terms and all quantum corrections are assigned to $\Delta(s, b_e)$. However, from the conservative perspective, one could expect that certain quantum terms that originate from the potential region should still exponentiate and lead to quantum corrections of the classical eikonal phase $\delta(s, b_e)$ and only quantum radiation pieces need not resum to a phase. We do not pursue this separation further and leave a detailed investigation to future work. The momentum-space amplitude $\mathcal{A}(s, -q^2)$ is Fourier-transformed to the $D-2$-dimensional impact-parameter space, conjugate to the (space-like) momentum-transfer q

$$\widetilde{\mathcal{A}}(s, b_e) = \int \frac{d^{D-2}q}{(2\pi)^{D-2}} \frac{\mathcal{A}(s, -q^2)}{4m_1 m_2 \sqrt{\sigma^2 - 1}} e^{ib_e \cdot q} \,. \tag{1.97}$$

Here, we distinguish the eikonal impact parameter b_e from the asymptotic impact parameter b related by the geometric identity

$$b_e = \frac{b}{\cos \frac{\chi}{2}} \,, \tag{1.98}$$

where χ is the scattering angle. The momentum-space scattering amplitude $\mathcal{A}(s, -q^2)$ entering in Eq. (1.97) has an expansion in terms of the coupling constant (loop-expansion) as well as an expansion in powers of $-q^2$. Via standard Fourier integrals, the power-series expansion in $-q^2$ gets converted to a similar expansion in impact-parameter space

$$\mathcal{A}_4^{(0)} = \frac{a_{-1}^{(0)}}{-q^2} \quad \to \quad \widetilde{\mathcal{A}}_4^{(0)} = \frac{\widetilde{a}_{-1}^{(0)}}{(-b_e^2)^{-\epsilon}} \,, \tag{1.99}$$

$$\mathcal{A}_4^{(1)} = \frac{a_{-1}^{(1)}}{(-q^2)^{1+\epsilon}} + \frac{a_{-1/2}^{(1)}}{(-q^2)^{\frac{1}{2}+\epsilon}} + \frac{a_0^{(1)}}{(-q^2)^{\epsilon}} \quad \to \quad \widetilde{\mathcal{A}}_4^{(1)} = \frac{\widetilde{a}_{-1}^{(1)}}{(-b_e^2)^{-2\epsilon}} + \frac{\widetilde{a}_{-1/2}^{(1)}}{(-b_e^2)^{\frac{1}{2}-2\epsilon}} + \frac{\widetilde{a}_0^{(1)}}{(-b_e^2)^{1-2\epsilon}} \,, \tag{1.100}$$

$$\mathcal{A}_4^{(2)} = \frac{a_{-1}^{(2)}}{(-q^2)^{1+2\epsilon}} + \frac{a_{-1/2}^{(2)}}{(-q^2)^{\frac{1}{2}+2\epsilon}} + \frac{a_0^{(2)}}{(-q^2)^{2\epsilon}} \quad \to \quad \widetilde{\mathcal{A}}_4^{(2)} = \frac{\widetilde{a}_{-1}^{(2)}}{(-b_e^2)^{-3\epsilon}} + \frac{\widetilde{a}_{-1/2}^{(2)}}{(-b_e^2)^{\frac{1}{2}-3\epsilon}} + \frac{\widetilde{a}_0^{(2)}}{(-b_e^2)^{1-3\epsilon}} \,, \tag{1.101}$$

where the impact-parameter space coefficients $\widetilde{a}_j^{(\ell)}$ are directly related to the momentum-space expressions around $D = 4 - 2\epsilon$ dimensions via

$$\int \frac{\mathrm{d}^{D-2}q}{(2\pi)^{D-2}} \frac{e^{\mathrm{i}b_e \cdot q}}{(-q^2)^{\alpha}} = \frac{\Gamma\left(D/2 - 1 - \alpha\right)}{2^{2\alpha+2}(\pi)^{\frac{D-2}{2}}\Gamma\left(\alpha\right)} \frac{1}{(-b_e^2)^{\frac{D-2-2\alpha}{2}}} \,. \tag{1.102}$$

Furthermore, the $a_i^{(\ell)}$ are simply related to the $a_{i,j}^{(\ell)}$ of Eqs. (1.89), (1.90), and (1.92). Expanding the right-hand-side of the eikonal ansatz in Eq. (1.96) perturbatively in the coupling α

$$\delta = \delta^{(0)} + \delta^{(1)} + \delta^{(2)} + \cdots \,, \qquad \Delta = \Delta^{(1)} + \cdots \,, \tag{1.103}$$

one can match both sides of Eq. (1.96) to the desired order in α to determine the eikonal quantities in terms of fixed-order amplitude results. Note that all classically divergent (or 'super-classical') terms are completely determined by lower order data and serve as nontrivial cross-check of the computation. Equipped with the eikonal phase, one can Fourier-transform back to momentum space which allows for the identification of the *classical* momentum transfer Q^μ from a stationary-phase approximation

$$Q^\mu = -\frac{\partial \,\mathrm{Re}\; 2\,\delta(s, b_e)}{\partial b_e^\mu} \,, \tag{1.104}$$

which is related to the scattering angle χ via

$$|Q| = 2p \sin\frac{\chi}{2} \,, \tag{1.105}$$

where $p = \frac{\sqrt{\sigma^2-1}m_1 m_2}{\sqrt{m_1^2+m_2^2+2m_1m_2\sigma}}$ is the asymptotic center of mass momentum.
In terms of the asymptotic impact parameter that is tied to the center-of-mass angular momentum $J = p\; b$ (see Eq. (1.98)), the scattering angle is

$$\tan\frac{\chi}{2} = -\frac{1}{2p}\frac{\partial\, 2\,\mathrm{Re}\;\delta}{\partial b} \,. \tag{1.106}$$

We can now take the perturbative expansion of Eq. (1.96) together with the explicit values of the tree-, one-loop, and two-loop amplitudes in momentum space of Eqs. (1.89), (1.90), and (1.92) to convert the variables to the normal masses m_i and to σ in order to obtain the explicit values for the $a_i^{(\ell)}(s)$ coefficients in Eq. (1.99) from which we can extract the eikonal parameters

$$\delta^{(0)}(s,b_e) = \frac{1}{(-b_e^2)^{-\epsilon}} \frac{\pi^\epsilon\,\Gamma(-\epsilon)}{32\pi\, m_1 m_2 \sqrt{\sigma^2-1}}\; a_{-1}^{(0)}\,, \tag{1.107}$$

$$\delta^{(1)}(s,b_e) = \frac{1}{(-b_e^2)^{\frac{1}{2}-2\epsilon}} \frac{2^{-2\epsilon}\pi^\epsilon\,\Gamma\left(\frac{1}{2}-2\epsilon\right)}{16\pi\, m_1 m_2 \sqrt{\sigma^2-1}\,\Gamma\left(\epsilon+\frac{1}{2}\right)}\; a_{-1/2}^{(1)}\,, \tag{1.108}$$

$$\begin{aligned}\delta^{(2)}(s,b_e) = \frac{1}{(-b_e^2)^{1-3\epsilon}} \frac{1}{2m_1 m_2} \Bigg[&\frac{4^{-2\epsilon}\pi^\epsilon\,\Gamma(1-3\epsilon)}{4\pi\,\sqrt{\sigma^2-1}\Gamma(2\epsilon)}\; a_0^{(2)} \\ &- \mathrm{i}\frac{2^{-2\epsilon}\pi^{2\epsilon}\,\Gamma(1-2\epsilon)\Gamma(-\epsilon)}{64\pi^2\, m_1 m_2\,(\sigma^2-1)\,\Gamma(\epsilon)}\; a_{-1}^{(0)}\, a_0^{(1)} \Bigg]\,,\end{aligned} \tag{1.109}$$

and the one-loop quantum remainder,

$$\Delta^{(1)}(s,b_e) = \frac{1}{(-b_e^2)^{1-2\epsilon}} \frac{2^{-2\epsilon}\pi^\epsilon\,\Gamma(1-2\epsilon)}{8\pi\, m_1 m_2 \sqrt{\sigma^2-1}\Gamma(\epsilon)}\; a_0^{(1)}\,. \tag{1.110}$$

We note that the imaginary part of the two-loop eikonal, $\delta^{(2)}$, still contains a $1/\epsilon$ infrared singularity (due to the $1/\epsilon^2$ contribution of $a_0^{(2)}$ in Eq. (1.110)), consistent with a similar feature in gravity [144], whereas the real part of the phase which is relevant for the physical scattering angle is IR finite.

With the explicit values of the eikonal parameters at hand, we can take Eq. (1.106), convert the eikonal impact parameter in Eq. (1.107) with the help of Eq. (1.98), and perturbatively expand the angle $\chi = \chi^{(0)} + \chi^{(1)} + \chi^{(2)} + \cdots$. This allows us to solve Eq. (1.106) order by order in the coupling in terms of expressions that we know from the scattering ampliutudes. In particular, we find

$$\chi^{(0)} = -(\alpha q_1 q_2)\frac{2\sigma}{J\sqrt{\sigma^2-1}}\,, \tag{1.111}$$

$$\chi^{(1)} = (\alpha q_1 q_2)^2 \frac{\pi(m_1+m_2)}{2J^2\sqrt{m_1^2+m_2^2+2m_1 m_2\,\sigma}}\,, \tag{1.112}$$

$$\begin{aligned}\chi^{(2)} = (\alpha q_1 q_2)^3 &\frac{(m_1^2{+}m_2^2)\,(6\sigma{-}4\sigma^3) + 4m_1 m_2\left(3 + (\sigma^2{-}3\sigma\sqrt{\sigma^2{-}1}{-}3)\sigma^2 + 6\sigma^2 \mathrm{arcsinh}\sqrt{\frac{\sigma-1}{2}}\right)}{3J^3\,(\sigma^2{-}1)^{3/2}\,(m_1^2+m_2^2+2m_1 m_2\,\sigma)} \\ &+ \alpha^3 q_1^2 q_2^2 \frac{4\sigma^2\,(m_2^2 q_1^2 + m_1^2 q_2^2)}{3J^3\,(m_1^2+m_2^2+2m_1 m_2\,\sigma)}\,,\end{aligned} \tag{1.113}$$

where the second line of Eq. (1.113) originates from the mushroom sector. Our results are in complete agreement with those of Saketh et al. [99], once we take into account the different conventions $\chi^{(L)}_{\text{us}} = -\chi^{(L)}_{[99]}$. Before discussing these results in a bit more detail, it is beneficial to split the $\mathcal{O}(\alpha^3)$ scattering angle into conservative and radiative parts,

$$\chi^{(2)} = \chi^{(2)}_{\text{cons.}} + \chi^{(2)}_{\text{rad.}}\,, \tag{1.114}$$

where

$$\chi^{(2)}_{\text{cons.}} = (\alpha q_1 q_2)^3\,\frac{2\left(\sigma\left(3-2\sigma^2\right)\left(m_1^2+m_2^2\right)+2m_1m_2\left(\sigma^4-3\sigma^2+3\right)\right)}{3J^3\left(\sigma^2-1\right)^{3/2}\left(m_1^2+m_2^2+2m_1m_2\,\sigma\right)}\,, \tag{1.115}$$

$$\begin{aligned}\chi^{(2)}_{\text{rad.}} = &-(\alpha q_1 q_2)^3\,\frac{4m_1m_2\,\sigma^2\left(\sigma\sqrt{\sigma^2-1}-2\,\text{arcsinh}\sqrt{\frac{\sigma-1}{2}}\right)}{J^3\left(\sigma^2-1\right)^{3/2}\left(m_1^2+m_2^2+2m_1m_2\,\sigma\right)}\\ &+\alpha^3 q_1^2 q_2^2\frac{4\sigma^2\left(m_2^2q_1^2+m_1^2q_2^2\right)}{3J^3\left(m_1^2+m_2^2+2m_1m_2\,\sigma\right)}\,.\end{aligned} \tag{1.116}$$

The radiative part of the angle can also be used to extract or compare to the radiated angular momentum [139, 155] at one order lower via the linear response relation

$$\chi_{\text{rad.}} = \frac{1}{2}\frac{\partial\chi_{\text{cons.}}}{\partial J}J_{\text{rad.}} + \mathcal{O}(\alpha^4)\,. \tag{1.117}$$

where $\chi_{\text{cons.}}$ starts at $\mathcal{O}(\alpha)$.

High-energy limit of scattering angle

Similar to the discussion in Ref. [99], we can investigate the behavior of our generic scattering angles of Eq. (1.113) in special kinematic limits. One interesting regime is the high-energy limit which corresponds to the center-of-mass energy $E{=}\sqrt{m_1^2+m_2^2+2m_1m_2\,\sigma} \gg (m_1+m_2)$ for m_1 and m_2 held fixed. This is achieved by taking $\sigma \gg 1$. Note that this limit is *not* equivalent to the massless limit where $m_1, m_2{\to}0$, which is outside the range of validity of our classical approximation $m_i^2 \gg |q|^2$, since the Compton wavelength of the particles $\lambda_c \sim 1/m$ becomes large compared to the impact parameter $|b| \sim 1/|q|$, whereas classical physics requires $\lambda_c \ll |b|$. The exact details of the high-energy limit depend on the parameters that are held fixed in the scattering experiment. In particular, so far we have opted to write the scattering angle in terms of the large angular momentum J, related to the impact parameter b,

$$J = \frac{m_1 m_2 \sqrt{\sigma^2-1}|b|}{\sqrt{m_1^2+m_2^2+2m_1 m_2\,\sigma}} \quad \overset{\text{HE}}{\longrightarrow} \quad \frac{|b|E}{2} + \mathcal{O}(1/E)\,, \tag{1.118}$$

by an additional factor of E in the high energy limit which shifts the overall energy dependence of the answer by overall powers of E in the conversion of L-loop results which are proportional to $1/J^{L+1}$.

We are now in the position to discuss the high energy limit of the scattering angles, both conservative and radiative. Up to $\mathcal{O}(\alpha^3)$ and to leading order in the high-energy limit (in each individual charge sector), we find

$$\chi_{\text{cons.}}\Big|_{\text{HE}} = \chi^{(0)}\Big|_{\text{HE}} + \chi^{(1)}\Big|_{\text{HE}} + \chi^{(2)}_{\text{cons.}}\Big|_{\text{HE}} + \mathcal{O}(\alpha^4)\,, \tag{1.119}$$

where we have the explicit high-energy values of the scattering angles

$$\chi^{(0)}\Big|_{\text{HE}} = -\frac{4\alpha m_1 m_2}{E\,|b|}\left[\frac{q_1}{m_1}\right]\left[\frac{q_2}{m_2}\right], \tag{1.120}$$

$$\chi^{(1)}\Big|_{\text{HE}} = \frac{2\pi\alpha^2 m_1^2 m_2^2\,(m_1+m_2)}{E^3\,|b|^2}\left[\frac{q_1}{m_1}\right]^2\left[\frac{q_2}{m_2}\right]^2, \tag{1.121}$$

$$\chi^{(2)}_{\text{cons.}}\Big|_{\text{HE}} = \frac{16\alpha^3 m_1^3 m_2^3}{3E^3\,|b|^3}\left[\frac{q_1}{m_1}\right]^3\left[\frac{q_2}{m_2}\right]^3, \tag{1.122}$$

in terms of the charge-to-mass ratios $r_i \equiv q_i/m_i$. The radiative angle is more interesting,

$$\chi^{(2)}_{\text{rad.}}\Big|_{\text{HE}} = -\frac{16\alpha^3 m_1^3 m_2^3}{E^3\,|b|^3}\left[\frac{q_1}{m_1}\right]^3\left[\frac{q_2}{m_2}\right]^3 + \frac{8\alpha^3 m_1^2 m_2^2}{3\,E\,|b|^3}\left(\left[\frac{q_1}{m_1}\right]^4\left[\frac{q_2}{m_2}\right]^2 + \left[\frac{q_1}{m_1}\right]^2\left[\frac{q_2}{m_2}\right]^4\right), \tag{1.123}$$

which, as has been pointed out in Ref. [99], develops a mass singularity in the mushroom sector due to uncanceled $1/m_i^2$ in the second term of Eq. (1.123). From our perspective, one should not take this as a true singularity of the result but rather as a breakdown of the classical approximation which requires $|q|^2 \ll m_i^2$, or equivalently $m_i^2|b|^2 \gg 1$, which prevents us from setting $m_i \to 0$. Presumably, one could take into account coherence effects to discuss the classical scattering of light states [48]. There, however, the particle interpretation breaks down and one should instead talk about the scattering of classical waves described by coherent states.

Note that the mushroom contribution is dominant in the high-energy limit and behaves like $1/E$ at $\mathcal{O}(\alpha^3)$ whereas the $q_1^3 q_2^3$ sector scales like $1/E^3$ at large E. Combining the high-energy limit of the conservative angle in Eq. (1.122) with the high-energy limit of the $q_1^3 q_2^3$-sector of the radiative angle, we find

$$\chi^{(2)}_{q_1^3 q_2^3}\Big|_{\text{HE}} = -\frac{32\alpha^3 m_1^3 m_2^3}{3E^3\,|b|^3}\left[\frac{q_1}{m_1}\right]^3\left[\frac{q_2}{m_2}\right]^3 = \frac{\left[\chi^{(0)}\Big|_{\text{HE}}\right]^3}{3!}\,, \tag{1.124}$$

which is given in terms of the third power of the high-energy limit of the tree-level angle. The contribution from the mushroom diagrams on the other hand does not follow such an iterative structure at high energies.

As noted in the introduction, we view QED as a useful model for gravitational calculations that not only lets us test computational setups in a simpler context, but also sheds light on important physical questions. To this end, we would like to compare the results of some classical observables in electrodynamics to the ones in GR. One of the simplest places of comparison is the high-energy limit of the scattering angle. First, at tree- and one-loop level, the leading order behavior of the gravitational scattering angle is [33]

$$\chi_{\text{GR}}\Big|_{\text{HE}} = \chi^{(0)}_{\text{GR}}\Big|_{\text{HE}} + \chi^{(1)}_{\text{GR}}\Big|_{\text{HE}} + \mathcal{O}(G^3) = \frac{4GE}{|b|} + \frac{15\pi G^2 E(m_1+m_2)}{4\,|b|^2} + \mathcal{O}(G^3)\,. \tag{1.125}$$

The high-energy-limit of the tree-level gravitational scattering angle, $\chi^{(0)}_{\text{GR}}\Big|_{\text{HE}}$ is the double-copy of the QED angle with the replacement $q_i \to E$ and $\alpha \to G$. This is a direct consequence of the fact that the tree-level amplitude is dominated by the t-channel exchange diagram which is obtained as the product of two three-particle amplitudes. In the high-energy limit, these have the double-copy property. At one-loop, there is still some residual double-copy property present that is exposed by the same replacement as above. However, the numerical prefactor does not directly match anymore.

At two-loop order, it is worthwhile to recall that the conservative scattering angle in GR [41, 42] contains a logarithmic high-energy singularity that is canceled by radiative contributions [138, 139]

$$\chi^{(2),\mathrm{GR}}_{\mathrm{rad.}}\Big|_{\mathrm{HE}} = \frac{8G^3E^3\left(6\log\left(\frac{E^2}{m_1m_2}\right)-5\right)}{3\,|b|^3}\,, \tag{1.126}$$

$$\chi^{(2),\mathrm{GR}}_{\mathrm{cons.}}\Big|_{\mathrm{HE}} = -\frac{8G^3E^3\left(6\log\left(\frac{E^2}{m_1m_2}\right)-9\right)}{3\,|b|^3}\,, \tag{1.127}$$

$$\left(\chi^{(2),\mathrm{GR}}_{\mathrm{cons.}}+\chi^{(2),\mathrm{GR}}_{\mathrm{rad.}}\right)\Big|_{\mathrm{HE}} = \frac{32G^3E^3}{3|b|^3} = \frac{\left[\chi^{(0)}_{\mathrm{GR}}\Big|_{\mathrm{HE}}\right]^3}{3!}\,. \tag{1.128}$$

The fact that the leading high-energy limit of the full scattering angle in gravity is given by the third power of the tree-level angle is furthermore responsible for the observed high-energy universality of gravitational scattering at $\mathcal{O}(G^3)$ [138, 139]. In comparison, for QED, only the box-sector ($\sim q_1^3q_2^3$) angle follows the same iteration structure (see Eq. (1.124)), whereas the mushroom terms (that are actually leading in the high-energy limit) do not.

Nonetheless, as was the case at one-loop order, the structure of the high-energy limit of the angle still follows a double-copy-like relation between QED and gravity under the replacement $q_i/m_i \to 1$, $m_i \to E$, and $\alpha \to G$. Notably, at two-loops in gravity, the logarithmic high-energy singularity of the individual conservative and radiative contributions to the angle is directly entangled with the mass singularity. This is due to the fact that both quantities appear linked as the argument of a logarithm $\log\frac{E^2}{m_1m_2}$ so that one can think about mass or high-energy divergences interchangeably. In QED, this is no longer true, as we have explicitly seen in Eqs. (1.123) and (1.122) above.

Interestingly, in the conservative sector of GR at $\mathcal{O}(G^4)$, dimensional analysis and explicit computation exposed a $1/m$ singularity [59] whose fate is unclear once radiation effects will ultimately be taken into account. Ref. [59] speculated that the $1/m$ is canceled by radiative contributions similar to the cancellation of the $\log m$ at $\mathcal{O}(G^3)$; however, it is also possible that this term remains and merely signals the breakdown of the classical approximation which requires that $m^2 \gg |q|^2$. As such, QED seems to be an ideal toy example that exposes these features already at lower-loop order than gravity which is a consequence of the different mass dimensions of the electromagnetic (α) and gravitational (G) coupling constants. An explicit investigation of this aspect in gravity is an interesting open problem.

1.4.3 Radiative impulse, energy loss, and scattering angle via KMOC

Besides the eikonal analysis of the previous subsection, we have furthermore analyzed the classical two-loop scalar QED observables in the KMOC framework in complete analogy to the gravitational case that has been obtained by two of the authors [47]. Due to the linearity of QED, the present analysis is a lot simpler due to the limited number of diagrams appearing in the computation. In fact, we were able to use exactly the same analysis pipeline from before, just substituting in the new QED integrands from section 1.2.2.

We first assemble all relevant terms for the transverse part of the impulse, which receives both *virtual* and *real* contributions according to (1.45). Now that we are in the soft region, we do have situations where internal photons are allowed to go on-shell, so that we have to both consider two- and three-particle cuts at $\mathcal{O}(\alpha^3)$ to find

$$\Delta p^{\mu}_{1,\perp} = \frac{(\alpha q_1 q_2)^3}{m_1 m_2}\left[\frac{8\sigma^2 \text{arcsinh}\sqrt{\frac{\sigma-1}{2}}}{(\sigma^2-1)^{5/2}} - \frac{4\sigma^3}{(\sigma^2-1)^2} + \frac{2\left(2m_1 m_2\left(\sigma^4-\sigma^2+1\right)+\left(m_1^2+m_2^2\right)\sigma\right)}{m_1 m_2\left(\sigma^2-1\right)^{5/2}}\right]\frac{b^\mu}{|b|^4}$$
$$+ \alpha^3 q_1^2 q_2^2 \frac{4\sigma^2\left(m_2^2 q_1^2 + m_1^2 q_2^2\right)}{3m_1^2 m_2^2\left(\sigma^2-1\right)}\frac{b^\mu}{|b|^4}\,. \tag{1.129}$$

In comparison to the conservative sector, we now have two different charge sectors, the one with $(q_1 q_2)^3$ dependence and the other with $q_i^2 q_j^4$. In QED, these sectors are independently gauge-invariant and do not interfer. This is distinct from the gravitational setting, where all results were proportional to G^3 which can be roughly understood from a double-copy point of view where the charges in gauge theory q_i get replaced by the gravitational charges, i.e. the masses m_i. Unlike in the conservative sector, now the $\text{arcsinh}\sqrt{\frac{\sigma-1}{2}}$ appears, but is not proportional to any leading power of σ so that the ultrarelativistic limit is well-behaved. From the above result, we can subtract the conservative contribution to single out the radiative part of the impulse

$$\Delta p_{1,\perp}^{\mu,\text{rad.}} = \frac{\alpha^3 q_1^2 q_2^2}{m_1 m_2} \frac{b^\mu}{|b|^4} \left[q_1 q_2 \left(\frac{8\sigma^2 \text{arcsinh}\sqrt{\frac{\sigma-1}{2}}}{(\sigma^2-1)^{5/2}} - \frac{4\sigma^3}{(\sigma^2-1)^2} \right) + \frac{4\sigma^2 \left(m_2^2 q_1^2 + m_1^2 q_2^2\right)}{3 m_1 m_2 (\sigma^2-1)} \right] . \tag{1.130}$$

From the radiative transverse impulse, one can extract the radiative correction to the scattering angle [47, 99] which equally splits into different charge sectors

$$\chi_{\text{rad}}^{(2)} = \alpha^3 q_1^2 q_2^2 \frac{4\sigma^2 \left[3 m_1 m_2 q_1 q_2 \left(2\text{arcsinh}\sqrt{\frac{\sigma-1}{2}} - \sigma\sqrt{\sigma^2-1} \right) + \left(m_2^2 q_1^2 + m_1^2 q_2^2\right) (\sigma^2-1)^{\frac{3}{2}} \right]}{3 J^3 (\sigma^2-1)^{3/2} \left(m_1^2 + m_2^2 + 2 m_1 m_2 \sigma\right)} . \tag{1.131}$$

For the longitudinal part, we only give the additional contribution due to radiation effects. In order to obtain the full longitudinal part, one would have to add the conservative result from Eq. (1.88)

$$\begin{aligned} \Delta p_{1,u}^{\mu,\text{rad.}} = \frac{\alpha^3 q_1^2 q_2^2 \pi}{m_1 m_2 |b|^3} \check{u}_2^\mu \Bigg[& q_1 q_2 \frac{(3\sigma^3 - 4\sigma^2 + 9\sigma - 4)(\sigma^2-1) - 2(3\sigma^2+1)\sqrt{\sigma^2-1}\,\text{arcsinh}\sqrt{\frac{\sigma-1}{2}}}{4(\sigma^2-1)^{5/2}} \\ & - \frac{(3\sigma^2+1)\left(m_2^2 \sigma\, q_1^2 + m_1^2\, q_2^2\right)}{12 m_1 m_2 \sqrt{\sigma^2-1}} \Bigg] , \end{aligned} \tag{1.132}$$

where the radiative part of the momentum change on particle 1 is purely in the direction of $\check{u}_2^\mu$. We now can compute the radiated momentum in the scattering of two charged scalars in QED in two different ways. First, we simply take the impulse on particle 1 plus the impulse on particle 2 (which can be obtained from the above results by simple relabeling) together with momentum conservation $\Delta p_1^\mu + \Delta p_2^\mu + \Delta R^\mu = 0$. Alternatively, we can directly compute the radiated momentum from KMOC, see Eq. (1.47) to find

$$\begin{aligned} \Delta R^\mu = \frac{\alpha^3 q_1^2 q_2^2 \pi}{|b|^3} \Bigg[& \frac{q_1 q_2}{m_1 m_2} \frac{u_1^\mu + u_2^\mu}{\sigma+1} \left\{ \frac{2(3\sigma^2+1)\,\text{arcsinh}\sqrt{\frac{\sigma-1}{2}} - \sqrt{\sigma^2-1}\,(3\sigma^3 - 4\sigma^2 + 9\sigma - 4)}{4(\sigma^2-1)^2} \right\} \\ & + \frac{(3\sigma^2+1)\left(m_2^2 q_1^2 u_1^\mu + m_1^2 q_2^2 u_2^\mu\right)}{12 m_1^2 m_2^2 \sqrt{\sigma^2-1}} \Bigg] , \end{aligned} \tag{1.133}$$

which points entirely along the longitudinal directions u_1^μ and u_2^μ with appropriate strength proportional to the charge-to-mass ratios q_i/m_i of the scattering particles. In comparison to the GR results obtained previously [46], where the masses are always positive, the electric charges can change sign. For the $q_1^3 q_2^2$ charge sector, this implies that the contribution to the radiated energy can be positive or negative. However, the combined energy loss e.g. in the center-of-mass system

$$\Delta E_{\text{c.m}} = \Delta R \cdot (u_1 + u_2)\,, \tag{1.134}$$

is numerically positive for arbitrary values of the charge q_1/q_2 and mass m_1/m_2 ratios.

1.4.4 Radiative radial action

For completeness, we give the explicit results for the *soft radial action* for which we found an empirical shortcut in terms of explicit subtractions of master integrals that has been described in section 1.2.4. Upon Fourier-transforming to impact-parameter space b, the two-loop soft radial action is

$$\begin{aligned} I_r^{(2)}(J,\sigma) = {} & \frac{(\alpha q_1 q_2)^3}{3J^2\left(\sigma^2-1\right)^{3/2}\left(m_1^2+m_2^2+2m_1m_2\sigma\right)}\Bigg[\left(m_1^2+m_2^2\right)\sigma\left(2\sigma^2-3\right) \\ & - 2m_1m_2\left\{3+\left(\sigma^2-3\sigma\sqrt{\sigma^2-1}-3\right)\sigma^2+6\sigma^2\operatorname{arcsinh}\sqrt{\frac{\sigma-1}{2}}\right\}\Bigg] \\ & -\frac{2\alpha^3 q_1^2 q_2^2\ \sigma^2\left(m_2^2 q_1^2+m_1^2 q_2^2\right)}{3J^2\left(m_1^2+m_2^2+2m_1m_2\sigma\right)}\,, \end{aligned} \tag{1.135}$$

from which we find the scattering angle

$$\chi^{(2)} = \frac{\partial I_r^{(2)}(J,\sigma)}{\partial J}\,, \tag{1.136}$$

which exactly agrees with our eikonal result in Eq. (1.113) and the ones that can be obtained from the impulse via the KMOC setup. At this point, our prescription for the modification of the boundary conditions for the soft master integrals was inspired by an analogous procedure in the conservative sector and it would be interesting to understand this method more systematically so that it can be applied at higher orders. It would be very interesting to find a direct computational method for the phase of the S-matrix in the representation of Ref. [102] and the relation to the velocity cuts of Ref. [149] as well as the heavy-particle effective theory implementation of related ideas of Ref. [150].

1.5 Conclusions

In this chapter we applied scattering amplitude techniques to study the classical two-body scattering problem in scalar electrodynamics in a regime similar to the post-Minkowskian expansion of general relativity. Scalar QED has many similarities to GR, except that it is far simpler because the underlying interactions are linear, making it useful as a toy model of the gravitational problem [33, 140]. The recent calculation of the scattering angle through $\mathcal{O}(\alpha^3)$, including radiative effects, by iteratively solving the classical equations of motion [99] motivated the computation of the corresponding results from amplitudes based approaches. We derived the classical scattering angle from both the eikonal phase [104] of the amplitude, and from the KMOC formalism [39]. We also noted a simplified computation of the radial action including radiative effects. The 'soft radial action' was obtained by a change in the boundary conditions of the differential equations for the soft master integrals. This automatically removes classically singular iterations and directly yields the radial action (including radiative contributions) up to two-loop order from which we obtain the classical scattering angle. All three approaches give the same scattering angle which furthermore agrees with the one found by solving the classical equations of motion [99].

An interesting feature of the scattering angle in QED is that, at $\mathcal{O}(\alpha^3)$, it contains factors of $1/m_i$ which are singular for $m_i \to 0$, despite having included both conservative and radiative effects consistently. Of course, this region is outside the validity of our setup since it violates the classical requirement that the Compton wavelength is smaller than the inter-particle separation. Translated to momentum space this amounts to the classical hierarchy of scales $-q^2 \ll m_i^2$ where the masses are larger than the momentum transfer which is violated for $m_i \to 0$. The same breakdown of the approximation was found in Ref. [99], where it was tied to terms generated via the ALD force [141–143]. In the classical setup, the ALD force has to be added 'by hand' to account for radiation loss during the scattering event. In contrast, in amplitudes-based frameworks, the radiation loss is taken into account automatically and is on an equal footing with other terms in the amplitudes. The appearance of the mass singularities in QED may be contrasted with the corresponding $\mathcal{O}(G^3)$ scattering angle in GR: once radiative effects are included the mass singularity cancels [138, 139]. On the other hand, at $\mathcal{O}(G^4)$ the pure potential contributions to the scattering angle contain a $1/m$ singularity [59]. Our results for the electrodynamics suggest that these may not cancel even after including gravitational radiation.

Following Refs. [96, 97, 99, 101] many physical observables can be analytically continued from the scattering problem to the bound-state problem. In particular, the scattering angle is directly tied to the periastron advance. In gravity, at $\mathcal{O}(G^4)$ this is greatly complicated by the nonlocal-in-time tail effect [92, 93, 95, 101, 104]. Since the tail effect arises from gravitational radiation interacting with potential gravitons (due to nonlinear graviton couplings in GR), electrodynamics should be immune from this complication, given that photons do not self interact classically in the absence of nonlinear higher derivative corrections to QED.

In summary, we expect electrodynamics to continue to serve as a useful toy model for the classical gravitational binary dynamics.

CHAPTER 2

The Eikonal Phase and Spinning Observables

2.1 Introduction

Now we will move on to incorporating spin to the calculation. In this chapter we will focus on the one-loop calculation of the impulse and spin kick observables up to linear order in spin. This will familiarize us with the complications spin brings to amplitudes calculations and it may affect things at higher orders.

Including spin in the scattering observable calculations has been a rich topic in the PM and PL expansions; calculations have been performed for the impulse and the spin kick using fixed spin states [40, 156–158], and worldline QFT [159–163]. More recently, work has been done in including spin to waveform, memory effect, and radiation calculations [164–169]. For including spin in the impulse and the spin kick, much progress has been made in performing these calculations using general spin QFT [121, 122, 170]. Traditionally, massive higher spin [171–176] requires the inclusion of lower spin auxiliary fields to eliminate nonphysical degrees of freedom; however, these introduce complicated propagator structures. The general spin QFT avoids the complicated propagator structure by using unconstrained, non-transverse fields that are spin-s representations of the Lorentz group; however, multiple spins can propagate with allowed transitions.

An interesting puzzle that arises in general spin QFT when multiple spins can propagate with allowed transitions is that extra independent Wilson coefficients appear in the derived physical results [177]. Ref. [170] showed that at least in the context of electrodynamics similar extra Wilson coefficients are obtained using a worldline formalism without a spin supplementary condition imposed. Here we confirm these results using the KMOC formalism.

The study of spinning amplitudes and their observables has also provided a greater understanding to some underlying structures in two-body scattering. In Refs. [50, 121, 122, 170], it has been shown that there is a direct link between spinning scattering observables and the eikonal phase. While in Refs. [121, 122] such a formula was found for the impulse and spin vector impulse via ansatz, Ref. [50] has found a way to partially derive these formulae by directly working with the eikonal phase in the KMOC formalism. This has since left a mystery about how the complete formula in Refs. [121, 122], especially the $D_L(f, g)$ terms, could be derived.

In this chapter, we will calculate the impulse Δp^μ and the spin kick $\Delta S^{\mu\nu}$ of a spinning body scattering off a non-spinning body to one loop, linear-in-spin order. We propose a procedure using the non-transverse properties of general spin fields in KMOC, which will allow us to derive a formula relating the eikonal phase of general spin amplitudes to their classical observables, including $D_L(f, g)$-like terms. To verify our results we will plug in amplitudes for general spin field theory coupled to electrodynamics and compare to Ref. [170], which we match when taking in to account differences in convention. Throughout the chapter we will be using the mostly minus metric signature.

2.2 Review

2.2.1 The Classical Scaling with Spin

We will be taking the classical limit of two-body scattering of particles mediated by electrodynamics separated by impact parameter b with charge eq_i, momentum p_i, mass m_i and spin S_i. In electrodynamics, the classical limit implies a hierarchy between the particle Compton wavelength, $\lambda_{c_i} = \hbar/m_i c$, and the classical charge radius, $r_{Q_i} = e^2 q_i^2/4\pi m_i$; namely, $\lambda_{c_i} \ll r_{Q_i}$, which corresponds to the large charge limit in QED [39, 178]. We will also be performing the Post-Lorentzian (PL) expansion, whose expansion parameter $r_{Q_i}/b \ll 1$, amounts to a large separation limit. Performed together, the classical limit and PL expansion gives us the following hierarchy of length scales

$$\lambda_{c_i} \ll r_{Q_i} \ll b. \tag{2.1}$$

For scattering amplitudes, it is more natural to consider the above hierarchy in momentum space. In two-body scattering the momentum transfer q is the conjugate variable to the impact parameter b,

$$|b| \sim \frac{1}{|q|} \gg \frac{1}{m_i}, \tag{2.2}$$

which implies

$$|q| \ll m_i \sim |p_i|, \tag{2.3}$$

where p is some external four-momentum with natural units $\hbar = c = 1$. We also know, for two-body classical systems, the angular momentum can be expressed as

$$|J_i| \equiv |p_i||b| \gg 1. \tag{2.4}$$

We make the same assumption as Ref. [121] for the magnitudes of the spin and angular momentum, $|J_i| \sim |S_i|$. The above is summarized in the following scaling,

$$p \to \lambda^0 p, \qquad q \to \lambda q, \qquad b \to \lambda^{-1} b, \qquad S \to \lambda^{-1} S, \tag{2.5}$$

where $\lambda \ll 1$, which helps us organize the classical limit.

2.2.2 Definition of Spin

We follow Refs. [121, 122, 170], and model the massive scattering bodies with complex general spin-s fields $\Phi_s^{\mu_1 \cdots \mu_s} = \Phi_s^{\mu(s)}$, where we choose $s \in \mathbb{Z}^{0+}$. These fields are symmetric and traceless but not transverse; therefore we do not need to include lower-spin auxiliary fields, such as those in Refs. [171–173]. As a result, from the rank-s polarization tensors associated with the non-transverse fields, we construct the following completeness relation

$$\delta^{\mu(s)}_{\ \nu(s)} = \sum_a \epsilon_a^{\mu(s)}(p)\epsilon^{*\,a}_{\nu(s)}(p), \tag{2.6}$$

where we sum over the little group indices a.

We use the spin tensor, which we define as

$$[S^{\mu\nu}(p)]^{a'}_{\ a} \equiv \epsilon^{*\,a'}_{\alpha(s)}(p)\,(M^{\mu\nu})^{\alpha(s)}_{\ \ \beta(s)}\,\epsilon_a^{\beta(s)}(p), \tag{2.7}$$

where $(M^{\mu\nu})^{\alpha(s)}_{\ \ \beta(s)}$ is the spin-s representation of the Lorentz generator

$$(M^{\mu\nu})^{\alpha(s)}_{\ \ \beta(s)} = is\,\delta^{[\mu}_{(\beta_1}\eta^{\nu](\alpha_1}\delta^{\alpha_2}_{\beta_2}\cdots\delta^{\alpha_s)}_{\beta_s)}, \tag{2.8}$$

satisfying the Lorentz algebra

$$[M^{\mu\nu}, M^{\rho\sigma}] = -i\left(\eta^{\mu\rho}M^{\sigma\nu} + \eta^{\nu\rho}M^{\mu\sigma} - \eta^{\mu\sigma}M^{\rho\nu} - \eta^{\nu\sigma}M^{\mu\rho}\right). \tag{2.9}$$

Note that because we have constructed the spin tensor from our unconstrained polarization tensors, the spin tensor does not necessarily obey the covariant spin supplementary condition (SSC), $p_\mu S^{\mu\nu}(p) = 0$ [170]. We relax the SSC in order to include boost degrees of freedom in the spin tensor, as in Ref. [170], although these can be set to zero at any point.

2.2.3 Basics of Observable Impulses

We now review the methods covered in Refs. [39, 47] to arrive at different observable impulses. However, we will now include the spin modifications that were first introduced in Ref. [40]. First, we measure the expectation value of some quantum operator $\mathbb{O}$ from the asymptotic past ("in") to the asymptotic future ("out") and take the difference; this results in an impulse of some corresponding observable $\mathcal{O}$,

$$\Delta\mathcal{O} = \langle \text{out}|\mathbb{O}|\text{out}\rangle - \langle \text{in}|\mathbb{O}|\text{in}\rangle. \tag{2.10}$$

We then relate these out-states to in-states by the S matrix, $S = 1 + iT$. We model our in-state by some N-particle wavepacket $|\Psi\rangle$, which depends on scalar wavefunctions $\phi(p_i)$, little group dependent parts of the wavefunction ξ_{a_i}, and momentum eigenstates $|p_i; a_i\rangle$, where a_i are little group indices. Doing so gives a natural separation that has come to be known as the "virtual" and "real" part of the impulse [39, 47]

$$\Delta\mathcal{O} = \langle\Psi|i[\mathbb{O}, T]|\Psi\rangle + \langle\Psi|T^\dagger[\mathbb{O}, T]|\Psi\rangle, \tag{2.11}$$

where

$$|\Psi\rangle = \bigotimes_{i=1}^{N} \sum_{a_i} \frac{1}{N!} \int d\Phi(p_i)\, \phi(p_i)\, \xi^{a_i}\, e^{ib_i\cdot p_i}\, |p_i; a_i\rangle. \tag{2.12}$$

Here we write the integration over Lorentz invariant phase space as

$$\int d\Phi(p_i) \equiv \int \hat{d}^D p_i\, \hat{\delta}^{(+)}(p_i^2 - m_i^2), \tag{2.13}$$

where $D = 4 - 2\epsilon$, $\hat{d}^D p_i \equiv d^D p_i/(2\pi)^4$, and $\hat{\delta}^{(+)}(k^2 - m^2) \equiv 2\pi\delta^{(+)}(k^2 - m^2)$, which only takes into account positive energy states; in the future, we will drop the $(+)$ superscript on the δ-function, since in the classical limit we do not have to make this distinction. We also assume a displacement b_i for each single-particle wavepacket with respect to some arbitrary origin. We now fix ourselves to $N = 2$ body scattering, where we take

$$\frac{|p_1; a_1\rangle \otimes |p_2; a_2\rangle}{2!} = |p_1 p_2; a_1 a_2\rangle. \tag{2.14}$$

Now we can write the observable impulse for two-body scattering as

$$\Delta\mathcal{O} = \prod_{i=1}^{2} \sum_{a_i, a_i'} \int d\Phi(p_i)\, d\Phi(p_i')\, \phi^*(p_i')\phi(p_i)\, \xi^*_{a_i'}\, \xi^{a_i}\, e^{-ib_i\cdot(p_i'-p_i)}\, (\mathcal{I}_{v\ \{a_i\}}^{\{a_i'\}} + \mathcal{I}_{r\ \{a_i\}}^{\{a_i'\}}), \tag{2.15}$$

where

$$\mathcal{I}_{v\ \{a_i\}}^{\{a_i'\}} = \langle p_1' p_2'; a_1' a_2'|i[\mathbb{O}, T]|p_1 p_2; a_1 a_2\rangle, \quad \mathcal{I}_{r\ \{a_i\}}^{\{a_i'\}} = \langle p_1' p_2'; a_1' a_2'|T^\dagger[\mathbb{O}, T]|p_1 p_2; a_1 a_2\rangle, \tag{2.16}$$

are known as the virtual kernel and real kernel, respectively.

For simplicity, we consider only one of our scattering bodies to be spinning; therefore, we can neglect one of these bodies' little group information. Using these states, we define our two-body scattering amplitude as

$$\begin{aligned}\langle p_1'p_2';a_1'|T|p_1p_2;a_1\rangle &= \hat{\delta}^{(4)}(p_1'+p_2'-p_1-p_2)\,[\mathcal{A}(p_1,p_2,p_1',p_2',S_1)]^{a_1'}{}_{a_1}\\ &\equiv \hat{\delta}^{(4)}(p_1'+p_2'-p_1-p_2)\,\epsilon^{*\,a_1'}(p_1')\cdot\mathbb{A}(p_1,p_2,p_1',p_2')\cdot\epsilon_{a_1}(p_1),\end{aligned}\tag{2.17}$$

where in the last line we stripped the amplitude of its polarizations, allowing us to work with the Lorentz generator as opposed to the spin tensor; we also define $S^{\mu\nu}(p_1)\equiv S_1^{\mu\nu}$. We leave the summation over representation indices in the second line of Eq. (2.17) implicit.

We expand the amplitudes in powers of the coupling constant g and powers of spin,

$$\begin{aligned}\mathcal{A}(p_i,p_i',S_1) =& g^2\left(\mathcal{A}^{(1,0)}(p_i,p_i')+\mathcal{A}^{(1,1)}(p_i,p_i',S_1)+\cdots\right)\\ &+g^4\left(\mathcal{A}^{(2,0)}(p_i,p_i')+\mathcal{A}^{(2,1)}(p_i,p_i',S_1)+\cdots\right)+\cdots\end{aligned}\tag{2.18}$$

where, for $\mathcal{A}^{(i,j)}$, i tracks the powers of g^2 and j tracks the powers of the spin tensor. In the case of two-body scattering of general spin fields coupled to electrodynamics, we expand in $g^2=4\pi\alpha q_1q_2$, where $\alpha=e^2/4\pi$ is the QED fine structure constant. Note that our amplitude in the first line of Eq. (2.17) is a matrix with respect to the little group indices, which it inherits from its dependence on $S^{\mu\nu}$. When contracted with the $\xi^{a_i},\xi^*_{a_i'}$ and integrated over the initial momentum phase space, we arrive at the expectation value of the spin tensor

$$\int d\Phi(p_1)\sum_{a_1a_1'}\xi^*_{a_1'}\,\xi^{a_1}\,[S_1^{\mu\nu}]^{a_1'}{}_{a_1}=\langle S_1^{\mu\nu}\rangle.\tag{2.19}$$

We are only concerned with the classical limit of these impulses. Therefore, following the arguments of Refs. [39, 50, 156], these wavepackets sharply peak about their classical values, amounting to the appearance of on-shell δ-functions. Similarly, since we are taking the classical limit of quantum expectation values, we must take our states to be spin coherent states, i.e. they minimize the standard deviations of the spin degrees of freedom of the observables [121, 156]. As a result, we are allowed to simplify Eq. (2.15)

$$\Delta\mathcal{O}=\int \hat{d}^Dq\,\hat{\delta}(2p_1\cdot q)\,\hat{\delta}(2p_2\cdot q)\,e^{-ib\cdot q}\,\langle(\mathcal{I}_v+\mathcal{I}_r)\rangle\equiv\int \hat{\mathcal{D}}q\,e^{-ib\cdot q}\,(\mathcal{I}_v+\mathcal{I}_r),\tag{2.20}$$

where $q^\mu = p_1'^\mu - p_1^\mu$ is the small momentum transfer conjugate to the impact parameter $b^\mu = b_2^\mu - b_1^\mu$, and we have absorbed the δ-functions into the measure via the $\not{D}$ notation. We will leave the expectation value brackets implicit. It should be emphasized that the amplitudes, $\mathcal{A}$ or $\mathbb{A}$, spin tensor $S^{\mu\nu}$, and Lorentz generator $M^{\mu\nu}$ are matrix valued in their respective representation indices; in the case of $\mathcal{A}$ and $S^{\mu\nu}$, these are the little group indices a_i, a_i'; for $\mathbb{A}$ and $M^{\mu\nu}$, these are the Lorentz group representation indices $\alpha(s)$.

We will be calculating both the impulse Δp^μ and the spin kick $\Delta S^{\mu\nu}$ to linear order in spin and next to leading order in the coupling constant; therefore, we need to consider the corresponding operators $\mathbb{P}^\mu$ and $\mathbb{S}^{\mu\nu}$, respectively, and their expectation values.

2.2.4 Impulse Set Up

Starting with the easier case, we consider the impulse. The following treatment was presented in Refs. [39, 40, 47, 50, 156] for the scalar and fixed spin cases; however, we are working with general spin fields and therefore some new nuances need to be considered.

First, we consider the virtual kernel of the impulse,

$$\begin{aligned}\langle\Psi|i[\mathbb{P}^\mu, T]|\Psi\rangle = \int \not{D}q\, e^{-ib\cdot q}\, \mathcal{I}_v^\mu &= \int \not{D}q\, e^{-ib\cdot q}\, iq^\mu\, \epsilon^*(p_1+q)\cdot\mathbb{A}(p_1,p_2,q)\cdot\epsilon(p_1) \\ &= \int \not{D}q\, e^{-ib\cdot q}\, iq^\mu\, \epsilon^*(p_1+q)\cdot\epsilon(p_1)\,\mathcal{A}(p_1,p_2,S_1),\end{aligned} \quad (2.21)$$

where we insert a complete set of states, Eq. (2.6), on either side of the polarization stripped amplitude to arrive at the last line. The product of polarizations in the second line of Eq. (2.21) can be re-expressed as an exponential

$$\epsilon^*(p_1+q)\cdot\epsilon(p_1) = \exp\left(iq_\mu \frac{S_1^{\mu\nu}(k_\nu + p_{1\,\nu})}{p_1\cdot k + m_1^2}\right) = \exp(iq\cdot\omega), \quad (2.22)$$

where k is some arbitrary reference frame from which one boosts from to arrive at either momentum p_1 or p_1+q; in our case, it is the rest frame of the mass m_1 body. A derivation can be found in Appendix B as well as in Refs. [116, 170]. This naturally leads us to introduce a new conjugate variable to q, which we call the covariant impact parameter [121, 122]

$$b^\mu_{\rm cov} = b^\mu - \omega^\mu = b^\mu - \frac{S_1^{\mu\nu}(k_\nu + p_{1\,\nu})}{p_1\cdot k + m_1^2}. \tag{2.23}$$

This leaves us with the all orders in spin and coupling constant result

$$\langle \Psi | i[\mathbb{P}^\mu, T] | \Psi \rangle = \int \not{D}q \, e^{-ib_{\rm cov}\cdot q} \, iq^\mu \, \mathcal{A}(p_1, p_2, S_1). \tag{2.24}$$

Now we consider the real kernel of the impulse,

$$\int \not{D}q \, e^{-ib\cdot q} \, \mathcal{I}_r^\mu = \langle \Psi | T^\dagger [\mathbb{P}_1^\mu, T] | \Psi \rangle = \bigotimes_i^N \int \frac{d\rho_i}{N!} \langle \Psi | T^\dagger | \rho_i \rangle \langle \rho_i | [\mathbb{P}_1^\mu, T] | \Psi \rangle, \tag{2.25}$$

where we inserted some complete set of states ρ_i. By choosing the content of our complete set of states, we automatically fix the order in the coupling constant g to which we can calculate. By virtue of the external states, we must insert a minimum of one massive state per matter line so as to preserve the mass content. In principle, we can insert additional massless states but this leads to higher-order contributions in g, which we are not concerned with in this chapter. Choosing the minimal complete set of states fixes us to the next to leading order in g real kernel for the impulse

$$\begin{aligned}
\mathcal{I}_r^{(2)\,\mu} &= \int \not{D}l \, l^\mu \, \epsilon^*(p_1+q) \cdot \mathbb{A}^{(1)}(q-l, p_1+l, p_2-l) \cdot \mathbb{A}^{(1)}(l, p_1, p_2) \cdot \epsilon(p_1) \\
&= e^{iq\cdot\omega} \int \not{D}l \, l^\mu \, \mathcal{A}^{(1)}(q-l, p_1+l, p_2-l, S_1) \, \mathcal{A}^{(1)}(l, p_1, p_2, S_1) \\
&= \int \hat{d}^D l \; l^\mu \, \epsilon^*(p_1+q) \cdot \text{[cut diagram]} \cdot \epsilon(p_1),
\end{aligned} \tag{2.26}$$

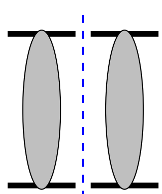

where l^μ is the loop momentum. In the last line, we relate the real kernel to the two-particle unitarity cut of the polarization stripped one loop amplitude, which replaces the cut momentum with on-shell δ-functions; in fact, the same ones that are in the definition of $\not{D}l$.

From Eq. (2.26), we can expand in orders of the spin tensor. Naively, one might expect for $\mathcal{I}_r^{(2,1)\,\mu}$ one would only need linear-in-spin combinations of the amplitudes in Eq. (2.26). However, one can decompose any product of Lorentz generators into combinations of symmetric and anti-symmetric products; in fact, one can always construct a completely antisymmetric product, which reduces to be linear in $M^{\mu\nu}$. For example, in the case of a quadratic product

$$M^{\mu\nu}M^{\rho\sigma} = \frac{1}{2}\{M^{\mu\nu}, M^{\rho\sigma}\} + \frac{1}{2}[M^{\mu\nu}, M^{\rho\sigma}], \tag{2.27}$$

where the curly braces are an anti-commutator and the last term, by virtue of the Lorentz algebra, is linear in the Lorentz generator. At the level of the spin tensor one can summarize this in the following spin counting

$$S^{\mu\nu} \sim \mathcal{O}(s), \qquad [\quad,\quad] \sim \mathcal{O}(s^{-1}), \qquad \{\quad,\quad\} \sim \mathcal{O}(1), \tag{2.28}$$

where s is some spin counting parameter. Fixing ourselves to linear order in spin, we express the real kernel for the impulse as

$$\begin{aligned}\mathcal{I}_r^{(2,1)\,\mu} = \\ e^{iq\cdot\omega}\int \hat{d}l\, l^\mu \big(&\mathcal{A}^{(1,0)}(q-l)\mathcal{A}^{(1,1)}(l,p_1,p_2,S_1) + \mathcal{A}^{(1,1)}(q-l,p_1+l,p_2-l,S_1)\mathcal{A}^{(1,0)}(l) \\ &+ \frac{1}{2}\left[\mathcal{A}^{(1,1)}(q-l,p_1+l,p_2-l,S_1), \mathcal{A}^{(1,1)}(l,p_1,p_2,S_1)\right]\Big).\end{aligned} \tag{2.29}$$

2.2.5 Spin Kick Set Up

Whereas the momentum operator was easy to work with because we are using momentum eigenstates, the spin operator expectation value is more complicated

$$\langle p'; a'|\mathbb{S}^{\mu\nu}|p; a\rangle = -\frac{1}{2}\,\hat{\delta}_\Phi(p'-p)\,\epsilon^{*\,a'}(p')\cdot M^{\mu\nu}\cdot\epsilon_a(p), \tag{2.30}$$

where $\hat{\delta}_\Phi(p'-p)$ is the δ-function for the Lorentz invariant phase space integral such that $\int d\Phi(p)\, f(p)\,\hat{\delta}_\Phi(p'-p) = f(p')$. A derivation for Eq. (2.30) can be found in Appendix A.

Plugging in Eq. (2.30) to the virtual kernel we get

$$\begin{aligned}\langle\Psi|i[\mathbb{S}_1^{\mu\nu}, T]|\Psi\rangle = \int \hat{d}q\, e^{-ib\cdot q}\,\mathcal{I}_v^{\mu\nu} &= \frac{i}{2}\int \hat{d}q\, e^{-ib\cdot q}\,\epsilon^*(p_1+q)\cdot[\mathbb{A}(q,p_1,p_2), M^{\mu\nu}]\cdot\epsilon(p_1) \\ &= \frac{i}{2}\int \hat{d}q\, e^{-ib_{\rm cov}\cdot q}\,\left[\mathcal{A}(q,p_1,p_2,S_1), S^{\mu\nu}(p_1)\right].\end{aligned} \tag{2.31}$$

For the real kernel at next to leading order in the coupling constant to all orders in spin

$$\mathcal{I}_r^{(2)\,\mu\nu} = \frac{1}{2}\int \hat{D}l\, \epsilon^*(p_1+q)\cdot \mathbb{A}^{(1)}(q-l,p_1+l,p_2-l)\cdot \left[\mathbb{A}^{(1)}(l,p_1,p_2), M^{\mu\nu}\right]\cdot \epsilon(p_1)$$
$$= \frac{e^{iq\cdot\omega}}{2}\int \hat{D}l\, \mathcal{A}^{(1)}(q-l,p_1+l,p_2-l,S_1)\left[\mathcal{A}^{(1)}(l,p_1,p_2,S_1), S_1^{\mu\nu}\right], \tag{2.32}$$

where if we use the spin scaling in Eq. (2.28) and expand to linear order in spin counting s,

$$\mathcal{I}_r^{(2,1)\,\mu\nu} = \frac{e^{iq\cdot\omega}}{2}\int \hat{D}l \Big(\mathcal{A}^{(1,0)}(q-l)\left[\mathcal{A}^{(1,1)}(l,p_1,p_2), S_1^{\mu\nu}\right]$$
$$+\frac{1}{2}\left[\mathcal{A}^{(1,1)}(q-l,p_1+l,p_2-l,S_1), \left[\mathcal{A}^{(1,1)}(l,p_1,p_2,S_1), S_1^{\mu\nu}\right]\right]\Big). \tag{2.33}$$

Before we move on to deriving the eikonal formulae for the impulse and the spin kick, we must first consider some properties of general spin amplitudes.

2.3 General Spin Amplitudes

We use general spin fields whose specifics beyond their non-transversality are not important for our derivation. For the derivation of the eikonal formula, we will keep our amplitudes general and grounded on minimal assumptions.

To verify our results, we use the following Lagrangian density from Ref. [170],

$$\mathcal{L} = \mathcal{L}_{\text{min}} + \mathcal{L}_{\text{EM}} + \sum_i \mathcal{L}^{(i)}_{\text{non-min}}, \tag{2.34}$$

where the sum is over powers of the Lorentz generator. In this chapter we expand only to leading order in powers of the Lorentz generator

$$\mathcal{L}_{\text{min}} = (D^\mu\Phi_s)^\dagger\, D_\mu\Phi_s - m^2\,\Phi_s^\dagger\,\Phi_s, \tag{2.35}$$

$$\mathcal{L}_{\text{EM}} = -\frac{1}{4}F^{\mu\nu}F_{\mu\nu}, \tag{2.36}$$

$$\mathcal{L}^{(1)}_{\text{non-min}} = C_1 F_{\mu\nu}\,\Phi_s^\dagger\,\mathbb{M}^{\mu\nu}\,\Phi_s + \frac{D_1}{m^2}\,F_{\mu\nu}\,\left((D_\rho\Phi_s)^\dagger\,\mathbb{M}^{\rho\mu}\,D^\nu\Phi_s + (D^\nu\Phi_s)^\dagger\,\mathbb{M}^{\rho\mu}\,D_\rho\Phi_s\right), \tag{2.37}$$

where

$$D^\mu\Phi_s = \partial^\mu\Phi_s - i\sqrt{4\pi\alpha}\,qA^\mu\Phi_s, \quad F_{\mu\nu} = 2\,\partial_{[\mu}A_{\nu]}, \tag{2.38}$$

Φ_s are the general spin fields, C_1 and D_1 are free parameters that, in principle, depend on macroscopic properties of the scattering bodies. In the usual worldline construction [179–183], where a spin supplementary condition is imposed, only the analog of the C_1 coefficients appears. D_1 is an example of an "extra Wilson coefficient" that appears when no SSC is imposed on the worldline, or when multiple spin states with allowed transitions propagate on field theory, as we allow here. Summations over representation indices of the fields and the Lorentz generators are left implicit. We are not including lower spin auxiliary fields to Φ_s, meaning we do not have transverse fields and therefore we are able to construct a simple completeness relation as in Eq. (2.6).

We take the classical limit of two-body, general spin scattering amplitudes by using the scaling in Eq. (2.5) and expanding in the $\lambda \to 0$ limit. We also demand that we are calculating the long-range contributions of these amplitudes, which amounts to the omission of any term that may cancel any massless exchange propagators in the two-body amplitude. To facilitate taking the classical limit of amplitudes, we use special variables [47, 76, 178]

$$\bar{p}_1 = p_1 + q/2 \qquad \bar{p}_2 = p_2 - q/2 \qquad y = \frac{\bar{p}_1 \cdot \bar{p}_2}{\bar{m}_1 \bar{m}_2} = \bar{u}_1 \cdot \bar{u}_2 \qquad \bar{m}_i^2 = \bar{p}_i^2 = m_i^2 - q^2/4, \quad (2.39)$$

where $\bar{u}_i = \bar{p}_i/\bar{m}_i$; this simplifies the scale counting of our calculation by making $\bar{u}_i \cdot q = 0$.

2.3.1 Tree Level

At tree level, we expect the the classical limit of the scalar amplitude to be of the form

$$\mathbb{A}^{(1,0)}(q) = \frac{\mathcal{N}^{(1,0)}}{q^2} \sim \mathcal{O}(\lambda^{-2}), \quad (2.40)$$

where, for Eq. (2.34), $\mathcal{N}^{(1,0)} = 4y\bar{m}_1\bar{m}_2$. Note that the numerator is taken to be a constant and therefore the amplitude only has a dependence on the momentum transfer q.

For the linear-in-spin tree amplitude, we have a more complicated structure. We expect the same propagator structure as in the scalar case, however we can have the following monomials in the numerator

$$\bar{u}_{1\,\mu}M^{\mu\nu}q_{\nu}, \qquad \bar{u}_{2\,\mu}M^{\mu\nu}q_{\nu}, \qquad \bar{u}_{1\,\mu}M^{\mu\nu}\bar{u}_{2\,\nu}. \tag{2.41}$$

If we expect all tree level amplitudes to scale classically i.e. $\mathcal{O}(\lambda^{-2})$ and if we require only long-range contributions, then only the first two monomials contribute to our amplitudes. With this in mind, we write our amplitude as

$$\mathbb{A}^{(1,1)}(q,\bar{u}_1,\bar{u}_2) = \frac{iq_{\nu}M^{\mu\nu}\left(c_1\bar{u}_{1\,\mu} + c_2\bar{u}_{2\,\mu}\right)}{q^2} \equiv \frac{iq_{\nu}M^{\mu\nu}\mathcal{N}^{(1,1)}_{\mu}(\bar{u}_1,\bar{u_2})}{q^2}, \tag{2.42}$$

where we have assumed that the Lorentz generator scales the same way as the spin tensor since they are simply related by Eq. (2.7).

2.3.2 One Loop

As has been shown in Refs. [170, 178, 184], when calculating the classical limit of the two-body, one loop amplitude using the soft expansion, it is possible to separate contributions into box diagram and triangle diagram contributions

$$\mathcal{A}^{(2)} = c_{\Delta}I_{\Delta} + c_{\nabla}I_{\nabla} + d_{\mathrm{B}}(I_{\mathrm{B}} + I_{\mathrm{xB}}) + \cdots\,. \tag{2.43}$$

The associated integrals are the following

$$I_{\mathrm{B}} = \int \hat{d}^D l \frac{1}{l^2(q-l)^2(2\bar{u}_1\cdot l + i0)(-2\bar{u}_2\cdot l + i0)} \sim \mathcal{O}(\lambda^{-2}), \tag{2.44}$$

$$I_{\mathrm{xB}} = \int \hat{d}^D l \frac{1}{l^2(q-l)^2(2\bar{u}_1\cdot l + i0)(2\bar{u}_2\cdot l + i0)} \sim \mathcal{O}(\lambda^{-2}), \tag{2.45}$$

$$I_{\Delta} = \int \hat{d}^D l \frac{1}{l^2(q-l)^2(2\bar{u}_1\cdot l + i0)} \sim \mathcal{O}(\lambda^{-1}), \tag{2.46}$$

$$I_{\nabla} = \int \hat{d}^D l \frac{1}{l^2(q-l)^2(-2\bar{u}_2\cdot l + i0)} \sim \mathcal{O}(\lambda^{-1}), \tag{2.47}$$

where we see two different scalings for the same amplitude. The triangle contributions have the expected one loop classical scaling, $\mathcal{O}(\lambda^{-1})$. On the other hand, the box integral terms scale lower than the expected classical scaling; this is known as super-classical or classically singular scaling [39, 47, 178].

The classically singular parts of the one loop amplitude, $\mathcal{O}(\lambda^{-2})$, carry an infrared divergence that cancels non-trivially when calculating observables. Therefore, it is convenient to systematically separate classically singular and classical terms in the one loop amplitude. We do this by separating the one loop amplitude into real and imaginary parts

$$\mathcal{A}^{(2)} = \mathrm{Re}\,\mathcal{A}^{(2)} + i\,\mathrm{Im}\,\mathcal{A}^{(2)}, \tag{2.48}$$

and using unitarity,

$2\,\mathrm{Im}$ 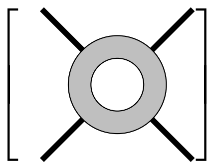 $= \int d\Phi_2$ 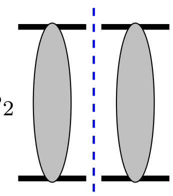 , (2.49)

where the dashed lines signal unitarity cuts along the massive propagators and the integration is over the complete set of states inserted between the two tree level amplitudes. It can be shown that the combination of classically singular terms in Eq. (2.43) is contained in the imaginary part of the one loop amplitude, therefore the real part is the combination of classical terms i.e. the triangle contributions. In the case of scalar particles, the imaginary part is exactly the classically singular term; the situation is less straightforward when we introduce spin.

We now consider $\mathrm{Im}\,\mathbb{A}^{(2,1)}$ explicitly

$$\begin{aligned} &2\,\mathrm{Im}\,\mathbb{A}^{(2,1)}(q,p_1,p_2) \\ &\quad= \int \hat{d}l\, \Big(\mathbb{A}^{(1,1)}(q-l,p_1+l,p_1-l)\mathbb{A}^{(1,0)}(l) + \mathbb{A}^{(1,0)}(q-l)\mathbb{A}^{(1,1)}(l,p_1,p_2) \\ &\qquad\qquad + \frac{1}{2}\left[\mathbb{A}^{(1,1)}(q-l,p_1+l,p_2-l),\mathbb{A}^{(1,1)}(l,p_1,p_2)\right]\Big)\,. \end{aligned} \tag{2.50}$$

We are interested in the amplitude with special kinematic variables, Eq. (2.39); therefore, we have to consider shifts in the external momentum by the small momentum transfer q as well as the shifts coming from the amplitudes with propagator $(q-l)^{-2}$. These shifts cause the promotion of certain terms from classically singular to classical contributions. It should be noted that the last line in Eq. (2.50) already scales classically and therefore is not promoted.

The promotions come from the following transformations

$$\mathbb{A}^{(1,1)}(l, p_1, p_2) \to \left(1 - \left(\frac{q-l}{2}\right) \cdot \left(\frac{\partial}{\partial \bar{p}_1} - \frac{\partial}{\partial \bar{p}_2}\right)\right) \mathbb{A}^{(1,1)}(l, \bar{p}_1, \bar{p}_2), \tag{2.51}$$

$$\mathbb{A}^{(1,1)}(q-l, p_1+l, p_2-l) \to \left(1 + \frac{l}{2} \cdot \left(\frac{\partial}{\partial \bar{p}_1} - \frac{\partial}{\partial \bar{p}_2}\right)\right) \mathbb{A}^{(1,1)}(q-l, \bar{p}_1, \bar{p}_2). \tag{2.52}$$

We rewrite Eq. (2.50) in terms of the barred variables,

$$\begin{aligned} 2\,\mathrm{Im}\,\mathbb{A}^{(2,1)}(q, p_1, p_2) = \int \hat{d}l \, \Big(& \mathbb{A}^{(1,1)}(q-l, \bar{p}_1, \bar{p}_2)\mathbb{A}^{(1,0)}(l) + \mathbb{A}^{(1,0)}(q-l)\mathbb{A}^{(1,1)}(l, \bar{p}_1, \bar{p}_2) \\ & + \frac{1}{2}\left[\mathbb{A}^{(1,1)}(q-l, \bar{p}_1, \bar{p}_2), \mathbb{A}^{(1,1)}(l, \bar{p}_1, \bar{p}_2)\right] \\ & + l \cdot \left(\frac{\partial}{\partial \bar{p}_1} - \frac{\partial}{\partial \bar{p}_2}\right) \mathbb{A}^{(1,1)}(q-l, \bar{p}_1, \bar{p}_2)\mathbb{A}^{(1,0)}(l) \Big). \end{aligned} \tag{2.53}$$

Now only the top line of Eq. (2.53) is classically singular while the rest of the terms scale classically; later on, these same shifts and transformations will occur in the real kernels of the impulse and the spin kick.

2.4 The Eikonal Formula

Before we begin deriving the eikonal formula, we first briefly review the eikonal phase. A detailed discussion on the eikonal phase can be found in Refs. [144, 185, 186]. In impact parameter space, one can write the following exponentiation of the two-body scattering amplitude

$$1 + i\,\mathcal{A}(b) = (1 + i\Delta(b))\, e^{i\delta(b)}, \tag{2.54}$$

where $\delta(b)$ is the eikonal phase, $\Delta(b)$ is a quantum remainder, and

$$\mathcal{A}(b) = \int \hat{d}q \, \mathcal{A}(q)\, e^{-ib\cdot q} \equiv \mathrm{FT}[\mathcal{A}(q)], \tag{2.55}$$

where in a center of mass momentum configuration, with total energy E and center of mass momentum $\vec{p}$,

$$\delta(2\bar{p}_1 \cdot q)\delta(2\bar{p}_2 \cdot q) \to \frac{1}{4|\vec{p}|E}\delta(q^0)\delta(q^i) = \frac{1}{4\bar{m}_1\bar{m}_2\sqrt{y^2-1}}\delta(q^0)\delta(q^i), \tag{2.56}$$

where $i = 1, 2, 3$. We are suppressing the amplitude's dependence on other parameters such as the momentum or masses, for the sake of clarity. By expanding Eq. (2.54) in powers of the coupling constant g and in powers of classical scaling parameter λ, one can relate the classical scaling amplitude order by order to the eikonal phase. To next to leading order in the coupling constant,

$$\delta^{(1)}(b) = \mathrm{FT}[\mathcal{A}^{(1)}(q)], \qquad \delta^{(2)}(b) = \mathrm{FT}[\mathrm{Re}\,\mathcal{A}^{(2)}]. \tag{2.57}$$

The relationship between the eikonal phase and classical amplitudes becomes more complicated at higher orders in the coupling constant; however, this is beyond the scope of this chapter. We assume that Eq. (2.57) holds to all orders in the spin expansion.

In Ref. [121], based on the structure of their results for the impulse and spin kick to one loop order, the authors introduced an ansatz relating the eikonal phase to the observables in the center of mass frame, which can be expressed as

$$\Delta\mathbf{p}_1 = \frac{\partial\delta}{\partial\mathbf{b}} + \frac{1}{2}\left\{\delta, \frac{\partial\delta}{\partial\mathbf{b}}\right\} + \mathcal{D}_L\left(\delta, \frac{\partial\delta}{\partial\mathbf{b}}\right) - \frac{1}{2}\frac{\partial}{\partial\mathbf{b}}\mathcal{D}_L(\delta,\delta) - \frac{\mathbf{p}}{2\mathbf{p}^2}\left(\frac{\partial\delta}{\partial\mathbf{b}}\right)^2 + \mathcal{O}(\delta^3), \tag{2.58}$$

$$\Delta\mathbf{S}_1 = \{\delta, \mathbf{S}_1\} + \frac{1}{2}\{\delta, \{\delta, \mathbf{S}_1\}\} + \mathcal{D}_L(\delta, \{\delta, \mathbf{S}_1\}) - \frac{1}{2}\{\mathcal{D}_L(\delta,\delta), \mathbf{S}_1\} + \mathcal{O}(\delta^3), \tag{2.59}$$

where the bold variables are three-vectors, $\mathbf{p}$ is the center of mass momentum, $\mathbf{b}$ is the canonical impact parameter, and $\mathbf{S}$ is the rest frame spin three-vector. The spin three-vector is defined as

$$S^i = \frac{1}{2}\epsilon^{ijk}S_{jk}, \tag{2.60}$$

where $i, j, k = 1, 2, 3$ and we use $\epsilon^{123} = 1$ as our convention for the Levi-Civita tensor. $\mathcal{D}_L$ is defined as

$$\mathcal{D}_L(f,g) \equiv -\epsilon_{ijk}S^i_1\frac{\partial f}{\partial S_{1\,j}}\frac{\partial g}{\partial L_k}, \tag{2.61}$$

where we are ignoring the explicit inclusion of boost degrees of freedom since we are not making this distinction. The brackets are defined by the $SO(3)$ algebra

$$\left\{S^i, S^j\right\} = \epsilon^{ijk}S_k, \tag{2.62}$$

and L_k is the orbital angular momentum $L^i = \epsilon^{ijk} b_j p_k$.

As of the writing of this chapter, Eqs. (2.58) and (2.59) have been verified to quadratic order in spin, next to leading order in the coupling constant for QED and GR [122, 170]; however, there is no derivation. While we will be deriving an eikonal formula, we will not be deriving Eqs. (2.58) and (2.59) exactly because we will not be fixing our system to the center of mass frame and we will not explicitly break covariance. Nonetheless, we will derive an eikonal formula similar to Eqs. (2.58) and (2.59) that are written in terms of the spin tensor as opposed to the spin vector and in a covariant form.

2.4.1 Eikonal Formula Derivation

We now derive an eikonal formula for the impulse and the spin kick. We start with the comparatively simpler, linear-in-spin impulse starting at tree level and then move to the one loop correction. We then do the same for the linear-in-spin spin kick. We compare all calculations to the results in [170] by applying the two-body scattering amplitudes associated with Eq. (2.34). We expand the general spin QED impulses in the following manner

$$\Delta\mathcal{O} = \alpha q_1 q_2 (\Delta^{(1,0)}\mathcal{O} + \Delta^{(1,1)}\mathcal{O} + \cdots) + (\alpha q_1 q_2)^2 (\Delta^{(2,0)}\mathcal{O} + \Delta^{(2,1)}\mathcal{O} + \cdots) + \cdots \quad (2.63)$$

where the superscript count in the same way as in the amplitudes in Eq. (2.18).

2.4.2 Impulse

2.4.2.1 Tree Level

At tree level, the impulse only receives contributions from the virtual kernel. Also, because the virtual kernel already scales classically, the momentum shift to barred variables does not result in new promoted contributions. Therefore, we have the following result to all orders in spin

$$\Delta^{(1)}p_1^\mu = \int \hat{d}^4 q\, e^{-ib_{\rm cov}\cdot q}\, iq^\mu\, \mathcal{A}^{(1)}(q,\bar{p}_1,\bar{p}_2,S_1)$$
$$= -\frac{\partial}{\partial b_\mu}\int \hat{d}^4 q e^{-ib_{\rm cov}\cdot q}\, \mathcal{A}^{(1)}(q,\bar{p}_1,\bar{p}_2,S_1), \tag{2.64}$$

where the singular superscript counts the powers in the coupling constant. We can now identify the Fourier transform with respect to the new impact parameter $b_{\rm cov}$ as the "covariant" eikonal phase

$$\Delta^{(1)}p_1^\mu = -\frac{\partial}{\partial b_\mu}\delta^{(1)}_{\rm cov}, \tag{2.65}$$

where $\delta(b_{\rm cov},\bar{u}_1,\bar{u}_2,S_1) \equiv \delta_{\rm cov}$.

Fixing to the linear-in-spin impulse and using the linear-in-spin tree level amplitude for general spin QED,

$$\mathbb{A}^{(1,1)}(q,\bar{u}_1,\bar{u}_2) = \frac{iq_\beta M^{\alpha\beta}(yD_1\bar{u}_{1\,\alpha} - C_1\bar{u}_{2\,\alpha})}{q^2}, \tag{2.66}$$

we compute the result

$$\Delta^{(1,1)}p_1^\mu = \frac{2}{\bar{m}_1\sqrt{y^2-1}}\frac{S_1^{\nu\rho}}{|b_{\rm cov}|^2}\left(\Pi^\mu_{\ \nu} + \frac{2\, b^\mu_{\rm cov}\, b_{{\rm cov}\,\nu}}{|b_{\rm cov}|^2}\right)(yD_1\bar{u}_{1\,\rho} - C_1\bar{u}_{2\,\rho})\,, \tag{2.67}$$

which matches the result in Ref. [170]. Here $|b_{\rm cov}|^2 = -b^2_{\rm cov}$ and $\Pi^\mu_{\ \nu}$ is the projective derivative of the impact parameter

$$\Pi^\mu_{\ \nu} = \delta^\mu_{\ \nu} + \frac{1}{y^2-1}\left(\bar{u}_1^\mu\check{\bar{u}}_{1\,\nu} + \bar{u}_2^\mu\check{\bar{u}}_{2\,\nu}\right), \tag{2.68}$$

where $\check{\bar{u}}_{1,2} \equiv \bar{u}_{1,2} - y\,\bar{u}_{2,1}$. To satisfy the orthogonality constraints of b^μ with respect to the scattering plane, i.e. $\bar{u}_i\cdot b = 0$, we require the projector $\Pi^\mu_{\ \nu}$ in place of the naive derivative, which does not take this into account.

2.4.2.2 One Loop

At one loop, we must include the real kernel in order to ensure that all classically singular terms cancel. In the same way as $\mathrm{Im}\,\mathbb{A}^{(2,1)}$, we need to change to special kinematic variables in Eq. (2.29) and keep track of terms promoted to classical scaling. This results in

$$\mathcal{I}_r^{(2,1)\,\mu} = \int \hat{d}l\; l^\mu\, \epsilon^*(p_1+q)\cdot \big\{ \mathbb{A}^{(1,0)}(q-l)\mathbb{A}^{(1,1)}(l,\bar{p}_1,\bar{p}_2) + \mathbb{A}^{(1,1)}(q-l,\bar{p}_1,\bar{p}_2)\mathbb{A}^{(1,0)}(l)$$
$$+ \mathbb{A}^{(1,0)}(l)\, l\cdot\left(\frac{\partial}{\partial \bar{p}_1} - \frac{\partial}{\partial \bar{p}_2}\right)\mathbb{A}^{(1,1)}(q-l,\bar{p}_1,\bar{p}_2)$$
$$+ \frac{1}{2}\left[\mathbb{A}^{(1,1)}(q-l,\bar{p}_1,\bar{p}_2), \mathbb{A}^{(1,1)}(l,\bar{p}_1,\bar{p}_2)\right]\Bigg\}\cdot \epsilon(p_1), \tag{2.69}$$

which is near identical to Eq. (2.53) except for the explicit factor of l^μ. In fact, when combining the virtual kernel, $\mathcal{I}_v^{(2,1)\,\mu}$, with Eq. (2.69) and focusing on the classically singular pieces, we observe the following

$$\int \hat{d}q\, e^{-iq\cdot b_{\text{cov}}} \int \hat{d}l \left(\frac{2l^\mu - q^\mu}{2}\right) \big\{ \mathcal{A}^{(1,0)}(q-l)\mathcal{A}^{(1,1)}(l,\bar{p}_1,\bar{p}_2,S_1)$$
$$+ \mathcal{A}^{(1,1)}(q-l,\bar{p}_1,\bar{p}_2,S_1)\mathcal{A}^{(1,0)}(l)\big\}\,. \tag{2.70}$$

The cancellation of the classically singular pieces must occur upon integration; to make this manifest at the integrand level we make the following decomposition of factors of loop momentum vector

$$l^\mu \to \frac{q^\mu}{2} - \frac{(l\cdot\bar{u}_1\,\check{u}_1^\mu + l\cdot\bar{u}_2\,\check{u}_2^\mu)}{y^2-1}, \tag{2.71}$$

and apply the δ-functions in the integrand, $\hat{\delta}(2\bar{p}_1\cdot l - q\cdot l)\hat{\delta}(2\bar{p}_2\cdot l + q\cdot l)$. Because we are only interested in long range interactions, we can make the replacement $q\cdot l \to q^2/2$; this results in the promotion of the remaining term in Eq. (2.70) to scale classically. We now have a uniformly classical scaling expression for the impulse

$$\Delta^{(2,1)}p_1^\mu = \int \hat{d}q\, e^{-iq\cdot b_{\text{cov}}}\, iq^\mu\, \mathrm{Re}\,\mathcal{A}^{(2,1)}(q,\bar{u}_1,\bar{u}_2,S_1)$$
$$+ \int \hat{d}q e^{-iq\cdot b_{\text{cov}}} \int \hat{d}l \left\{ \left(\frac{2l^\mu - q^\mu}{4}\right)\left[\mathcal{A}^{(1,1)}(q-l,\bar{u}_1,\bar{u}_2,S_1), \mathcal{A}^{(1,1)}(l,\bar{u}_1,\bar{u}_2,S_1)\right]\right.$$
$$+ \mathcal{A}^{(1,0)}(l)\left(\frac{2l^\mu - q^\mu}{2}\right) l^\alpha \left(\frac{1}{\bar{m}_1}\frac{\partial}{\partial \bar{u}_1^\alpha} - \frac{1}{\bar{m}_2}\frac{\partial}{\partial \bar{u}_2^\alpha}\right)\mathcal{A}^{(1,1)}(q-l,\bar{u}_1,\bar{u}_2,S_1)$$
$$+ \frac{-q^2}{4(y^2-1)}\left(\frac{\check{u}_1^\mu}{\bar{m}_1} - \frac{\check{u}_2^\mu}{\bar{m}_2}\right)\big(\mathcal{A}^{(1,0)}(q-l)\mathcal{A}^{(1,1)}(l,\bar{u}_1,\bar{u}_2,S_1)$$
$$\left. + \mathcal{A}^{(1,1)}(q-l,\bar{u}_1,\bar{u}_2,S_1)\mathcal{A}^{(1,0)}(l)\big)\right\}. \tag{2.72}$$

To be able to re-express the amplitudes that depend on the loop momentum in terms of their respective eikonal phases, we make the shift $q \to q + l$ and substitute explicit factors of $q, l \to i\frac{\partial}{\partial b}$,

$$\begin{aligned}\Delta^{(2,1)}p_1^\mu = &-\frac{\partial\,\delta_{\rm cov}^{(2,1)}}{\partial b_\mu} + \frac{i}{2}\left[\delta_{\rm cov}^{(1,1)}, \frac{\partial\delta_{\rm cov}^{(1,1)}}{\partial b_\mu}\right] + \frac{1}{(y^2-1)}\left(\frac{\check{\bar{u}}_1^\mu}{\bar{m}_1} - \frac{\check{\bar{u}}_2^\mu}{\bar{m}_2}\right)\frac{\partial\delta_{\rm cov}^{(1,0)}}{\partial b}\cdot\frac{\partial\delta_{\rm cov}^{(1,1)}}{\partial b}\\ &+\frac{1}{2}\left[\frac{\partial}{\partial b_\mu}, \left(\frac{1}{\bar{m}_1}\frac{\partial}{\partial\bar{u}_1^\alpha} - \frac{1}{\bar{m}_2}\frac{\partial}{\partial\bar{u}_2^\alpha}\right)\delta_{\rm cov}^{(1,1)}\right]\frac{\partial\delta_{\rm cov}^{(1,0)}}{\partial b_\alpha}.\end{aligned} \tag{2.73}$$

To verify Eq. (2.73), we plug in the appropriate tree level amplitudes and linear-in-spin, one loop amplitude,

$$\mathrm{Re}\mathbb{A}^{(2,1)} = \mathbb{A}_{\triangle+\triangledown}(q, \bar{u}_1, \bar{u}_2) = \frac{1}{4\sqrt{-q^2}} i q_\nu \mathbb{M}^{\mu\nu}\left(\beta_{(1)}\bar{u}_{1\,\mu} + \beta_{(2)}\bar{u}_{2\,\mu}\right), \tag{2.74}$$

$$\begin{aligned}\beta_{(1)} = &\frac{-1}{(y^2-1)\bar{m}_1}\Big(\left[(y^2+1)C_1 + (y^2-1)D_1\right]\bar{m}_1\\ &+\left[C_1^2 - (y^2+1)C_1D_1 + y^2D_1^2 + (3y^2-1)D_1\right]\bar{m}_2\Big),\end{aligned} \tag{2.75}$$

$$\beta_{(2)} = \frac{y}{(y^2-1)\bar{m}_1}\left(2C_1\bar{m}_1 + \left[C_1^2 - 2C_1D_1 + D_1^2 + 2D_1\right]\bar{m}_2\right), \tag{2.76}$$

and compute the result

$$\begin{aligned}\Delta^{(2,1)}p_1^\mu = &\frac{\pi\left(3\,b_{\rm cov}^\mu\,b_{{\rm cov}\,\nu} + |b_{\rm cov}|^2\,\Pi^\mu_\nu\right)S_1^{\nu\rho}}{2|b_{\rm cov}|^5(y^2-1)^{3/2}\,\bar{m}_1^2\,\bar{m}_2}\left\{\check{\bar{u}}_{1\,\rho}[\bar{m}_1(D_1 - C_1) - \bar{m}_2(C_1^2 - C_1D_1 - D_1)]\right.\\ &\left.+ y\check{\bar{u}}_{2\,\rho}[\bar{m}_1(C_1 + D_1) - \bar{m}_2D_1(C_1 - D_1 - 3)]\right\}\\ &-\frac{2b_{\rm cov}^\nu S_{1\,\nu\rho}\Pi^\mu_\rho}{|b_{\rm cov}|^4(y^2-1)\,\bar{m}_1^2\,\bar{m}_2}\left\{2C_1y\bar{m}_1 + \bar{m}_2(C_1^2 - y^2D_1(2C_1 - D_1 - 2))\right\}\\ &+\frac{4y(\bar{m}_2\check{\bar{u}}_1^\mu - \bar{m}_1\check{\bar{u}}_2^\mu)b_{\rm cov}^\nu S_{1\,\nu\rho}}{|b_{\rm cov}|^4(y^2-1)^3\,\bar{m}_1^2\,\bar{m}_2}\left\{\check{\bar{u}}_1^\rho(D_1 - C_1) + \check{\bar{u}}_2^\rho(y^2D_1 - C_1)\right\},\end{aligned} \tag{2.77}$$

where we match the result in Ref. [170], taking into account our impact parameters point in opposite directions.

We notice a similarity between Eq. (2.73) and Eq. (2.58). The first obvious caveat is that we express our result in terms of the spin tensor as opposed to Refs. [50, 121, 122, 170], which use the spin three-vector. The second is that in Eq. (2.73) we work with the covariant impact parameter whereas Refs. [50, 121, 122, 170] use the canonical rest frame impact parameter, which are related by Eq. (2.23). Nevertheless, structural similarities are hard to not notice when comparing to Eq. (2.58), particularly in the terms independent of $\mathcal{D}_L(f,g)$. Because we have verified Eq. (2.73) using the result in Ref. [170], we conclude that we have derived an eikonal formula for the one loop, linear-in-spin impulse that takes into account the contributions of the $\mathcal{D}_L(f,g)$ terms in Refs. [121, 122, 170].

2.4.3 Spin Kick

2.4.3.1 Tree Level

Same as in the impulse case, for the tree level spin kick we only need the contribution from the virtual kernel. We also do not have to worry about any promotions coming from the shift when changing to barred variables because the tree level amplitude already scales classically

$$\Delta^{(1)} S_1^{\mu\nu} = \frac{i}{2} \int \hat{d}q \, e^{-ib_{\text{cov}}\cdot q} \left[\mathcal{A}^{(1)}(q, \bar{u}_1, \bar{u}_2, S_1), S_1^{\mu\nu}\right]. \tag{2.78}$$

Re-expressing Eq. (2.78) in terms of the eikonal phase and covariant coordinates we get

$$\Delta^{(1)} S_1^{\mu\nu} = \frac{i}{2} \left[\delta^{(1)}_{\text{cov}}, S_1^{\mu\nu}\right]. \tag{2.79}$$

We check Eq. (2.79) by fixing ourselves to linear order in spin and plugging in Eq. (2.66) for the amplitude

$$\Delta^{(1,1)} S_1^{\mu\nu} = \frac{4}{\bar{m}_1\sqrt{y^2-1}} \frac{\left(yD_1 b_{\text{cov}\,[\sigma}\bar{u}_{1\,\rho]} - C_1 b_{\text{cov}\,[\sigma}\bar{u}_{2\,\rho]}\right)\eta^{\rho[\mu}S_1^{\nu]\sigma}}{|b_{\text{cov}}|^2}, \tag{2.80}$$

where the brackets around the indices signals their anti-symmetrization,

$$a_{[\sigma}c_{\rho]} \equiv \frac{1}{2}\left(a_\sigma c_\rho - a_\rho c_\sigma\right), \tag{2.81}$$

for some four-vectors a, c, and $\eta^{\rho\mu}$ is the Minkowski metric. Eq. (2.80) matches the result in Ref. [170] taking into account our impact parameters point in opposite directions and an overall factor of $1/2$, which comes from our definition of the spin operator expectation value.

2.4.3.2 One Loop

Same as in the impulse case, for the one loop calculation we need to include the real kernel contribution. After shifting to barred variables and making explicit the classical scaling, we have the following real kernel contribution to the spin kick

$$\begin{aligned}\mathcal{I}_r^{(2,1)\,\mu\nu} =& \frac{e^{iq\cdot\omega}}{2}\int \hat{d}l\ \Big\{\mathcal{A}^{(1,0)}(q-l)\left[\mathcal{A}^{(1,1)}(l,\bar{u}_1,\bar{u}_2,S_1),S_1^{\mu\nu}\right] \\ &+\mathcal{A}^{(1,0)}(l)\frac{l^\alpha}{2}\left(\frac{1}{\bar{m}_1}\frac{\partial}{\partial\bar{u}_1^\alpha}-\frac{1}{\bar{m}_2}\frac{\partial}{\partial\bar{u}_2^\alpha}\right)\left[\mathcal{A}^{(1,1)}(q-l,\bar{u}_1,\bar{u}_2,S_1),S_1^{\mu\nu}\right] \\ &+\frac{1}{2}\left[\mathcal{A}^{(1,1)}(q-l,\bar{u}_1,\bar{u}_2,S_1),\left[\mathcal{A}^{(1,1)}(l,\bar{u}_1,\bar{u}_2,S_1),S_1^{\mu\nu}\right]\right]\Big\}, \end{aligned} \tag{2.82}$$

where only the top line of Eq. (2.82) has classically singular scaling. The cancellation of the classically singular terms in the real kernel and $\operatorname{Im}\mathbb{A}^{(2,1)}$ is more subtle in the spin kick case; namely, when attempting to cancel the classically singular terms, we end up with the following

$$\frac{e^{iq\cdot\omega}}{4}\int\hat{d}l\ \left[\mathcal{A}^{(1,0)}(q-l)\mathcal{A}^{(1,1)}(l,\bar{u}_1,\bar{u}_2,S_1)-\mathcal{A}^{(1,0)}(l)\mathcal{A}^{(1,1)}(q-l,\bar{u}_1,\bar{u}_2,S_1),S_1^{\mu\nu}\right], \tag{2.83}$$

which does not obviously cancel. However, if we schematically plug in for the amplitudes using Eq. (2.40) and Eq. (2.42), the necessary steps become clearer

$$\frac{e^{iq\cdot\omega}}{4}\int\hat{d}l\,\frac{i\mathcal{N}^{(1,0)}\mathcal{N}_\alpha^{(1,1)}(\bar{u}_1,\bar{u}_2)}{l^2(q-l)^2}(2l_\beta-q_\beta)\left[S_1^{\alpha\beta},S_1^{\mu\nu}\right]. \tag{2.84}$$

Because the cancellation of classically singular terms occurs upon integration, we can make the same replacement for the loop momentum as in Eq. (2.71) and apply the δ-functions in $\hat{d}l$. Doing so gives us the uniformly classical spin kick

$$\begin{aligned}\Delta^{(2,1)}S_1^{\mu\nu} =& \frac{i}{2}\int\hat{d}q\,e^{-iq\cdot b_{\rm cov}}\Big\{\left[\operatorname{Re}\mathcal{A}^{(2,1)}(q,\bar{u}_1,\bar{u}_2,S_1),S_1^{\mu\nu}\right] \\ &+\int\hat{d}l\Big\{\frac{(-q^2)}{4(y^2-1)}\frac{\mathcal{A}^{(1,0)}(l)\mathcal{N}_\alpha^{(1,1)}(\bar{u}_1,\bar{u}_2)}{(q-l)^2}\left(\frac{\check{\bar{u}}_{1\,\beta}}{\bar{m}_1}-\frac{\check{\bar{u}}_{2\,\beta}}{\bar{m}_2}\right)\left[S_1^{\alpha\beta},S_1^{\mu\nu}\right] \\ &-\frac{i}{2}\left[\mathcal{A}^{(1,1)}(q-l,\bar{u}_1,\bar{u}_2,S_1),\left[\mathcal{A}^{(1,1)}(l,\bar{u}_1,\bar{u}_2,S_1),S_1^{\mu\nu}\right]\right] \\ &+\frac{i}{4}\left[\left[\mathcal{A}^{(1,1)}(q-l,\bar{u}_1,\bar{u}_2,S_1),\mathcal{A}^{(1,1)}(l,\bar{u}_1,\bar{u}_2,S_1)\right],S_1^{\mu\nu}\right]\Big\}\Big\}. \end{aligned} \tag{2.85}$$

Note that the last line in Eq. (2.85) evaluates to zero due to the horizontal flip symmetry of the cut, i.e. $l \to q - l$. Once again, we systematically replace our amplitudes with eikonal phases by shifting $q \to q + l$ and replacing explicit factors of q, l with $i\frac{\partial}{\partial b}$,

$$\Delta^{(2,1)} S_1^{\mu\nu} = \frac{i}{2}\left[\delta_{\text{cov}}^{(2,1)}, S_1^{\mu\nu}\right] + \frac{1}{4}\left[\delta_{\text{cov}}^{(1,1)}, \left[\delta_{\text{cov}}^{(1,1)}, S_1^{\mu\nu}\right]\right] + \frac{i\mathcal{N}_\alpha^{(1,1)}(\bar{u}_1, \bar{u}_2)}{32\pi \bar{m}_1 \bar{m}_2 (y^2-1)^{3/2}} \left(\frac{\check{\bar{u}}_{1\,\beta}}{\bar{m}_1} - \frac{\check{\bar{u}}_{2\,\beta}}{\bar{m}_2}\right)\left[S_1^{\alpha\beta}, S_1^{\mu\nu}\right] \frac{\partial \delta_{\text{cov}}^{(1,0)}}{\partial b^\gamma} \frac{b_{\text{cov}}^\gamma}{|b_{\text{cov}}|^2}. \tag{2.86}$$

We verify Eq. (2.86) by plugging in the appropriate amplitudes from Eq. (2.34)

$$\begin{aligned}
\Delta^{(2,1)} S_1^{\mu\nu} = & \frac{\pi S_1^{\rho[\nu}\eta^{\mu]\sigma}}{|b_{\text{cov}}|^3 (y^2-1)^{3/2}\, \bar{m}_1^2 \bar{m}_2} \Big[b_{\text{cov}\,[\sigma} \check{\bar{u}}_{1\,\rho]} \big(\bar{m}_1 (D_1 - C_1) - \bar{m}_2 (C_1^2 - D_1 - C_1 D_1)\big) \\
& + b_{\text{cov}\,[\sigma} \check{\bar{u}}_{2\,\rho]} y \left(\bar{m}_1 (D_1 + C_1) - \bar{m}_2 D_1 (C_1 - D_1 - 3)\right) \Big] \\
& - \frac{2}{|b_{\text{cov}}|^4 (y^2-1)\, \bar{m}_1^2} \Big[2 b_{\text{cov}\,\rho} S_1^{\rho\sigma} \left(C_1 \bar{u}_{2\,\sigma} - D_1 y \bar{u}_{1\,\sigma}\right) \Big(C_1 b_{\text{cov}}^{[\mu} \bar{u}_2^{\nu]} - y D_1 b_{\text{cov}}^{[\mu} \bar{u}_1^{\nu]} \Big) \\
& - b_{\text{cov}\,\rho} S_1^{\rho[\nu} b_{\text{cov}}^{\mu]} (C_1^2 - D_1 (2C_1 - D_1) y^2) \Big] \\
& - \frac{2}{|b_{\text{cov}}|^2 (y^2-1)^3\, \bar{m}_1^2 \bar{m}_2} \Big[\bar{m}_2 \Big(y^2 (C_1 - D_1)^2 S_1^{\rho[\nu} \check{\bar{u}}_1^{\mu]} \check{\bar{u}}_{1\,\rho} + (C_1 - D_1 y^2)^2 S_1^{\rho[\nu} \check{\bar{u}}_2^{\mu]} \check{\bar{u}}_{2\,\rho} \Big) \\
& + S_1^{\rho[\nu} \check{\bar{u}}_1^{\mu]} \check{\bar{u}}_{2\,\rho} \big(\bar{m}_1 (C_1 - D_1) y^2 + y \bar{m}_2 (C_1 - y^2 D_1)(C_1 - D_1 + 1)\big) \\
& - S_1^{\rho[\nu} \check{\bar{u}}_2^{\mu]} \check{\bar{u}}_{1\,\rho} (\bar{m}_1 (C_1 - D_1) y^2 - y \bar{m}_2 (C_1 - y^2 D_1)(C_1 - D_1 - 1)) \Big],
\end{aligned} \tag{2.87}$$

which matches the results in Ref. [170] taking in to account the difference in an overall factor of 1/2 due to our definition of the spin operator and our impact parameters pointing in opposite directions. Taking into account the fact that we use the spin tensor and the covariant impact parameter, we see that the top line of Eq. (2.86) has a similar form to Eq. (2.59) not including the $\mathcal{D}_L(f, g)$ terms. Because we have verified Eq. (2.86) using the result in Ref. [170], we conclude that we have derived an eikonal formula for the one loop, linear-in-spin spin kick that takes into account the contributions of the $\mathcal{D}_L(f, g)$ terms in Ref. [170].

2.5 Conclusion and Discussion

We derived covariant eikonal formulae relating the eikonal phase to the impulse and spin kick to linear order in spin and next to leading order in the coupling constant. To do so we used the KMOC formalism [39], which directly gives physical observables in terms of scattering amplitudes in impact parameter space, which is connected to the eikonal phase. This is the first next-to-leading order spin dependent calculation using the KMOC formalism and general spin QFT. To simplify the evaluation, we used the non-transverse property of unconstrained massive general spin fields [170] to construct the completeness relation Eq. (2.6) for the polarization tensors. This non-transverse property also allows us to construct SSC-violating spin tensors, as in the worldline and field theory calculations of [170]. The choice of barred variables [47, 76] simplified the cancellation of classically singular terms in the integrand and facilitated the appearance of terms proportional to external momentum derivatives. We verified our results by comparing to the results in Ref. [170], which were based on worldline and field theory matched to a general spin EFT. Based on this match, we also conclude that our eikonal formulae, Eqs. (2.73) and (2.86), capture the effects of the $\mathcal{D}_L(f, g)$ terms in Eqs. (2.58) and (2.59).

There are obvious future directions, including extending this work to higher order in spin and coupling constant. The eikonal formulae, based on rest-frame spin introduced in Ref. [121], have been explicitly verified to quadratic order in spin [122] and next to leading order in the coupling. Though our covariant construction is different, extending this work to quadratic-in-spin order (and beyond) will provide insight to the relationship between the eikonal phase and spinning scattering observables. It would, of course, be very interesting to extend the derivation of the eikonal formulae to higher orders in the coupling as well.

A more thorough investigation of the relation between the eikonal formulae for the impulse and spin kick presented here and those in Refs. [170] would be very interesting. It would also be interesting to use the procedure presented here to incorporate spin in the calculation of other observables such as the direct waveform calculations [166–168, 187, 188], absorption effects [189], or even to observables in the three-body case [190].

CHAPTER 3

Spinning Observables from Field Theory

3.1 Introduction

In this chapter, we will generalize the work in the previous chapter to all orders in spin. We will also be comparing to gravity as opposed to electrodynamics; however, we will consider the general structure of general-spin amplitudes and then check against gravity calculations. For the sake of clarity, we will re-include our base assumption and review about the classical limit and spin.

The way in which one takes into account spin effects in their amplitude is crucial when calculating spin corrections to observables. Refs. [115, 116, 120, 191] have shown that, up to quartic order in spin, spin effects on the Compton amplitude for massive spinning fields minimally coupled to gravity exponentiate in the classical limit; however, at higher orders in spin, this exponentiation breaks down. Ref. [192] showed, by matching higher-spin Compton amplitudes to solutions to the Teukolsky equation, that there are corrections to the amplitude that break the exponentiation, which have been related to subtleties in the Teukolsky solution [193, 194]. These subtleties will not affect our derivations in this work for a few reasons. Namely, we are not worried about constructing amplitudes, we only care about their general structure when it comes to their momentum scaling in the classical limit. In fact, we only need to know this scaling at tree level for two-body scattering. Another reason is that we are checking our formulas up to quadratic order in spin. While an explicit comparison to higher orders in spin would solidify the validity of our derivation at those orders, our derivation will not rely on truncating to quadratic order in spin; in fact, we will be using properties of non-transverse, higher-spin fields for our calculation.

While a lot of work has been done using fixed-spin representations of massive fields to model scattering bodies [40, 156, 157, 166, 195], the calculations in Refs. [170, 196, 197] use non-transverse massive spinning fields, which allow for lower-spin states to propagate in their amplitudes, and with allowed transitions between them. This difference in models effectively implies a difference in choice of spin supplementary condition (SSC) and spin-vector-magnitude conservation: the former enforces it while the latter does not. Ref. [170] showed that one can go from SSC-violating to SSC-enforcing observables by properly tuning the Wilson coefficients in their QFT. This relationship implies that systems with the SSC imposed can be thought of as subsets of those that allow for SSC-violating degrees of freedom. In contrast to the non-transverse formalism, the fixed-spin formalism would have to introduce auxiliary fields at higher orders in spin that would result in complicated spin-s propagators, such as those used in the massive higher-spin literature [170–173]. In this paper, we will use the simplifications allowed by SSC-violating degrees of freedom to calculate higher-spin corrections to the momentum impulse and spin kick.

The exponentiated S-matrix approach to calculate PM observables also has a rich history, with the use of the radial action [62, 178, 198–202] and eikonal phase [195–197, 203–206] providing very useful semi-classical approaches. While much of the work using these methods has been done for non-spinning matter, recent work has incorporated spin degrees of freedom to their formalisms. Based on their results using an EFT Hamiltonian, a formula was reverse engineered in Ref. [121] that directly related the eikonal phase to the one-loop correction of the momentum impulse and spin kick. These eikonal formulas have the nice property of only having simple operations acting on the eikonal phase such as differentiation and commutation. In Chapter 2 and Ref. [195], eikonal formulas were derived, where the former used non-transverse massive spinning fields to calculate up to linear order in spin, while the latter used fixed-spin fields and provided an expression the was verified up to quadratic order in spin.

In this paper, we expand upon the work in Chapter 2 and generalize it to all orders in spin; this is a first for a derivation from field theory that does not rely on specific spin representations and KMOC. We use the KMOC formalism and take advantage of the properties of non-transverse massive spinning fields to simplify the derivation. Compared to other methods of calculating spinning observables, the origin of the terms in our formulas are very trackable by virtue of the approach of the KMOC formalism. In Section 2, we re-review the key elements for performing the derivation for the sake of clarity. In Section 3, we discuss properties of the amplitudes we will be working with. In Section 4 and 5, we carry out the derivation for the momentum impulse and spin kick eikonal formulas, respectively. In Section 6, we point out an underlying pattern in our eikonal formulas and discuss this in the context of the existing literature. In Section 7, we summarize our results and consider possible new directions to elaborate on this work. We also provide appendices that clarify the details of our calculation and comparison.

3.2 Review

We review the necessary building blocks for deriving the eikonal formulas for the momentum impulse and the spin kick. First, we will review the scaling arguments that will allow us to sensibly take a classical limit. Next, we briefly touch on the basic assumption of our massive higher-spin fields. Then, we briefly cover the KMOC formalism with spin included. Later, we present the momentum shift used to simplify the organization of the classical limit. Finally, we review the eikonal-phase formalism and recent efforts in deriving eikonal formulas.

3.2.1 The Classical Scaling with Spin

In this work we will be working in the long-range, relativistic, classical limit, allowing us to model our two-body system in terms of point-like massive particles. Taking the classical limit, in the context of two-body scattering amplitudes, amounts to determining the relevant length scales of the problem: there are three general length scales in the massive two-body context [207]. We must consider the de Broglie wavelength, $\lambda_{dB} = \hbar/|\mathbf{p}|$, where $\mathbf{p}$ is the three-momentum of either body, which is associated with the scale where the wave nature of the bodies becomes important; the impact parameter b, which is the macroscopic length of separation between the two bodies; and the Compton wavelength $\lambda_C = \hbar/m$ where m is the mass of either body, which is associated with the scale at which QFT effects, such as particle production, become relevant. For our purposes, we take the long-range, relativistic, classical limit,

$$b \gg \lambda_{dB} \sim \lambda_C, \tag{3.1}$$

otherwise known as the eikonal limit [207].

We also must consider the classical particle size when determining length scales for specific theories. For example, in the case of electrodynamics, we would consider the classical charge radius $r_Q = \frac{\alpha Q^2}{m}$; combined with Eq.(3.1) this would give us the Post-Lorentzian expansion parameter $\frac{\alpha Q^2}{mb}$. For gravity, we would consider the Schwarzschild radius $r_G = Gm$, which would give us the Post-Minkowskian expansion parameter $\frac{Gm}{b}$ [178].

For scattering amplitudes, it is more convenient to talk about this scaling in momentum space. To do this, we need the conjugate variable to the impact parameter, which is the momentum transfer $|q| \sim 1/|b|$. This implies the following scaling relation of our momenta,

$$|q| \sim \hbar \ll m \sim |\mathbf{p}|. \tag{3.2}$$

We can also relate the total angular momentum to the impact parameter by $|J| \sim |b||\mathbf{p}|$, which implies $J \gg \hbar$ in the eikonal limit. Of course, we are interested in the spin angular momentum S of the scattering; therefore, we will assume that when we distinguish S from the orbital angular momentum L, their magnitudes scale similarly, $|S| \sim |L| \gg \hbar$ [121].

From now on, we will be working in natural units $\hbar = c = 1$. To organize the scaling, we will use a small unitless parameter $\lambda \ll 1$ and have the following scaling in mind for our variables

$$p \to p, \quad q \to \lambda q, \quad b \to \lambda^{-1} b, \quad S \to \lambda^{-1} S, \tag{3.3}$$

when taking the eikonal limit. This is the standard scaling used throughout the amplitudes community to calculate the classical limit of spinning amplitudes [39, 40, 42, 47, 76, 121, 189, 207].

3.2.2 Higher-Spin Fields

To model our scattering bodies, we will be following the work done in Refs. [121, 170, 196], which use symmetric, non-transverse, massive higher-spin fields; we will refer to these as general-spin fields. By choosing general-spin fields, we allow for lower-spin states to propagate in our amplitudes, thus allowing for spin-transitions in our scattering events. Ref. [170] showed that allowing these lower-spin states to propagate violates the covariant spin supplementary condition (SSC),

$$p_\mu S^{\mu\nu}(p) = 0, \tag{3.4}$$

therefore allowing for extra degrees of freedom in our QFT. This can be seen in the decomposition of the spin tensor in to SSC-preserving and SSC-violating pieces

$$S^{\mu\nu}(p) = \frac{1}{m}\epsilon^{\mu\nu\rho\sigma} p_\rho s_\sigma(p) + \frac{1}{m}\left(p^\mu K^\nu(p) - p^\nu K^\mu(p)\right), \tag{3.5}$$

where $s_\sigma(p)$ is the spin vector and $K^\mu(p)$ is the boost vector or "mass dipole" [196, 208, 209]. It should be noted that, while the SSC is violated, the spin-tensor magnitude remains a conserved quantity; this is achieved by squaring Eq.(3.5) and perturbing

$$\Delta S^2 = 2\Delta K^2 - 2\Delta s^2, \tag{3.6}$$

where the right-hand side must vanish. This has been observed in explicit calculation [170].

When taking the classical limit of observables, Ref. [170] showed that imposing the SSC is the same as fixing Wilson coefficients in the general spin QFT. This implies that imposing the SSC on the general-spin fields eliminates these extra degrees of freedom in the classical limit, thus recovering the finite-spin-s result. This also implies that we can impose the SSC after we have calculated observables using general-spin fields and recover those that obey it.

A major advantage in using the general-spin fields is that we are able to construct a simple completeness relation for the spin-s polarization tensors

$$\sum_a \epsilon_a^{\mu(s)}(p)\epsilon^{*\,a}_{\nu(s)}(p) = \delta^{\mu(s)}_{\nu(s)}, \tag{3.7}$$

where we sum over the little group indices a and $\delta^{\mu(s)}_{\nu(s)}$ is the appropriate Kronecker delta such that for a rank-s tensor $\delta^{\mu(s)}_{\nu(s)}T^{\nu(s)} = T^{\mu(s)}$.

We define the spin tensor using these polarization tensors

$$[S^{\mu\nu}(p)]_a^{\ a'} \equiv \epsilon^{*\,a'}_{\alpha(s)}(p)\,(M^{\mu\nu})^{\alpha(s)}_{\ \ \beta(s)}\,\epsilon_a^{\beta(s)}(p), \tag{3.8}$$

where $(M^{\mu\nu})^{\alpha(s)}_{\ \ \beta(s)}$ is the spin-s representation of the Lorentz generator

$$(M^{\mu\nu})^{\alpha(s)}_{\ \ \beta(s)} = is\,\delta^{[\mu}_{(\beta_1}\eta^{\nu](\alpha_1}\delta^{\alpha_2}_{\beta_2}\cdots\delta^{\alpha_s)}_{\beta_s)}, \tag{3.9}$$

satisfying the Lorentz algebra

$$[M^{\mu\nu}, M^{\rho\sigma}] = -i\left(\eta^{\mu\rho}M^{\sigma\nu} + \eta^{\nu\rho}M^{\mu\sigma} - \eta^{\mu\sigma}M^{\rho\nu} - \eta^{\nu\sigma}M^{\mu\rho}\right). \tag{3.10}$$

Because the commutator in the Lorentz algebra reduces the number of Lorentz generators by one, for the purposes of classical scaling, we will take the commutator to scale as $\mathcal{O}(\lambda)$.

We define products of spin tensors in the same way as Refs. [121, 170, 196], where for a product of s spin tensors,

$$[S^{\mu_1\nu_1}(p)\cdots S^{\mu_s\nu_s}(p)]_a^{a'} = \frac{1}{s!}\epsilon^{*\,a'}(p)\ \mathrm{Sym}\left[M^{\mu_1\nu_1}M^{\mu_2\nu_2}\cdots M^{\mu_{s-1}\nu_{s-1}}M^{\mu_s\nu_s}\right]\epsilon_a(p), \tag{3.11}$$

where

$$\text{Sym}\left[M^{\mu_1\nu_1}\cdots M^{\mu_n\nu_n}\right] = \left[\sum_{\sigma\in S_n}\prod_{i=1}^{n} M^{\mu_{\sigma(i)}\nu_{\sigma(i)}}\right]. \tag{3.12}$$

For convenience we will use the shorthand,

$$\left[S^{\mu(s)\nu(s)}(p)\right]_a^{\ a'} \equiv \left[S^{\mu_1\nu_1}(p)\cdots S^{\mu_s\nu_s}(p)\right]_a^{\ a'}. \tag{3.13}$$

3.2.3 KMOC with Spin

The KMOC formalism calculates the change in some observable $\mathcal{O}$ by measuring the difference in the expectation value of some corresponding quantum operator $\mathbb{O}$ from the asymptotic past to the asymptotic future [39],

$$\Delta\mathcal{O} = \langle\text{out}|\mathbb{O}|\text{out}\rangle - \langle\text{in}|\mathbb{O}|\text{in}\rangle. \tag{3.14}$$

We can relate the "out" states to the "in" state via the S-matrix, $S = 1 + iT$

$$\Delta\mathcal{O} = \langle\Psi|i[\mathbb{O}, T]|\Psi\rangle + \langle\Psi|T^\dagger[\mathbb{O}, T]|\Psi\rangle, \tag{3.15}$$

where $|\Psi\rangle$ is the scattering wave packet. For a two-body wave packet we have

$$|\Psi\rangle = \sum_{a_1,a_2}\int d\Phi(p_1)d\Phi(p_2)\,\phi(p_1)\phi(p_2)\,\xi^{a_1}\,\xi^{a_2}\,e^{ib_1\cdot p_1}\,e^{ib_2\cdot p_2}\,|p_1p_2;a_1a_2\rangle, \tag{3.16}$$

where a_i are the little group indices of the scattering bodies, $\phi(p_i)$ are the wavefunctions associated with the bodies, ξ^{a_i} are vectors that take in to account the little group dependence of the wavefunction, and we use momentum eigenstates [39, 40, 50, 195]. Both parts of the wavefunction are defined such that $\int d\Phi(p)|\phi(p)|^2 = \sum_i |\xi_i|^2 = 1$.

We write the Lorentz invariant phase space as

$$\int d\Phi(p_i) \equiv \int \hat{d}^D p_i\,\hat{\delta}(p_i^2 - m_i^2), \tag{3.17}$$

where $D = 4 - 2\epsilon$, $\hat{d}^D p_i \equiv d^D p_i/(2\pi)^D$, and $\hat{\delta}(p_i^2 - m_i^2) \equiv 2\pi\theta(p_i^0)\delta(p_i^2 - m^2)$. Because we will be taking the classical limit, we will ignore the positive energy enforcing θ-function from now on. We also assume a displacement b_i for each particle in the wavepacket with respect to some arbitrary origin.

We can re-express the change in the observable for two-body scattering as

$$\Delta\mathcal{O} = \prod_{i=1}^{2}\sum_{a_i,a_i'}\int d\Phi(p_i)\, d\Phi(p_i')\, \phi^*(p_i')\phi(p_i)\, \xi^*_{a_i'}\, \xi^{a_i}\, e^{-ib_i\cdot(p_i'-p_i)}\, (\mathcal{I}_{v\ \{a_i\}}^{\{a_i'\}} + \mathcal{I}_{r\ \{a_i\}}^{\{a_i'\}}), \tag{3.18}$$

where

$$\mathcal{I}_{v\ \{a_i\}}^{\{a_i'\}} = \langle p_1'p_2'; a_1'a_2'|i[\mathbb{O},T]|p_1p_2;a_1a_2\rangle, \qquad \mathcal{I}_{r\ \{a_i\}}^{\{a_i'\}} = \langle p_1'p_2'; a_1'a_2'|T^\dagger[\mathbb{O},T]|p_1p_2;a_1a_2\rangle, \tag{3.19}$$

are known in the literature as the virtual kernel and real kernel, respectively.

We define the amplitude as

$$\begin{aligned}\langle p_1'p_2'; a_1'a_2'|T|p_1p_2;a_1a_2\rangle &= \hat{\delta}^{(4)}(p_1'+p_2'-p_1-p_2)\,[\mathcal{A}\left(p_1,p_2,p_1',p_2',S(p_1),S(p_2)\right)]^{a_1'a_2'}_{a_1a_2}\\ &\equiv \hat{\delta}^{(4)}(p_1'+p_2'-p_1-p_2)\,\epsilon^{*\,a_1'}(p_1')\epsilon^{*\,a_2'}(p_2')\cdot\mathbb{A}(p_1,p_2,p_1',p_2')\cdot\epsilon_{a_1}(p_1)\epsilon_{a_2}(p_2),\end{aligned} \tag{3.20}$$

where we leave products over representation indices implicit and $\mathbb{A}$ is the polarization-stripped amplitude, which helps clarify the little group dependence of the amplitude. Note that $\mathbb{A}$ depends only on the momenta and not on the spin tensors because we have stripped the polarization tensors, leaving us with Lorentz generators.

Recalling Eq. (3.8), we can see that all the little group dependence of the amplitude is in the spin tensor. Therefore, an important quantity we need to consider is the expectation value of the spin tensors

$$\prod_{i=1}^{2}\int d\Phi(p_i)|\phi(p_i)|^2\sum_{a_ia_i'}\xi^*_{a_i'}\,\left[S^{\mu(s_i)\nu(s_i)}(p_i)\right]^{a_i'}_{\ a_i}\xi^{a_i} = \langle S_1^{\mu(s_1)\nu(s_1)}\rangle\langle S_2^{\mu(s_2)\nu(s_2)}\rangle. \tag{3.21}$$

In the classical limit, following the arguments in Refs. [39, 40, 50, 195], the wave packets $\phi(p_i), \phi^*(p_i')$ sharply peak about their classical value. Similarly, when we consider the ξ_{a_i} to be spin coherent states, the spin tensors will be sharply fixed to their classical value with minimal variance, which we have labeled as $S_i^{\mu\nu}$ for each spin tensor. Because all the little group information is contained in the spin tensor, we will ignore the little group indices for the amplitude under the understanding that the $S_i^{\mu(s_i)\nu(s_i)}$ are matrix valued in them; we will also ignore the angle brackets in the classical limit.

With these simplifications in mind, when we take the classical limit we can express Eq. (3.18) more simply

$$\Delta\mathcal{O} = \int \hat{d}^D q\, \hat{\delta}(2p_1\cdot q + q^2)\, \hat{\delta}(2p_2\cdot q - q^2)\, e^{-ib\cdot q}\,(\mathcal{I}_v + \mathcal{I}_r) \equiv \int \not{D} q\, e^{-ib\cdot q}\,(\mathcal{I}_v + \mathcal{I}_r), \quad (3.22)$$

where $q^\mu = p_1'^\mu - p_1^\mu$ is the small momentum transfer conjugate to the impact parameter $b^\mu = b_2^\mu - b_1^\mu$, and we have absorbed the δ-functions into the the measure via the $\not{D}$ notation.

3.2.4 Special Kinematic Variables

When deriving the eikonal formulas, we want to explicitly show that our expressions uniformly scale classically; however the current kinematic set up makes this difficult. For example, in either of the momentum-conserving δ-functions in Eq. (3.22), we can see an inhomogeneity in the classical scaling

$$\hat{\delta}(2p_1\cdot q + q^2) \to \hat{\delta}(2\lambda p_1\cdot q + \lambda^2 q^2), \quad (3.23)$$

which makes it difficult to keep track of the overall scaling of our integrands. A convenient reparameterization of the momenta for the calculation of two-body scattering observables in the eikonal limit that simplifies this issue are the following,

$$\bar{p}_1 = p_1 + q/2, \qquad \bar{p}_2 = p_2 - q/2, \qquad y = \frac{\bar{p}_1\cdot\bar{p}_2}{\bar{m}_1\bar{m}_2}, \qquad \bar{m}_i^2 = \bar{p}_i^2 = m_i^2 - q^2/4. \quad (3.24)$$

This new set of momenta special kinematic variables [47, 76] simplify our δ-functions to be $\hat{\delta}(2\bar{p}_1\cdot q)\hat{\delta}(2\bar{p}_2\cdot q)$, however the momentum shift will have other effects on our observable integrands.

3.2.5 The Eikonal Phase

We will briefly review the eikonal-phase formalism and recent developments in this subject in the context of scattering observables. A detailed discussion on the eikonal phase can be found in [144, 185, 186, 210]. In impact parameter space, it has been observed that the two-body scattering amplitude exponentiates

$$1 + i\,\mathcal{A}(b) = (1 + i\Delta(b))\, e^{i\delta(b)}, \tag{3.25}$$

where $\delta(b)$ is the eikonal phase, $\Delta(b)$ is a quantum remainder, and

$$\mathcal{A}(b) = \int \hat{d}q\, \mathcal{A}(q)\, e^{-ib\cdot q} \equiv \mathrm{FT}[\mathcal{A}(q)], \tag{3.26}$$

where we leave the dependence of the amplitude on other variables such as external momenta and spins implicit.

By expanding Eq. (3.25) in powers of the coupling constant and in powers of classical scaling parameter λ, one can relate the amplitude order by order to the eikonal phase. Up to next to leading order in the coupling constant,

$$\delta^{(1)}(b) = \mathrm{FT}[\mathcal{A}^{(1)}(q)], \qquad \delta^{(2)}(b) = \mathrm{FT}[\mathrm{Re}\,\mathcal{A}^{(2)}], \tag{3.27}$$

where we assume that Eq. (3.27) holds to all orders in the spin expansion and the superscript counts powers of the coupling constant.

In Ref. [121], the authors calculated scattering observables for gravity by calculating amplitudes using general-spin QFT, relating this to an EFT potential and then used Hamilton's equations to calculate the momentum impulse and spin kick. This procedure has been used to calculate observables up to fifth power in spin at one loop [177]. From their results, they were able to construct an ansatz that relates the eikonal phase to these observables via simple operations such as commutation or differentiation. In Refs. [195, 197], both works were able to derive an eikonal formula at one loop. In particular Ref. [195], who used the eikonal formalism, was able to show that these one-loop eikonal formulas come from half variable shifts of their tree-level observables, suggesting an iterative pattern.

While Ref. [195] was able to derive an one-loop eikonal formula that they validated to quadratic order in spin, they did so assuming a SSC and using fixed-spin states. In this work, we will refrain from imposing a SSC in our derivation in order to have as general a result as possible. As stated earlier, by allowing lower spin states to propagate in our fields we imply a violation of the SSC, which allows us to use simple relations such as Eq. (3.7) to derive the one-loop eikonal formulas. We will show that, after deriving the formulas, we can properly impose the SSC to recover the result found in Ref. [195].

3.3 General-Spin Amplitudes

When calculating the observables from general spin amplitudes we perform a perturbative expansion in the coupling constant g^2 in our QFT; for example, this could be the fine structure constant α or the gravitational constant G. We will organize this expansion in the following way

$$\mathcal{A}(q, p_1, p_2, S_1, S_2) = g^2 \mathcal{A}^{(1)}(q, p_1, p_2, S_1, S_2) + g^4 \mathcal{A}^{(2)}(q, p_1, p_2, S_1, S_2) + \cdots \tag{3.28}$$

where g is some coupling constant and we will refer to $\mathcal{A}^{(1)}$ as the tree-level amplitude and $\mathcal{A}^{(2)}$ as the one-loop amplitude. There are basic structures of these amplitudes in the eikonal limit that are crucial to the calculation of the eikonal formulas.

3.3.1 Tree-level Amplitudes

We know that the tree-level amplitude should have the following properties in the eikonal limit:

1. Model elastic scattering;

2. Lead to a Coulomb potential: $V(b) \propto 1/b$;

3. Have the same classical scaling as the $s_1 = s_2 = 0$ case: $\mathcal{A}^{(1)} \to \mathcal{O}(\lambda^{-2})\mathcal{A}^{(1)}$.

With these properties we can construct an ansatz for the tree-level amplitude

$$\mathcal{A}^{(1)}(q,p_i,S_i) = e^{iq\cdot(\omega_1-\omega_2)}\sum_{s_1,s_2}\mathcal{A}^{(1,\,s_1,\,s_2)}(q,p_i,S_i) \tag{3.29}$$

$$\mathcal{A}^{(1,\,s_1,\,s_2)}(q,p_i,S_i) = i^{(s_1+s_2)}\frac{q_{\mu(s_1)}q_{\rho(s_2)}}{q^2}S_1^{\mu(s_1)\nu(s_1)}S_2^{\rho(s_2)\sigma(s_2)}\Upsilon^{(1)}_{\nu(s_1)\sigma(s_2)}(p_1,p_2), \tag{3.30}$$

where $q_{\mu(s_1)} = q_{\mu_1}q_{\mu_2}\cdots q_{\mu_{s_1}}$, $S_1^{\mu(s_1)\nu(s_1)}S_2^{\rho(s_2)\sigma(s_2)}$ can be read off from Eq.(3.13), and $\Upsilon^{(1)}_{\nu(s_1)\sigma(s_2)}(p_1,p_2)$ is some s_1+s_2 ranked tensor at tree-level that is a function of the external momenta. One can construct an ansatz for Υ, however, for the purposes of deriving the eikonal formulas this will not be necessary. We include in the Appendix the ansatz we used to perform our checks. For clarity, we will provide a few examples:

$$\mathcal{A}^{(1,\,0,\,0)}(q,p_1,p_2) = \frac{\Upsilon^{(1)}(p_1,p_2)}{q^2}, \tag{3.31}$$

$$\mathcal{A}^{(1,\,1,\,0)}(q,p_1,p_2) = iq_{\mu_1}S_1^{\mu_1\nu_1}\frac{\Upsilon^{(1)}_{\nu_1}(p_1,p_2)}{q^2}, \tag{3.32}$$

$$\mathcal{A}^{(1,\,1,\,1)}(q,p_1,p_2) = -q_{\mu_1}q_{\rho_2}S_1^{\mu_1\nu_1}S_2^{\rho_1\sigma_1}\frac{\Upsilon^{(1)}_{\nu_1\sigma_2}(p_1,p_2)}{q^2}, \tag{3.33}$$

$$\mathcal{A}^{(1,\,2,\,0)}(q,p_1,p_2) = -q_{\mu_1}q_{\mu_2}S_1^{\mu_1\nu_1}S_1^{\mu_2\nu_2}\frac{\Upsilon^{(1)}_{\nu_1\nu_2}(p_1,p_2)}{q^2}, \tag{3.34}$$

where the different $\Upsilon^{(1)}$ can be found in the Appendix.

The exponential prefactor in Eq. (3.29) comes from the exponentiation of the product of the polarization tensors [116, 121, 170, 197], which are a universal feature in scattering amplitudes,

$$\epsilon^*(p_1+q)\cdot\epsilon(p_1) = e^{iq\cdot\omega_1}, \qquad \epsilon^*(p_2-q)\cdot\epsilon(p_2) = e^{-iq\cdot\omega_2} \tag{3.35}$$

where $\omega_i^\mu(p_i) = S_i^{\mu\nu}(k_{i\,\nu}+p_{i\,\nu})/(p_i\cdot k_i+m_i^2)$. We can think of these as matrix exponentials in the little group space. Here k_i are the reference momenta of each scattering body, which is taken to be the rest frame. In the context of the KMOC formalism, we can absorb these exponentials into our impact parameter, such that we shift into a new position space coordinate

$$b_{cov} \equiv b - (\omega_1-\omega_2), \tag{3.36}$$

which we will refer to as the covariant impact parameter. From now on we will be working with b_{cov} and therefore we will ignore the exponential prefactor when considering Eq. (3.29). For a discussion on changing between the canonical impact parameter, b, and b_{cov}, see Ref. [211].

3.3.2 One-Loop Amplitudes

The one-loop amplitude in the eikonal limit can be broken down into box, triangle, and bubble diagrams [47, 76, 184]. Equivalently, we can decompose the one-loop amplitude into real and imaginary contributions. These two decompositions are related in the following way

$$\mathcal{A}^{(2)} = \mathrm{Re}\,\mathcal{A}^{(2)} + i\mathrm{Im}\,\mathcal{A}^{(2)}, \tag{3.37}$$

$$\mathrm{Re}\,\mathcal{A}^{(2)} = \mathcal{A}^{(2)}_{\Delta} + \mathcal{A}^{(2)}_{\nabla} \to (\lambda^{-1})\mathrm{Re}\,\mathcal{A}^{(2)}, \tag{3.38}$$

$$\mathrm{Im}\,\mathcal{A}^{(2)} = \mathcal{A}^{(2)}_{\text{Box}} + \mathcal{A}^{(2)}_{\text{xBox}} \to (\lambda^{-2})\mathrm{Im}\,\mathcal{A}^{(2)}, \tag{3.39}$$

where we ignore the bubble contributions, since they do not contribute in the eikonal limit at this loop order. We have also highlighted the fact that the real and imaginary contributions have different classical scalings. The real contribution has the expected scaling to be a classical contribution. The imaginary contribution has a lower than expected scaling which is known in the literature as a super-classical or classically-singular contribution [39, 47, 178]. The classically-singular contribution is associated with the infrared divergence that arises from the sum of the box and cross-box diagrams; this divergence must vanish when calculating IR safe observables, such as the momentum impulse and spin kick, and we will show how this explicitly occurs when deriving the eikonal formulas.

We can also construct an ansatz for $\mathrm{Re}\,\mathcal{A}^{(2)}$ in a similar fashion to the tree-level ansatz,

$$\mathrm{Re}\,\mathcal{A}^{(2)} = \sum_{s_1,s_2} \frac{i^{(s_1+s_2)} S_1^{\mu(s_1)\nu(s_1)} S_2^{\rho(s_2)\sigma(s_2)}}{\sqrt{-q^2}} \Big\{ q_{\mu(s_1)} q_{\rho(s_2)} \Upsilon^{(2)}_{\nu(s_1)\sigma(s_2)}$$
$$+q^2 \Big(q_{\mu(s_1-2)} q_{\rho(s_2)} \Upsilon^{(2)}_{\mu_{s_1}\mu_{s_1-1}\nu(s_1)\sigma(s_2)} + q_{\mu(s_1)} q_{\rho(s_2-2)} \Upsilon^{(2)}_{\nu(s_1)\rho_{s_2}\rho_{s_2-1}\sigma(s_2)}$$
$$+q_{\mu(s_1-1)} q_{\rho(s_2-1)} \Upsilon^{(2)}_{\mu_{s_1}\nu(s_1)\rho_{s_2}\sigma(s_2)} \Big) + \cdots \Big\}, \tag{3.40}$$

where, in principle, we can continue to replace factors of $q_{\mu_i} q_{\mu_j}, q_{\mu_i} q_{\rho_j}, q_{\rho_i} q_{\rho_j}$ with factors of q^2 since this will not create contact terms. While Eq. (3.40) is not necessary to derive the eikonal formulas, it will be necessary when verifying them up to quadratic order in spin. We adopt the convention that $q_{\mu(-1)} = q_{\rho(-1)} = 0$ and $q_{\mu(0)} = q_{\rho(0)} = 1$. We also suppress the momentum dependence with the understanding the $\Upsilon^{(2)} \equiv \Upsilon^{(2)}(p_1, p_2)$.

3.3.3 Unitarity with Higher Spin

As mentioned before, the imaginary part of the one-loop amplitude is the sum of the box and cross box diagrams. It is well known that this combination can be expressed as the on-shell product of tree-level amplitudes, which can be seen using unitarity and truncating to one-loop order

$$2\,\mathrm{Im}\,\mathcal{A}^{(2)}(q, p_1, p_2) = \int \not{D}l\, \mathcal{A}^{(1)}(q-l, p_1+l, p_2-l)\, \mathcal{A}^{(1)}(l, p_1, p_2), \tag{3.41}$$

where l is the loop momentum and we have left the dependence on the spin tensors implicit. However, this product is obscures the full picture. Recall that when we take products of Lorentz generator we need to decompose terms into symmetric and anti-symmetric products. Stripping the amplitudes of their polarizations makes this clearer

$$2\,\mathrm{Im}\,\mathbb{A}^{(2)}(q, p_1, p_2) = \int \not{D}l\, \mathbb{A}^{(1)}(q-l, p_1+l, p_2-l)\, \mathbb{A}^{(1)}(l, p_1, p_2)$$
$$= \frac{1}{2} \int \not{D}l \left(\left[\mathbb{A}^{(1)}(q-l, p_1+l, p_2-l), \mathbb{A}^{(1)}(l, p_1, p_2) \right] \right.$$
$$\left. + \left\{ \mathbb{A}^{(1)}(q-l, p_1+l, p_2-l), \mathbb{A}^{(1)}(l, p_1, p_2) \right\} \right). \tag{3.42}$$

Now the anti-symmetric term has the same classical scaling as the real part of the one-loop amplitude i.e. it has been promoted from a classically-singular to a classical contribution. On the other hand, the symmetric product continues to be classically-singular.

We still have yet to shift to the barred variables $\bar{p}_i$, which has the potential to promote the classical scaling of the amplitudes. Assuming that q and l have the same scaling, we can expand the amplitudes in small λ (or Equivalently soft internal momenta q, l) resulting in the following transformations to our tree-level amplitudes

$$\mathbb{A}^{(1)}(l, p_1, p_2) \to \left(1 - \left(\frac{q-l}{2}\right) \cdot \left(\frac{\partial}{\partial \bar{p}_1} - \frac{\partial}{\partial \bar{p}_2}\right)\right) \mathbb{A}^{(1)}(l, \bar{p}_1, \bar{p}_2), \tag{3.43}$$

$$\mathbb{A}^{(1)}(q-l, p_1+l, p_2-l) \to \left(1 + \frac{l}{2} \cdot \left(\frac{\partial}{\partial \bar{p}_1} - \frac{\partial}{\partial \bar{p}_2}\right)\right) \mathbb{A}^{(1)}(q-l, \bar{p}_1, \bar{p}_2). \tag{3.44}$$

This transformation does not affect the anti-symmetric term in Eq. (3.42) because it already scales classically and any promotion would over-correct it to a quantum contribution.

The shift to barred variables also has another more subtle yet crucial effect. Recall that we are integrating over $\not{D}l$, which upon shifting to barred variables becomes

$$\not{D}l \to \hat{d}^D l\, \hat{\delta}(2\bar{p}_1 \cdot l - q^2/2)\, \hat{\delta}(2\bar{p}_2 \cdot l + q^2/2) \tag{3.45}$$

where, while keeping in mind that we are only interested in long-range scattering, we make the replacement $q \cdot l \to q^2/2$ in order to avoid canceling any massless propagators. Once again we have a δ-function that is inhomogenous in classical scaling, which allows us to expand it,

$$\not{D}\, l \to \left(1 + \frac{q^2}{4}\left(\frac{\check{u}_2^\alpha}{\bar{m}_2} - \frac{\check{u}_1^\alpha}{\bar{m}_1}\right)\frac{\partial}{\partial l^\alpha}\right) \hat{\delta}\left(2\bar{p}_1 \cdot l\right)\, \hat{\delta}\left(2\bar{p}_2 \cdot l\right), \tag{3.46}$$

where we truncate to the leading correction. Here $\check{u}_{1,2} \equiv (u_{1,2} - y u_{2,1})/(1-y^2)$, such that $\check{u}_i \cdot u_j = \delta_{i,j}$, where $u_i \equiv \bar{p}_i/\bar{m}_i$ is the classical velocity. We will eventually integrate by parts to remove the derivative from the δ-functions, which will result in new classical contributions. Ref. [168] used this procedure in a similar context.

With the barred variables applied, and restoring the polarization tensors, we have the following imaginary contribution to the one-loop amplitude

$$\begin{aligned}
&2\,\mathrm{Im}\,\mathcal{A}^{(2)}(q,p_1,p_2) \\
&= \int \hat{d}\!\!\!/ l \left\{ \mathcal{A}^{(1)}(l,\bar{p}_1,\bar{p}_2)\mathcal{A}^{(1)}(q-l,\bar{p}_1,\bar{p}_2) + \frac{1}{2}\left[\mathcal{A}^{(1)}(q-l,\bar{p}_1,\bar{p}_2), \mathcal{A}^{(1)}(l,\bar{p}_1,\bar{p}_2)\right] \right. \\
&\qquad + \mathcal{A}^{(1)}(l,\bar{p}_1,\bar{p}_2)\,\frac{l}{2}\cdot\left(\frac{\partial}{\partial\bar{p}_1}-\frac{\partial}{\partial\bar{p}_2}\right)\mathcal{A}^{(1)}(q-l,\bar{p}_1,\bar{p}_2) \\
&\qquad \left. - \mathcal{A}^{(1)}(q-l,\bar{p}_1,\bar{p}_2)\frac{(q-l)}{2}\cdot\left(\frac{\partial}{\partial\bar{p}_1}-\frac{\partial}{\partial\bar{p}_2}\right)\mathcal{A}^{(1)}(l,\bar{p}_1,\bar{p}_2) \right\} \\
&\quad + \left(\frac{\check{u}_2^{\alpha}}{\bar{m}_2}-\frac{\check{u}_1^{\alpha}}{\bar{m}_1}\right)\frac{q^2}{4}\int \hat{d}^D l\,\mathcal{A}^{(1)}(l,\bar{p}_1,\bar{p}_2)\,\mathcal{A}^{(1)}(q-l,\bar{p}_1,\bar{p}_2)\frac{\partial}{\partial l^{\alpha}}\left(\hat{\delta}\left(2\bar{p}_1\cdot l\right)\,\hat{\delta}\left(2\bar{p}_2\cdot l\right)\right),
\end{aligned} \tag{3.47}$$

where only the symmetric product in the first line, which is the naive unitarity relation, is still classically-singular.

In principle, $\mathrm{Im}\,\mathcal{A}^{(2)}$ should obey what is known as the horizontal-flip symmetry [47, 189], which is to say that the integrand in Eq. (3.47) should be invariant under the exchange of massless propagators $l \leftrightarrow q-l$. This is clear to see diagrammatically,

$2\,\mathrm{Im}\,\mathcal{A}^{(2)}(q,p_1,p_2) = \int \hat{d}^D l$ 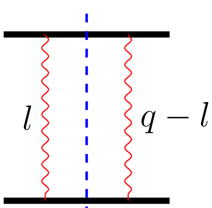

$= \int \hat{d}^D l$ 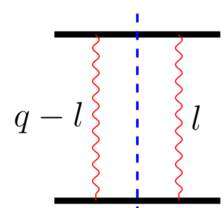

, (3.48)

where the dashed line represents a unitarity cut. Note that if we were to enforce this symmetry, only the symmetric product and last line of Eq. (3.47) would survive, since the other terms are parity-odd under this exchange. In the context of KMOC, the integrand in Eq.(3.47) will be acted on by operators which may affect the parity of the integrand with respect to the horizontal-flip symmetry, which we will see in the upcoming sections.

3.4 Momentum Impulse from KMOC with Spin

We will start by deriving the eikonal formula for the momentum impulse. Because our wavepackets are expressed in terms of momentum eigenstates, the momentum operator acts in the following way:

$$\mathbb{P}_1^\mu|p_1,p_2\rangle = p_1^\mu|p_1p_2\rangle. \tag{3.49}$$

We will first calculate the virtual contribution followed by the real contribution. We will then reorganize the contributions to the momentum impulse into non-iteration and iteration pieces, focusing on the latter since it is more non-trivial.

3.4.1 Virtual and Real Kernel Contribution

Applying the momentum operator, for the virtual contribution we get

$$\langle\Psi|i[\mathbb{P}^\mu,T]|\Psi\rangle = \int \not{D}q e^{-ib_{\mathrm{cov}}\cdot q}\mathcal{I}_v^\mu = \int \not{D}q e^{-ib_{\mathrm{cov}}\cdot q} iq^\mu \mathcal{A}(q,p_1,p_2). \tag{3.50}$$

At tree level, this is the only contribution to the momentum impulse

$$\begin{aligned}\Delta^{(1)}p_1^\mu &= \int \not{D}q e^{-ib_{\mathrm{cov}}\cdot q} iq^\mu \mathcal{A}^{(1)}(q,p_1,p_2)\\ &= -\frac{\partial}{\partial(b_{\mathrm{cov}\,\mu})_\perp}\int \not{D}q e^{-ib_{\mathrm{cov}}\cdot q}\mathcal{A}^{(1)}(q,p_1,p_2) = -\Pi^{\mu\nu}\frac{\partial\delta^{(1)}_{\mathrm{cov}}}{\partial b^\nu_{\mathrm{cov}}},\end{aligned} \tag{3.51}$$

where we use the shorthand $\delta_{\mathrm{cov}} = \delta(b_{\mathrm{cov}},u_1,u_2,S_1,S_2)$ and

$$\Pi^{\mu\nu} = \eta^{\mu\nu} - u_1^\mu\check{u}_1^\nu - u_2^\mu\check{u}_2^\nu, \tag{3.52}$$

is a projector that we are free to introduce due to the on-shell energy-conserving δ-functions in $\not{D}q$. When exchanging q^μ for $i\partial/\partial b_{\mathrm{cov}\,\mu}$, the projector preserves the on-shell condition upon taking derivatives. Anytime we are able to apply the on-shell conditions, we can introduce the projector in our integrand via the transformation $q^\mu \to \Pi^\mu{}_\nu q^\nu$. Note that because the transfer momentum and impact parameter obey the same on-shell conditions ($b_{\mathrm{cov}}\cdot p_i = 0$), we can also freely make the exchange $b^\mu_{\mathrm{cov}} \to \Pi^\mu{}_\nu b^\nu_{\mathrm{cov}}$. As a result, we impose that all scalar products involving b_{cov}, q must be broken down in the following way to protect the on-shell conditions

$$v\cdot b_{\mathrm{cov}} \to v_\mu b_{\mathrm{cov}\,\nu}\Pi^{\mu\nu}, \quad v\cdot q \to v_\mu q_\nu \Pi^{\mu\nu}, \tag{3.53}$$

for some vector v. This subtlety will become important once we move on to the one-loop case.

At tree level, we do not need to worry how switching to barred variables will affect the scaling, since any promotions associated with the momentum shift would be an over-correction i.e., result in quantum contributions. Therefore, we can make the simple replacement $p_i \to \bar{p}_i$ and then take the classical value of the momenta $\bar{p}_i^\mu = \bar{m}_i u_i^\mu$.

At one loop, the virtual part of the momentum impulse can be broken down into contributions from the real and the imaginary part of the one-loop amplitude,

$$\int \hat{d}q e^{-ib_{\text{cov}}\cdot q} \left(iq^\mu \text{Re}\mathcal{A}^{(2)}(q,p_1,p_2) - q^\mu \text{Im}\,\mathcal{A}^{(2)}(q,p_1,p_2)\right) \equiv \Delta^{(2)} p^\mu_{1\,v,\text{Re}} + \Delta^{(2)} p^\mu_{1\,v,\text{Im}}. \quad (3.54)$$

The contribution from $\Delta^{(2)} p^\mu_{1\,v,\text{Re}}$ will follow the same procedure in the tree-level case since it is already at the correct scaling to be considered classical,

$$\Delta^{(2)} p^\mu_{1\,v,\text{Re}} = \int \hat{d}q e^{-ib_{\text{cov}}\cdot q} iq^\mu \text{Re}\mathcal{A}^{(2)}(q,\bar{p}_1,\bar{p}_2) = -\frac{\partial \delta^{(2)}_{\text{cov}}}{\partial (b_{\text{cov}\,\mu})_\perp}. \quad (3.55)$$

The real kernel only starts contributing at one loop. Plugging in for the momentum operator we get

$$\begin{aligned}\langle\Psi|T^\dagger[\mathbb{P}_1^\mu, T]|\Psi\rangle|_{\text{NLO}} = \Delta^{(2)} p_r^\mu &= \int \hat{d}q e^{-ib_{\text{cov}}\cdot q} \mathcal{I}_r^{(2)\,\mu} \\ &= \int \hat{d}q e^{-ib_{\text{cov}}\cdot q} \int \hat{d}l\, l^\mu \mathcal{A}^{(1)}(q-l, p_1+l, p_2-l)\mathcal{A}^{(1)}(l,p_1,p_2). \quad (3.56)\end{aligned}$$

As was the case for $\text{Im}\,\mathcal{A}^{(2)}$, we will need to strip the amplitudes of their polarizations, break down the product of amplitudes into symmetric and anti-symmetric parts, apply the momentum shift to barred variables, and expand the shifted integrand. In the momentum impulse case, this procedure produces the same result as Eq. (3.47) except for the prefactor of l^μ, which leads to a new organization of our momentum impulse contributions.

3.4.2 Iterative Contribution

We organize the remaining contributions to the momentum impulse, in the following way

$$\Delta^{(2)} p^\mu_{it} \equiv \Delta^{(2)} p^\mu_{r} + \Delta^{(2)} p^\mu_{1\,v,\mathrm{Im}} = \Delta^{(2)} p^\mu_{it,*} + \Delta^{(2)} p^\mu_{it,\partial u} + \Delta^{(2)} p^\mu_{it,\partial l}. \tag{3.57}$$

We will refer to Eq. (3.57) as the iterative contribution since it is proportional to on-shell products of tree amplitudes.

The first term, $\Delta^{(2)} p^\mu_{it,*}$, is proportional to the symmetric and anti-symmetric product of the amplitudes

$$\Delta^{(2)} p^\mu_{it,*} \equiv \int \hat{d}q e^{-ib_{\mathrm{cov}}\cdot q} \int \hat{d}l \left(\frac{l^\mu - (q^\mu - l^\mu)}{2}\right) \\ \left(\mathcal{A}^{(1)}(q-l,\bar{p}_1,\bar{p}_2)\mathcal{A}^{(1)}(l,\bar{p}_1,\bar{p}_2) + \frac{1}{2}\left[\mathcal{A}^{(1)}(q-l,\bar{p}_1,\bar{p}_2), \mathcal{A}^{(1)}(l,\bar{p}_1,\bar{p}_2)\right]\right), \tag{3.58}$$

where the symmetric product still is classically-singular. To simplify Eq. (3.58), we will enforce the horizontal-flip symmetry. Because the prefactor $(l^\mu - (q^\mu - l^\mu))/2$ is parity-odd under the exchange $l \to q - l$, the only term that will survive is the anti-symmetric product

$$\Delta^{(2)} p^\mu_{it,*} = \int \hat{d}q e^{-ib_{\mathrm{cov}}\cdot q} \int \hat{d}l \left[\mathcal{A}^{(1)}(q-l,\bar{p}_1,\bar{p}_2), \frac{l^\mu}{2}\mathcal{A}^{(1)}(l,\bar{p}_1,\bar{p}_2)\right], \tag{3.59}$$

where we exploited the overall horizontal-flip symmetry to write the above in a more compact form. By enforcing the horizontal-flip symmetry, we got rid of the only classically-singular term left in the calculation.

To express $\Delta^{(2)} p^\mu_{it,*}$ in terms of eikonal phases, we need to change the loop integral into a Fourier transform; to do this we perform the shift $q \to q + l$,

$$\begin{aligned} \Delta^{(2)} p^\mu_{it,*} &= \int \hat{d}q e^{-ib_{\mathrm{cov}}\cdot q} \int \hat{d}l e^{-ib_{\mathrm{cov}}\cdot l} \left[\mathcal{A}^{(1)}(q,\bar{p}_1,\bar{p}_2), \frac{l^\mu}{2}\mathcal{A}^{(1)}(l,\bar{p}_1,\bar{p}_2)\right] \\ &= \frac{i}{2}\left[\delta^{(1)}_{\mathrm{cov}}, \frac{\partial \delta^{(1)}_{\mathrm{cov}}}{\partial (b_{\mathrm{cov}\,\mu})_\perp}\right]. \end{aligned} \tag{3.60}$$

The second term in Eq. (3.57), $\Delta^{(2)}p^{\mu}_{it,\partial u}$, is proportional to the external momentum derivatives

$$\Delta^{(2)}p^{\mu}_{it,\partial u} \equiv \int \hat{d}q e^{-ib_{\rm cov}\cdot q}\int \hat{d}l \left(\frac{l^{\mu}-(q^{\mu}-l^{\mu})}{2}\right) \left(\mathcal{A}^{(1)}(l,\bar{p}_1,\bar{p}_2)\frac{l}{2}\cdot\left(\frac{\partial}{\partial\bar{p}_1}-\frac{\partial}{\partial\bar{p}_2}\right)\mathcal{A}^{(1)}(q-l,\bar{p}_1,\bar{p}_2) -\mathcal{A}^{(1)}(q-l,\bar{p}_1,\bar{p}_2)\frac{(q-l)}{2}\cdot\left(\frac{\partial}{\partial\bar{p}_1}-\frac{\partial}{\partial\bar{p}_2}\right)\mathcal{A}^{(1)}(l,\bar{p}_1,\bar{p}_2)\right), \quad (3.61)$$

For Eq. (3.61), we will repeat the same procedure of enforcing the horizontal-flip symmetry, shifting the transfer momentum $q\to q+l$, and then re-expressing the amplitudes in terms of eikonal phases,

$$\Delta^{(2)}p^{\mu}_{it,\partial u} = -\frac{1}{2}\frac{\partial\delta^{(1)}_{\rm cov}}{\partial(b_{{\rm cov}\,\alpha})_{\perp}}\frac{\overleftrightarrow{\partial}}{\partial(b_{{\rm cov}\,\mu})_{\perp}}\left(\frac{1}{\bar{m}_1}\frac{\partial}{\partial u_1^{\alpha}}-\frac{1}{\bar{m}_2}\frac{\partial}{\partial u_2^{\alpha}}\right)\delta^{(1)}_{\rm cov}, \quad (3.62)$$

where

$$f(x)\frac{\overleftrightarrow{\partial}}{\partial x}g(x) \equiv \frac{\partial f(x)}{\partial x}g(x) - f(x)\frac{\partial g(x)}{\partial x}. \quad (3.63)$$

The last term remaining, $\Delta^{(2)}p^{\mu}_{it,\partial l}$, comes from the expansion of the on-shell δ-functions

$$\Delta^{(2)}p^{\mu}_{it,\partial l} \equiv \int \hat{d}q e^{-ib_{\rm cov}\cdot q}\int \hat{d}^D l \left(\frac{l^{\mu}-(q^{\mu}-l^{\mu})}{2}\right)\frac{q^2}{4}\left(\frac{\check{u}_2^{\alpha}}{\bar{m}_2}-\frac{\check{u}_1^{\alpha}}{\bar{m}_1}\right) \mathcal{A}^{(1)}(l,\bar{p}_1,\bar{p}_2)\mathcal{A}^{(1)}(q-l,\bar{p}_1,\bar{p}_2)\frac{\partial}{\partial l^{\alpha}}\left(\hat{\delta}\left(2\bar{p}_1\cdot l\right)\,\hat{\delta}\left(2\bar{p}_2\cdot l\right)\right), \quad (3.64)$$

which will prove to be complicated to express in terms of eikonal phases. Say we integrate by parts to remove the derivative acting on the δ-functions, carry out the derivatives, and repeat the procedure we used for the previous contributions

$$\Delta^{(2)}p^{\mu}_{it,\partial l} = -\frac{1}{2}\left(\frac{\check{u}_2^{\mu}}{\bar{m}_2}-\frac{\check{u}_1^{\mu}}{\bar{m}_1}\right)\left(\frac{\partial\delta^{(1)}_{\rm cov}}{\partial(b_{\rm cov})_{\perp}}\right)^2 + \frac{1}{2}\left(\frac{\check{u}_1^{\alpha}}{\bar{m}_1}-\frac{\check{u}_2^{\alpha}}{\bar{m}_2}\right)\frac{\partial\delta^{(1)}_{\rm cov}}{\partial(b_{{\rm cov}\,\gamma})_{\perp}}\frac{\overleftrightarrow{\partial}}{\partial(b_{{\rm cov}\,\mu})_{\perp}}\int \hat{d}l e^{-ib_{\rm cov}\cdot l}l_{\gamma}\frac{\partial}{\partial l^{\alpha}}\mathcal{A}^{(1)}(l,\bar{p}_1,\bar{p}_2). \quad (3.65)$$

We are still left with a term that does not neatly lend itself to being expressed as an eikonal phase. We must also be careful when applying the on-shell conditions in $\hat{d}l$. Because the on-shell δ-functions were being acted on by derivatives, we are not necessarily able to freely introduce the projector Eq. (3.52) into our amplitude prior to integrating by parts. As a result, when evaluating the integrand above, we must first apply the derivative on the amplitude, and only then we are free to introduce the on-shell projector, making this a correction to the cut condition of the internal massive lines in Eq. (3.48).

To eventually express Eq. (3.65) fully in terms of eikonal phases, we plug in the ansatz for the tree-level general-spin amplitude Eq. (3.29). After recognizing that the loop momentum derivative effectively replaces the projector $\Pi^{\mu\nu}$ with other variables, we prescribe the following replacement rule

$$\int \hat{d}l e^{-ib_{\text{cov}}\cdot l} l_\gamma \frac{\partial}{\partial l^\alpha} \mathcal{A}^{(1)}(l, \bar{p}_1, \bar{p}_2) \to 2\frac{\partial \delta^{(1)}_{\text{cov}}}{\partial \Pi^{\alpha\gamma}}, \tag{3.66}$$

where we define the derivative with respect to the projector as

$$\frac{\partial \Pi_{\mu\nu}}{\partial \Pi_{\alpha\beta}} \equiv \frac{1}{2}\left(\delta^\alpha_\mu \delta^\beta_\nu + \delta^\beta_\mu \eta^\alpha_\nu\right), \tag{3.67}$$

due to its symmetric nature. We must emphasize that taking the derivative with respect to the projector is more of a bookkeeping strategy that arrives at the desired expression; in the appendix, we provide an analysis of how we arrived at this resolution and an alternative way of expressing it. Note that as a result of our prescription for scalar products, Eq.(3.53), $\frac{\partial}{\Pi^{\alpha\beta}} b\cdot v = v^{(\alpha}b^{\beta)}$. We also emphasize that if we had taken the derivative with the on-shell projector already applied Eq. (3.65) would have vanished.

We now combine all of our contributions to the impulse to derive the higher-spin eikonal formula for the one-loop momentum impulse

$$\begin{aligned}\Delta^{(2)} p_1^\mu = &-\frac{\partial \delta^{(2)}_{\text{cov}}}{\partial (b_{\text{cov}\,\mu})_\perp} + \frac{i}{2}\left[\delta^{(1)}_{\text{cov}}, \frac{\partial \delta^{(1)}_{\text{cov}}}{\partial (b_{\text{cov}\,\mu})_\perp}\right] - \frac{1}{2}\left(\frac{\check{u}_1^\mu}{\bar{m}_1} - \frac{\check{u}_2^\mu}{\bar{m}_2}\right)\left(\frac{\partial \delta^{(1)}_{\text{cov}}}{\partial (b_{\text{cov}})_\perp}\right)^2 \\ &+ \frac{\partial \delta^{(1)}_{\text{cov}}}{\partial (b_{\text{cov}\,\alpha})_\perp} \frac{\overleftrightarrow{\partial}}{\partial (b_{\text{cov}\,\mu})_\perp}\left(\left(\frac{\check{u}_1^\beta}{\bar{m}_1} - \frac{\check{u}_2^\beta}{\bar{m}_2}\right)\frac{\partial}{\partial \Pi^{\alpha\beta}} - \frac{1}{2}\left(\frac{1}{\bar{m}_1}\frac{\partial}{\partial u_1^\alpha} - \frac{1}{\bar{m}_2}\frac{\partial}{\partial u_2^\alpha}\right)\right)\delta^{(1)}_{\text{cov}}.\end{aligned} \tag{3.68}$$

We compared Eq. (3.68) to the results in Ref. [195] up to quadratic order in spin and found full agreement. As another check we have verified that Eq. (3.68) also satisfies momentum conservation, which can be easily seen if we make explicit the factors of $\Pi^{\mu\nu}$ in the derivative $\partial/\partial(b_{\mathrm{cov}\,\mu})_\perp$.

Note that we have not made use of any specific spin representation to arrive at Eq.(3.68), implying that it is valid to all orders in spin; it would be interesting to see if this holds at higher than quadratic orders in spin.

We can also rewrite Eq. (3.68) in terms of the tree-level momentum impulse to simplify our expression and reveal the iterative nature of the impulse formula,

$$\Delta^{(2)}p_1^\mu = -\frac{\partial\delta^{(2)}_{\mathrm{cov}}}{\partial(b_{\mathrm{cov}\,\mu})_\perp} - \frac{i}{2}\left[\delta^{(1)}_{\mathrm{cov}}, \Delta^{(1)}p_1^\mu\right] - \frac{1}{2}\left(\frac{\check{u}_1^\mu}{\bar{m}_1} - \frac{\check{u}_2^\mu}{\bar{m}_2}\right)\left(\Delta^{(1)}p_1\right)^2 \\ + \frac{1}{2}\Delta^{(1)}p_{1\,\alpha}\frac{\overleftrightarrow{\partial}}{\partial(b_{\mathrm{cov}\,\mu})_\perp}\nabla^\alpha_{p_{\mathrm{cm}}}\delta^{(1)}_{\mathrm{cov}}, \tag{3.69}$$

where we define

$$\nabla^\alpha_{p_{\mathrm{cm}}} \equiv \left(\frac{1}{\bar{m}_1}\frac{\partial}{\partial u_{1\,\alpha}} - \frac{1}{\bar{m}_2}\frac{\partial}{\partial u_{2\,\alpha}}\right) - 2\left(\frac{\check{u}_{1\,\beta}}{\bar{m}_1} - \frac{\check{u}_{2\,\beta}}{\bar{m}_2}\right)\frac{\partial}{\partial\Pi_{\alpha\beta}} \tag{3.70}$$

as some derivative that respects the center-of-mass symmetry of the two-body system. We find that imposing a SSC removes the derivative part of the cut-correction contribution, Eq. (3.65), leading to the replacement $\nabla^\alpha_{p_{\mathrm{cm}}} \to \left(\frac{1}{\bar{m}_1}\frac{\partial}{\partial u_{1\,\alpha}} - \frac{1}{\bar{m}_2}\frac{\partial}{\partial u_{2\,\alpha}}\right)$. This is an interesting consequence of imposing the SSC and hints at some relation between these cut corrections and the choice of using non-transverse, massive spinning fields.

3.5 Spin Kick from KMOC with Spin

In this section we will derive the higher-spin eikonal formula for the one-loop spin kick. Similarly to the momentum impulse case, we will begin by looking at the virtual and real kernels by applying the appropriate spin tensor operator

$$\langle p_1'p_2'|\mathbb{S}_1^{\mu\nu}|p_1p_2\rangle = \hat{\delta}_\Phi(p_1'-p_1)\hat{\delta}_\Phi(p_2'-p_2)\,\epsilon^*(p_1')\cdot M^{\mu\nu}\cdot\epsilon(p_1), \tag{3.71}$$

where $\hat{\delta}_\Phi(p'-p)$ is the δ-function for the Lorentz invariant phase space integral such that $\int d\Phi(p)\, f(p)\, \hat{\delta}_\Phi(p'-p) = f(p')$. We have rescaled our operator from the one in Ref. [197] in order to simplify our comparison to the literature. We will then reorganize our contributions to isolate the iteration terms and then simplify them into expressions proportional to products of eikonal phases.

It will be more clear to work in polarization stripped amplitudes in this section, therefore we will introduce the shorthand $\epsilon \equiv \epsilon(p_1)\epsilon(p_2)$, $\epsilon^* \equiv \epsilon^*(p_1+q)\epsilon^*(p_2-q)$.

3.5.1 Virtual and Real Kernel Contributions

Applying Eq. (3.71), the virtual kernel reduces to

$$\begin{aligned}\langle\Psi|i[\mathbb{S}_1^{\mu\nu},T]|\Psi\rangle = \int \hat{d}^4 q\, e^{-ib\cdot q}\, \mathcal{I}_v^{\mu\nu} &= -i\int \hat{d}^4 q\, e^{-ib\cdot q}\, \epsilon^* \cdot [\mathbb{A}(q,p_1,p_2), M^{\mu\nu}]\cdot\epsilon \\ &= -i\int \hat{d}^4 q\, e^{-ib_{\rm cov}\cdot q}\, [\mathcal{A}(q,p_1,p_2), S_1^{\mu\nu}]\,, \end{aligned} \tag{3.72}$$

where it is understood that $\epsilon^*_{2'}, \epsilon_2$ do not contract with $M^{\mu\nu}$ and only interacts with the amplitude $\mathbb{A}(q,p_1,p_2)$.

At tree level, this is the only contribution and already scales classically; therefore we can shift to barred variables without worrying about the scaling,

$$\Delta^{(1)} S_1^{\mu\nu} = -i\left[\delta^{(1)}_{\rm cov}, S_1^{\mu\nu}\right]. \tag{3.73}$$

As a preliminary check, we can see whether Eq. (3.73) satisfies spin-tensor-magnitude conservation

$$2S_{1\,\mu\nu}\Delta S_1^{\mu\nu} + \Delta S_{1\,\mu\nu}\Delta S_1^{\mu\nu} = 0, \tag{3.74}$$

which is conserved regardless of whether we impose a SSC or not [170, 196]. Plugging in the eikonal phase related to our amplitude ansatz, Eq. (3.29), we see that spin-tensor-magnitude conservation is satisfied

$$-2iS_{1\,\mu\nu}\left[\delta^{(1)}_{\rm cov}, S_1^{\mu\nu}\right] = 0, \tag{3.75}$$

however this does not obviously vanish at the level of the eikonal phase. This signals that we are free to make a modification to the commutator that explicitly shows tree-level spin-tensor-magnitude conservation. In fact, we find a new projector for the commutator of the form

$$\Sigma_{1\ \rho\sigma}^{\mu\nu} = \delta^{\mu}_{\ \rho}\delta^{\nu}_{\ \sigma} - \frac{S_1^{\mu\nu}\, S_{1\,\rho\sigma}}{S_1^2}, \tag{3.76}$$

which leaves the commutator unchanged

$$\left[S_1^{\mu\nu}, S_1^{\alpha\beta}\right] = \Sigma_{1\ \rho\sigma}^{\mu\nu}\left[S_1^{\rho\sigma}, S_1^{\alpha\beta}\right] = \Sigma_{1\ \gamma\delta}^{\alpha\beta}\left[S_1^{\mu\nu}, S_1^{\gamma\delta}\right] = \Sigma_{1\ \rho\sigma}^{\mu\nu}\Sigma_{1\ \gamma\delta}^{\alpha\beta}\left[S_1^{\rho\sigma}, S_1^{\gamma\delta}\right], \tag{3.77}$$

while satisfying $\Sigma_{1\ \rho\sigma}^{\mu\nu} S_1^{\rho\sigma} = 0$.

We can see this spin projector $\Sigma_{1\ \rho\sigma}^{\mu\nu}$ in analogy to the momentum projector $\Pi^{\mu\nu}$. The momentum projector arises as a result of the on-shell delta functions in our integrands, which are associated with momentum conservation of the two-body system, allowing us to make the prescription Eq.(3.53). This leads us to a similar conclusion as Ref [195], that $\Pi^{\mu\nu}$ can be seen as a shift freedom associated with the on-shell δ-functions. Similarly, the spin projector $\Sigma_{1\ \rho\sigma}^{\mu\nu}$ arises as a result of spin-tensor-magnitude conservation Eq.(3.74), while conserving the Lorentz algebra. Because the spin projector makes spin-tensor-magnitude conservation manifest at the level of the eikonal phase, and because it leaves the Lorentz algebra unaffected, we conclude that $\Sigma_{1\ \rho\sigma}^{\mu\nu}$ is a shift freedom of the Lorentz algebra associated with spin-tensor-magnitude conservation. We view the above shift freedoms as prescriptions on the operators that act on our eikonal phases

$$\text{impulse operator}: \frac{\partial \delta_{\text{cov}}}{\partial b_{\text{cov}\,\mu}} \xrightarrow[\text{momentum conservation}]{\text{two-body}} \frac{\partial \delta_{\text{cov}}}{\partial (b_{\text{cov}\,\mu})_{\perp}} \equiv \Pi^{\mu\nu}\frac{\partial \delta_{\text{cov}}}{\partial b^{\nu}_{\text{cov}}}, \tag{3.78}$$

$$\text{spin kick operator}: [\delta_{\text{cov}}, S_1^{\mu\nu}] \xrightarrow[S_{\mu\nu}S^{\mu\nu}\ \text{conservation}]{} [\delta_{\text{cov}}, S_1^{\mu\nu}]_{\perp} \equiv \Sigma_{1\ \rho\sigma}^{\mu\nu}[\delta_{\text{cov}}, S_1^{\rho\sigma}]\,. \tag{3.79}$$

Both of these projectors are required to manifestly conserve their respective conservation conditions at the level of the eikonal phase. We will see in the one-loop calculation that the spin projector will be just as crucial to calculating the correct spin kick as the momentum projector is to calculating the correct momentum impulse.

Moving on to the one-loop correction, we must now decompose the amplitude into real and imaginary contributions in order to faithfully keep track of classical scaling. We will use a similar notation to that of the impulse case where

$$\langle\Psi|i[\mathbb{S}_1^{\mu\nu},T]|\Psi\rangle|_{NLO} = \Delta^{(2)}S^{\mu\nu}_{1\,v,\mathrm{Re}} + \Delta^{(2)}S^{\mu\nu}_{1\,v,\mathrm{Im}}, \tag{3.80}$$

where

$$\Delta^{(2)}S^{\mu\nu}_{1\,v,\mathrm{Re}} = -i\int \hat{d}q\, e^{-ib_{\mathrm{cov}}\cdot q}\,\left[\mathrm{Re}\mathcal{A}^{(2)}(q,p_1,p_2), S_1^{\mu\nu}\right] = -i\left[\delta^{(2)}_{\mathrm{cov}}, S_1^{\mu\nu}\right], \tag{3.81}$$

and

$$\Delta^{(2)}S^{\mu\nu}_{1\,v,\mathrm{Im}} = \int \hat{d}q\, e^{-ib_{\mathrm{cov}}\cdot q}\,\left[\mathrm{Im}\mathcal{A}^{(2)}(q,p_1,p_2), S_1^{\mu\nu}\right], \tag{3.82}$$

where we will defer the expansion until later, when we consider the full iteration contribution.

Plugging in the spin operator for the real kernel and fixing ourselves to one-loop order we get

$$\begin{aligned}\Delta^{(2)}S^{\mu\nu}_{1\,r} &\equiv \langle\Psi|\,T^{\dagger}\,[\mathbb{S}_1^{\mu\nu},\,T]\,|\Psi\rangle\\ &= -\int \hat{d}q e^{-ib\cdot q}\int \hat{d}l\,\epsilon^{*}\cdot\mathbb{A}^{(1)}(q-l,p_1+l,p_2-l)\cdot\left[\mathbb{A}^{(1)}(l,p_1,p_2),M^{\mu\nu}\right]\cdot\epsilon,\end{aligned} \tag{3.83}$$

which we will need to decompose into symmetric and antisymmetric parts, shift to barred variables, and enforce the horizontal-flip symmetry.

3.5.2 Iterative Contribution

We organize the iterative contribution in a similar manner as in the momentum impulse case,

$$\Delta^{(2)}S^{\mu\nu}_{1\,it} \equiv \Delta^{(2)}S^{\mu\nu}_{1\,r} + \Delta^{(2)}S^{\mu\nu}_{1\,v,\mathrm{Im}} = \Delta^{(2)}S^{\mu\nu}_{1\,it,*} + \Delta^{(2)}S^{\mu\nu}_{1\,it,\partial u} + \Delta^{(2)}S^{\mu\nu}_{1\,it,\partial l}. \tag{3.84}$$

Beginning with $\Delta^{(2)} S^{\mu\nu}_{1\,it,\partial u}$, this contribution is proportional to the external momentum derivatives

$$\begin{aligned}\Delta^{(2)} S^{\mu\nu}_{1\,it,\partial u} \equiv & -\frac{1}{2}\int \hat{D}q e^{-ib\cdot q}\int \hat{D}l \\ & \epsilon^* \left(\left\{ \left[\mathbb{A}^{(1)}(l,\bar{p}_1,\bar{p}_2), M^{\mu\nu}\right], \frac{l}{2}\cdot\left(\frac{\partial}{\partial \bar{p}_1}-\frac{\partial}{\partial \bar{p}_2}\right)\mathbb{A}^{(1)}(q-l,\bar{p}_1,\bar{p}_2)\right\} \right. \\ & \left. - \left\{ \mathbb{A}^{(1)}(q-l,\bar{p}_1,\bar{p}_2), \left[\frac{q-l}{2}\cdot\left(\frac{\partial}{\partial \bar{p}_1}-\frac{\partial}{\partial \bar{p}_2}\right)\mathbb{A}^{(1)}(l,\bar{p}_1,\bar{p}_2), M^{\mu\nu}\right]\right\}\right)\epsilon.\end{aligned} \tag{3.85}$$

Because Eq. (3.85) already scales classically and applying the horizontal-flip symmetry will not change the expression, we can immediately shift the momentum transfer and then express this contribution in terms of eikonal phases,

$$\begin{aligned}\Delta^{(2)} S^{\mu\nu}_{1\,it,\partial u} = & \frac{i}{2}\left[\left(\frac{1}{\bar{m}_1}\frac{\partial}{\partial u_1^\alpha}-\frac{1}{\bar{m}_2}\frac{\partial}{\partial u_2^\alpha}\right)\delta^{(1)}_{\text{cov}}, S^{\mu\nu}_1\right]\frac{\partial \delta^{(1)}_{\text{cov}}}{\partial (b_{\text{cov}\,\alpha})_\perp} \\ & -\frac{i}{2}\left[\frac{\partial \delta^{(1)}_{\text{cov}}}{\partial (b_{\text{cov}\,\alpha})_\perp}, S^{\mu\nu}_1\right]\left(\frac{1}{\bar{m}_1}\frac{\partial}{\partial u_1^\alpha}-\frac{1}{\bar{m}_2}\frac{\partial}{\partial u_2^\alpha}\right)\delta^{(1)}_{\text{cov}}.\end{aligned} \tag{3.86}$$

For the contribution proportional to the products of the amplitudes and the Lorentz generator

$$\begin{aligned}\Delta^{(2)} S^{\mu\nu}_{1\,it,*} \equiv & -\frac{1}{2}\int \hat{D}q e^{-ib\cdot q}\int \hat{D}l \\ & \epsilon^* \left(\left[\mathbb{A}^{(1)}(q-l,\bar{p}_1,\bar{p}_2), \left[\mathbb{A}^{(1)}(l,\bar{p}_1,\bar{p}_2), M^{\mu\nu}\right]\right] \right. \\ & + \left\{\mathbb{A}^{(1)}(q-l,\bar{p}_1,\bar{p}_2), \left[\mathbb{A}^{(1)}(l,\bar{p}_1,\bar{p}_2), M^{\mu\nu}\right]\right\} \\ & \left. -\frac{1}{2}\left[\left\{\mathbb{A}^{(1)}(q-l,\bar{p}_1,\bar{p}_2), \mathbb{A}^{(1)}(l,\bar{p}_1,\bar{p}_2)\right\}, M^{\mu\nu}\right]\right)\epsilon,\end{aligned} \tag{3.87}$$

we still need to cancel the classically-singular contribution in the last two lines. When we examine these terms in Eq. (3.87) and apply commutator identities, we find that they are parity-odd under the horizontal-flip symmetry

$$\begin{aligned}& \left\{\mathbb{A}^{(1)}(q-l), \left[\mathbb{A}^{(1)}(l), M^{\mu\nu}\right]\right\} - \frac{1}{2}\left[\left\{\mathbb{A}^{(1)}(q-l), \mathbb{A}^{(1)}(l)\right\}, M^{\mu\nu}\right] \\ & \quad = \frac{1}{2}\left(\left\{\mathbb{A}^{(1)}(q-l), \left[\mathbb{A}^{(1)}(l), M^{\mu\nu}\right]\right\} - \left\{\mathbb{A}^{(1)}(l), \left[\mathbb{A}^{(1)}(q-l), M^{\mu\nu}\right]\right\}\right),\end{aligned} \tag{3.88}$$

where we leave the external momenta dependence implicit. Because the operator does not affect the parity of this contribution, the classically-singular terms vanish. Now that we have a fully classical contribution, we can follow the same procedure as before and rewrite Eq. (3.87) in terms of tree-level eikonal phases

$$\Delta^{(2)} S^{\mu\nu}_{1\,it,*} = -\frac{1}{2}\left[\delta^{(1)}_{\rm cov}, \left[\delta^{(1)}_{\rm cov}, S^{\mu\nu}_1\right]\right]. \tag{3.89}$$

For $\Delta^{(2)} S^{\mu\nu}_{1\,it,\partial l}$, we first need to integrate by parts in order to apply the horizontal-flip symmetry. Doing so results in the same cancellation of classically-singular terms as in $\Delta^{(2)} S^{\mu\nu}_{1\,it,*}$, where using Eq. (3.88) results in a parity-odd contribution. However, we run in to the same obstacle as in the momentum impulse case,

$$\begin{aligned}\Delta^{(2)} S^{\mu\nu}_{1\,it,\partial l} = &-\int \hat{d}q e^{-ib\cdot q}\int \hat{d}l \frac{-q^2}{4}\left(\frac{\check{u}_2^\alpha}{\bar{m}_2}-\frac{\check{u}_1^\alpha}{\bar{m}_1}\right)\\ &\left(\mathcal{A}^{(1)}(q-l)\left[\frac{\partial}{\partial l^\alpha}\mathcal{A}^{(1)}(l), S^{\mu\nu}_1\right]-\frac{\partial}{\partial l^\alpha}\mathcal{A}^{(1)}(l)\left[\mathcal{A}^{(1)}(q-l), S^{\mu\nu}_1\right]\right),\end{aligned} \tag{3.90}$$

which is overall parity-even and scales classically. As before, we have to resolve the $\partial/\partial l^\alpha$ derivative; luckily the combination is the same as in the momentum impulse case. Therefore, we can perform the transfer momentum shift and use the same replacement rule Eq. (3.66) to express $\Delta^{(2)} S^{\mu\nu}_{1\,it,\partial l}$ in terms of eikonal phases

$$\Delta^{(2)} S^{\mu\nu}_{1\,it,\partial l} = -i\left(\frac{\check{u}_1^\alpha}{\bar{m}_1}-\frac{\check{u}_2^\alpha}{\bar{m}_2}\right)\left(\left[\frac{\partial\delta^{(1)}_{\rm cov}}{\partial\Pi^{\alpha\gamma}}, S^{\mu\nu}_1\right]\frac{\partial\delta^{(1)}_{\rm cov}}{\partial(b_{{\rm cov}\,\gamma})_\perp}-\left[\frac{\partial\delta^{(1)}_{\rm cov}}{\partial(b_{{\rm cov}\,\gamma})_\perp}, S^{\mu\nu}_1\right]\frac{\partial\delta^{(1)}_{\rm cov}}{\partial\Pi^{\alpha\gamma}}\right). \tag{3.91}$$

With the full iterative contribution in terms of eikonal phases, we now have the higher-order-in-spin eikonal formula to one-loop order for the spin kick. However, we would like to first make one-loop spin-tensor-magnitude conservation explicit by incorporating the projector Eq. (3.76) associated with the Lorentz algebra into our commutators. For most of the contributions no appreciable difference occurs, but in the case of $\Delta^{(2)} S^{\mu\nu}_{1\,it,*}$ the double commutator has a non-trivial effect

$$\Delta^{(2)} S^{\mu\nu}_{1\,it,*} = -\frac{1}{2}\Sigma^{\mu\nu}_{1\;\rho\sigma}\left[\delta^{(1)}_{\rm cov}, \left[\delta^{(1)}_{\rm cov}, S^{\rho\sigma}_1\right]\right] + S^{\mu\nu}_1\frac{\left[\delta^{(1)}_{\rm cov}, S^{\rho\sigma}_1\right]\left[\delta^{(1)}_{\rm cov}, S_{1\,\rho\sigma}\right]}{2S_1^2}. \tag{3.92}$$

Now we can combine our iteration terms knowing that our eikonal formula for the spin kick will explicitly satisfy one-loop spin-tensor-magnitude conservation

$$\begin{aligned}\Delta^{(2)} S_1^{\mu\nu} = &-i\left[\delta^{(2)}_{\text{cov}}, S_1^{\mu\nu}\right] - \frac{1}{2}\Sigma^{\mu\nu}_{1\,\rho\sigma}\left[\delta^{(1)}_{\text{cov}}, \left[\delta^{(1)}_{\text{cov}}, S_1^{\rho\sigma}\right]\right] + \frac{1}{2} S_1^{\mu\nu} \frac{\left[\delta^{(1)}_{\text{cov}}, S_1^{\rho\sigma}\right]\left[\delta^{(1)}_{\text{cov}}, S_{1\,\rho\sigma}\right]}{S_1^2} \\ &- \frac{i}{2}\left[\frac{\partial \delta^{(1)}_{\text{cov}}}{\partial (b^\alpha_{\text{cov}})_\perp}, S_1^{\mu\nu}\right]\nabla^\alpha_{p_{\text{cm}}}\delta^{(1)}_{\text{cov}} + \frac{i}{2}\frac{\partial \delta^{(1)}_{\text{cov}}}{\partial (b^\alpha_{\text{cov}})_\perp}\nabla^\alpha_{p_{\text{cm}}}\left[\delta^{(1)}_{\text{cov}}, S_1^{\mu\nu}\right]. \end{aligned} \tag{3.93}$$

This is a first-of-its-kind derivation of the spin kick using KMOC and general spin amplitudes. We have verified Eq. (3.93) to the results in Ref. [195] up to quadratic order in spin. We also find that the cut-correction effects vanish when we impose a SSC. We have also verified that Eq. (3.93) respects spin-tensor-magnitude conservation. Once again, we have not used any properties of specific spin representations making Eq.(3.93), in principle, valid to all orders in spin; however, a direct comparison will be required to solidify this claim.

Once again we can rewrite Eq. (3.93) in terms of tree-level spin kicks and momentum impulses

$$\begin{aligned}\Delta^{(2)} S_1^{\mu\nu} = &-i\left[\delta^{(2)}_{\text{cov}}, S_1^{\mu\nu}\right] - \frac{i}{2}\Sigma^{\mu\nu}_{1\,\rho\sigma}\left[\delta^{(1)}_{\text{cov}}, \Delta^{(1)} S_1^{\rho\sigma}\right] - \frac{S_1^{\mu\nu}}{2S_1^2}(\Delta^{(1)} S_1)^2 \\ &+ \frac{i}{2}\left[\Delta^{(1)} p_{1\,\alpha}, S_1^{\mu\nu}\right]\nabla^\alpha_{p_{\text{cm}}}\delta^{(1)}_{\text{cov}} - \frac{i}{2}\Delta^{(1)} p_{1\,\alpha}\left[\nabla^\alpha_{p_{\text{cm}}}\delta^{(1)}_{\text{cov}}, S_1^{\mu\nu}\right], \end{aligned} \tag{3.94}$$

which bears a striking resemblance to the impulse eikonal formula Eq. (3.69), signaling a more general representation of these eikonals formulas.

3.6 Comparing the Eikonal Formulas

As can be seen in Eq. (3.69) and Eq. (3.94), after taking into account conservation of momentum and the spin tensor magnitude, both the impulse and spin kick formulas exhibit the following pattern

$$\Delta^{(2)}\mathcal{O} = \mathbb{O}\circ\delta^{(2)}_{\text{cov}} - \frac{i}{2}\left[\delta^{(1)}_{\text{cov}}, \mathbb{O}\circ\delta^{(1)}_{\text{cov}}\right] - \frac{1}{2}\mathbb{O}\overleftrightarrow{\circ}\left(\Delta^{(1)} p_{1\,\alpha}\nabla^\alpha_{p_{\text{cm}}}\delta^{(1)}_{\text{cov}}\right), \tag{3.95}$$

where $\Delta\mathcal{O}$ can be either observable $\Delta p_1^\mu, \Delta S_1^{\mu\nu}$ and $\mathbb{O}$ is the operator associated with the observable such that

$$\mathbb{S}_1^{\mu\nu} \circ \delta \equiv -i\left[\delta, S_1^{\mu\nu}\right]_\perp, \qquad \mathbb{P}_1^\mu \circ \delta \equiv -\frac{\partial\delta}{\partial(b_{\text{cov}\,\mu})_\perp}. \tag{3.96}$$

We define the operation $\overleftrightarrow{\circ}$ as

$$\mathbb{O}\overleftrightarrow{\circ}\left(\nabla^\alpha_{p_{\text{cm}}}\delta^{(1)}_{\text{cov}}\,\Delta^{(1)}p_{1\,\alpha}\right) \equiv \left(\mathbb{O}\circ\nabla^\alpha_{p_{\text{cm}}}\delta^{(1)}_{\text{cov}}\right)\,\Delta^{(1)}p_{1\,\alpha} - \nabla^\alpha_{p_{\text{cm}}}\delta^{(1)}_{\text{cov}}\,\left(\mathbb{O}\circ\Delta^{(1)}p_{1\,\alpha}\right). \tag{3.97}$$

While it is unclear where such a pattern would arise from, there have been suggestions in the literature of sources for eikonal formulas. In Ref. [121], the authors suggest that their eikonal formula arises from an exponential operation on the observables of the following form

$$\Delta\mathcal{O} = e^{-i\delta\mathcal{D}}\left[\mathcal{O}, e^{i\delta\mathcal{D}}\right], \tag{3.98}$$

where $\mathcal{D}$ is some differential operator, which is defined in Eq. (7.21) of Ref. [121]. In Refs. [159, 195], both works show that the higher-order corrections to observables can be generated by making half variable shifts to their observables

$$\Delta\mathcal{O}(u_i, s_i, b) \to \Delta\mathcal{O}\left(u_i + \frac{\Delta u_i}{2}, s_i + \frac{\Delta s_i}{2}, b + \frac{\Delta b}{2}\right), \tag{3.99}$$

where expanding to next to leading order produces their one-loop corrections, which we agree with. It is clear that if we interpret the exponential operator in Eq. (3.98) as some translation operators then these two formulas are related. In fact, Ref. [195] showed that the eikonal formulas in Refs. [121, 170], with the SSC freedom, can be expressed as directional derivatives, which would come from expanding a small shift on the variables of the observables. We believe that our formulas can also be expressed in such a form, however, an explicit calculation still needs to be done.

3.7 Conclusion

In this paper we used the KMOC formalism and general spin amplitudes to derive one-loop formulas that relate the eikonal phase to the momentum impulse and the spin kick with spin effects included. While other derivations exist in the literature [195], the methods presented here are the first to use general spin amplitudes that do not rely on an SSC or properties of specific spin representations. We have verified these equations up to quadratic order in spin by comparing to Ref. [195], though we expect our results to hold at higher orders in spin; this remains to be explicitly checked. We found that our eikonal formulas, Eq. (3.69) and Eq. (3.94), follow a Baker-Campbell-Hausdorff expansion pattern, Eq. (3.95), similar to those found in Refs. [121, 122, 170, 196]; Ref. [195] found this pattern is related to half-variable shifts in the observables, signaling that the eikonal formulas can be generated by some translation operator on the observables. We also found that it was crucial to include the impulse projector Eq. (3.52) and the new spin kick projector Eq. (3.76), which are associated with the conservation of energy and spin tensor magnitude, respectively.

We chose to use non-transverse massive spinning fields in order to capture SSC-violating effects, such as spin vector magnitude violation, with the understanding that we can later impose the SSC to match results using transverse fixed-spin fields [170, 196]: this simplified our calculations considerably. As a result, we were able to use simplified completeness relations for the polarization tensors of massive spinning fields; this allowed for the easy manipulation of integrands proportional to the on-shell product of tree-level amplitudes. We were also able to assume an analytic structure of our tree-level amplitudes; we did this in order to resolve the cut-correction effect in Eq. (3.65) that resulted from expanding the on-shell δ-functions of the two-particle cut integral associated with the iteration contributions. We found that, upon imposing a SSC, this effect no longer contributes to our observables. This relationship works well with our understanding that, by using SSC-violating fields, we allow for lower spin states to propagate in our amplitudes, which would be eliminated by enforcing a SSC. Since these cut-correction contributions come from the unitarity cut of the internal massive lines, and imposing the SSC removes them, we believe they may be shown to be related to the effects of the lower spin states propagating in our amplitudes, such as the spin vector magnitude change. It would be interesting to see an explicit calculation showing the relationship between the cut corrections and the spin vector magnitude change.

A number of avenues exist to expand on this work. Because we checked our equations up to quadratic order in spin, we were not able to see the subtleties associated with higher-spin amplitudes starting at quintic order in spin [192]. Though, in principle, our derivation is valid to any order in spin, it would be important to check how these higher-spin subtleties show up in the context of this work. Another extension would be to see how to derive an eikonal formula at two loops, especially since the iteration pieces in this order will also include one-loop contributions as well as on-shell massless particles for the tree-level iterations. It would also be interesting to see how non-conservative effects, such as radiation and absorption, are affected by spin degrees of freedom. Recently, work in Refs. [212, 213] have explored the effects of spin on mass absorption and the momentum impulse. Exploring how absorption affects the spin kick would also be insightful, particularly in understanding how spin transitions play a role. Furthermore, it would be interesting to see shifts like those in Ref. [159], which preserve the symmetry in the worldline [195], affect the eikonal formulas in a similar way as the momentum-conserving projector Eq. (3.52) or the spin-tensor-magnitude-conserving projector Eq. (3.76).

CHAPTER 4

Classical Spin Transitions and Absorptive Scattering

4.1 Introduction

So far, we have explored dissipative and spin effects separately. In this chapter, we will synthesize these treatments to calculate absorptive effects with spin included. Once again, we will review techniques like KMOC and the soft limit in order to place them in the context of absorptive effects.

Absorptive and horizon effects have been calculated throughout the years, such as works [214–229]. More recently, [189, 213] have calculated the mass shift due to absorptive effects for black holes using the KMOC formalism; the latter included spin effects up to $\mathcal{O}(S^2)$. While both works provided results for black holes by matching to calculations from black hole perturbation theory, [189] provided a framework for calculating absorptive effects for generic compact spinning bodies.

In this chapter, we describe an on-shell, amplitudes-based approach to incorporating radiation absorption effects in the Post-Minkowskian scattering of generic, compact, spinning bodies. Classical spinning observables are recovered by extrapolating results calculated with finite quantum spin-s particles using the properties of spin universality and Casimir interpolation. At leading-order our results give a completely general and non-redundant parametrization of absorptive observables in terms of a finite number of Wilson coefficients associated with 3-particle mass/spin changing on-shell amplitudes. We denote these underlying microscopic processes as *classical spin transitions*. Explicit results for the leading-order impulse due to the absorption of scalar, electromagnetic and gravitational radiation, for spin transitions $\Delta s = 0, \pm 1, \pm 2$ are given in a complete form up to $\mathcal{O}(S^2)$. Our explicit results reveal some surprising universal patterns. We find that, up to a non-trivial identification of Wilson coefficients, the impulse for spinning-up and spinning-down by the same magnitude $|\Delta s|$ are identical. For processes where the quantum $\Delta s < 0$ transition is forbidden, the corresponding classical observable is suppressed in powers of S by a predictable amount. Additionally we find that, while for generic non-aligned spin configurations there is a non-zero scattering angle at leading-order, for aligned spin, similar to non-spinning absorption, the scattering angle vanishes and the impulse is purely longitudinal. The formalism and results presented provide a significant extension of the amplitudes-based calculational pipeline for gravitational waveforms from binary black hole and neutron star systems beyond the point-particle approximation.

The chapter is organized in the following manner. In Section 4.2 we review the KMOC formalism and the soft limit in the context of absorptive and spin effects while focusing on the impulse as our classical observable. In Section 4.3, we go in to detail of how we use definite-spin representations to calculate spin effects in our amplitudes. We also consider unavoidable ambiguities in this scheme that come from the Casimir operator S^2. In Section 4.4, we describe the building blocks for the spin-transition amplitudes and introduce some over-arching results in our impulse calculation. In the Appendix F we provide the explicit three-point amplitudes and in Appendix G we provide the explicit impulse results.

Notation and conventions: Throughout this chapter, unless otherwise indicated, we use natural units $\hbar = c = 1$. Lorentz covariant expressions are defined with the mostly minus metric signature $\eta_{\mu\nu} = \eta^{\mu\nu} = \text{diag}(+1, -1, -1, -1)$. For expressions involving Levi-Civita symbols we employ Schoonschip notation: $\varepsilon^{abcd} \equiv \varepsilon^{\mu\nu\rho\sigma} a_\mu b_\nu c_\rho d_\sigma$, $\varepsilon^{\mu bcd} \equiv \varepsilon^{\mu\nu\rho\sigma} b_\nu c_\rho d_\sigma$, etc. We also use the normalization for the Levi-Civita symbol $\varepsilon^{0123} = 1$. Tensor indices are symmetrized and anti-symmetrized as

$$T^{(\mu_1\cdots\mu_n)} \equiv \frac{1}{n!}\sum_{\sigma\in S_n} T^{\mu_{\sigma(1)}\cdots\mu_{\sigma(n)}}, \qquad T^{[\mu_1\cdots\mu_n]} \equiv \frac{1}{n!}\sum_{\sigma\in S_n} \mathrm{sgn}\,(\sigma)\, T^{\mu_{\sigma(1)}\cdots\mu_{\sigma(n)}}, \tag{4.1}$$

respectively. Loop and phase space integrals are evaluated using dimensional regularization, in $D = 4 - 2\epsilon$ dimensions. The following shorthand is used to suppress factors of 2π: $\hat{\mathrm{d}}^D p_i \equiv \mathrm{d}^D p_i/(2\pi)^D$, and $\hat{\delta}(p_i^2 - m_i^2) \equiv 2\pi\delta(p_i^2 - m_i^2)$.

4.2 Classical Observables from Quantum Amplitudes

We will use the KMOC formalism [39, 40] to calculate classical observables from quantum amplitudes, however, with a slight modification in order to incorporate absorption effects. These absorption modifications are aligned with those in Ref. [189]. We will also go in to some detail on how we account for spin-transitions in our integrands. We will also touch on our integration technique and the vector basis we use in our calculation.

4.2.1 Dissipative Observables

In this chapter the physical observable we study is the impulse imparted on body-1 during a 2-to-2 scattering event. Quantum mechanically, this given by the asymptotic change in the expectation value of the 4-momentum operator $\mathbb{P}_1^\mu$

$$\Delta p_1^\mu \equiv \langle \mathrm{in}|S^\dagger \mathbb{P}_1^\mu S|\mathrm{in}\rangle - \langle \mathrm{in}|\mathbb{P}_1^\mu|\mathrm{in}\rangle. \tag{4.2}$$

Following [39], and assuming body-2 is non-spinning, we choose the in-state to be

$$|\mathrm{in}\rangle \equiv \sum_{a_1=1}^{2s_1+1} \int \mathrm{d}\Phi(p_1, m_1^2)\mathrm{d}\Phi(p_2, m_2^2)\, \phi(p_1)\phi(p_2)\, \xi^{a_1}\, e^{ib_1\cdot p_1}\, e^{ib_2\cdot p_2}\, |p_1, \{s_1, a_1\}; p_2\rangle, \tag{4.3}$$

where s_1 is the *spin magnitude* and a_1 is an index labeling the components of the $2s_1 + 1$ dimensional representation of $SU(2)$, the *little-group* of body-1. The state $|p_1, \{s_1, a_1\}; p_2\rangle$ is a 2-body momentum eigenstate and the minimal-uncertainty wavepacketabss $\phi(p_i)e^{ib_i\cdot p_i}$

are peaked around 4-momenta $p_i^\mu \approx m_i u_i^\mu$ and impact parameter b_i^μ [39, 40, 50, 195]. The little-group vector ξ^{a_1} defines a *spin-coherent* state approximating the classical spin vector S_1^μ in the correspondence limit [156]. For simplicity, in this chapter body-2 is assumed to be non-spinning. Both parts of the wavefunction are normalized such that $\int \mathrm{d}\Phi(p, m^2)|\phi(p)|^2 = \sum_a |\xi^a|^2 = 1$; where the Lorentz invariant phase space measure is defined as

$$\int \mathrm{d}\Phi(p_i, m_i^2) \equiv \int \hat{\mathrm{d}}^D p_i \, \hat{\delta}^{(+)}(p_i^2 - m_i^2). \tag{4.4}$$

Assuming the standard unitarity relation $T^\dagger T = i(T - T^\dagger)$, where $S \equiv 1 + iT$, it is useful to rewrite (4.2) as the sum of so-called *virtual* and *real* contributions

$$\Delta p_1^\mu = \underbrace{\langle \mathrm{in}| i[\mathbb{P}_1^\mu, T]|\mathrm{in}\rangle}_{\text{virtual}} + \underbrace{\langle \mathrm{in}| T^\dagger[\mathbb{P}_1^\mu, T]|\mathrm{in}\rangle}_{\text{real}}. \tag{4.5}$$

We re-express the change in the observable for 2-body scattering as

$$\Delta p_1^\mu = \sum_{a_1, a_1'=1}^{2s_1+1} \int \left(\prod_{i=1}^{2} \mathrm{d}\Phi(p_i, m_i^2)\, \mathrm{d}\Phi(p_i', m_i^2)\, \phi^*(p_i')\phi(p_i)\, e^{-ib_i\cdot(p_i'-p_i)} \right) \xi^*_{a_1'} \, (\mathcal{I}_v^\mu + \mathcal{I}_r^\mu)^{a_1'}_{a_1} \, \xi^{a_1}, \tag{4.6}$$

where

$$\begin{aligned} \mathcal{I}_v^\mu &\equiv \langle p_1', \{s_1, a_1'\}; p_2'| i[\mathbb{P}_1^\mu, T]|p_1, \{s_1, a_1\}; p_2\rangle, \\ \mathcal{I}_r^\mu &\equiv \langle p_1', \{s_1, a_1'\}; p_2'| T^\dagger[\mathbb{P}_1^\mu, T]|p_1, \{s_1, a_1\}; p_2\rangle, \end{aligned} \tag{4.7}$$

are the virtual and real *kernels* respectively. The virtual kernel is simply related to the elastic scattering amplitude

$$\mathcal{I}_v^\mu = i\hat{\delta}^{(D)}\left(\sum_{i=1}^{2} p_i - \sum_{i=1}^{2} p_i'\right)(p_1'^\mu - p_1^\mu)\mathcal{A}_4\left(\phi_1^{a_1}(p_1)\phi_2(p_2) \to \phi_1^{a_1'}(p_1')\phi_2(p_2')\right). \tag{4.8}$$

The real kernel is evaluated by inserting a complete set of states between $T^\dagger$ and $[\mathbb{P}_1^\mu, T]$. Different sectors of the Hilbert space give different contributions, and at leading-order these are separately well-defined and gauge invariant. Contributions of the form

$$\mathbb{1} \supset \sum_{b_1=1}^{2s_1+1} \int \mathrm{d}\Phi(r_1, m_1^2)\mathrm{d}\Phi(r_2, m_2^2)|r_1, \{s_1, b_1\}; r_2\rangle\langle r_1, \{s_1, b_1\}; r_2|, \tag{4.9}$$

define the *conservative* sector; other contributions, including radiation modes and internal excited states, define the *dissipative* sector. We are interested in contributions corresponding to excited single-particle states of body-1

$$\mathbb{1} \supset \sum_{s_1',\pm} \sum_{b_1=1}^{2s_1'+1} \int_{m_{1*}^2}^{\infty} \mathrm{d}\mu^2 \rho_{s_1'}^{\pm}(\mu^2) \int \mathrm{d}\Phi(r_1,\mu^2)\mathrm{d}\Phi(r_2,m_2^2)|r_1,\{s_1',b_1\},\mu^2;r_2\rangle\langle r_1,\{s_1',b_1\},\mu^2;r_2|. \tag{4.10}$$

Here the excited-state in general is labeled by its Lorentz invariant quantum numbers: mass μ^2, spin magnitude s_1', and (if a symmetry of the system) an intrinsic parity $\pm$. All of these may be different from body-1 in the in-state. For a given spin and parity there may be contributions of states with a range of masses, and in general we do not assume these are narrow-width particle-like excitations. Consequently we include an integration over μ^2 weighted by an unknown spectral density function $\rho_{s_1'}^{\pm}(\mu^2)$. For macroscopic spinning bodies we expect that it should be possible to *decrease* the total rest-mass by the spontaneous emission of a superradiant mode [230], and so for at least some contributions $m_{1*}^2 < m_1^2$.

The excited-state contributions to the real kernel then takes the form

$$\begin{aligned}\mathcal{I}_r^{\mu} &= \sum_{s_1',\pm} \sum_{b_1=1}^{2s_1'+1} \int_{m_{1*}^2}^{\infty} \mathrm{d}\mu^2 \rho_{s_1'}^{\pm}(\mu^2) \int \mathrm{d}\Phi(r_1,\mu^2)\mathrm{d}\Phi(r_2,m_2^2) \\ &\quad \langle p_1',\{s_1,a_1'\};p_2'|T^{\dagger}|r_1,\{s_1',b_1\},\mu^2;r_2\rangle\langle r_1,\{s_1',b_1\},\mu^2;r_2|[\mathbb{P}_1^{\mu},T]|p_1,\{s_1,a_1\};p_2\rangle \\ &= \hat{\delta}^{(D)}\left(\sum_{i=1}^{2} p_i - p_i'\right) \sum_{s_1',\pm} \sum_{b_1=1}^{2s_1'+1} \int_{m_{1*}^2}^{\infty} \mathrm{d}\mu^2 \rho_{s_1'}^{\pm}(\mu^2) \int \mathrm{d}\Phi(r_1,\mu^2)\mathrm{d}\Phi(r_2,m_2^2)\hat{\delta}^{(D)}\left(\sum_{i=1}^{2} p_i - r_i\right) \\ &\quad (r_1^{\mu} - p_1^{\mu})\, \mathcal{A}_4^*\left(\phi_1^{a_1'}(p_1)\phi_2(p_2) \to X_{s_1',\pm}^{b_1}(r_1)\phi_2(r_2)\right) \mathcal{A}_4\left(\phi_1^{a_1}(p_1)\phi_2(p_2) \to X_{s_1',\pm}^{b_1}(r_1)\phi_2(r_2)\right).\end{aligned} \tag{4.11}$$

We have written the T-matrix elements as scattering amplitudes involving excited states, denoted generically as X. Since the excited X-states are unstable, their inclusion in the asymptotic Hilbert space (4.10) and the associated scattering amplitudes in (4.11) exist only in the usual formal sense in perturbation theory, stability of these states being recovered in the limit of zero coupling [231].[1] In the calculation of *inclusive* observables, such as the impulse Δp_1^μ, we are summing over the X-states, the *exclusive* amplitudes $\mathcal{M}(\phi_1\phi_2 \to X\phi_2')$ should be regarded as formal devices for organizing the intermediate kinematics.

4.2.2 Soft Expansion

We use the framework described in the previous subsection to calculate dissipative contributions to the impulse in a kinematic regime defined by the hierarchy of scales (in natural units $\hbar = c = 1$)

$$\lambda_C^{(i)} \ll R^{(i)} \ll b^\mu, \tag{4.12}$$

where $\lambda_C^{(i)} \sim \frac{1}{m_i}$ and $R^{(i)}$ are the *Compton wavelength* and *classical charge radius* of body-i respectively, and $b^\mu \equiv b_1^\mu - b_2^\mu$ the (relative) covariant impact parameter. The classical charge radii have different definitions depending on the force mediating particle being used to probe them

$$R_\psi^{(i)} \sim \frac{g_i^2}{m_i^3}, \qquad R_\gamma^{(i)} \sim \frac{e^2 Q_i^2}{m_i}, \qquad R_h^{(i)} \sim G m_i, \tag{4.13}$$

where g_i and Q_i are the scalar and electric charges of body-i, e is the dimensionless electromagnetic gauge coupling and G is Newton's constant. For bodies that carry multiple charges we will not assume a hierarchy between these scales. We make no assumptions about the relative velocity, and all of the results presented are manifestly Lorentz covariant. Together, this regime describes the scattering of (semi-)classical, relativistic point-particles at large impact parameter; in the gravitational context this is usually referred to as *post-Minkowskian (PM)* scattering, and in the electromagnetic context as *post-Lorentzian (PL)* scattering.

In practice this double-hierarchy is implemented by first expanding in the couplings g, e and G, the usual Feynman diagrammatic loop expansion, and then subsequently expanding the momentum space KMOC kernels $\mathcal{I}_{r,v}^\mu(q)$ in the limit of small momentum transfer ($q \sim \frac{1}{b}$)

$$q^\mu \ll m_1 u_1^\mu \sim m_2 u_2^\mu, \tag{4.14}$$

[1] In the presence of superradiant modes, even the incoming state with mass m_1^2 is unstable.

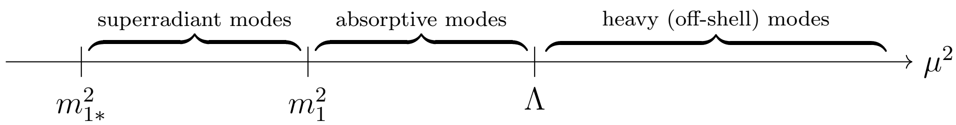

Figure 4.1: Schematic representation of contributions to the spectral integral.

where our kinematic conventions are depicted in Figure 4.2. Loop integrals are expanded in this limit prior to integration using the *method of regions* [145]. In this context the dominant long-range contribution corresponds to a single relativistic region, the *soft region* defined as $\ell^\mu \sim q^\mu$, where ℓ^μ is the momentum associated with an internal massless mediator.

Macroscopic compact bodies are expected to exhibit a nearly continuous spectrum of excited states, corresponding to excitations of the enormous number of (possibly unknown) internal degrees of freedom. As discussed in the previous section, we can incorporate these excited states into the calculation of dissipative observables using the KMOC in-in formalism, by including the contributions of (formal) particle-like X-states with spins s_1' and invariant mass-squared μ^2 with an integral over an *a priori* unknown spectral density $\rho^{\pm}_{s_1'}(\mu^2)$. As depicted in Figure 4.1, it is useful to separate this integration into three distinct regions:

1. $m_{1*}^2 \leq \mu^2 < m_1^2$: *superradiant modes*,
2. $m_1^2 \leq \mu^2 \leq \Lambda$: *absorptive modes*,
3. $\Lambda < \mu^2$: *heavy (off-shell) modes.*

At leading-order, corresponding to diagrams of the form depicted in Figure 4.2, contributions from region (i) describe the spontaneous emission of a superradiant mode. We will discuss prospects for incorporating these contributions further in Section 4.5.

Absorption (of positive energy radiation), by definition, corresponds to the contributions of regions (ii) and (iii) for which the mass of the internal state exceeds the mass of the incoming body: $\mu^2 > m_1^2$. The scale Λ is chosen (somewhat arbitrarily) to separate modes that can and cannot go on-shell during scattering in the regime of small momentum transfer. The contributions from region (iii) can be consistently integrated out to produce higher-derivative effective (tidal response) operators; we will assume this has been parametrized as part of the calculation in the conservative sector [130, 137]. For the rest of the chapter, *absorption* will refer to the contributions from region (ii).

In the classical limit we take angular momentum to be very large such that, if we restore powers of $\hbar$, $J \gg \hbar$. With this in mind, we will also take the magnitude of the spin to be large.

As discussed in [189], it is convenient to re-define the spectral integration in the formal X-state propagator as

$$\int_{m_1^2}^{\Lambda} \mathrm{d}\mu^2 \, \rho(\mu^2) \, \frac{i \, \Pi^{\alpha_1 \cdots \alpha_s}_{\beta_1 \cdots \beta_s}(k)}{k^2 - \mu^2 + i0} \to \frac{1}{2m_1} \int_0^{\infty} \mathrm{d}x \, \rho(x) \frac{i\Pi^{\alpha_1 \cdots \alpha_s}_{\beta_1 \cdots \beta_s}(k)}{k^2 - m_1^2 - 2m_1 x + i0}, \tag{4.15}$$

where $\mu^2 \equiv m_1^2 + 2m_1 x$, and $\Pi^{\alpha_1 \ldots \alpha_s}_{\beta_1 \ldots \beta_s}$ is the projector for a massive, symmetric-traceless spin-s field. Here we have replaced the hard-cutoff Λ with a form of analytic regularization and expand the spectral function to leading-order near the mass of the incoming state, $\mu^2 \approx m_1^2$. In what follows we will assume that this has the form of a power law[2]

$$\rho(x) \sim x^{1+\alpha}, \qquad \text{as} \qquad x \to 0^+. \tag{4.16}$$

The definition of the analytic regularization is that the integral on the right-hand-side is evaluated for some range of values of α for which it convergent, and then analytically continued to the physical value. In [189], these low-energy spectral functions were determined for scalar, photon and graviton absorption by a Schwarzschild black hole by matching with the known absorption cross-section. In each case the spectral function was found to be a *linear* function at low-energies, meaning $\rho(x) \sim x$ as $x \to 0^+$. For the rest of this chapter we will continue to make this assumption, defining the spectral integral by continuation to

[2] Without loss of generality we can absorb the overall coefficient of the spectral function into a redefinition of the Wilson coefficients appearing in the 3-point amplitudes.

$\alpha \to 0$. In principle however, this represents a further UV parameter to be determined by matching; it is straightforward to repeat our calculations for other values.

If body-1 is incoming with momentum p_1^μ and absorbs radiation with momentum q^2, the invariant mass of the excited state is $\mu^2 \approx m_1^2 + 2p_1 \cdot q$. The X-states that are relevant for absorption in the soft region therefore scale as $x \sim q^\mu$.

All together, we define the soft limit by the following scaling relations

$$l^\mu \sim q^\mu \sim x \sim \lambda, \qquad u_1^\mu \sim u_2^\mu \sim \lambda^0, \qquad \frac{S_1^\mu}{m_1} \sim \lambda^{-1}, \tag{4.17}$$

the leading-order impulse corresponds to expanding the KMOC kernel to leading-order in the

This allows us to simplify the impulse formula

$$\Delta p_1^\mu \to \frac{1}{4m_1 m_2} \int \hat{d}^D q \, \hat{\delta}\left(u_1 \cdot q\right) \, \hat{\delta}\left(u_2 \cdot q\right) \, e^{-ib\cdot q} \left(\mathcal{I}_v^\mu + \mathcal{I}_r^\mu\right), \tag{4.18}$$

where $u_i = p_i/m_i$ is the classical velocity. Details of evaluating the different kernels can be found in the literature [39, 47, 178, 189, 197]; taking in to account absorption in our scheme does not affect these details.

4.2.3 Leading Absorptive Impulse

In the case of absorption, the leading contribution to the impulse begins with the one-loop amplitude, $\mathcal{A}_4^{(s_1,s_1',|h|)}$ where s_1, s_1' are the spin of the external and excited field, respectively, and $|h|$ is the helicity of the massless mediator.

The blue dashed lines represent unitarity cuts, keeping in mind the need to insert physical state projectors when cutting spinning propagators. We expand the amplitude in the soft limit, giving us the expansion

$$\mathcal{A}_4^{(s_1,s_1',|h|)} = \mathcal{A}_{4(\mathrm{LO})}^{(s_1,s_1',|h|)} + \mathcal{A}_{4(\mathrm{NLO})}^{(s_1,s_1',|h|)} + \mathcal{A}_{4(\mathrm{N^2LO})}^{(s_1,s_1',|h|)} + \cdots, \tag{4.19}$$

where the leading order one-loop amplitude $\mathcal{A}_{s_1,s_1',|h|}^{(\mathrm{LO})}$ is a sum of box and cross box diagrams, which can be expressed as iterative combinations of tree-level amplitudes via reverse

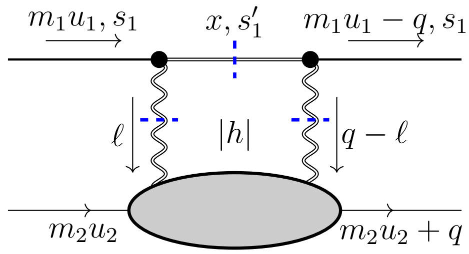

Figure 4.2: Unitarity cut required to reconstruct the integrand for the leading-order absorptive impulse. Pinched mediator contributions are scaleless in the soft region of ℓ-integration and pinched excited-state contributions are scaleless in the region of x-integration corresponding to absorptive modes.

unitarity,

$$\hat{\delta}(z) = \frac{i}{z + i0} - \frac{i}{z - i0}. \tag{4.20}$$

While previous work on absorption has been focused on matching to black hole results, we have instead decided to make our results more generally applicable to compact objects. As in [189], one can in principle compare cross sections with [232] and determine the spectral density function $\rho(x)$. In this work, we use the leading non-zero value $\rho(x) \propto x$ in order to obtain the leading order contributions, which may vanish in the case of black holes.

For any choice of spins there are strictly finitely many independent such amplitudes and therefore we can give a completely general parametrization; the explicit amplitudes used in this section are given in Appendix F.[3] We then input these amplitudes to the integrand in Fig. (4.2) and sew them with the scalar Compton amplitude with the appropriate physical state projectors for the given massless mediator.

Unlike in the non-absorptive, no-spin-transition case, triangle and Y-diagrams (in the graviton case) are sub-leading; as a result, there are no divergent super-classical contributions

[3]Because we are using definite spin representations, i.e. symmetric, transverse, traceless fields, the 3-point amplitudes are related to the coupling of massive spinning fields from familiar Lagrangian constructions such as the Proca Lagrangian (spin-1), Pauli-Fierz Lagrangian (spin-2), and the higher spin Lagrangians constructed in Refs. [171].

in the one-loop amplitude. This shift in the soft scaling of the diagrams is due to the Källen-Lehman form of the internal massive propagators in the soft limit and absorptive regime

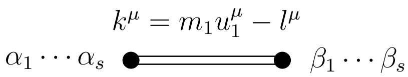

$$= \int_{m_1^2}^{\Lambda} d\mu^2\, \rho(\mu^2)\, \frac{i\, \Pi^{\alpha_1 \cdots \alpha_s}_{\beta_1 \cdots \beta_s}(\mu^2, k)}{k^2 - \mu^2 + i0} \xrightarrow[\text{absorptive}]{\text{soft limit}} -\frac{i}{2m_1} \int_0^\infty dx\, x^{1+\alpha} \frac{\Pi^{\alpha_1 \cdots \alpha_s}_{\beta_1 \cdots \beta_s}(x, m_1 u_1 - \ell)}{u_1 \cdot \ell + x - i0}, \tag{4.21}$$

which in the soft region is higher order than the usual linearized propagators in conservative dynamics, $i/(u \cdot l + i0)$. Here $\Pi^{\alpha_1 \cdots \alpha_s}_{\beta_1 \cdots \beta_s}$ is the completeness relation of the internal spin-s field. We also omit sub-leading terms in the soft expansion.

Also unique to the absorptive case, as was found in [189], when examining the integrand of the absorptive impulse only the iterative contributions of the amplitude are non-vanishing. This simplification is due to the horizontal flip symmetry of the integrand

$$\mathcal{I}^\mu \Big|_{l \leftrightarrow q-l} = \mathcal{I}^\mu, \qquad \mathcal{I}^\mu \equiv \mathcal{I}^\mu_v + \mathcal{I}^\mu_r. \tag{4.22}$$

Therefore, we only concern ourselves with the following integrand when computing the absorptive impulse

$$(\Delta p_1^\mu)^{s \to s'}_{|h|} = \frac{1}{4m_1 m_2} \int_0^\infty dx\, x^{1+\alpha} \int \hat{d}^D q\, \hat{\delta}(u_1 \cdot q)\, \hat{\delta}(u_2 \cdot q)\, e^{-ib\cdot q}$$

$$\times \int \hat{d}^D \ell \left(\frac{2\ell^\mu - q^\mu}{2} \right)$$

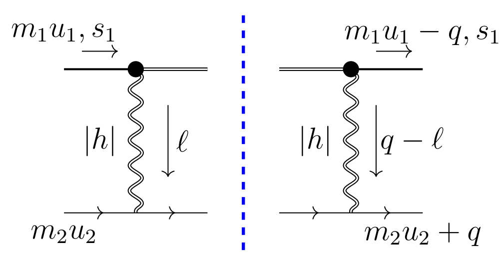

$$, \tag{4.23}$$

where the indices on the internal lines signal that we need to take in to account the completeness relation of the internal spin representation, i.e. insert physical state projectors; this is due to the summing over internal states. For example, for spin-1 and spin-2 representations with momentum k^μ, the projectors are,

$$\Pi^{\alpha_1}_{\beta_1}(\mu^2,k) = \delta^{\alpha_1}_{\beta_1} - \frac{k^{\alpha_1}k_{\beta_1}}{\mu^2}, \tag{4.24}$$

$$\begin{aligned}\Pi^{\alpha_1\alpha_2}_{\beta_1\beta_2}(\mu^2,k) = &\frac{1}{2}\Pi^{\alpha_1}_{\beta_1}(\mu^2,k)\Pi^{\alpha_2}_{\beta_2}(\mu^2,k) + \frac{1}{2}\Pi^{\alpha_1}_{\beta_2}(\mu^2,k)\Pi^{\alpha_2}_{\beta_1}(\mu^2,k)\\ &- \frac{1}{3}\Pi^{\alpha_1\alpha_2}(\mu^2,k)\Pi_{\beta_1\beta_2}(\mu^2,k),\end{aligned} \tag{4.25}$$

where $\mu^2 = 2m_1x + m_1^2$ is the mass of the excited field. These completeness relations are determined by the symmetry of the indices, transversality, and the number of little group states being $2s_1'+1$. Because the amplitude contributions begin at one-loop order, we do not have to worry about super-classical pieces polluting our results, unlike in the conservative case [39, 47, 178, 233].

Another consequence of not performing the cross-section matching done in Ref. [189] is that we will need to account for missing factors of G via dimensional analysis if we want to compare to works that have . Based on the units of the spin vector and the dimensionless perturbative expansion parameters (Eq.(4.13)) we use the following scaling scheme for each mediator exchange

$$(\Delta p_1^\mu)^{s\to s'}_{|0|} \propto \left(\frac{g^2/m_1^2}{|b|}\right)\left(\frac{Gm_1}{|b|}\right)^{\alpha_1}\left(\frac{|S_1|/m_1}{|b|}\right)^{\alpha_2}, \tag{4.26}$$

$$(\Delta p_1^\mu)^{s\to s'}_{|1|} \propto \left(\frac{e^2/m_1^2}{|b|}\right)\left(\frac{Gm_1}{|b|}\right)^{\alpha_1}\left(\frac{|S_1|/m_1}{|b|}\right)^{\alpha_2}, \tag{4.27}$$

$$(\Delta p_1^\mu)^{s\to s'}_{|2|} \propto \left(\frac{Gm_1}{|b|}\right)^{\alpha_1}\left(\frac{|S_1|/m_1}{|b|}\right)^{\alpha_2}, \tag{4.28}$$

where we will be solving for powers of Gm_1 based on how many powers of $|b|$ are left over after accounting for the spin scaling and the perturbative expansion scaling.

After we expand in the softlimit, we make a vNV decomposition of tensor integrals by making the replacement

$$\ell^\mu \to \frac{1}{2}q^\mu - x\check{u}_1^\mu + \left(\frac{\tilde{n}\cdot\ell}{\tilde{n}^2}\right)\tilde{n}^\mu + \ell^\mu_{[-2\epsilon]}, \tag{4.29}$$

where

$$\check{u}_1^\mu = \frac{u_1^\mu - y\,u_2^\mu}{1-y^2}, \qquad \check{u}_2^\mu = \frac{u_2^\mu - y\,u_1^\mu}{1-y^2}, \qquad y = u_1\cdot u_2, \qquad \tilde{n}^\mu \equiv \varepsilon^{\mu u_1 u_2 q}. \tag{4.30}$$

The master integrals we require (4.32) turn out to be finite in the cases of interest, so we can ignore the $[-2\epsilon]$-dimensional component of ℓ^μ when making the reduction. In (4.29) we have used the replacements $u_1 \cdot \ell \to -x$ and $q \cdot \ell \to \frac{1}{2}q^2$; the corresponding expressions differ only by integrals that are scaleless in the soft region.

Note that odd factors of $n \cdot \ell$ would violate the horizontal flip symmetry and therefore vanish upon integration; so we should only consider even powers of this term. Also note that we make the following replacement due to our choice of decomposition

$$\frac{(\tilde{n} \cdot \ell)^2}{\tilde{n}^2} \to \frac{x^2}{y^2-1} - \frac{q^2}{4}. \tag{4.31}$$

After tensor reduction, and dropping integrals that vanish due to the horizontal flip symmetry of the integrand, the remaining integrals are of the form

$$I_{k,n}[q^{\mu_1}...q^{\mu_r}] \equiv \int_0^\infty \mathrm{d}x x^k \int \hat{\mathrm{d}}^4 q \hat{\delta}(u_2 \cdot q) \hat{\delta}(u_1 \cdot q) e^{iq\cdot b} q^{\mu_1}...q^{\mu_r} \left(-q^2\right)^n \int \hat{\mathrm{d}}^4 \ell \frac{\hat{\delta}(u_1 \cdot \ell + x)\hat{\delta}(u_2 \cdot \ell)}{\ell^2 (q-\ell)^2}. \tag{4.32}$$

As shown in Appendix E of [189], the scalar integrals evaluate to

$$I_{k,n}[1] = \frac{(-1)^n 4^{n-2} \Gamma\left(\frac{k+1}{2}\right)^3 \left(\frac{k+1}{2}\right)_n^2}{\pi^{3/2}\Gamma\left(\frac{k}{2}+1\right)} \frac{(y^2-1)^{\frac{k-1}{2}}}{(-b^2)^{\frac{2n+1+k}{2}}}. \tag{4.33}$$

Tensor integrals can be generated by taking appropriate transverse b-derivatives

$$I_{k,n}[q^{\mu_1}...q^{\mu_r}] = \prod_{j=1}^{r} \left(-i\, \Xi^{\mu_j \nu_j} \frac{\partial}{\partial b^{\nu_j}}\right) I_{k,n}[1], \tag{4.34}$$

where the projector onto the space transverse to $\{u_1^\mu, u_2^\mu\}$ is [40]

$$\Xi^{\mu\nu} \equiv \eta^{\mu\nu} - u_1^\mu \check{u}_1^\nu - u_2^\mu \check{u}_2^\nu. \tag{4.35}$$

Because of our decomposition of the loop momentum vector, Eq. (4.29), one might naively believe, based on Eq. (4.23), that there no transverse contributions to the impulse. However, after integration, we have made the choice of basis $\{b^\mu, u_1^\mu, u_2^\mu, n^\mu\}$, where

$$n^\mu \equiv \varepsilon^{\mu u_1 u_2 b}. \tag{4.36}$$

Therefore, we also decompose the spin vector in this same basis

$$S_1^\mu = \left(\frac{b \cdot S_1}{b^2}\right) b^\mu + \left(\frac{n \cdot S_1}{b^2(y^2-1)}\right) n^\mu + (u_2 \cdot S_1)\check{u}_2^\mu. \tag{4.37}$$

As a result, in this basis choice, we have transverse components in the impulse on top of the longitudinal ($\check{u}_1$) and dual (n) components. This also means we must also decompose products of spin vectors, i.e. S_1^2, in order to consistently be in the basis.

4.3 Classical Spin from Finite Representations

In this section, we will define the spin vector and lay out how we express polarization tensors in terms of the spin vector. We will also cover our strategy for resolving ambiguities associated with definite-spin representations, which follows the method done in Refs. [198, 234].

4.3.1 Classical Spin Vector

All of the spin-dependent information in our amplitudes is contained in the polarization tensors; in particular, in the universal combination $\epsilon^{\mu_1\cdots\mu_{s_1}}(p_1-q)\epsilon^{\nu_1\cdots\nu_{s_1}}(p_1)$, which can be translated to spin vectors. In order to extract spin information from the polarization tensors, we use the definition for the spin tensor

$$\epsilon_{\mu_1\cdots\mu_{s_1}}(p_1)\,[M^{\mu\nu}]^{\mu_1\cdots\mu_{s_1}}{}_{\nu_1\cdots\nu_{s_1}}\,\epsilon^{\nu_1\cdots\nu_{s_1}}(p_1) \to S_1^{\mu\nu}, \tag{4.38}$$

where

$$[M^{\mu\nu}]^{\mu_1\cdots\mu_s}{}_{\nu_1\cdots\nu_s} = 2is\,\delta^{[\mu}_{(\nu_1}\eta^{\nu](\mu_1}\delta^{\mu_2}_{\nu_2}\cdots\delta^{\mu_s)}_{\nu_s)}, \tag{4.39}$$

are the generators of the spin-s representation of the Lorentz algebra

$$[M^{\mu\nu}, M^{\rho\sigma}] = -i\left(\eta^{\mu\rho}M^{\nu\sigma} - \eta^{\nu\rho}M^{\mu\sigma} + \eta^{\nu\sigma}M^{\mu\rho} - \eta^{\mu\sigma}M^{\nu\rho}\right). \tag{4.40}$$

Note that we are suppressing the little-group dependence of the polarizations, since these will eventually be summed over in the KMOC formalism, as explained in Section 4.2.1.

With that being said, it should be kept in mind that until we take the classical limit, the spin vector/tensor is a matrix in little-group space.

We model our system using transverse, traceless fields; therefore we will elect to use the spin vector

$$S_1^\mu = -\frac{1}{2m_1}\varepsilon^{\mu\nu\rho\sigma} p_{1\,\nu} S_{1\,\rho\sigma} \tag{4.41}$$

without having to worry about extra boost degrees of freedom i.e. obey the covariant spin supplementary condition (SSC) [170, 196, 235].

For products of spin vectors, we first symmetrize over the pair of free indices of the Lorentz generator in eq.(4.38)

$$\frac{1}{n!}\epsilon_{\alpha_1\cdots\alpha_{s_1}}(p_1)\,\mathrm{Sym}\left[M^{\mu_1\nu_1}\cdots M^{\mu_n\nu_n}\right]^{\alpha_1\cdots\alpha_{s_1}}_{\phantom{\alpha_1\cdots\alpha_{s_1}}\beta_1\cdots\beta_{s_1}}\;\epsilon^{\beta_1\cdots\beta_{s_1}}(p_1) \to S_1^{\mu_1\nu_1}\cdots S_1^{\mu_n\nu_n}. \tag{4.42}$$

We define the Sym$[\cdots]$ operator in the following way

$$\mathrm{Sym}\left[M^{\mu_1\nu_1}\cdots M^{\mu_n\nu_n}\right]^{\alpha_1\cdots\alpha_{s_1}}_{\phantom{\alpha_1\cdots\alpha_{s_1}}\beta_1\cdots\beta_{s_1}} \equiv \left[\sum_{\sigma\in S_n}\prod_{i=1}^{n} M^{\mu_{\sigma(i)}\nu_{\sigma(i)}}\right]^{\alpha_1\cdots\alpha_{s_1}}_{\phantom{\alpha_1\cdots\alpha_{s_1}}\beta_1\cdots\beta_{s_1}}, \tag{4.43}$$

where S_n is the symmetric group of n elements. We provide a couple of examples

$$\mathrm{Sym}[M^{\mu_1\nu_1}M^{\mu_2\nu_2}]^{\alpha_1\cdots\alpha_{s_1}}_{\phantom{\alpha_1\cdots\alpha_{s_1}}\beta_1\cdots\beta_{s_1}} = [M^{\mu_1\nu_1}M^{\mu_2\nu_2}]^{\alpha_1\cdots\alpha_{s_1}}_{\phantom{\alpha_1\cdots\alpha_{s_1}}\beta_1\cdots\beta_{s_1}} + [M^{\mu_2\nu_2}M^{\mu_1\nu_1}]^{\alpha_1\cdots\alpha_{s_1}}_{\phantom{\alpha_1\cdots\alpha_{s_1}}\beta_1\cdots\beta_{s_1}}, \tag{4.44}$$

$$\begin{aligned}\mathrm{Sym}[M^{\mu_1\nu_1}M^{\mu_2\nu_2}M^{\mu_3\nu_3}]^{\alpha_1\cdots\alpha_{s_1}}_{\phantom{\alpha_1\cdots\alpha_{s_1}}\beta_1\cdots\beta_{s_1}} &= [M^{\mu_1\nu_1}M^{\mu_2\nu_2}M^{\mu_3\nu_3}]^{\alpha_1\cdots\alpha_{s_1}}_{\phantom{\alpha_1\cdots\alpha_{s_1}}\beta_1\cdots\beta_{s_1}} + [M^{\mu_2\nu_2}M^{\mu_1\nu_1}M^{\mu_3\nu_3}]^{\alpha_1\cdots\alpha_{s_1}}_{\phantom{\alpha_1\cdots\alpha_{s_1}}\beta_1\cdots\beta_{s_1}}\\ &+ [M^{\mu_3\nu_3}M^{\mu_2\nu_2}M^{\mu_1\nu_1}]^{\alpha_1\cdots\alpha_{s_1}}_{\phantom{\alpha_1\cdots\alpha_{s_1}}\beta_1\cdots\beta_{s_1}} + [M^{\mu_1\nu_1}M^{\mu_3\nu_3}M^{\mu_2\nu_2}]^{\alpha_1\cdots\alpha_{s_1}}_{\phantom{\alpha_1\cdots\alpha_{s_1}}\beta_1\cdots\beta_{s_1}}\\ &+ [M^{\mu_2\nu_2}M^{\mu_3\nu_3}M^{\mu_1\nu_1}]^{\alpha_1\cdots\alpha_{s_1}}_{\phantom{\alpha_1\cdots\alpha_{s_1}}\beta_1\cdots\beta_{s_1}} + [M^{\mu_3\nu_3}M^{\mu_1\nu_1}M^{\mu_2\nu_2}]^{\alpha_1\cdots\alpha_{s_1}}_{\phantom{\alpha_1\cdots\alpha_{s_1}}\beta_1\cdots\beta_{s_1}},\end{aligned} \tag{4.45}$$

where ordering matters because these are matrix valued elements. We explain our notation for the product of matrices

$$[A_1A_2\cdots A_{n-1}A_n]^{\alpha_1\cdots\alpha_s}_{\beta_1\cdots\beta_s} \equiv [A_1]^{\alpha_1\cdots\alpha_s}_{\gamma_1\cdots\gamma_s}\,[A_2]^{\gamma_1\cdots\gamma_s}_{\delta_1\cdots\delta_s}\cdots[A_{n-1}]^{\eta_1\cdots\eta_s}_{\zeta_1\cdots\zeta_s}\,[A_n]^{\zeta_1\cdots\zeta_s}_{\beta_1\cdots\beta_s}, \tag{4.46}$$

for some matrix A_i.

With the spin variable well defined, we can proceed with obtaining spin information from our amplitudes.

The first step in extracting spin vectors from this product of polarization tensors is to expand $\epsilon^*_{\mu_1\cdots\mu_{s_1}}(p_1-q)$ in the soft limit. The procedure for the perturbative expansion of the polarization can be found in [116, 170, 197]. In our work, we choose the reference momentum[4] to be p_1, which allows us to use the following resummed expression

$$\epsilon^*_{\alpha(s_1)}(p_1-q)\,\epsilon_{\gamma_{(s_1)}}(p_1) = \exp\left[\frac{iq_\mu p_{1\,\nu}}{m_1^2}\frac{\arcsin\left(\sqrt{\frac{-q^2}{4m_1^2}}\right)}{\sqrt{\frac{-q^2}{4m_1^2}}\sqrt{1+\frac{q^2}{4m_1^2}}}M^{\mu\nu}\right]_{\alpha(s_1)}^{\quad\beta(s_1)}\epsilon^*_{\beta(s_1)}(p_1)\,\epsilon_{\gamma_{(s_1)}}(p_1). \tag{4.47}$$

Prior to expanding Eq. (4.47), we need to replace the product of polarization tensors to spin vectors. To do this, we construct a system of equations relating the polarization tensors to different powers of spin vectors. We start by taking the unordered outer product of $2s_1$ Lorentz generators with the polarization tensors, plugging in for the spin-s_1 representation. We then construct a system of equations by successively symmetrizing and anti-symmetrizing the generators and identifying these combinations with the appropriate spin vector structure. For example, for a spin-1 representation we start with

$$\begin{aligned}&-\Pi^{\mu_1\mu_2}(m_1^2,p_1)+\epsilon^{*\,\mu_2}(p_1)\epsilon^{\mu_1}(p_1)\\&\qquad=\left(\frac{-1}{2m_1}\right)^2\varepsilon^{\mu_1\nu_1\rho_1\sigma_1}\varepsilon^{\mu_2\nu_2\rho_2\sigma_2}p_{1\,\nu_1}p_{1\,\nu_2}\epsilon^*_{\alpha_1}(p_1)\left(M_{\rho_1\sigma_1}\right)^{\alpha_1}{}_{\beta}\left(M_{\rho_2\sigma_2}\right)^{\beta}{}_{\alpha_2}\epsilon^{\alpha_2}(p_1).\end{aligned} \tag{4.48}$$

Then we symmetrize and anti-symmetrize over the μ_1,μ_2 indices to get a system of equations

$$\begin{aligned}S_1^{\mu_1}S_1^{\mu_2} &= -\Pi^{\mu_1\mu_2}(m_1^2,p_1)+\frac{1}{2}\epsilon^{*\,\mu_2}(p_1)\epsilon^{\mu_1}(p_1)+\frac{1}{2}\epsilon^{*\,\mu_1}(p_1)\epsilon^{\mu_2}(p_1),\\ [S_1^{\mu_1},S_1^{\mu_2}] \equiv -\frac{i}{m_1}\varepsilon^{\mu_1\mu_2 p_1\,S_1} &= \epsilon^{*\,\mu_2}(p_1)\epsilon^{\mu_1}(p_1)-\epsilon^{*\,\mu_1}(p_1)\epsilon^{\mu_2}(p_1),\end{aligned} \tag{4.49}$$

[4]For spinning fields, the polarization tensor is defined with respect to some reference frame; the choice of reference frame is arbitrary. It is from this choice of frame that one boosts to the desired frame. For a detailed discussion there are numerous sources [116, 170, 197, 236].

which we solve for either unordered product of the polarization tensors

$$\epsilon^{\mu_1}(p_1)\epsilon^{*\,\mu_2}(p_1) \to \Pi^{\mu_1\mu_2}(m_1^2, p_1) + -\frac{i}{2m_1}\varepsilon^{\mu_1\mu_2 p_1 S_1} + S_1^{\mu_1}S_1^{\mu_2}. \tag{4.50}$$

With Eq. (4.50) and Eq. (4.47), we can reliably expand the universal polarization product in our amplitudes in the softlimit to any desired order for the spin-1 representation.

At this point, we are able to take the universal product of polarization tensors, $\epsilon^{\mu_1\cdots\mu_{s_1}}(p_1-q)\epsilon^{\nu_1\cdots\nu_{s_1}}(p_1)$, and translate it to a function of spin vectors and momenta. If we were only interested in leading order contributions, we would expand Eq. 4.47 to $\mathcal{O}(q^{2s_1})$; this is because for a spin-s_1 representation we can access spin vector contributions up to $\mathcal{O}(S_1^{2s_1})$. Therefore, in the soft limit we would be expanding up to $\mathcal{O}(\lambda^0)$. However, as well will see in the next section, we will need to expand to higher contributions in the soft limit.

4.3.2 Spin Universality and Interpolation

When calculating classical observables with fixed spin representation, special care must be taken for the Casimir operator

$$S_1^{\mu}S_{1\,\mu} \equiv S_1^2 = -s_1(s_1+1), \tag{4.51}$$

which creates an ambiguity in our results [198, 234]. It is easy to see this ambiguity in Eq. (4.51), where the left-hand side scales as $\mathcal{O}(\lambda^{-2})$ while the right-hand side is scaleless. This implies that terms that are naively suppressed in the softlimit actually should be multiplied by a factor of S_1^2, promoting them to classical-scaling terms. This ambiguity calls for what Refs. [198, 234] refer to as *Spin Interpolation*. A guiding principle in fixing this ambiguity is *spin universality*, where it is assumed that the amplitude for a spin-s_1 representation should contain the amplitude of a spin-s_1' representation if $s_1 > s_1'$ and if both amplitudes are describing the same interaction. For example, we assume that the amplitude $\mathcal{A}_4^{(1,2,h)}$ should contain the amplitude for $\mathcal{A}_4^{(0,1,h)}$ since they both involve a $\Delta s = 1$ change in angular momentum.

In this section, we will provide a concrete example for the spin interpolation procedure for the case of $\mathcal{A}_4^{(1,2,0)}$ and $\mathcal{A}_4^{(0,1,0)}$. [5] We interpolate the amplitudes prior to integration, therefore we will use the following decomposition of the amplitude

$$\mathcal{A}_4^{(s,s',h)} = \frac{1}{4m_1m_2}\int \hat{d}^4\ell\,\hat{\delta}(u_2\cdot\ell)\frac{\mathcal{N}^{(s,s',h)}}{\ell^2\,(q-l)^2[u_1\cdot\ell+x-i0]}, \tag{4.52}$$

where we will be focusing on the numerator $\mathcal{N}^{(s,s',h)}$. For the case that we are studying, the amplitude indeed takes this form; however, this is not strictly necessary for all cases.

We also interpolate in the soft limit, therefore we can express the relevant amplitudes in the following way

$$\mathcal{A}_{1,2,0} = \mathcal{A}_{1,2,0}^{(\mathrm{LO})} + \mathcal{A}_{1,2,0}^{(\mathrm{NLO})} + \mathcal{A}_{1,2,0}^{(\mathrm{N^2LO})} + \cdots\,, \quad \mathcal{A}_{0,1,0} = \mathcal{A}_{0,1,0}^{(\mathrm{LO})} + \mathcal{A}_{0,1,0}^{(\mathrm{NLO})} + \mathcal{A}_{0,1,0}^{(\mathrm{N^2LO})} + \cdots\,, \tag{4.53}$$

$$\mathcal{A}_{1,2,0}^{(\mathrm{LO})} = \tilde{\mathcal{A}}_{1,2,0}^{(\mathrm{LO})} + S_1^2\tilde{\mathcal{A}}_{1,2,0}^{(\mathrm{LO},\,1)},$$

where the tildes signal that these are the naive results before interpolation and we construct the interpolation ansatz $\tilde{\mathcal{A}}_{1,2,0}^{(\mathrm{LO},\,1)}$ based on the possible structures that, when multiplied by S_1^2, have the same soft scaling and spin scaling as $\tilde{\mathcal{A}}_{1,2,0}^{(\mathrm{LO})}$. In this case, because

$$\tilde{\mathcal{N}}_{1,2,0}^{(\mathrm{LO})} = -\frac{g^2\left(g_1^{(1,2,0)}\right)^2}{6}\left(\ell\cdot S_1\right)\left((q-\ell)\cdot S_1\right), \tag{4.54}$$

we construct the ansatz

$$\tilde{\mathcal{N}}_{1,2,0}^{(\mathrm{LO},\,1)} = f_1^{(1,2,0)}x^2 + f_2^{(1,2,0)}q^2, \tag{4.55}$$

since these are the only two independent structures that scale as $\mathcal{O}(\lambda^2 S_1^0)$. This could also have been informed by the structure of $\tilde{\mathcal{A}}_{0,1,0}^{(\mathrm{N^2LO})}$,

$$\tilde{\mathcal{N}}_{0,1,0}^{(\mathrm{N^2LO})} = \frac{g^2\left(g_1^{(0,1,0)}\right)^2}{2}\left(2x^2+q^2\right). \tag{4.56}$$

[5] The choice of scalar, photon, or graviton does not change the procedure.

We will not be considering NLO contributions because these would only contribute to Casimir ambiguity at $\mathcal{O}(S_1^3)$, which we cannot consider in a spin-1 representation. In higher-spin representations, however, this will certainly be a contribution to take into account.

According to spin universality, the following must hold

$$\mathcal{A}_{1,2,0} - \mathcal{A}_{0,1,0} = 0 \qquad \text{at} \qquad \mathcal{O}(S_1^0), \tag{4.57}$$

which is to say that all of the $\mathcal{O}(S_1^0)$ information of $\mathcal{A}_{1,2,0}$ must contain all of $\mathcal{A}_{0,1,0}$. If we enforce this condition in the soft limit and input the value for the Casimir operator (in this case $S_1^2 = -2$), we have the following set of equations

$$\begin{aligned} &\tilde{\mathcal{A}}^{(\text{LO})}_{1,2,0} - \mathcal{A}^{(\text{LO})}_{0,1,0} = 0, \\ &\tilde{\mathcal{A}}^{(\text{N}^2\text{LO})}_{1,2,0} - 2\tilde{\mathcal{A}}^{(C1,\text{LO})}_{1,2,0} - \mathcal{A}^{(\text{N}^2\text{LO})}_{0,1,0} = 0, \end{aligned} \tag{4.58}$$

where it is implied that we are only considering spinless information. Solving the second equation fixes the free coefficients in the ansatz such that

$$f_1^{(1,2,0)} = -\frac{g^2}{6}\left(3\left(g_1^{(0,1,0)}\right)^2 + \left(g_1^{(1,2,0)}\right)^2\right), \quad f_2^{(1,2,0)} = -\frac{g^2}{12}\left(3\left(g_1^{(0,1,0)}\right)^2 + \left(g_1^{(1,2,0)}\right)^2\right). \tag{4.59}$$

In the case of this spin transition, $\Delta s = 1$, the amplitude is suppressed by a power of $\mathcal{O}(S_1^2)$; this means that there is no spinless information at leading order and therefore the first equation is satisfied trivially. This is not always the case; for example, the leading contribution for the $\Delta s = 0$ transition for scalar exchange starts at $\mathcal{O}(S_1^0)$. It turns out the scaling of the spin suppression is predictable but we will explore this later in the next section.

With the interpolation procedure completed, we now have the unambiguous answer $\mathcal{A}^{(\text{LO})}_{1,2,0}$, which also includes the Wilson coefficient of $\mathcal{A}_{0,1,0}$. We will later see that it is possible to reduce the number of Wilson coefficients further by exploiting an unexpected symmetry. In the example we have been using, this would be

$$\mathcal{A}^{(\mathrm{LO})}_{1,2,0} - \mathcal{A}^{(\mathrm{LO})}_{1,0,0} = 0, \tag{4.60}$$

where both of these amplitudes describe a $|\Delta s| = 1$ change in spin. This is a feature we have observed for different spin transitions Δs and different massless exchange helicities, which we will comment on further in the next section.

The spin interpolation procedure should be valid as long spin universality holds; under this assumption we expect this procedure to work to arbitrary spin-s_1 representations. Therefore we can in principle have Casimir terms up to $(S_1^2)^{s_1}$. This means that we will have to expand our amplitudes to 2^{s_1} extra orders in the soft expansion in order to account for all Casimir ambiguities associated with a spin-s_1 representation.

After the spin interpolation is complete, we need to replace the factors of S_1^2 with the correct basis by squaring Eq. (4.37), such that

$$S_1^2 = -\left(\frac{(b \cdot S_1)^2}{(-b^2)} + \frac{(n \cdot S_1)^2}{(-b^2)\,(y^2-1)} + \frac{(u_2 \cdot S_1)^2}{y^2-1}\right). \tag{4.61}$$

This implies that there are a set of spin monomials up to $\mathcal{O}(S_1^3)$ that are obviously unambiguous prior to spin interpolation; namely,

$$\text{at } \mathcal{O}(S_1) \qquad b \cdot S_1,\ n \cdot S_1,\ u_2 \cdot S_1, \tag{4.62}$$

$$\text{at } \mathcal{O}(S_1^2) \qquad b \cdot S_1\, n \cdot S_1,\ n \cdot S_1\, u_2 \cdot S_1,\ b \cdot S_1\, u_2 \cdot S_1, \tag{4.63}$$

$$\text{at } \mathcal{O}(S_1^3) \qquad b \cdot S_1\, n \cdot S_1\, u_2 \cdot S_1, \tag{4.64}$$

where at $\mathcal{O}(S_1^4)$ there are no obvious spin monomials that are not affected by spin interpolation.

If we had not performed the spin interpolation but still knew that we had an ambiguity in our results, we could construct the impulse generally as

$$(\Delta p_1^\mu)^{s\to s'}_{|h|} = (u_1 \cdot \Delta p_1)^{s\to s'}_{|h|}\,\check{u}_1^\mu + \frac{(b \cdot \Delta p_1)^{s\to s'}_{|h|}}{b^2} b^\mu + \frac{(n \cdot \Delta p_1)^{s\to s'}_{|h|}}{(y^2-1)\,b^2} n^\mu, \tag{4.65}$$

where we can generically parametrize the coefficients of the components[6],

$$(u_1 \cdot \Delta p_1)^{s\to s'}_{|h|} = \frac{\sqrt{y^2-1}}{\sqrt{-b^2}} \sum_{j_1,j_2,j_3} (c_u)^{(s,s',|h|)}_{j_1,j_2,j_3} (b\cdot S_1)^{j_1} (n\cdot S_1)^{j_2} \left(\sqrt{-b^2}\, u_2\cdot S_1\right)^{j_3}, \tag{4.66}$$

$$\frac{(b \cdot \Delta p_1)^{s\to s'}_{|h|}}{b^2} = \frac{\sqrt{y^2-1}}{\sqrt{-b^2}}, \sum_{j_1,j_2,j_3} (c_b)^{(s,s',|h|)}_{j_1,j_2,j_3} (b\cdot S_1)^{j_1} (n\cdot S_1)^{j_2} \left(\sqrt{-b^2}\, u_2\cdot S_1\right)^{j_3}, \tag{4.67}$$

$$\frac{(n \cdot \Delta p_1)^{s\to s'}_{|h|}}{(y^2-1)\, b^2} = \frac{\sqrt{y^2-1}}{\sqrt{-b^2}} \sum_{j_1,j_2,j_3} (c_n)^{(s,s',|h|)}_{j_1,j_2,j_3} (b\cdot S_1)^{j_1} (n\cdot S_1)^{j_2} \left(\sqrt{-b^2}\, u_2\cdot S_1\right)^{j_3}, \tag{4.68}$$

where the $(c_i)^{(s,s',|h|)}_{j_1,j_2,j_3}$ would be the ambiguous coefficients. At $\mathcal{O}(S_1^2)$, the addition of the ambiguity has the following effect on the coefficients,

$$(c_i)^{(s,\,s',\,|h|)}_{2,0,0} \to (c_i)^{(s,\,s',\,|h|)}_{2,0,0} + \frac{\beta^{(s,s',|h|)}}{b^2}, \tag{4.69}$$

$$(c_i)^{(s,\,s',\,|h|)}_{0,2,0} \to (c_i)^{(s,\,s',\,|h|)}_{0,2,0} + \frac{\beta^{(s,s',|h|)}}{b^2(y^2-1)}, \tag{4.70}$$

$$(c_i)^{(s,\,s',\,|h|)}_{0,0,2} \to (c_i)^{(s,\,s',\,|h|)}_{0,0,2} + \frac{\beta^{(s,s',|h|)}}{b^2(y^2-1)}, \tag{4.71}$$

where we assume the ambiguity can affect any component of the impulse and $\beta^{(s,s',|h|)}$ is the ambiguity coefficient that would be fixed by the spin interpolation procedure. From this mapping, we also see that prior to interpolation it is possible to construct combinations of coefficients that are unaffected by the ambiguity coefficient, namely

$$\begin{aligned} d^{(s,s',h)}_{2,1} &\equiv (c_i)^{(s,s',|h|)}_{0,0,2} - \frac{(c_i)^{(s,s',|h|)}_{2,0,0}}{y^2-1}, \\ d^{(s,s',h)}_{2,2} &\equiv (c_i)^{(s,s',|h|)}_{0,2,0} - \frac{(c_i)^{(s,s',|h|)}_{2,0,0}}{y^2-1}, \end{aligned} \tag{4.72}$$

where $c_i \in \{c_b, c_n, c_u\}$; for the coefficients $d^{(s,s',h)}_{i,j}$, i tracks the power of spin and j tracks the number. The coefficients $(c_i)^{(s,s',|h|)}_{0,1,1}$, $(c_i)^{(s,s',|h|)}_{1,0,1}$, and $(c_i)^{(s,s',|h|)}_{1,1,0}$ are individually Casimir independent.

[6] In the next section, we will comment on the structure of Eq. (4.65); specifically, the additional components when compared to the non-spinning case [189].

At $\mathcal{O}(S_1^3)$ the following 6 non-trivial combinations of coefficients are Casimir independent

$$\begin{aligned}
d_{3,1}^{(s,s',h)} &\equiv (c_i)_{0,0,3}^{(s,s',|h|)} - \frac{(c_i)_{2,0,1}^{(s,s',|h|)}}{y^2-1}, \\
d_{3,2}^{(s,s',h)} &\equiv (c_i)_{0,1,2}^{(s,s',|h|)} - \frac{(c_i)_{2,1,0}^{(s,s',|h|)}}{y^2-1}, \\
d_{3,3}^{(s,s',h)} &\equiv (c_i)_{0,2,1}^{(s,s',|h|)} - \frac{(c_i)_{2,0,1}^{(s,s',|h|)}}{y^2-1}, \\
d_{3,4}^{(s,s',h)} &\equiv (c_i)_{0,3,0}^{(s,s',|h|)} - \frac{(c_i)_{2,1,0}^{(s,s',|h|)}}{y^2-1}, \\
d_{3,5}^{(s,s',h)} &\equiv (c_i)_{1,0,2}^{(s,s',|h|)} - \frac{(c_i)_{3,0,0}^{(s,s',|h|)}}{y^2-1}, \\
d_{3,6}^{(s,s',h)} &\equiv (c_i)_{1,2,0}^{(s,s',|h|)} - \frac{(c_i)_{3,0,0}^{(s,s',|h|)}}{y^2-1},
\end{aligned} \tag{4.73}$$

and the coefficient $(c_i)_{1,1,1}^{(s,s',|h|)}$ is individually Casimir independent.

At $\mathcal{O}(S_1^4)$ the following 9 non-trivial combinations of coefficients are Casimir independent

$$\begin{aligned}
d_{4,1}^{(s,s',h)} &\equiv (c_i)_{0,0,4}^{(s,s',|h|)} - \frac{(c_i)_{2,0,2}^{(s,s',|h|)}}{y^2-1} + \frac{(c_i)_{4,0,0}^{(s,s',|h|)}}{(y^2-1)^2}, \\
d_{4,2}^{(s,s',h)} &\equiv (c_i)_{0,1,3}^{(s,s',|h|)} - \frac{(c_i)_{2,1,1}^{(s,s',|h|)}}{y^2-1}, \\
d_{4,3}^{(s,s',h)} &\equiv (c_i)_{0,2,2}^{(s,s',|h|)} - (c_i)_{0,4,0}^{(s,s',|h|)} - \frac{(c_i)_{2,0,2}^{(s,s',|h|)}}{y^2-1} + \frac{(c_i)_{4,0,0}^{(s,s',|h|)}}{(y^2-1)^2}, \\
d_{4,4}^{(s,s',h)} &\equiv (c_i)_{0,3,1}^{(s,s',|h|)} - \frac{(c_i)_{2,1,1}^{(s,s',|h|)}}{y^2-1}, \\
d_{4,5}^{(s,s',h)} &\equiv (c_i)_{1,0,3}^{(s,s',|h|)} - \frac{(c_i)_{3,0,1}^{(s,s',|h|)}}{y^2-1}, \\
d_{4,6}^{(s,s',h)} &\equiv (c_i)_{1,1,2}^{(s,s',|h|)} - \frac{(c_i)_{3,1,0}^{(s,s',|h|)}}{y^2-1}, \\
d_{4,7}^{(s,s',h)} &\equiv (c_i)_{1,2,1}^{(s,s',|h|)} - \frac{(c_i)_{3,0,1}^{(s,s',|h|)}}{y^2-1}, \\
d_{4,8}^{(s,s',h)} &\equiv (c_i)_{1,3,0}^{(s,s',|h|)} - \frac{(c_i)_{3,1,0}^{(s,s',|h|)}}{y^2-1}, \\
d_{4,9}^{(s,s',h)} &\equiv (c_i)_{0,4,0}^{(s,s',|h|)} - \frac{(c_i)_{2,2,0}^{(s,s',|h|)}}{y^2-1} + \frac{(c_i)_{4,0,0}^{(s,s',|h|)}}{(y^2-1)^2}.
\end{aligned} \tag{4.74}$$

While not interpolating the amplitudes makes the impulses ambiguous, these combinations of the un-interpolated coefficients being unaffected by the Casimir ambiguities allows us to draw conclusions from un-interpolated results without worrying about missing information. In fact, we can construct combinations of coefficients for higher powers of spin that are not affected by the Casimir ambiguity.

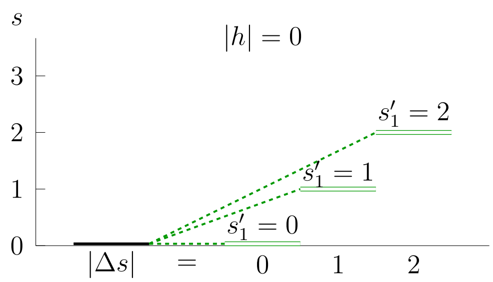

(a) Spin transition spectrum of the spin-0 field under massless scalar exchange.

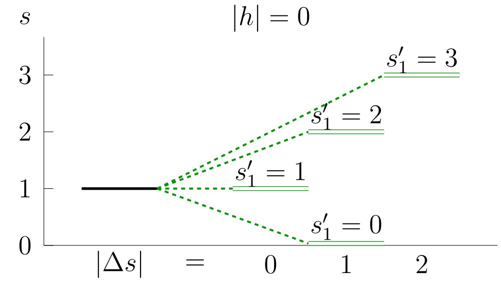

(b) Spin transition spectrum of the spin-1 field under massless scalar exchange.

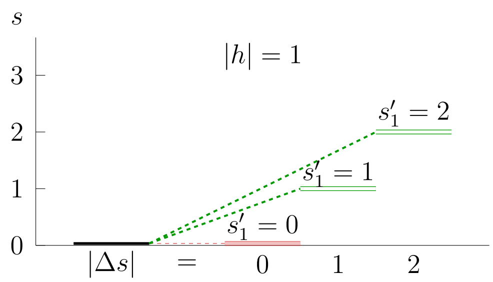

(c) Spin transition spectrum of the spin-0 field under photon exchange.

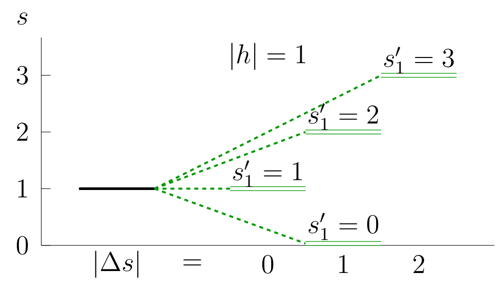

(d) Spin transition spectrum of the spin-1 field under photon exchange.

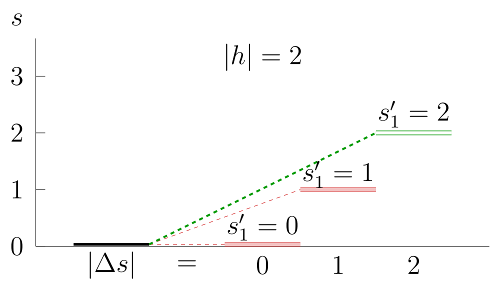

(e) Spin transition spectrum of the spin-0 field under graviton exchange.

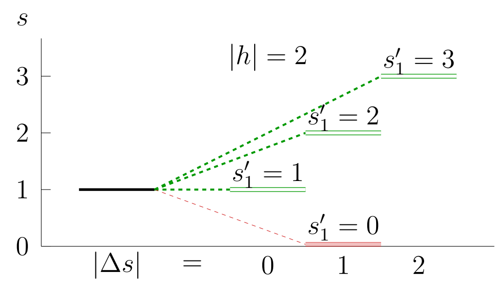

(f) Spin transition spectrum of the spin-1 field under graviton exchange.

Figure 4.3: Calculated spin transition spectrum of the external spin-0 and spin-1 field. The bold line represents the mass-m field while the double line represents the excited mass-μ field. The red transitions are forbidden because they would violate gauge invariance. The green transitions are allowed. We refer to transitions above the $\Delta s = 0$ horizontal the "ceiling" and those below the "floor".

4.4 Results

Here we summarize our calculation method and some structural aspects of the results. We use the spin transitions spectra in Fig. 4.3 to guide the explanation of our results. Our observations are informed by behavior in external spin-1 and spin-0 calculations.

4.4.1 Classical Spin Transitions and Absorption

We will provide a 5-step breakdown of our approach to calculating the impulse. We will go from constructing the amplitude to leading order through arriving at a final impulse.

1. Construct the Integrand

We construct the one-loop integrand by the method of generalized unitarity. We sew together the minimal coupling Compton amplitude to the absorptive 3-point amplitudes in Appendix F via physical state projectors for the scalar, photon, and graviton and completeness relations for the internal excited spin states. For the spectral mass function, we choose $\rho(x) \sim x$; however, it should be noted for different physical objects this proportionality may change.

2. Replace Polarization Tensors with Spin Vectors

After sewing together the integrand, we replace the universal product of polarization tensors with Eq. (4.47). At this point, we can follow the procedure of Sec. (4.3.1) and replace the polarization tensors with spin vectors and projectors.

3. Expand the Integrand

Now that the integrand is fully in terms of momenta and spin vectors, we can perform the soft expansion. As explained in Sec. (4.3.2), we will need to expand to 2^{s_1} extra orders of λ in order to be able to carry out the interpolation procedure. The leading order contribution should reduce to the sum of box and cross-box contributions, which leads to the cuts in the impulse integrand of Eq. (4.23).

4. Interpolate the Integrand

With the integrand expanded in the soft limit, we can perform the spin interpolation procedure laid out in Sec. (4.3.2). This should only be done if there is a corresponding transition that has a lower external spin-s_1' field whose contribution should be entirely contained by the spin-s_1 calculation, as dictated by spin universality. Once the interpolation is complete, we have the unambiguous integrand, which may carry Wilson coefficients associated with lower external spin 3-point amplitudes.

5. Integrate

Now that we have the unambiguous integrand, the final step now is to vNV decompose tensor integrals (Eq. (4.29)), and integrate using the master formula Eq. (4.32). After placing all leftover vectors in to the basis $\{b^\mu, u_1^\mu, u_2^\mu, n^\mu\}$, we have successfully calculated the impulse. This also means that we replace all factors of S_1^2 with Eq. (4.61).

At this point we arrive at the final impulse, which we parameterize into components as in Eq. (4.65), and organize the coefficients those components in Eqs. (4.67 - 4.66). We provide the results for the interpolated impulses in Appendix G, up to $\mathcal{O}(S_1^2)$. For the non-interpolated results, we provide the combination of coefficients that are immune to the Casimir ambiguity discussed in Section (4.3.2).

4.4.2 Basic Structure of the Impulse

In contrast to the spinless case [189], the impulse that we have calculated has components along the b^μ and n^μ directions. Naively, if one were to follow the steps we have provided, one might expect the n^μ component but certainly not b^μ. After all, if we were to look at the impulse integrand, Eq. (4.23), and the decomposition of the loop momentum, Eq. (4.29), the factors of q^μ exactly cancel, which is what typically Fourier transforms to b^μ. The only possible source for the resulting b^μ component of the impulse is the $\tilde{n}^\mu$ component of the impulse integrand after decomposing the loop momentum.

From our calculation, at $\mathcal{O}(S_1^2)$, there are only two non-vanishing contributions for both the n^μ and b^μ component: $(c_n)_{1,0,1}^{(s,s',|h|)}, (c_n)_{0,1,1}^{(s,s',|h|)}$ and $(c_b)_{1,0,1}^{(s,s',|h|)}, (c_b)_{0,1,1}^{(s,s',|h|)}$. The only spin monomials in momentum space that would generate the spin monomials associated with these coefficients are $\tilde{n} \cdot S_1 u_2 \cdot S_1$ and $q \cdot S_1 u_2 \cdot S_1$. If we focus on this part of the integrand, replace vectors of q with projected derivatives, as done in Eq. (4.34), make sure to project all vectors on to the basis $\{\check{u}_1^\mu, \check{u}_2^\mu, b^\mu, n^\mu\}$, and assume that prior to taking derivatives the integral is proportional to $(-b^2)^\alpha$, we find the following correspondence

$$\begin{aligned} &\tilde{n}^\mu\, \tilde{n} \cdot S_1\, u_2 \cdot S_1 \longrightarrow b^\mu\, u_2 \cdot S_1\, b \cdot S_1 + n^\mu\, u_2 \cdot S_1\, n \cdot S_1 \left(\frac{2\alpha - 1}{y^2 - 1}\right), \\ &\tilde{n}^\mu\, \tilde{q} \cdot S_1\, u_2 \cdot S_1 \longrightarrow b^\mu\, u_2 \cdot S_1\, n \cdot S_1 - n^\mu\, u_2 \cdot S_1\, b \cdot S_1\, (2\alpha - 1), \end{aligned} \tag{4.75}$$

where extra overall numerical factors are dropped for clarity. As we have established, these are the only combinations in which the non-longitudinal contributions to the impulse occur. This also explains why the coefficients associated with these contributions are always related to each other, which can be seen in the results in Appendix G.

We also find that the space of spin monomials at each order in spin is not spanned by the spin monomials in any of the contributions to the impulse, i.e. several of the $(c_i)_{j_1,j_2,j_3}^{(s,s',|h|)}$ are zero. This is apriori not expected and must be a feature of the kinematics of the system we are studying, since this appears to be a universal feature regardless of the helicity exchanged.

4.4.3 Floor-Ceiling Symmetry

We have observed that in all cases the calculated absorptive impulse satisfies the following relation

$$(\Delta p_1^\mu)_{|h|}^{s\to s-\Delta s} \cong (\Delta p_1^\mu)_{|h|}^{s\to s+\Delta s}\,, \tag{4.76}$$

where $\cong$ means that the two expressions are equal up to a non-trivial mapping of Wilson coefficients. In words, the impulse associated with a *decrease* of the spin magnitude by Δs (the *floor*) is identical to the impulse associated with an *increase* of spin magnitude by Δs (the *ceiling*).

In this framework, this seems far from obvious. In general the 3-point amplitude in the ceiling transition involves strictly more Wilson coefficients than the corresponding floor transition. For Eq. (4.76) to be possible, most of the ceiling Wilson coefficients must be irrelevant in the classical limit, at least to leading order.

The simplest illustrative example is to compare $(\Delta p_1^\mu)_0^{1\to 2}$ with $(\Delta p_1^\mu)_0^{1\to 0}$. Comparing the relevant three-point amplitudes in Section (4.4.1) does not make any symmetry obvious. However, if we looked at the relevant impulse coefficients in Section (G), we would find that there exists a mapping between Wilson coefficients that would make these results identical

$$g_1^{(1,0,0)} \mapsto \frac{1}{6}\, g_1^{(1,2,0)}, \qquad\qquad g_1^{(0,1,0)} \mapsto \frac{2\,i}{3} g_1^{(1,2,0)}. \tag{4.77}$$

The second mapping has an interesting implication. $g_1^{(0,1,0)}$ comes from the Casimir interpolation between $\mathcal{A}_{1,2,0}$ and $\mathcal{A}_{0,1,0}$. Prior to invoking the Floor-Ceiling symmetry, there was no direct relationship between the Wilson coefficients of these amplitudes; we only had a mixing of coefficients from different (yet related) amplitudes. Once we take in to account the symmetry, we are finally able to express $(\Delta p_1^\mu)_0^{1\to 2}$ fully in terms of Wilson coefficients in its three-point amplitude. This suggests there is an extra condition in the Casimir interpolation scheme

$$\mathcal{A}^{(LO)}_{s,s+\Delta s,|h|} - \mathcal{A}^{(LO)}_{s,s-\Delta s,|h|} = 0. \tag{4.78}$$

We have observed this for the photon case as well. We have also observed this symmetry for spin-2 external fields for the $|\Delta s| = 1, 2$ transitions, however without Casimir interpolation i.e. without an equivalent mapping to the second one in Eq. (4.77).

4.4.4 Spin Suppression

We have also observed a suppression that is universal across all massless mediators. When examining the scaling between different spin transitions we find that those channels that are missing a floor are suppressed in the soft expansion. However, this does not mean that this is a true quantum suppression; rather, because these are by definition leading order absorptive contributions, we interpret this to be a suppression in the gravitational Newton constant G . This implies that transitions from spin-0 are always G suppressed because there's nowhere to transition to but towards a ceiling.

For example, if we look at Fig. 4.3 we see the spectrum of spin transitions that we calculated, where graphs in a row share the same massless mediator and graphs in a column share the same external spin representation. Looking at the $|\Delta s| = 1$ channel in Fig. 4.3a, we see that the external spin-0 spectrum is missing a floor. Looking one spectrum over in Fig. 4.3b, we see that in the same channel the external spin-1 spectrum has both a floor and a ceiling. When comparing the amplitudes for these channels in the soft limit, we find the following scalings

$$\mathcal{A}_{0,1,0} \propto \mathcal{O}\left(\lambda^2\right), \qquad \mathcal{A}_{1,0,0}, \mathcal{A}_{1,2,0} \propto \mathcal{O}\left(\lambda^0\right), \tag{4.79}$$

where $\mathcal{O}\left(\lambda^0\right)$ is the lowest allowed order for any channel or any massless mediator. In position space, this difference in scalings translates to an extra factor of $1/(-b^2)$ in $(\Delta p_1^\mu)_0^{0\to 1}$. We can determine the G-scaling of the impulse by dimensional analysis; for the current example we find

$$(\Delta p_1^\mu)_0^{0\to 1} \propto \mathcal{O}\left(G^4 S_1^0\right), \qquad (\Delta p_1^\mu)_0^{1\to 2}, (\Delta p_1^\mu)_0^{1\to 0} \propto \mathcal{O}\left(G^2 S_1^2\right), \tag{4.80}$$

where we include the spin scaling to illustrate an interesting point that we observed universally. Clearly the spectrum that included a floor and a ceiling are leading in the PM expansion, while the floor-less spectrum is sub-leading, as if trading the spin scaling $\mathcal{O}(S_1^2)$ for G scaling $\mathcal{O}(G^2)$. We can instead consider this pattern a spin suppression, since the leading G contribution occurs at a higher order in spin.

As another example, let us consider the $|\Delta s| = 2$ channel. Here we observe a similar scaling pattern to that of the $|\Delta s| = 1$ channel,

$$\begin{aligned} &\mathcal{A}_{0,2,0} \propto \mathcal{O}\left(\lambda^4\right), \qquad &&\mathcal{A}_{1,3,0} \propto \mathcal{O}\left(\lambda^2\right), \\ &(\Delta p_1^\mu)_0^{0\to 2} \propto \mathcal{O}\left(G^6 S_1^0\right), \qquad &&(\Delta p_1^\mu)_0^{1\to 3}, \propto \mathcal{O}\left(G^4 S_1^2\right), \end{aligned} \tag{4.81}$$

however, the external spin-1 transition is still sub-leading in the λ/G scaling. No-Floor suppression suggests that we need to go to $O(S_1^4)$ to see the leading λ/G contribution, i.e. an external spin-2 calculation. Because the overall scaling of the amplitude is not affected by Casimir ambiguity, we can confidently verify that for the spin-2, $|\Delta s| = 2$ channel, the amplitudes and impulses scale in the following way

$$\begin{aligned} &\mathcal{A}_{2,4,0}, \mathcal{A}_{2,0,0} \propto \mathcal{O}\left(\lambda^0\right), \\ &(\Delta p_1^\mu)_0^{2\to 4}, (\Delta p_1^\mu)_0^{2\to 0} \propto \mathcal{O}\left(G^2 S_1^4\right), \end{aligned} \tag{4.82}$$

which follows the expected trend, i.e. the first spin-s field with a floor and a ceiling for a given channel starts the spin scaling at $\mathcal{O}(S_1^{2s})$ at the leading λ/G scaling.

From this exchange between powers of G and powers of S_1, which we call No-Floor suppression, we can predict the leading order PM scaling of graviton absorption. In Ref. [189], the Källen-Lehman projector for graviton radiation is equivalent to summing over the states of a spin-2 field; in our language, this would correspond to the $(\Delta p_1^\mu)_2^{0\to 2}$ calculation. For the graviton $|\Delta s| = 2$ channel, (Figures 4.3e and 4.3f) we see that both the spin-0 and spin-1 representations are missing a floor; in fact, we must go to a spin-2 representation to find the leading G order result. No-Floor suppression implies that

$$\mathcal{A}_{0,2,2} \propto \mathcal{O}\left(\lambda^4\right), \qquad \mathcal{A}_{1,3,2} \propto \mathcal{O}\left(\lambda^2\right), \qquad \mathcal{A}_{2,4,2}, \mathcal{A}_{2,0,2} \propto \mathcal{O}\left(\lambda^0\right)$$
$$(\Delta p_1^\mu)_2^{0\to 2} \propto \mathcal{O}\left(G^7 S_1^0\right), \quad (\Delta p_1^\mu)_2^{1\to 3} \propto \mathcal{O}\left(G^5 S_1^2\right), \quad (\Delta p_1^\mu)_2^{2\to 4}, (\Delta p_1^\mu)_2^{2\to 0} \propto \mathcal{O}\left(G^3 S_1^4\right), \tag{4.83}$$

where we have verified this scaling argument by dimensional analysis. Therefore we predict that the leading absorptive effect should occur at 3-PM at $\mathcal{O}\left(S_1^4\right)$. However, when comparing to Ref. [213], we find that while we match the leading G scaling, we are off by a power of S_1. A similar situation occurs for the leading PL scaling of photon absorption. The reason for this mismatch in the spin scaling is that we do not include super-radiance effects in our calculation. By avoiding the spectral mass function matching, we also miss non-analytic in spin contributions that Ref. [213] would be sensitive to.

For the cases of absorption without spin-transitions ($\Delta s = 0$), the suppression is more straightforward. In this channel, if $s_1 < |h|$, then the impulse either is suppressed or does not exist; this is due to gauge invariance and is related to the discussion in Appendix F. More specifically, if $s_1 + s_1' < |h|$ then the channel does not exist. If $s_1 + s_1' = |h|$, then the channel is suppressed. As a result, relative to the spin-2, $\Delta s = 0$ channel under graviton exchange, the spin-1 case is suppressed by a factor of G^2. Note that, in the case of graviton exchange, the gauge invariance restriction suppresses the spin-1, $|\Delta s| = 1$ channel (Fig. 4.3f), making it just as G-suppressed as the $|\Delta s| = 2$ channel.

This No-Floor suppression has an interesting implication when it comes leading spin scaling for the impulse. Say we were to consider a spin-1/2 field and look at its spin transition spectrum; it would look like the first column of Fig. 4.3, i.e. all ceilings and no floors. If we only transition in units of integer spin there would be no floors to consider for any massless mediator; therefore, we find that the leading G contribution to the impulse for any channel can never be linear in spin. This might be related to the absence of super-radiance for Dirac fermions on a Kerr background [230, 237], though a more thorough study would be necessary

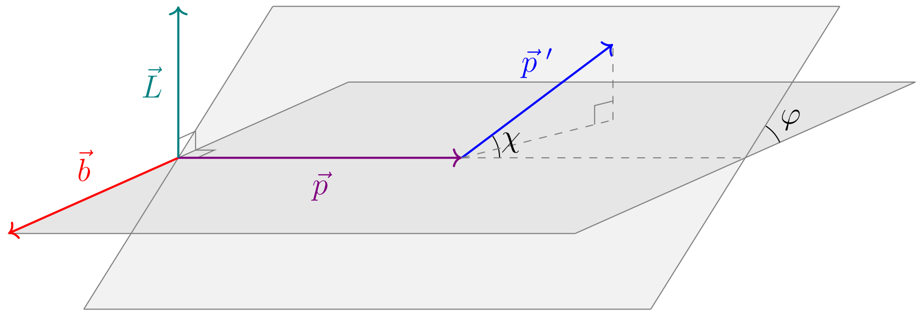

Figure 4.4: The *polar* χ, and *azimuthal* φ, scattering angles defined in the COM frame in terms of the incoming 3-momentum $\vec{p}$, outgoing 3-momentum $\vec{p}\,'$ and impact parameter $\vec{b}$. The azimuthal angle φ measures the degree of *non-planarity* of the scattering; in the limit of aligned spin ($\vec{S}_1 \propto \vec{L}$) the scattering is planar ($\vec{p}\,'$ lies in the plane spanned by $\vec{p}$ and $\vec{b}$) and consequently $\varphi = 0$.

to make this connection concrete.

4.4.5 Scattering Angles and Mass Shift

To calculate the scattering angle, we use the center-of-mass frame

$$\begin{aligned} u_1^\mu &= \left(\frac{E_1}{m_1}, 0, 0, \frac{|\vec{p}\,|}{m_1}\right), \qquad u_2^\mu = \left(\frac{E_2}{m_2}, 0, 0, -\frac{|\vec{p}\,|}{m_2}\right), \\ b^\mu &= |\vec{b}|\,(0,1,0,0)\,, \qquad n^\mu = |\vec{b}|\frac{|\vec{p}\,|}{\mu_{cm}}\frac{E}{M}\,(0,0,1,0)\,, \end{aligned} \tag{4.84}$$

where $M = m_1 + m_2$ is the total mass, $\mu_{cm} = m_1 m_2/M$ is the reduced mass, $E = E_1 + E_2$ is the total energy, and $|p|$ is the center of mass momentum. In this frame the vector n is proportional to the orbital angular momentum, $\vec{L} = \vec{b} \times \vec{p}$, specifically

$$\vec{n} = -\frac{E}{\mu_{cm}\,M}\vec{L}, \tag{4.85}$$

they are anti-aligned in our set up.

To parametrize the spin in the center-of-mass frame we first perform a standard boost from the rest frame. We define the ring radius in the rest frame

$$a_1^\mu \equiv \frac{s_1^\mu}{m_1} = |\vec{a}_1|(0,\, \cos\phi\sin\theta,\, \sin\phi\sin\theta,\, \cos\theta), \tag{4.86}$$

where s_1^μ is the rest-frame spin of particle 1. Boosting from the rest frame to the center-of-mass frame results in

$$S_1^\mu = m_1\,|\vec{a}_1|\left(\frac{|\vec{p}\,|}{m_1}\cos\theta, \cos\phi\sin\theta, \sin\phi\sin\theta, \frac{E_1}{m_1}\cos\theta\right), \tag{4.87}$$

where in our choice of spherical coordinates $\theta \in [0,\pi]$ and $\phi \in [0, 2\pi]$.

To leading order in the center-of-mass frame, we define the scattering angle as

$$\chi_{|h|}^{s\to s'} = \frac{\sqrt{m_1^2+m_2^2+2m_1m_2y}}{m_1m_2\sqrt{y^2-1}}\sqrt{-\left(\Delta p_1^2\right)_{|h|}^{s\to s'} - \frac{(\Delta m_1^2)_{|h|}^{s\to s'}}{y^2-1}}, \tag{4.88}$$

where we ignore higher order contributions. At leading order, we define the mass shift as

$$(\Delta m_1)_{|h|}^{s\to s'} = (u_1\cdot\Delta p_1)_{|h|}^{s\to s'}\,, \tag{4.89}$$

which comes from momentum conservation. We also consider the *azimuthal scattering angle* φ,

$$\varphi_{|h|}^{s\to s'} = \frac{1}{\sqrt{y^2-1}}\frac{(n\cdot\Delta p_1)_{|h|}^{s\to s'}}{(b\cdot\Delta p_1)_{|h|}^{s\to s'}}, \tag{4.90}$$

which measures the non-planarity of the scattering.

From Eq. (4.88) and our coordinate choices, one can use the results in Appendix G to calculate the full scattering angle. However, it is more instructive to study certain alignments of S_1^μ with the basis $\{u_2^\mu, b^\mu, n^\mu\}$. The relevant dot products are

$$u_2\cdot S_1 = m_1|\vec{a}_1|\frac{|\vec{p}\,|E}{\mu_{cm}M}\cos\theta, \tag{4.91}$$

$$b\cdot S_1 = -m_1|\vec{a}_1||\vec{b}|\sin\theta\cos\phi, \tag{4.92}$$

$$n\cdot S_1 = m_1|\vec{a}_1||\vec{b}|\frac{|\vec{p}\,|E}{\mu_{cm}M}\sin\theta\sin\phi. \tag{4.93}$$

For our set up, choosing $\theta = \pi/2$, $\phi = 3\pi/2$ isolates what is known as the *spin-aligned* scattering angle, $\tilde{\chi}_{|h|}^{s\to s'}$, which is when the spin and the angular momentum are aligned. In this alignment, there is no precession in our system and only the dot product Eq. (4.93) contributes.

We find for transitions with a Floor and Ceiling, the spin-aligned scattering angle is proportional to coefficients that vanish when one considers Floor-Ceiling Symmetry. For example, in the massless scalar exchange case

$$\tilde{\chi}_{|0|}^{1\to 0} = 0 \tag{4.94}$$

$$\tilde{\chi}_{|0|}^{1\to 2} \propto \left(3\left(g_1^{(0,1,0)}\right)^2 + 2\left(g_1^{(1,2,0)}\right)^2\right), \tag{4.95}$$

where the mapping from Floor-Ceiling symmetry in Eq. (4.77) eliminates $\tilde{\chi}_{|0|}^{1\to 2}$.

This feature holds for the same transition channel in photon exchange

$$\tilde{\chi}_{|1|}^{1\to 0} = 0 \tag{4.96}$$

$$\begin{aligned}\tilde{\chi}_{|1|}^{1\to 2} \propto\, & 32M^2\mu_{cm}^2\left(3\left(g_1^{(0,1,1)}\right)^2 + 2\left(g_1^{(1,2,1)}\right)^2\right) \\ & + 5(E^2-M^2)(E^2-M^2+4M\mu_{cm})\left[3\left(h_1^{(0,1,1)}\right)^2 + \left(h_1^{(1,2,1)}\right)^2\right. \\ & \left. +3\left(g_1^{(0,1,1)}\right)^2 + 2\left(g_1^{(1,2,1)}\right)^2\right],\end{aligned} \tag{4.97}$$

where the mapping from Floor-Ceiling Symmetry would be

$$\begin{aligned}&\left(g_1^{(1,0,1)}\right) \to 1/\sqrt{6}\left(g_1^{(1,2,1)}\right), \qquad && \left(g_1^{(0,1,1)}\right)^2 \to -2/3\left(g_1^{(1,2,1)}\right)^2, \\ &\left(h_1^{(1,0,1)}\right) \to 1/\sqrt{6}\left(h_1^{(1,2,1)}\right), && \left(h_1^{(0,1,1)}\right)^2 \to -1/3\left(h_1^{(1,2,1)}\right)^2,\end{aligned} \tag{4.98}$$

which eliminates $\tilde{\chi}_{|1|}^{1\to 2}$.

In the end, we find that all transitions that we calculate have a vanishing scattering angle in the spin-aligned case at leading order. This is easier to see by making the replacement in Eq. (4.88),

$$\chi_{|h|}^{s\to s'} = \frac{\sqrt{m_1^2+m_2^2+2m_1m_2y}}{m_1m_2\sqrt{y^2-1}}\sqrt{-\frac{\left((b\cdot\Delta p_1)_{|h|}^{s\to s'}\right)^2}{b^2} - \frac{\left((n\cdot\Delta p_1)_{|h|}^{s\to s'}\right)^2}{b^2(y^2-1)}} \tag{4.99}$$

which comes from our parameterization of the absorptive impulse Eq. (4.65) using the substitution Eq. (4.89).

By studying the coefficients in Appendix G, we see that there are always terms proportional to $b \cdot S_1$ and $u_2 \cdot S_1$, which vanish in the spin-aligned case. Apriori, this is a non-obvious property of the absorptive impulse; the fact that this property persists for all massless mediators signals that this is due to some property of the kinematics and should be universal.

Because we always have a vanishing scattering angle in the spin-aligned case, we have an undefined azimuthal scattering angle φ. This is, of course, expected when it comes to spherical coordinates; the azimuthal angle is ill-defined at the poles.

On top of the scattering angle, we have also calculated the leading order mass shift, $(\Delta m_1)_{|h|}^{s\to s'}$, for spin transition $|\Delta s| = 0, 1, 2$ up to $\mathcal{O}(S_1^2)$ in the spin expansion. When comparing to the results for Schwarzschild black holes in [189], we find that at first we have too many free coefficients in our results; namely, we have the Wilson coefficients from parity-even ($g_i^{(s,s',|h|)}$) and parity-odd ($h_i^{(s,s',|h|)}$) terms from the 3-point amplitude. However, when we set these Wilson coefficients equal to each other, we find that we reproduce the Schwarzschild results up to an overall constant. This matching hints that equating the parity-even and parity-odd Wilson coefficients corresponds to enforcing *Self-Duality* of the absorptive body, which in [189] arises from determining the 2-point function of absorptive operators in the portal action. This hints that there may be similar simplifications when one considers Kerr black holes.

4.5 Discussion

In this chapter we explored the effects of absorption and spin-transitions on 2-body scattering in the soft limit. We modeled the spin dependence of our bodies by using fields of definite spin s, allowing us to take in to account up to $\mathcal{O}\left(S_1^{2s}\right)$ contributions. We calculated the impulse by inputting absorptive amplitudes constructed from generalized unitarity, Fig. (1.3), in to the KMOC formalism. These amplitudes were calculated by appropriately sewing the 3-point amplitudes in Appendix F to the spinless Compton amplitude for scalar, photon, and graviton radiation.

By examining the results for the impulse, we have been able to see universal structural behaviors. We have observed Spin Universality, which is to say that higher spin representations entirely contain the information of lower spin representations. This fact is crucial for the spin interpolation procedure, which resolves any ambiguities due to Casimir terms.

We have also observed a pattern relating impulses of mirror transitions, i.e, $s \to s + \Delta s$ and $s \to s - \Delta s$, which we call Floor-Ceiling symmetry. The floor ($s \to s - \Delta s$) transition is related to the ceiling ($s \to s + \Delta s$) transition by a mapping of Wilson coefficients. This symmetry is also consequential for the spin-interpolation procedure by providing an extra condition to match Wilson coefficients of lower spin representations to higher spin ones.

We further find a scaling relationship for spin transition channels of different external spin representations across different massless mediators. What we call No-Floor suppression, we find that transitions without a floor are always suppressed in the λ/PM expansion. This results in the spin scaling at the leading PM order for a given transition channel is determined by the external spin representation of the first spectrum with a floor. In other words, there is an exchange between G scaling and spin scaling for spectra without a floor. Another consequence of No-Floor suppression is that, at leading PM order and $|\Delta s| > 0$, the impulse can never start below $\mathcal{O}(S_1^2)$, which can be seen in the results in Appendix G. This may be related to arguments forbidding fermionic radiation in Kerr backgrounds [230, 237] but a more thorough analysis needs to be done on this.

The source of these observations is not clear at this time. There must be some relationship to little group symmetries and gauge invariance since this is how we construct our building blocks; however, how these restrictions carry through the calculation is not clear. Moreover, numerous operators in the 3-point amplitudes do not survive the soft expansion. At the same time only certain combinations of operators appear at certain orders of spin. In short, there is a lot to investigate in how these observations can be made manifest earlier in the calculation, e.g. at the amplitude level.

There a number of ways to build upon this work. While we were able to comment on aspects of the external spin-2 calculation, a complete calculation including spin interpolation needs to be done in order to have the full picture. On a similar vein, pushing the calculation of impulses to larger $|\Delta s|$ and higher loop order would be insightful in knowing how well the Floor-Ceiling symmetry and No-Floor suppression hold. As we noted in Section 4.2.3, we did not match to black hole cross section calculations [232] to fix the spectral mass function $\rho(x)$. It would be interesting to see how the matching procedure introduced in Ref. [189] changes when taking spin transitions in to account and how these changes might affect our observations.

APPENDIX A

The Spin Operator

We consider the operator promotion of angular momentum, as done in Appendix B of Ref. [40]

$$\mathbb{J}^{\mu\nu} = \int d^3x\, M^{0\mu\nu} = \int d^3x \left(x^\mu T^{0\nu} - x^\nu T^{0\mu} \right), \tag{A.1}$$

where $M^{\alpha\mu\nu}$ is the conserved Noether current associated with Lorentz symmetry and $T^{\mu\nu}$ is the Belinfante tensor

$$T^{\mu\nu} = \Theta^{\mu\nu} - \frac{i}{2}\partial_\rho \left(\frac{\partial \mathcal{L}_0}{\partial(\partial_\rho \Phi_s)} \cdot M^{\mu\nu} \cdot \Phi_s - \frac{\partial \mathcal{L}_0}{\partial(\partial_\mu \Phi_s)} \cdot M^{\rho\nu} \cdot \Phi_s - \frac{\partial \mathcal{L}_0}{\partial(\partial_\nu \Phi_s)} \cdot M^{\rho\mu} \cdot \Phi_s \right), \tag{A.2}$$

where $\Theta^{\mu\nu}$ is the stress-energy tensor, $\partial_\rho = \frac{\partial}{\partial x^\rho}$, $(M^{\mu\nu})^{\alpha(s)}{}_{\beta(s)}$ is the Lorentz generator, the dots surrounding the Lorentz generator implies summation over the representation indices, and $\Phi_s(x)$ is the complex free general spin field

$$\Phi_s(x) = \sum_a \int d\Phi(k) \left(a_a(k)\epsilon_a(k)e^{-ik\cdot x} + b_a^\dagger(k)\epsilon_a^*(k)e^{ik\cdot x} \right), \tag{A.3}$$

where a is the little group index and $a_a, b_a^\dagger$ are the particle and anti-particle annihilation operators, respectively. Assuming a reasonable free kinetic term from some Lagrangian $\mathcal{L}_0$, like Eq. (2.35) with $\alpha \to 0$, we obtain a natural separation of angular momentum in to what we call "orbital" and "spin" parts:

$$\mathbb{J}^{\mu\nu} = \int d^3x \, \left(x^\mu \Theta^{0\nu}(x) - x^\nu \Theta^{0\mu}(x) + i\Pi_s(x) \cdot M^{\mu\nu} \cdot \Phi_s(x) \right) = \mathbb{L}^{\mu\nu} + \mathbb{S}^{\mu\nu}, \tag{A.4}$$

$\Pi_s(x) = \frac{\partial \mathcal{L}}{\partial_0 \Phi_s}$ is the conjugate momentum to Φ_s. We call the term with the Lorentz generator the spin operator, $\mathbb{S}^{\mu\nu}$. Taking the normal ordered expectation value of the spin operator gives us the following for the free theory,

$$\langle p'; a'|\mathbb{S}^{\mu\nu}|p; a\rangle = \langle 0|a^{a'}(p') : \int d^3x\, i\, \Pi_s\, M^{\mu\nu}\Phi_s : a_a^\dagger(p)|0\rangle = -\frac{1}{2}\hat{\delta}_\Phi(p'-p)\, \epsilon^{a'}(p') \cdot M^{\mu\nu} \cdot \epsilon_a(p), \tag{A.5}$$

where we use the commutation relation

$$[a_i(p'), a_j^\dagger(p)] = 2E_p\, \hat{\delta}^{(3)}(\vec{p}\,' - \vec{p})\, \delta_{i,j} = \hat{\delta}_\Phi(p'-p)\, \delta_{i,j}, \tag{A.6}$$

and ignore terms proportional to $b^\dagger$ since we are only interested in positive energy states in the classical limit.

APPENDIX B

Polarization Tensors and their Products

We know that polarization tensors are not tensors in the usual sense. To boost from one arbitrary frame to another, one has to first perform a standard boost to some arbitrary reference frame followed by a boost to the final frame: Ref. [236] provides a thorough explanation using the rest frame as a reference frame explicitly. Refs. [117, 118] provide an alternative expression for the standard boost with some arbitrary reference frame k without explicitly breaking covariance. As in Ref. [118, 236], we write our spin-s polarization tensors as

$$\epsilon^{\mu(s)}(p) = D(L(p;k))^{\mu(s)}{}_{\nu(s)}\epsilon^{\nu(s)}(k), \tag{B.1}$$

where this D matrix boosts $\epsilon^{\mu(s)}$ from reference frame k to arbitrary frame p via some standard boost $L(p;k)$ and furnishes a representation of the homogeneous Lorentz group. For example, the scalar representation $D = 1$ and the vector representation $D = \Lambda^{\mu}{}_{\nu}$, which is what we normally think of as a standard Lorentz transformation.

While Refs. [116, 170, 236] have a thorough discussion on how to deal with this feature of polarization tensors, they eventually break covariance explicitly, which is inconvenient for the KMOC formalism. Ref. [118] provides an alternative expression for these D matrices

$$D(L(p;k))^{\alpha(s)}{}_{\beta(s)} = \text{Exp}[-i\lambda(p;k)p^{\mu}k^{\nu}M_{\mu\nu}]^{\alpha(s)}{}_{\beta(s)}, \tag{B.2}$$

$$\lambda(p;k) = \frac{\text{arcosh}\left(\frac{p\cdot k}{m^2}\right)}{\sqrt{(p\cdot k)^2 - m^4}} \equiv \frac{\Theta}{\sqrt{\Gamma}}. \tag{B.3}$$

The use of Θ and Γ is for later convenience and holds no significance beyond this discussion. We implicitly take k to be the rest frame but do not plug in this fact explicitly.

We now consider a small perturbation in the desired frame $p \to p+q$. We perturbatively expand the following polarization product about small q

$$\epsilon^*(p+q)\cdot\epsilon(p) = \epsilon^*(p+q)|_{q\to 0}\cdot\epsilon(p) + q^\alpha\left(\frac{\partial}{\partial p^\alpha}\epsilon^*(p+q)\right)|_{q\to 0}\cdot\epsilon(p) + \frac{q^\beta q^\alpha}{2!}\left(\frac{\partial}{\partial p^\beta}\frac{\partial}{\partial p^\alpha}\epsilon^*(p+q)\right)|_{q\to 0}\cdot\epsilon(p) + \cdots \tag{B.4}$$

where we suppress little group indices for clarity.

We start with the first non-trivial order in the expansion. Note we are now taking derivatives of a matrix exponential, therefore we must keep in mind the derivative of the exponential map

$$\frac{d}{dt}e^{X(t)} = \left(\frac{1-e^{-\mathrm{ad}_X}}{\mathrm{ad}_X}\frac{dX(t)}{dt}\right)e^{X(t)}, \tag{B.5}$$

where

$$\frac{1-e^{-\mathrm{ad}_X}}{\mathrm{ad}_X} = \sum_{k=0}^{\infty}\frac{(-1)^k}{(k+1)!}(\mathrm{ad}_X)^k, \tag{B.6}$$

and

$$\mathrm{ad}_X(Y) = [X,Y]. \tag{B.7}$$

Using this information, we expand the first derivative to sixth order in the exponential map expansion

$$\begin{aligned} q^\alpha\left(\frac{\partial}{\partial p^\alpha}\epsilon(p+q)\right)|_{q\to 0} = \Bigg\{ & p_\mu k_\nu \frac{m^2 q^2}{2}\left(\frac{\lambda^3}{3!}+\frac{\lambda^5\Gamma}{5!}+\frac{\lambda^7\Gamma^2}{7!}+\cdots\right) \\ & + k_\mu q_\nu\left(\left(\lambda+\frac{\lambda^3\Gamma}{3!}+\frac{\lambda^5\Gamma^2}{5!}+\frac{\lambda^7\Gamma^3}{7!}+\cdots\right)\right. \\ & \left. - k\cdot p\left(\frac{\lambda^2}{2!}+\frac{\lambda^4\Gamma}{4!}+\frac{\lambda^6\Gamma^2}{6!}+\cdots\right)\right) \\ & + p_\mu q_\nu m^2\left(\frac{\lambda^2}{2!}+\frac{\lambda^4\Gamma}{4!}+\frac{\lambda^6\Gamma^2}{6!}+\cdots\right)\Bigg\} iM^{\mu\nu}\epsilon(p), \end{aligned} \tag{B.8}$$

where we apply $k\cdot q = 0$ since q is assumed to be space-like and k is the rest frame, and $p\cdot q = -q^2/2$ due to momentum conservation. Recall that the λ carry factors of Γ; taking this into account results in equal scaling of Γ in each series resulting in the following resummation

$$q^\alpha \left(\frac{\partial}{\partial p^\alpha} \epsilon(p+q) \right) |_{q\to 0} = \Bigg\{ p_\mu k_\nu \frac{m^2 q^2}{2\Gamma} \left(\frac{\sinh\Theta}{\sqrt{\Gamma}} - \lambda \right) + k_\mu q_\nu \left(\frac{\sinh\Theta}{\sqrt{\Gamma}} - \frac{k\cdot p}{\Gamma} \left(\cosh\Theta - 1\right) \right) + p_\mu q_\nu \frac{m^2}{\Gamma} \left(\cosh\Theta - 1\right) \Bigg\} iM^{\mu\nu}\epsilon(p). \tag{B.9}$$

Finally, a couple of useful relations to know are $\cosh(\text{arcosh}x) = x$ and $\sinh(\text{arcosh}x) = \sqrt{x^2-1}$. With this in mind we arrive at the first term in the expansion

$$q^\alpha \left(\frac{\partial}{\partial p^\alpha} \epsilon(p+q) \right) |_{q\to 0} = \left((k+p)_\mu q_\nu + p_\mu k_\nu \frac{q^2(1-m^2\lambda)}{2(p\cdot k - m^2)} \right) \frac{iM^{\mu\nu}}{p\cdot k + m^2} \epsilon(p), \tag{B.10}$$

where we should note that the second term in the parentheses is higher order in our expansion parameter q, and will therefore be ignored in the future.

We now have an answer for the first order expansion of the product of polarization tensors

$$q^\alpha \left(\frac{\partial}{\partial p^\alpha} \epsilon^*(p+q) \right) |_{q\to 0} \cdot \epsilon(p) = iq_\mu \frac{S^{\mu\nu}(p)(k_\nu + p_\nu)}{p\cdot k + m^2} \equiv iq_\mu \omega^\mu. \tag{B.11}$$

Calculating higher orders in the perturbation series streamlines. We consider the second derivative of the exponential map

$$\frac{d^2}{dt^2} e^{X(t)} = \frac{d}{dt} \left(\frac{1-e^{-\text{ad}_X}}{\text{ad}_X} \frac{dX(t)}{dt} \right) e^{X(t)} + \left(\frac{1-e^{-\text{ad}_X}}{\text{ad}_X} \frac{dX(t)}{dt} \right)^2 e^{X(t)}. \tag{B.12}$$

We have just calculated the terms in the parentheses, so all we have to do is take our previous expression and simply plug in

$$\frac{q^\beta q^\alpha}{2!} \left(\frac{\partial}{\partial p^\beta} \frac{\partial}{\partial p^\alpha} \epsilon(p+q) \right) |_{q\to 0} = \frac{1}{2} \Bigg[-ik_\mu q_\nu M^{\mu\nu} \frac{q^2(1-m^2\lambda)}{2(p\cdot k^2 - m^4)} + \bigg((k+p)_\mu q_\nu \frac{iM^{\mu\nu}}{p\cdot k + m^2} + p_\mu k_\nu \frac{q^2(1-m^2\lambda)}{2(p\cdot k - m^2)} \frac{iM^{\mu\nu}}{p\cdot k + m^2} \bigg)^2 \Bigg] \epsilon(p). \tag{B.13}$$

Once again, looking at the q-scaling of our expression, we only have one term that contributes to the leading order, which gives us the truncated second order term

$$\frac{q^\beta q^\alpha}{2!}\left(\frac{\partial}{\partial p^\beta}\frac{\partial}{\partial p^\alpha}\epsilon^*(p+q)\right)|_{q\to 0}\cdot\epsilon(p) = q_\mu q_\rho \frac{-(k_\nu+p_\nu)(k_\sigma+p_\sigma)}{2(p\cdot k+m^2)^2}\epsilon^*(p)\frac{1}{2}\left\{M^{\mu\nu}, M^{\rho\sigma}\right\}\epsilon(p)$$
$$= q_\mu q_\rho \frac{-S^{\mu\nu}(p)(k_\nu+p_\nu)S^{\rho\sigma}(p)(k_\sigma+p_\sigma)}{2(p\cdot k+m^2)^2}, \qquad \text{(B.14)}$$

where we preemptively decomposed the quadratic product of Lorentz generators in to symmetric and anti-symmetric parts. We also use the identity introduced in Ref. [121] relating symmetric products of Lorentz generators and products of the spin tensor. Here we begin to notice a pattern

$$\frac{q^\beta q^\alpha}{2!}\left(\frac{\partial}{\partial p^\beta}\frac{\partial}{\partial p^\alpha}\epsilon^*(p+q)\right)|_{q\to 0}\cdot\epsilon(p) = \frac{(iq_\mu\omega^\mu)(iq_\rho\omega^\rho)}{2!}.$$

At this point, we see the same pattern of exponentiation as seen in Refs. [121, 122, 170, 177] and use the exponentiated form of the polarization tensor product Eq. (2.22).

APPENDIX C

Elements for Comparison

To compare our eikonal formulas to Ref. [195], we matched our amplitudes to theirs while imposing the SSC and changing to their basis of variables. We then calculated the eikonal phases for these amplitudes and plugged these into the eikonal formulas and compared observables.

Because Ref. [195] used the spin vector as their spin variable, we needed to use the relationship,

$$S^{\mu\nu}(p) = \frac{1}{m}\epsilon^{\mu\nu\rho\sigma}p_\rho s_\sigma(p). \tag{C.1}$$

Note that we could have included the mass dipole K^μ in Refs. [170, 196], but because we will be imposing the SSC this would be pointless.

We used the following coefficients for our amplitudes Eq. (3.29) and Eq. (3.40):

$$\Upsilon^{(1)} = c^{(1,0,0)}, \tag{C.2}$$

$$\Upsilon^{(1)}_{\nu_1} = c_1^{(1,1,0)} u_{1\,\nu_1} + c_2^{(1,1,0)} u_{2\,\nu_1}, \tag{C.3}$$

$$\Upsilon^{(1)}_{\nu_1\nu_2} = c_1^{(1,2,0)} \eta_{\nu_1\nu_2} + c_2^{(1,2,0)} u_{1\,\nu_1} u_{1\,\nu_2} + c_3^{(1,2,0)} u_{2\,\nu_1} u_{2\,\nu_2} + c_4^{(1,2,0)} \left(u_{1\,\nu_1} u_{2\,\nu_2} + u_{2\,\nu_1} u_{1\,\nu_2}\right), \tag{C.4}$$

$$\Upsilon^{(2)} = c^{(2,0,0)}, \tag{C.5}$$

$$\Upsilon^{(2)}_{\nu_1} = c_1^{(2,1,0)} u_{1\,\nu_1} + c_2^{(2,1,0)} u_{2\,\nu_1}, \tag{C.6}$$

$$\Upsilon^{(2)}_{\nu_1\nu_2} = c_1^{(2,2,0)} \eta_{\nu_1\nu_2} + c_2^{(2,2,0)} u_{1\,\nu_1} u_{1\,\nu_2} + c_3^{(2,2,0)} u_{2\,\nu_1} u_{2\,\nu_2} + c_4^{(2,2,0)} \left(u_{1\,\nu_1} u_{2\,\nu_2} + u_{2\,\nu_1} u_{1\,\nu_2}\right), \tag{C.7}$$

$$\begin{aligned}
\Upsilon^{(2)}_{\mu_1\nu_1\mu_2\nu_2} = {} & c_{q^2,1}^{(2,2,0)} \left(\eta_{\mu_1\mu_2}\eta_{\nu_1\nu_2} - \eta_{\nu_1\mu_2}\eta_{\mu_1\nu_2}\right) \\
& + c_{q^2,2}^{(2,2,0)} \left(\eta_{\mu_1\mu_2} u_{1\,\nu_1} u_{1\,\nu_2} + \eta_{\nu_1\nu_2} u_{1\,\mu_1} u_{1\,\mu_2} - \eta_{\nu_1\mu_2} u_{1\,\mu_1} u_{1\,\nu_2} - \eta_{\mu_1\nu_2} u_{1\,\nu_1} u_{1\,\mu_2}\right) \\
& + c_{q^2,3}^{(2,2,0)} \left(\eta_{\mu_1\mu_2} u_{2\,\nu_1} u_{2\,\nu_2} + \eta_{\nu_1\nu_2} u_{2\,\mu_1} u_{2\,\mu_2} - \eta_{\nu_1\mu_2} u_{2\,\mu_1} u_{2\,\nu_2} - \eta_{\mu_1\nu_2} u_{2\,\nu_1} u_{2\,\mu_2}\right) \\
& + c_{q^2,4}^{(2,2,0)} \big(\eta_{\mu_1\mu_2} \left(u_{1\,\nu_1} u_{2\,\nu_2} + u_{2\,\nu_1} u_{1\,\nu_2}\right) + \eta_{\nu_1\nu_2} \left(u_{1\,\mu_1} u_{2\,\mu_2} + u_{2\,\mu_1} u_{1\,\mu_2}\right) \\
& \qquad - \eta_{\nu_1\mu_2} \left(u_{1\,\mu_1} u_{2\,\nu_2} + u_{2\,\mu_1} u_{1\,\nu_2}\right) - \eta_{\mu_1\nu_2} \left(u_{1\,\nu_1} u_{2\,\mu_2} + u_{2\,\nu_1} u_{1\,\mu_2}\right)\big) \\
& + c_{q^2,5}^{(2,2,0)} \big(u_{1\,\mu_1} u_{1\,\mu_2} u_{2\,\nu_1} u_{2\,\nu_2} + u_{2\,\mu_1} u_{2\,\mu_2} u_{1\,\nu_1} u_{1\,\nu_2} \\
& \qquad - u_{1\,\nu_1} u_{1\,\mu_2} u_{2\,\mu_1} u_{2\,\nu_2} - u_{1\,\mu_1} u_{1\,\nu_2} u_{2\,\nu_1} u_{2\,\mu_2}\big),
\end{aligned} \tag{C.8}$$

where the superscript in the coefficients follow the pattern $c^{(\mathrm{nPM},\, s_1,\, s_2)}$ and the $c_{q^2,i}^{(2,2,0)}$ come from the extra contributions that appear starting at 2PM. The tensor structures above were chosen such that they followed the symmetries of the spin tensors and their products.

To properly compare amplitudes, we need to enforce the covariant SSC,

$$p_{1\,\mu} S_1^{\mu\nu} = 0, \tag{C.9}$$

on our coefficients. To do this, we perturbatively expand the SSC,

$$\left(p_{1\,\mu} + \Delta p_{1\,\mu}\right)\left(S_1^{\mu\nu} + \Delta S_1^{\mu\nu}\right) = 0, \tag{C.10}$$

and treat each order in PM and spin as an equation of constraint on our coefficients. After enforcing these constraints, and switching to the basis $\{q, u_1, u_2, \epsilon^{\mu\nu\rho\sigma} u_{1\,\nu} u_{2\,\rho} q_\sigma\}$ we can match our coefficients to those of the amplitudes in Ref. [195]. In principle, we can use this procedure to match to any amplitude.

Now that we are effectively using the same amplitudes, we can Fourier transform our amplitudes into eikonal phases using the following integral

$$\int \hat{d}^D q\, \hat{\delta}\left(2\bar{p}_1 \cdot q\right) \hat{\delta}\left(2\bar{p}_2 \cdot q\right) \frac{e^{-iq\cdot b_{\mathrm{cov}}}}{\left(-q^2\right)^{\alpha}} = \frac{1}{4\bar{m}_1 \bar{m}_2 \sqrt{y^2-1}} \frac{\Gamma(D/2-1-\alpha)}{2^{2\alpha}\pi^{(D/2-1)}\Gamma(\alpha)} \frac{1}{\left(-b_{\mathrm{cov}}^2\right)^{(D/2-1-\alpha)}}, \tag{C.11}$$

where we exchange any factors of iq^μ in the amplitude for $\Pi^{\mu\nu}\partial/\partial b^\nu_{\mathrm{cov}}$.

To compare the spin kick effect, we need to invert Eq. (C.1) to solve for s^μ and then perturbatively expand,

$$\Delta s_1^\mu = \frac{1}{2m_1} \epsilon^{\mu\nu\rho\sigma} \left(\Delta p_{1\,\nu} S_{1\,\rho\sigma} + p_{1\,\nu} \Delta S_{1\,\rho\sigma} + \Delta p_{1\,\nu} \Delta S_{1\,\rho\sigma}\right). \tag{C.12}$$

At this point, we have all we need to compare our formulas to the results of Ref. [195], which we find agreement with.

APPENDIX D

Polarization Tensors in Barred Variables

In principle, we should consider how shifting to barred variables would affect our polarizations, and therefore the spin tensor. However, as we see in the derivation, this effect does not affect our calculation due to reasons of horizontal-flip symmetry and classical counting.

When shifting Eq. (3.35) to barred variables, we arrive at the simple replacement $\omega_i(p_i) \to -\omega_i(\bar{p}_i) \equiv -\bar{\omega}_i$. Therefore the effect on $b_{\rm cov}$ can be taken into account entirely by the replacement $b_{\rm cov} \to \bar{b}_{\rm cov} = b + (\bar{\omega}_1 - \bar{\omega}_2)$.

The effect on the spin tensor is more complicated. Starting with $S^{\mu\nu}(p_1) \to S^{\mu\nu}(\bar{p}_1 - q/2)$, which occurs when we shift to barred variables, but in terms of polarization tensors, we see that

$$
\begin{aligned}
&\epsilon^*(\bar{p}_1 - q/2) \cdot M \cdot \epsilon(\bar{p}_1 - q/2) \\
&\qquad = \left(\epsilon^*(\bar{p}_1 - q/2) \cdot \epsilon(\bar{p}_1)\right) \left(\epsilon^*(\bar{p}_1) \cdot M \cdot \epsilon(\bar{p}_1)\right) \left(\epsilon^*(\bar{p}_1) \cdot \epsilon(\bar{p}_1 - q/2)\right) \\
&\qquad = \epsilon^*(\bar{p}_1) \cdot e^{iq\cdot\bar{\omega}_1/2} \cdot M \cdot e^{-iq\cdot\bar{\omega}_1/2} \cdot \epsilon(\bar{p}_1) \\
&\qquad = S^{\mu\nu}(\bar{p}_1) + \frac{1}{2}\left[iq \cdot \bar{\omega}_1, S^{\mu\nu}(\bar{p}_1)\right] + \cdots
\end{aligned}
\tag{D.1}
$$

where in the last line we expanded using the identity due to Baker, Campbell, and Hausdorff and truncated the expansion to leading order in q. The second term scales higher in classical scaling and therefore would be something to take into account when we keep track of classical contributions. Note that this correction results in the same one for the spin vector in Refs. [40, 50, 195] if we choose the reference momentum to be $k_i = \bar{p}_i$.

In our set up, we never have to include internal polarization tensors because these will just be turned to Kronecker deltas. Therefore the only correction relating to the shifted spin tensor we ever have to consider are proportional to q, which does not affect the horizontal-flip symmetry parity. Because the parity is unchanged when we use this effect to promote our classically-singular terms, we will find the odd parity of these terms will make them vanish. As a result, we can conclude that the barred variables shift on the spin tensor does not affect our calculation, unlike in the fixed-spin formalism of Refs. [40, 50, 195].

APPENDIX E

Resolving the Cut-Correction Term

Here we present how we arrive at the cut-correction contribution to our observables. We will first plug in the ansatz for our tree amplitudes in Eq. (3.29) to Eq. (3.65) and then compare this to a directional derivative with respect to the projector $\Pi^{\mu}_{\ \nu}$. We will be simplifying certain aspects of the integrand in the observables analysis without affecting the basic conclusions.

Plugging in our ansatz to the simplified integrand results in the following,

$$\begin{aligned}&\int \not{D} l e^{-ib\cdot l}\frac{u^\gamma}{m}\Delta p_\alpha l^\alpha \frac{\partial \mathcal{A}^{(1)}(l)}{\partial l^\gamma}\\&=\Delta p_\alpha \frac{u^\gamma}{m}(-1)^{(s_1+s_2)}\left(s_1\eta_{\gamma\mu_{s_1}}\Pi_{\rho_{s_2}\beta}+s_2\eta_{\rho_{s_2}\gamma}\Pi_{\mu_{s_1}\beta}\right)\frac{\partial}{\partial b_\alpha}\frac{\partial}{\partial b_\beta}\frac{\partial}{\partial b_\perp^{\mu(s_1-1)}}\frac{\partial}{\partial b_\perp^{\rho(s_2-1)}}f_{b^2}^{\mu(s_1)\rho(s_2)},\end{aligned} \tag{E.1}$$

where we absorb irrelevant terms into the function $f_{b^2}^{\mu(s_1)\rho(s_2)}$. Note that we drop all terms proportional to $u\cdot b=0$. Eq. (E.1) provides a clue of where to go: it would appear that we have replaced the original projector dressing the impact parameter derivatives with a new projector via some product rule. Let us now consider the following directional derivative

$$\begin{aligned}\frac{u^\gamma}{m}\Delta p^\alpha \frac{\partial \delta^{(1)}}{\partial \Pi^{\gamma\alpha}}&=\frac{u^\gamma}{m}\Delta p^\alpha(-1)^{(s_1+s_2)}\frac{\partial}{\partial \Pi^{\gamma\alpha}}\left(\Pi_{\mu(s_1)\nu(s_1)}\Pi_{\rho(s_2)\sigma(s_2)}\right)\frac{\partial}{\partial b_{\nu(s_1)}}\frac{\partial}{\partial b_{\sigma(s_2)}}f_{b^2}^{\mu(s_1)\rho(s_2)}\\&=(-1)^{(s_1+s_2)}\frac{u^\gamma}{2m}\Delta p_\alpha\left(s_1\eta_{\gamma\mu_{s_1}}\Pi_{\rho_{s_2}\beta}+s_2\eta_{\rho_{s_2}\gamma}\Pi_{\mu_{s_1}\beta}\right)\frac{\partial}{\partial b_\alpha}\frac{\partial}{\partial b_\beta}\frac{\partial}{\partial b_\perp^{\mu(s_1-1)}}\frac{\partial}{\partial b_\perp^{\rho(s_2-1)}}f_{b^2}^{\mu(s_1)\rho(s_2)}\\&=\frac{1}{2}\int \not{D} l e^{-ib\cdot l}\frac{u^\gamma}{m}\Delta p_\alpha l^\alpha\frac{\partial \mathcal{A}^{(1)}(l)}{\partial l^\gamma},\end{aligned} \tag{E.2}$$

where we define the derivative

$$\frac{\partial \Pi_{\mu\nu}}{\partial \Pi_{\alpha\beta}} \equiv \frac{1}{2}\left(\delta^{\alpha}_{\mu}\delta^{\beta}_{\nu} + \delta^{\beta}_{\mu}\eta^{\alpha}_{\nu}\right), \tag{E.3}$$

based on the symmetric nature of the projector. This is more of a bookkeeping notation rather than literally taking a derivative by a projector, which may prove to be a mathematically heretical thing to do. We could have obtained a similar result if we instead did not treat the projector as an independent variable and rather as a function of the velocities u_i,

$$\Delta p \cdot \frac{\partial \delta^{(1)}}{\partial u_i}\Big|_{\frac{\partial \Upsilon}{\partial u_i}\to 0} = -2\Delta p^{\alpha}\check{u}_i^{\gamma}\frac{\partial \delta^{(1)}}{\partial \Pi^{\alpha\gamma}}, \tag{E.4}$$

where we have isolated derivatives acting on the projectors. We will consider the derivative with respect to the projector as a sort of shorthand for the left-hand side of Eq. (E.4).

APPENDIX F

Three-Point Amplitudes for Absorption

Counting Independent Amplitudes

For larger values of s_i, due to the proliferation of kinematic and dimensionality constraints, it becomes non-trivial to construct a minimal basis of truly independent on-shell 3-point amplitudes. A convenient way to count the number of independent 3-point amplitudes in $D = 4$ is to make use of the massive spinor formalism[1]. As explained in [191], after solving all relevant constraints, the general form of a 3-point amplitude with two massive particles (of unequal mass) and one massless particle is

$$\mathcal{A}_3^{(s_1,s_2,h_3)} = \boldsymbol{\lambda}_1^{\alpha_1}...\boldsymbol{\lambda}_1^{\alpha_{2s_1}}\boldsymbol{\lambda}_2^{\beta_1}...\boldsymbol{\lambda}_2^{\beta_{2s_2}} \sum_{i=1}^{N(s_1,s_2,h_3)} g_i \left(u^{s_1+s_2+h_3} v^{s_1+s_2-h_3}\right)^{(i)}_{\alpha_1...\alpha_{2s_1}\beta_1...\beta_{2s_2}}, \tag{F.1}$$

where

$$u_\alpha \equiv \lambda_{3\alpha}, \qquad v_\alpha \equiv \frac{p_{1\alpha\dot{\beta}}}{m_1}\overline{\lambda}_3^{\dot{\beta}}, \qquad \boldsymbol{\lambda}_i \equiv z_{iI}\lambda_{i\alpha}^I, \qquad z_{iI}z_i^I = 0. \tag{F.2}$$

Details on the definitions of massive spinors are given in the original reference [191]. The number of independent 3-point amplitudes is equal to the number of distinct terms that can appear in the above sum. This is equivalent to a simple counting problem: given a set containing the letter u, $s_1 + s_2 + h_3$ times, and the letter v, $s_1 + s_2 - h_3$ times[2], how many

[1]This section is a review of Section 4.2.1 of [191]. The method presented in that reference is completely correct, but the final quoted formula is only applicable if $|h_3| \leq |s_1 - s_2|$. For completeness, in this Appendix we rederive the general case.

[2]If $|h_3| > s_1 + s_2$ then there are no structures we can write down with the correct helicity weights for all of the particles; the problem is only non-trivial for $|h_3| \leq s_1 + s_2$.

different ways can that set be partitioned into two disjoint subsets of length $2s_1$ and $2s_2$? The solution is given by

$$N\left(s_1, s_2, h_3\right) = \begin{cases} s_1 + s_2 - |s_1 - s_2| + 1 & \text{if} \quad |h_3| \leq |s_1 - s_2|, \\ s_1 + s_2 - |h_3| + 1 & \text{if} \quad |s_1 - s_2| < |h_3| \leq s_1 + s_2, \\ 0 & \text{if} \quad s_1 + s_2 < |h_3|. \end{cases} \tag{F.3}$$

This counting of on-shell amplitudes must agree with the counting of cubic Lagrangian operators modulo equations of motion and total derivatives. It is useful to classify the latter into *parity-even* (without a Levi-Civita symbol) and *parity-odd* (with a Levi-Civita symbol). Since parity changes the sign of the helicity for a massless particle, we identify

$$\mathcal{A}_3^{(s_1,s_2,h_3)}\Big|_{\lambda_3 \leftrightarrow \bar{\lambda}_3} = \mathcal{A}_3^{(s_1,s_2,-h_3)}, \qquad \tilde{\mathcal{A}}_3^{(s_1,s_2,h_3)}\Big|_{\lambda_3 \leftrightarrow \bar{\lambda}_3} = -\tilde{\mathcal{A}}_3^{(s_1,s_2,-h_3)}, \tag{F.4}$$

with the + sign for parity even operators and the − sign for parity odd. The formula (F.3) counts the number of on-shell amplitudes for a given helicity, and so for $|h_3| > 0$, $N\left(s_1, s_2, h_3\right)$ is separately the number of parity even operators and the number of parity odd operators; the total number of operators for a given massless spin $|h_3|$ is $2N\left(s_1, s_2, h_3\right)$. For $h_3 = 0$ (massless scalar mediators) $N\left(s_1, s_2, 0\right)$ counts the total number of operators, parity even plus parity odd. We will use this counting to verify that we have correctly constructed a complete basis of 3-point interactions.

Below we explicitly enumerate the on-shell 3-point amplitudes used in the calculation of the absorptive impulse. We use the all-outgoing convention, with momenta and spins/helicities labeled as:

$$\mathcal{A}_3^{(s_1,s_2,h_3)} \qquad \Longleftrightarrow$$

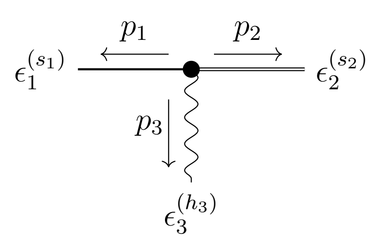

Without loss of generality, we represent the traceless-symmetric polarization tensor for the graviton as a product $\epsilon_i^{\mu\nu} = \epsilon_i^{\mu}\epsilon_i^{\nu}$, where $\epsilon_i^2 = 0$.

Scalar Absorption

Parity even interactions:

$$\mathcal{A}_3^{(0,0,0)} = g_1^{(0,0,0)}, \tag{F.5}$$

$$\mathcal{A}_3^{(0,1,0)} = -ig_1^{(0,1,0)}\left(p_3\cdot\epsilon_2\right), \tag{F.6}$$

$$\mathcal{A}_3^{(0,2,0)} = -g_1^{(0,2,0)}\left(p_3\cdot\epsilon_2\right)^2, \tag{F.7}$$

$$\mathcal{A}_3^{(1,0,0)} = -ig_1^{(1,0,0)}\left(p_3\cdot\epsilon_1\right), \tag{F.8}$$

$$\mathcal{A}_3^{(1,1,0)} = g_1^{(1,1,0)}(\epsilon_1\cdot\epsilon_2) - g_2^{(1,1,0)}(p_3\cdot\epsilon_1)(p_3\cdot\epsilon_2), \tag{F.9}$$

$$\mathcal{A}_3^{(1,2,0)} = -ig_1^{(1,2,0)}(p_3\cdot\epsilon_2)(\epsilon_1\cdot\epsilon_2) + ig_2^{(1,2,0)}(p_3\cdot\epsilon_1)(p_3\cdot\epsilon_2)^2, \tag{F.10}$$

$$\mathcal{A}_3^{(1,3,0)} = -g_1^{(1,3,0)}(p_3\cdot\epsilon_2)^2(\epsilon_1\cdot\epsilon_2) + g_2^{(1,3,0)}(p_3\cdot\epsilon_1)(p_3\cdot\epsilon_2)^3. \tag{F.11}$$

Parity odd interactions:

$$\tilde{\mathcal{A}}_3^{(1,1,0)} = h_1^{(1,1,0)}\varepsilon^{p_1p_3\epsilon_1\epsilon_2}, \tag{F.12}$$

$$\tilde{\mathcal{A}}_3^{(1,2,0)} = ih_1^{(1,2,0)}(p_3\cdot\epsilon_2)\varepsilon^{p_1p_3\epsilon_1\epsilon_2}, \tag{F.13}$$

$$\tilde{\mathcal{A}}_3^{(1,3,0)} = -h_1^{(1,3,0)}(p_3\cdot\epsilon_2)^2\varepsilon^{p_1p_3\epsilon_1\epsilon_2}. \tag{F.14}$$

Photon Absorption

Parity even interactions:

$$\mathcal{A}_3^{(0,1,\pm1)} = g_1^{(0,1,1)}\left[(p_1\cdot\epsilon_3)(p_3\cdot\epsilon_2) - \frac{1}{2}(\mu^2 - m_1^2)(\epsilon_2\cdot\epsilon_3)\right], \tag{F.15}$$

$$\mathcal{A}_3^{(0,2,\pm1)} = -ig_1^{(0,2,1)}(p_3\cdot\epsilon_2)\left[(p_1\cdot\epsilon_3)(p_3\cdot\epsilon_2) - \frac{1}{2}(\mu^2 - m_1^2)(\epsilon_2\cdot\epsilon_3)\right], \tag{F.16}$$

$$\mathcal{A}_3^{(1,0,\pm1)} = g_1^{(1,0,1)} \left[(p_2 \cdot \epsilon_3)(p_3 \cdot \epsilon_1) + \frac{1}{2}(\mu^2 + m_1^2)(\epsilon_1 \cdot \epsilon_3) \right], \tag{F.17}$$

$$\begin{aligned} \mathcal{A}_3^{(1,1,\pm1)} &= i g_1^{(1,1,1)} \left[(p_3 \cdot \epsilon_2)(\epsilon_1 \cdot \epsilon_3) - (p_3 \cdot \epsilon_1)(\epsilon_2 \cdot \epsilon_3) \right], \\ &\quad + i g_2^{(1,1,1)} \left[(p_3 \cdot \epsilon_2)(\epsilon_1 \cdot \epsilon_3) - (p_3 \cdot \epsilon_1)(\epsilon_2 \cdot \epsilon_3) \right] \end{aligned} \tag{F.18}$$

$$\begin{aligned} \mathcal{A}_3^{(1,2,\pm1)} &= g_1^{(1,2,1)} (p_3 \cdot \epsilon_2) \left[(p_3 \cdot \epsilon_2)(\epsilon_1 \cdot \epsilon_3) - (p_3 \cdot \epsilon_1)(\epsilon_2 \cdot \epsilon_3) \right] \\ &\quad + g_2^{(1,2,1)} (\epsilon_1 \cdot \epsilon_2) \left[(p_1 \cdot \epsilon_3)(p_3 \cdot \epsilon_2) - \frac{1}{2}(\mu^2 - m_1^2)(\epsilon_2 \cdot \epsilon_3) \right] \\ &\quad + g_3^{(1,2,1)} (p_3 \cdot \epsilon_1)(p_3 \cdot \epsilon_2) \left[\frac{1}{2}(\mu^2 - m_1^2)(\epsilon_2 \cdot \epsilon_3) - (p_1 \cdot \epsilon_3)(p_3 \cdot \epsilon_2) \right], \end{aligned} \tag{F.19}$$

$$\begin{aligned} \mathcal{A}_3^{(1,3,\pm1)} &= i g_1^{(1,3,1)} (p_3 \cdot \epsilon_2)^2 \left[(p_3 \cdot \epsilon_1)(\epsilon_2 \cdot \epsilon_3) - (p_3 \cdot \epsilon_2)(\epsilon_1 \cdot \epsilon_3) \right] \\ &\quad - i g_2^{(1,3,1)} (p_3 \cdot \epsilon_2)(\epsilon_1 \cdot \epsilon_2) \left[(p_1 \cdot \epsilon_3)(p_3 \cdot \epsilon_2) - \frac{1}{2}(\mu^2 - m_1^2)(\epsilon_2 \cdot \epsilon_3) \right] \\ &\quad + i g_3^{(1,3,1)} (p_3 \cdot \epsilon_1)(p_3 \cdot \epsilon_2)^2 \left[(p_1 \cdot \epsilon_3)(p_3 \cdot \epsilon_2) - \frac{1}{2}(\mu^2 - m_1^2)(\epsilon_2 \cdot \epsilon_3) \right]. \end{aligned} \tag{F.20}$$

Parity odd interactions:

$$\tilde{\mathcal{A}}_3^{(0,1,\pm1)} = h_1^{(0,1,1)} \varepsilon^{p_1 p_3 \epsilon_2 \epsilon_3}, \tag{F.21}$$

$$\tilde{\mathcal{A}}_3^{(0,2,\pm1)} = -i h_1^{(0,2,1)} (p_3 \cdot \epsilon_2)\, \varepsilon^{p_1 p_3 \epsilon_2 \epsilon_3}, \tag{F.22}$$

$$\tilde{\mathcal{A}}_3^{(1,0,\pm1)} = h_1^{(1,0,1)} \varepsilon^{p_2 p_3 \epsilon_1 \epsilon_3}, \tag{F.23}$$

$$\tilde{\mathcal{A}}_3^{(1,1,\pm1)} = -i h_1^{(1,1,1)} \varepsilon^{p_3 \epsilon_1 \epsilon_2 \epsilon_3} + i h_2^{(1,1,1)} (p_3 \cdot \epsilon_2) \varepsilon^{p_2 p_3 \epsilon_1 \epsilon_3}, \tag{F.24}$$

$$\begin{aligned} \tilde{\mathcal{A}}_3^{(1,2,\pm1)} &= h_1^{(1,2,1)} (\epsilon_1 \cdot \epsilon_2) \varepsilon^{p_1 p_3 \epsilon_2 \epsilon_3} - h_2^{(1,2,1)} (p_3 \cdot \epsilon_1)(p_3 \cdot \epsilon_2) \varepsilon^{p_1 p_3 \epsilon_2 \epsilon_3} \\ &\quad + h_3^{(1,2,1)} (p_3 \cdot \epsilon_2)^2 \varepsilon^{p_2 p_3 \epsilon_1 \epsilon_3}, \end{aligned} \tag{F.25}$$

$$\begin{aligned} \tilde{\mathcal{A}}_3^{(1,3,\pm1)} &= i h_1^{(1,3,1)} (p_3 \cdot \epsilon_2)^2 \varepsilon^{p_3 \epsilon_1 \epsilon_2 \epsilon_3} - i h_2^{(1,3,1)} (p_3 \cdot \epsilon_2)(\epsilon_1 \cdot \epsilon_2) \varepsilon^{p_1 p_3 \epsilon_2 \epsilon_3} \\ &\quad + i h_3^{(1,3,1)} (p_3 \cdot \epsilon_1)(p_3 \cdot \epsilon_2)^2 \varepsilon^{p_1 p_3 \epsilon_2 \epsilon_3}. \end{aligned} \tag{F.26}$$

Graviton Absorption

Parity even interactions:

$$\mathcal{A}_3^{(0,2,\pm2)} = -\frac{1}{2}g_1^{(0,2,2)}\left[(p_1\cdot\epsilon_3)(p_3\cdot\epsilon_2) - \frac{1}{2}(\mu^2 - m_1^2)(\epsilon_2\cdot\epsilon_3)\right]^2, \tag{F.27}$$

$$\begin{aligned}\mathcal{A}_3^{(1,1,\pm2)} = -\frac{1}{2}g_1^{(1,1,2)}&\left[(p_1\cdot\epsilon_3)(p_3\cdot\epsilon_1) - \frac{1}{2}(\mu^2 - m_1^2)(\epsilon_1\cdot\epsilon_3)\right]\\ &\times\left[(p_2\cdot\epsilon_3)(p_3\cdot\epsilon_2) + \frac{1}{2}(\mu^2 + m_1^2)(\epsilon_2\cdot\epsilon_3)\right],\end{aligned} \tag{F.28}$$

$$\begin{aligned}\mathcal{A}_3^{(1,2,\pm2)} = &-\frac{1}{2}ig_1^{(1,2,2)}\left[(p_1\cdot\epsilon_3)(p_3\cdot\epsilon_2) - \frac{1}{2}(\mu^2 - m_1^2)(\epsilon_2\cdot\epsilon_3)\right]\\ &\times\left[(p_3\cdot\epsilon_2)(\epsilon_1\cdot\epsilon_3) - (p_3\cdot\epsilon_1)(\epsilon_2\cdot\epsilon_3)\right]\\ &+\frac{1}{2}ig_2^{(1,2,2)}(p_3\cdot\epsilon_2)\left[(p_1\cdot\epsilon_3)(p_3\cdot\epsilon_1) - \frac{1}{2}(\mu^2 - m_1^2)(\epsilon_1\cdot\epsilon_3)\right]\\ &\times\left[(p_2\cdot\epsilon_3)(p_3\cdot\epsilon_2) + \frac{1}{2}(\mu^2 + m_1^2)(\epsilon_2\cdot\epsilon_3)\right],\end{aligned} \tag{F.29}$$

$$\begin{aligned}\mathcal{A}_3^{(1,3,\pm2)} = &-\frac{1}{2}g_1^{(1,3,2)}(p_3\cdot\epsilon_2)\left[(p_1\cdot\epsilon_3)(p_3\cdot\epsilon_2) - \frac{1}{2}(\mu^2 - m_1^2)(\epsilon_2\cdot\epsilon_3)\right]\\ &\times\left[(p_3\cdot\epsilon_2)(\epsilon_1\cdot\epsilon_3) - (p_3\cdot\epsilon_1)(\epsilon_2\cdot\epsilon_3)\right]\\ &+\frac{1}{2}g_2^{(1,3,2)}(p_3\cdot\epsilon_2)^2\left[(p_1\cdot\epsilon_3)(p_3\cdot\epsilon_1) - \frac{1}{2}(\mu^2 - m_1^2)(\epsilon_1\cdot\epsilon_3)\right]\\ &\times\left[(p_2\cdot\epsilon_3)(p_3\cdot\epsilon_2) + \frac{1}{2}(\mu^2 + m_1^2)(\epsilon_2\cdot\epsilon_3)\right]\\ &-\frac{1}{2}g_3^{(1,3,2)}(\epsilon_1\cdot\epsilon_2)\left[(p_1\cdot\epsilon_3)(p_3\cdot\epsilon_2) - \frac{1}{2}(\mu^2 - m_1^2)(\epsilon_2\cdot\epsilon_3)\right]^2.\end{aligned} \tag{F.30}$$

Parity odd interactions:

$$\tilde{\mathcal{A}}_3^{(0,2,\pm2)} = \frac{1}{2}h_1^{(0,2,2)}\left[(p_1\cdot\epsilon_3)(p_3\cdot\epsilon_2) - \frac{1}{2}(\mu^2 - m_1^2)(\epsilon_2\cdot\epsilon_3)\right]\varepsilon^{p_1p_3\epsilon_2\epsilon_3}, \tag{F.31}$$

$$\tilde{\mathcal{A}}_3^{(1,1,\pm2)} = -\frac{1}{2}h_1^{(1,1,2)}\left[(p_2\cdot\epsilon_3)(p_3\cdot\epsilon_2) + \frac{1}{2}(\mu^2 + m_1^2)(\epsilon_2\cdot\epsilon_3)\right]\varepsilon^{p_1p_3\epsilon_1\epsilon_3}, \tag{F.32}$$

$$\tilde{\mathcal{A}}_3^{(1,2,\pm 2)} = \frac{i}{2} h_1^{(1,2,2)} \left[(p_3 \cdot \epsilon_1)(\epsilon_2 \cdot \epsilon_3) - (p_3 \cdot \epsilon_2)(\epsilon_1 \cdot \epsilon_3) \right] \varepsilon^{p_1 p_3 \epsilon_2 \epsilon_3} + \frac{i}{2} h_2^{(1,2,2)} (p_3 \cdot \epsilon_2) \left[(p_2 \cdot \epsilon_3)(p_3 \cdot \epsilon_2) + \frac{1}{2}(\mu^2 + m_1^2)(\epsilon_2 \cdot \epsilon_3) \right] \varepsilon^{p_1 p_3 \epsilon_1 \epsilon_3}, \tag{F.33}$$

$$\tilde{\mathcal{A}}_3^{(1,3,\pm 2)} = \frac{i}{2} h_1^{(1,3,2)} (p_3 \cdot \epsilon_2) \left[(p_3 \cdot \epsilon_2)(\epsilon_1 \cdot \epsilon_3) - (p_3 \cdot \epsilon_1)(\epsilon_2 \cdot \epsilon_3) \right] \varepsilon^{p_1 p_3 \epsilon_2 \epsilon_3} + \frac{i}{2} h_2^{(1,3,2)} (\epsilon_1 \cdot \epsilon_2) \left[(p_1 \cdot \epsilon_3)(p_3 \cdot \epsilon_2) - \frac{1}{2}(\mu^2 - m_1^2)(\epsilon_2 \cdot \epsilon_3) \right] \varepsilon^{p_1 p_3 \epsilon_2 \epsilon_3} - \frac{i}{2} h_3^{(1,3,2)} (p_3 \cdot \epsilon_2)^2 \left[(p_2 \cdot \epsilon_3)(p_3 \cdot \epsilon_2) + \frac{1}{2}(\mu^2 + m_1^2)(\epsilon_2 \cdot \epsilon_3) \right] \varepsilon^{p_1 p_3 \epsilon_1 \epsilon_3}. \tag{F.34}$$

APPENDIX G

Impulse Results for Absorption

Below we give the Casimir interpolated impulse coefficients up to $\mathcal{O}(S_1^2)$ in terms of the Wilson coefficients appearing in the 3-point amplitudes constructed in Appendix F; coefficients which are not explicitly enumerated are zero. We organize each set of coefficients first by massless mediator and then by exchange channel, labeled as $(s, s', |h|)$. The definition of the coefficients is given in (4.65) and (4.67 - 4.66).

Scalar Absorption

- $(0,0,0)$:

$$(c_u)_{0,0,0}^{(0,0,0)} = -\frac{g^2}{2^{11}m_1^2m_2^2}\frac{\left(g_1^{(0,0,0)}\right)^2}{(-b^2)}. \tag{G.1}$$

- $(0,1,0)$:

$$(c_u)_{0,0,0}^{(0,1,0)} = -\frac{9g^2}{2^{15}m_1^2m_2^2}\frac{(3y^2+5)\left(g_1^{(0,1,0)}\right)^2}{(-b^2)^2}. \tag{G.2}$$

- $(0,2,0)$:

$$(c_u)_{0,0,0}^{(0,2,0)} = -\frac{75g^2}{2^{17}m_1^2m_2^2}\frac{(5y^4+26y^2+17)\left(g_1^{(0,2,0)}\right)^2}{(-b^2)^3}. \tag{G.3}$$

- $(1,0,0)$:

$$(c_u)_{2,0,0}^{(1,0,0)} = -\frac{45g^2}{2^{15}m_1^2m_2^2}\frac{\left(g_1^{(1,0,0)}\right)^2}{(-b^2)^3}, \tag{G.4}$$

$$(c_u)^{(1,0,0)}_{0,0,2} = -\frac{27g^2}{2^{15}(y^2-1)m_1^2m_2^2}\frac{y^2\left(g_1^{(1,0,0)}\right)^2}{(-b^2)^3}, \tag{G.5}$$

$$(c_b)^{(1,0,0)}_{1,0,1} = \frac{3g^2}{2^{14}(y^2-1)m_1^2m_2^2}\frac{y\left(g_1^{(1,0,0)}\right)^2}{(-b^2)^3}, \tag{G.6}$$

$$(c_n)^{(1,0,0)}_{0,1,1} = -\frac{4}{(y^2-1)}(c_b)^{(1,0,0)}_{1,0,1}. \tag{G.7}$$

- $(1,1,0)$:

For this transition there is a particular combination of Wilson coefficients,

$$\left(\tilde{g}_2^{(1,1,0)}\right)^2 := \left(g_1^{(1,1,0)}\right)^2 + 2m_1^2\left(g_1^{(1,1,0)}\right)\left(g_2^{(1,1,0)}\right), \tag{G.8}$$

that is more natural for the impulse.

$$(c_u)^{(1,1,0)}_{0,0,0} = \frac{g^2}{2^{11}m_1^2m_2^2}\frac{\left(g_1^{(1,1,0)}\right)^2}{\sqrt{-b^2}}, \tag{G.9}$$

$$(c_u)^{(1,1,0)}_{1,0,0} = \frac{3g^2}{2^{11}m_1m_2^2}\frac{\left(g_1^{(1,1,0)}h_1^{(1,1,0)}\right)}{(-b^2)^2}, \tag{G.10}$$

$$(c_u)^{(1,1,0)}_{2,0,0} = -\frac{3g^2}{2^{16}m_1^4m_2^2}\frac{(9y^2-43)\left(\tilde{g}_2^{(1,1,0)}\right)^2 - 30m_1^4\left(h_1^{(1,1,0)}\right)^2}{(-b^2)^3}, \tag{G.11}$$

$$(c_u)^{(1,1,0)}_{0,2,0} = -\frac{3g^2}{2^{16}(y^2-1)m_1^4m_2^2}\frac{(9y^2+7)\left(\tilde{g}_2^{(1,1,0)}\right)^2}{(-b^2)^3}, \tag{G.12}$$

$$(c_u)^{(1,1,0)}_{0,0,2} = -\frac{27g^2}{2^{16}(y^2-1)m_1^4m_2^2}\frac{(3y^2-1)\left(\tilde{g}_2^{(1,1,0)}\right)^2 - 2y^2m_1^4\left(h_1^{(1,1,0)}\right)^2}{(-b^2)^3}, \tag{G.13}$$

$$(c_b)^{(1,1,0)}_{1,0,1} = \frac{3yg^2}{2^{14}(y^2-1)m_1^4m_2^2}\frac{\left(\tilde{g}_2^{(1,1,0)}\right)^2 - m_1^4\left(h_1^{(1,1,0)}\right)^2}{(-b^2)^3}, \tag{G.14}$$

$$(c_n)^{(1,1,0)}_{0,1,1} = -\frac{4}{(y^2-1)}(c_b)^{(1,1,0)}_{1,0,1}. \tag{G.15}$$

- $(1,2,0)$:

$$(c_u)^{(1,2,0)}_{2,0,0} = -\frac{9g^2}{2^{16}m_1^2m_2^2}\frac{(3y^2+5)\left(g_1^{(1,2,0)}\right)^2+(2y^2+5)\left(g_1^{(0,1,0)}\right)^2}{(-b^2)^3}, \tag{G.16}$$

$$(c_u)^{(1,2,0)}_{0,2,0} = -\frac{3g^2(3y^2+5)}{2^{16}(y^2-1)m_1^2m_2^2}\frac{2\left(g_1^{(1,2,0)}\right)^2+3\left(g_1^{(0,1,0)}\right)^2}{(-b^2)^3}, \tag{G.17}$$

$$(c_u)^{(1,2,0)}_{0,0,2} = -\frac{3g^2}{2^{16}(y^2-1)m_1^2m_2^2}\frac{(9y^2+10)\left(g_1^{(1,2,0)}\right)^2+3(3y^2+5)\left(g_1^{(0,1,0)}\right)^2}{(-b^2)^3}, \tag{G.18}$$

$$(c_b)^{(1,2,0)}_{1,0,1} = \frac{yg^2}{2^{15}(y^2-1)m_1^2m_2^2}\frac{\left(g_1^{(1,2,0)}\right)^2}{(-b^2)^3}, \tag{G.19}$$

$$(c_n)^{(1,2,0)}_{0,1,1} = -\frac{4}{(y^2-1)}(c_b)^{(1,2,0)}_{1,0,1}. \tag{G.20}$$

For equivalence between (1,0,0) and (1,2,0) there exists the map of Wilson coefficients

$$g_1^{(1,0,0)} \to 1/6\, g_1^{(1,2,0)}, \qquad \left(g_1^{(0,1,0)}\right)^2 \to -2/3\left(g_1^{(1,2,0)}\right)^2, \tag{G.21}$$

which is determined by spin universality and Floor-Ceiling symmetry.

- $(1,3,0)$:

$$(c_u)^{(1,3,0)}_{2,0,0} = \frac{3g^2}{2^{18}m_1^2m_2^2}\frac{(75y^4+152y^2+101)\left(g_1^{(1,3,0)}\right)^2+25(5y^4+26y^2+17)\left(g_1^{(0,2,0)}\right)^2}{(-b^2)^4}, \tag{G.22}$$

$$(c_u)^{(1,3,0)}_{0,2,0} = \frac{3g^2}{2^{18}(y^2-1)m_1^2m_2^2}\frac{(75y^4+558y^2+199)\left(g_1^{(1,3,0)}\right)^2+25(5y^4+26y^2+17)\left(g_1^{(0,2,0)}\right)^2}{(-b^2)^4}, \tag{G.23}$$

$$(c_u)^{(1,3,0)}_{0,0,2} = \frac{15g^2}{2^{18}(y^2-1)m_1^2m_2^2}\frac{(5y^2(y^2+8)+59)\left(g_1^{(1,3,0)}\right)^2+5(5y^4+26y^2+17)\left(g_1^{(0,2,0)}\right)^2}{(-b^2)^4}, \tag{G.24}$$

$$(c_b)^{(1,3,0)}_{1,0,1} = \frac{3yg^2}{2^{16}(y^2-1)m_1^2m_2^2}\frac{(y^2+11)\left(g_1^{(1,3,0)}\right)^2}{(-b^2)^4}, \tag{G.25}$$

$$(c_n)^{(1,3,0)}_{0,1,1} = -\frac{6}{(y^2-1)}(c_b)^{(1,3,0)}_{1,0,1}. \tag{G.26}$$

Photon Absorption

- $(0,1,1)$:

$$(c_u)^{(0,1,1)}_{0,0,0} = -\frac{9e^2}{2^{13}}\frac{(5y^2+3)\left(g_1^{(0,1,1)}\right)^2 + 5(y^2-1)\left(h_1^{(0,1,1)}\right)^2}{(-b^2)^2}. \tag{G.27}$$

- $(0,2,1)$:

$$(c_u)^{(0,2,1)}_{0,0,0} = -\frac{225e^2}{2^{17}m_1^2m_2^2}\frac{(7y^4+50y^2+7)\left(g_1^{(0,2,1)}\right)^2 + 7(y^4+2y^2-3)\left(h_1^{(0,2,1)}\right)^2}{(-b^2)^3}. \tag{G.28}$$

- $(1,0,1)$:

$$(c_u)^{(1,0,1)}_{2,0,0} = -\frac{45e^2}{2^{13}}\frac{y^2\left(g_1^{(1,0,1)}\right)^2 - (y^2-1)\left(h_1^{(1,0,1)}\right)^2}{(-b^2)^3}, \tag{G.29}$$

$$(c_u)^{(1,0,1)}_{1,1,0} = \frac{45ye^2}{2^{12}}\frac{\left(g_1^{(1,0,1)}\right)\left(h_1^{(1,0,1)}\right)}{(-b^2)^3}, \tag{G.30}$$

$$(c_u)^{(1,0,1)}_{0,0,2} = -\frac{9e^2}{2^{13}(y^2-1)}\frac{3\left(g_1^{(1,0,1)}\right)^2 - 5(y^2-1)\left(h_1^{(1,0,1)}\right)^2}{(-b^2)^3}, \tag{G.31}$$

$$(c_b)^{(1,0,1)}_{1,0,1} = \frac{3ye^2}{2^{12}(y^2-1)}\frac{\left(g_1^{(1,0,1)}\right)^2}{(-b^2)^3}, \tag{G.32}$$

$$(c_b)^{(1,0,1)}_{0,1,1} = -\frac{3e^2}{2^{12}(y^2-1)}\frac{\left(g_1^{(1,0,1)}\right)\left(h_1^{(1,0,1)}\right)}{(-b^2)^3}, \tag{G.33}$$

$$(c_n)^{(1,0,1)}_{1,0,1} = 4\,(c_b)^{(1,0,1)}_{0,1,1}, \tag{G.34}$$

$$(c_n)^{(1,0,1)}_{0,1,1} = -\frac{4}{(y^2-1)}(c_b)^{(1,0,1)}_{1,0,1}. \tag{G.35}$$

- $(1,1,1)$:

$$(c_u)^{(1,1,1)}_{2,0,0} = -\frac{45e^2}{2^{13}m_1^2}\frac{(y^2-1)\left(g_1^{(1,1,1)}\right)^2 - y^2\left(h_1^{(1,1,1)}\right)^2}{(-b^2)^3}, \tag{G.36}$$

$$(c_u)_{1,1,0}^{(1,1,1)} = \frac{45ye^2}{2^{12}m_1^2}\frac{\left(g_1^{(1,1,1)}\right)\left(h_1^{(1,1,1)}\right)}{(-b^2)^3}, \tag{G.37}$$

$$(c_u)_{0,0,2}^{(1,1,1)} = -\frac{9e^2}{2^{13}(y^2-1)m_1^2}\frac{5(y^2-1)\left(g_1^{(1,1,1)}\right)^2 - 3\left(h_1^{(1,1,1)}\right)^2}{(-b^2)^3}, \tag{G.38}$$

$$(c_b)_{1,0,1}^{(1,1,1)} = -\frac{3ye^2}{2^{12}(y^2-1)m_1^2}\frac{\left(h_1^{(1,1,1)}\right)^2}{(-b^2)^3}, \tag{G.39}$$

$$(c_b)_{0,1,1}^{(1,1,1)} = -\frac{3e^2}{2^{12}m_1^2}\frac{\left(g_1^{(1,1,1)}\right)\left(h_1^{(1,1,1)}\right)}{(-b^2)^3}, \tag{G.40}$$

$$(c_n)_{1,0,1}^{(1,1,1)} = 4\,(c_b)_{0,1,1}^{(1,1,1)}, \tag{G.41}$$

$$(c_n)_{0,1,1}^{(1,1,1)} = -\frac{4}{(y^2-1)}\,(c_b)_{1,0,1}^{(1,1,1)}. \tag{G.42}$$

- $(1,2,1)$:

$$(c_u)_{2,0,0}^{(1,2,1)} = -\frac{9e^2}{2^{14}}\frac{1}{(-b^2)^3}\left((5y^2+2)\left(g_1^{(1,2,1)}\right)^2 + (5y^2+3)\left(g_1^{(0,1,1)}\right)^2\right. \tag{G.43}$$

$$\left.+5(y^2-1)\left(h_1^{(0,1,1)}\right)^2\right), \tag{G.44}$$

$$(c_u)_{1,1,0}^{(1,2,1)} = \frac{15ye^2}{2^{13}}\frac{\left(g_1^{(1,2,1)}\right)^2\left(h_1^{(1,2,1)}\right)^2}{(-b^2)^3}, \tag{G.45}$$

$$(c_u)_{0,2,0}^{(1,2,1)} = -\frac{3e^2}{2^{14}(y^2-1)}\frac{1}{(-b^2)^3}\left(2(5y^2+3)\left(g_1^{(1,2,1)}\right)^2 + 3(5y^2+3)\left(g_1^{(0,1,1)}\right)^2\right. \tag{G.46}$$

$$\left.+5(y^2-1)\left(h_1^{(1,2,1)}\right)^2 + 15(y^2-1)\left(h_1^{(0,1,1)}\right)^2\right), \tag{G.47}$$

$$(c_u)_{0,0,2}^{(1,2,1)} = -\frac{3e^2}{2^{14}(y^2-1)}\frac{1}{(-b^2)^3}\left((10y^2+9)\left(g_1^{(1,2,1)}\right)^2 + 3(5y^2+3)\left(g_1^{(0,1,1)}\right)^2\right. \tag{G.48}$$

$$\left.+15(y^2-1)\left(h_1^{(0,1,1)}\right)^2\right), \tag{G.49}$$

$$(c_b)_{1,0,1}^{(1,2,1)} = \frac{ye^2}{2^{13}(y^2-1)}\frac{\left(g_1^{(1,2,1)}\right)^2}{(-b^2)^3}, \tag{G.50}$$

$$(c_b)^{(1,2,1)}_{0,1,1} = -\frac{ye^2}{2^{13}(y^2-1)}\frac{\left(g_1^{(1,2,1)}\right)\left(h_1^{(1,2,1)}\right)}{(-b^2)^3}, \tag{G.51}$$

$$(c_n)^{(1,2,1)}_{1,0,1} = 4\,(c_b)^{(1,2,1)}_{0,1,1}, \tag{G.52}$$

$$(c_n)^{(1,2,1)}_{0,1,1} = -\frac{4}{(y^2-1)}(c_b)^{(1,2,1)}_{1,0,1}. \tag{G.53}$$

For equivalence between (1,0,1) and (1,2,1) there exists the map of Wilson coefficients

$$\begin{aligned}
&\left(g_1^{(1,0,1)}\right) \to 1/\sqrt{6}\left(g_1^{(1,2,1)}\right), && \left(g_1^{(0,1,1)}\right)^2 \to -2/3\left(g_1^{(1,2,1)}\right)^2, \\
&\left(h_1^{(1,0,1)}\right) \to 1/\sqrt{6}\left(h_1^{(1,2,1)}\right), && \left(h_1^{(0,1,1)}\right)^2 \to -1/3\left(h_1^{(1,2,1)}\right)^2,
\end{aligned} \tag{G.54}$$

which is determined by spin universality and Floor-Ceiling symmetry.

- $(1,3,1)$:

$$\begin{aligned}
(c_u)^{(1,3,1)}_{2,0,0} = \frac{3e^2}{2^{18}}\frac{1}{(-b^2)^4}\Bigg(&(175y^4+962y^2+175)\left(g_1^{(1,3,1)}\right)^2 + 75(7y^2+1)(y^2+1)\left(g_1^{(0,2,1)}\right)^2 \\
&+35(11y^4+4y^2-15)\left(h_1^{(1,3,1)}\right)^2 + 525(y^4+2y^2-3)\left(h_1^{(0,2,1)}\right)^2\Bigg),
\end{aligned} \tag{G.55}$$

$$(c_u)^{(1,3,1)}_{1,1,0} = \frac{63ye^2}{2^{16}}\frac{(5y^2+19)\left(g_1^{(1,3,1)}\right)\left(h_1^{(1,3,1)}\right)}{(-b^2)^4}, \tag{G.56}$$

$$\begin{aligned}
(c_u)^{(1,3,1)}_{0,2,0} = &\frac{3e^2}{2^{18}(y^2-1)}\frac{1}{(-b^2)^4} \\
&\Bigg((385y^4+2558y^2+385)\left(g_1^{(1,3,1)}\right)^2 + 75(7y^2+1)(y^2+7)\left(g_1^{(0,2,1)}\right)^2 \\
&\quad +175(y^4+2y^2-3)\left(\left(h_1^{(1,3,1)}\right)^2 + 3\left(h_1^{(0,2,1)}\right)^2\right)\Bigg),
\end{aligned} \tag{G.57}$$

$$\begin{aligned}
(c_u)^{(1,3,1)}_{0,0,2} = &\frac{15e^2}{2^{18}(y^2-1)}\frac{1}{(-b^2)^4} \\
&\Bigg((35y^4+346y^2+35)\left(g_1^{(1,3,1)}\right)^2 + 15(7y^2+1)(y^2+7)\left(g_1^{(0,2,1)}\right)^2
\end{aligned}$$

$$+7(5y^4+28y^2-33)\left(h_1^{(1,3,1)}\right)^2+105(y^4+2y^2-3)\left(h_1^{(0,2,1)}\right)^2\Big), \tag{G.58}$$

$$(c_b)^{(1,3,1)}_{1,0,1}=\frac{9ye^2}{2^{16}(y^2-1)}\frac{8(y^2+1)\left(g_1^{(1,3,1)}\right)^2+7(y^2-1)\left(h_1^{(1,3,1)}\right)^2}{(-b^2)^4}, \tag{G.59}$$

$$(c_b)^{(1,3,1)}_{0,1,1}=-\frac{9e^2}{2^{16}(y^2-1)}\frac{(y^2+7)\left(g_1^{(1,3,1)}\right)\left(h_1^{(1,3,1)}\right)}{(-b^2)^4}, \tag{G.60}$$

$$(c_n)^{(1,3,1)}_{1,0,1}=6\,(c_b)^{(1,3,1)}_{0,1,1}, \tag{G.61}$$

$$(c_n)^{(1,3,1)}_{0,1,1}=-\frac{6}{(y^2-1)}(c_b)^{(1,3,1)}_{1,0,1}. \tag{G.62}$$

Graviton Absorption

- $(0,2,2)$:

$$(c_u)^{(0,2,2)}_{0,0,0}=-\frac{225\kappa^2m_1^2m_2^2}{2^{21}}\;\frac{\left(g_1^{(0,2,2)}\right)^2(21y^4-14y^2+9)+7\left(h_1^{(0,2,2)}\right)^2(3y^4-2y^2-1)}{\left(-b^2\right)^3} \tag{G.63}$$

- $(1,1,2)$:

$$(c_u)^{(1,1,2)}_{2,0,0}=-\frac{45\kappa^2m_1^2m_2^2}{2^{22}}\;\frac{\left(g_1^{(1,1,2)}\right)^2(80y^4+29y^2-17)-5\left(h_1^{(1,1,2)}\right)^2(16y^4-9y^2-7)}{\left(-b^2\right)^4} \tag{G.64}$$

$$(c_u)^{(1,1,2)}_{1,1,0}=\frac{945y\kappa^2m_1^2m_2^2}{2^{19}}\;\frac{\left(g_1^{(1,1,2)}\right)\left(h_1^{(1,1,2)}\right)}{\left(-b^2\right)^4} \tag{G.65}$$

$$(c_u)^{(1,1,2)}_{0,2,0}=-\frac{45\kappa^2m_1^2m_2^2}{2^{19}(y^2-1)}\;\frac{\left(g_1^{(1,1,2)}\right)^2(10y^4-13y^2+4)-10y^2\left(h_1^{(1,1,2)}\right)^2(y^2-1)}{\left(-b^2\right)^4} \tag{G.66}$$

$$(c_u)^{(1,1,2)}_{0,0,2}=\frac{225y^2\kappa^2m_1^2m_2^2}{2^{22}(y^2-1)}\;\frac{\left(g_1^{(1,1,2)}\right)^2(5y^2-17)+37\left(h_1^{(1,1,2)}\right)^2(y^2-1)}{\left(-b^2\right)^4} \tag{G.67}$$

$$(c_b)^{(1,1,2)}_{1,0,1} = \frac{45y\kappa^2 m_1^2 m_2^2}{2^{21}(y^2-1)} \; \frac{\left(g_1^{(1,1,2)}\right)^2 (7y^2-3) + 7\left(h_1^{(1,1,2)}\right)^2 (y^2-1)}{(-b^2)^4} \tag{G.68}$$

$$(c_b)^{(1,1,2)}_{0,1,1} = -\frac{45\kappa^2 m_1^2 m_2^2}{2^{19}(y^2-1)} \; \frac{\left(g_1^{(1,1,2)}\right)\left(h_1^{(1,1,2)}\right)}{(-b^2)^4} \tag{G.69}$$

$$(c_n)^{(1,1,2)}_{1,0,1} = 6(c_b)^{(1,1,2)}_{0,1,1} \tag{G.70}$$

$$(c_n)^{(1,1,2)}_{0,1,1} = -\frac{6}{(y^2-1)}(c_b)^{(1,1,2)}_{1,0,1} \tag{G.71}$$

- $(1,2,2)$:

$$(c_u)^{(1,2,2)}_{2,0,0} = -\frac{45\kappa^2 m_2^2}{2^{23}} \; \frac{5\left(g_1^{(1,2,2)}\right)^2 (16y^4+5y^2-21) + \left(h_1^{(1,2,2)}\right)^2 (80y^4-407y^2+51)}{(-b^2)^4} \tag{G.72}$$

$$(c_u)^{(1,2,2)}_{1,1,0} = \frac{2835y\kappa^2 m_2^2}{2^{20}} \; \frac{\left(g_1^{(1,2,2)}\right)\left(h_1^{(1,2,2)}\right)}{(-b^2)^4} \tag{G.73}$$

$$(c_u)^{(1,2,2)}_{0,2,0} = -\frac{45\kappa^2 m_2^2}{2^{20}(y^2-1)} \; \frac{10y^2\left(g_1^{(1,2,2)}\right)^2 (y^2-1) + \left(h_1^{(1,2,2)}\right)^2 (10y^4-y^2-12)}{(-b^2)^4} \tag{G.74}$$

$$(c_u)^{(1,2,2)}_{0,0,2} = -\frac{225y^2\kappa^2 m_2^2}{2^{23}(y^2-1)} \; \frac{79\left(g_1^{(1,2,2)}\right)^2 (y^2-1) + \left(h_1^{(1,2,2)}\right)^2 (79y^2-115)}{(-b^2)^4} \tag{G.75}$$

$$(c_b)^{(1,2,2)}_{1,0,1} = -\frac{135y\kappa^2 m_2^2}{2^{22}(y^2-1)} \; \frac{7\left(g_1^{(1,2,2)}\right)^2 (y^2-1) + \left(h_1^{(1,2,2)}\right)^2 (7y^2-3)}{(-b^2)^4} \tag{G.76}$$

$$(c_b)^{(1,2,2)}_{0,1,1} = -\frac{135\kappa^2 m_2^2}{2^{20}(y^2-1)} \; \frac{\left(g_1^{(1,2,2)}\right)\left(h_1^{(1,2,2)}\right)}{(-b^2)^4} \tag{G.77}$$

$$(c_n)^{(1,2,2)}_{1,0,1} = 6(c_b)^{(1,2,2)}_{0,1,1} \tag{G.78}$$

$$(c_n)^{(1,2,2)}_{0,1,1} = -\frac{6}{(y^2-1)}(c_b)^{(1,2,2)}_{1,0,1} \tag{G.79}$$

- $(1,3,2)$:

$$(c_u)^{(1,3,2)}_{2,0,0} = \frac{3\kappa^2 m_1^2 m_2^2}{2^{22}} \frac{1}{(-b^2)^4}$$

$$\left(\left(g_1^{(1,3,2)}\right)^2 \left(1485y^4 - 296y^2 + 243\right) + 75\left(g_1^{(0,2,2)}\right)^2 \left(21y^4 - 14y^2 + 9\right) + 5(y^2-1)\left(\left(h_1^{(1,3,2)}\right)^2 \left(201y^2 - 7\right) + 105\left(h_1^{(0,2,2)}\right)^2 \left(3y^2+1\right)\right)\right) \tag{G.80}$$

$$(c_u)_{1,1,0}^{(1,3,2)} = \frac{189\kappa^2 y m_1^2 m_2^2}{2^{18}(y^2-1)} \left(\frac{\left(g_1^{(1,3,2)}\right)\left(h_1^{(1,3,2)}\right)}{\left(-b^2\right)^4}\right) \tag{G.81}$$

$$(c_u)_{0,2,0}^{(1,3,2)} = \frac{3\kappa^2 m_1^2 m_2^2}{2^{22}(y^2-1)} \frac{1}{(-b^2)^4} \left(\left(g_1^{(1,3,2)}\right)^2 \left(1485y^4 - 1094y^2 + 537\right) + 75\left(g_1^{(0,2,2)}\right)^2 \left(21y^4 - 14y^2 + 9\right) + 5(y^2-1)\left(\left(h_1^{(1,3,2)}\right)^2 \left(201y^2 + 35\right) + 105\left(h_1^{(0,2,2)}\right)^2 \left(3y^2+1\right)\right)\right) \tag{G.82}$$

$$(c_u)_{0,0,2}^{(1,3,2)} = \frac{15\kappa^2 m_1^2 m_2^2}{2^{22}(y^2-1)} \frac{1}{(-b^2)^4} \left(\left(g_1^{(1,3,2)}\right)^2 \left(171y^4 + 8y^2 + 69\right) + 15\left(g_1^{(0,2,2)}\right)^2 \left(21y^4 - 14y^2 + 9\right) + 5(y^2-1)\left(\left(h_1^{(1,3,2)}\right)^2 \left(15y^2 + 7\right) + 21\left(h_1^{(0,2,2)}\right)^2 \left(3y^2+1\right)\right)\right) \tag{G.83}$$

$$(c_b)_{1,0,1}^{(1,3,2)} = -\frac{9y\kappa^2 m_1^2 m_2^2}{2^{20}(y^2-1)} \frac{\left(g_1^{(1,3,2)}\right)^2 (7y^2-3) + 7\left(h_1^{(1,3,2)}\right)^2 (y^2-1)}{\left(-b^2\right)^4} \tag{G.84}$$

$$(c_b)_{0,1,1}^{(1,3,2)} = -\frac{9\kappa^2 m_1^2 m_2^2}{2^{18}(y^2-1)} \frac{\left(g_1^{(1,2,2)}\right)\left(h_1^{(1,3,2)}\right)}{\left(-b^2\right)^4} \tag{G.85}$$

$$(c_n)_{1,0,1}^{(1,3,2)} = 6(c_b)_{0,1,1}^{(1,3,2)} \tag{G.86}$$

$$(c_n)_{0,1,1}^{(1,3,2)} = -\frac{6}{(y^2-1)}(c_b)_{1,0,1}^{(1,3,2)} \tag{G.87}$$

Bibliography

[1] **LIGO Scientific, Virgo** Collaboration, B. Abbott et al., *Observation of Gravitational Waves from a Binary Black Hole Merger*, *Phys. Rev. Lett.* **116** (2016), no. 6 061102, [arXiv:1602.03837].

[2] **LIGO Scientific, Virgo** Collaboration, B. Abbott et al., *GW170817: Observation of Gravitational Waves from a Binary Neutron Star Inspiral*, *Phys. Rev. Lett.* **119** (2017), no. 16 161101, [arXiv:1710.05832].

[3] M. Punturo et al., *The Einstein Telescope: A third-generation gravitational wave observatory*, *Class. Quant. Grav.* **27** (2010) 194002.

[4] S. Dwyer, D. Sigg, S. W. Ballmer, L. Barsotti, N. Mavalvala, and M. Evans, *Gravitational wave detector with cosmological reach*, *Phys. Rev. D* **91** (2015), no. 8 082001, [arXiv:1410.0612].

[5] **LISA** Collaboration, P. Amaro-Seoane et al., *Laser Interferometer Space Antenna*, arXiv:1702.00786.

[6] D. Reitze et al., *Cosmic Explorer: The U.S. Contribution to Gravitational-Wave Astronomy beyond LIGO*, *Bull. Am. Astron. Soc.* **51** (7, 2019) 035, [arXiv:1907.04833].

[7] A. Buonanno and T. Damour, *Effective one-body approach to general relativistic two-body dynamics*, *Phys. Rev. D* **59** (1999) 084006, [gr-qc/9811091].

[8] F. Pretorius, *Evolution of binary black hole spacetimes*, *Phys. Rev. Lett.* **95** (2005) 121101, [gr-qc/0507014].

[9] M. Campanelli, C. O. Lousto, P. Marronetti, and Y. Zlochower, *Accurate evolutions of orbiting black-hole binaries without excision*, *Phys. Rev. Lett.* **96** (2006) 111101, [gr-qc/0511048].

[10] J. G. Baker, J. Centrella, D.-I. Choi, M. Koppitz, and J. van Meter, *Gravitational wave extraction from an inspiraling configuration of merging black holes*, *Phys. Rev. Lett.* **96** (2006) 111102, [gr-qc/0511103].

[11] Y. Mino, M. Sasaki, and T. Tanaka, *Gravitational radiation reaction to a particle motion*, *Phys. Rev. D* **55** (1997) 3457–3476, [gr-qc/9606018].

[12] T. C. Quinn and R. M. Wald, *An Axiomatic approach to electromagnetic and gravitational radiation reaction of particles in curved space-time*, *Phys. Rev. D* **56** (1997) 3381–3394, [gr-qc/9610053].

[13] J. Droste, *The field of n moving centres in Einstein's theory of gravitation*, *Proc. Acad. Sci. Amst.* **26** (1916) 447–455.

[14] A. Einstein, L. Infeld, and B. Hoffmann, *The Gravitational equations and the problem of motion*, *Annals Math.* **39** (1938) 65–100.

[15] W. D. Goldberger and I. Z. Rothstein, *An Effective field theory of gravity for extended objects*, *Phys. Rev. D* **73** (2006) 104029, [hep-th/0409156].

[16] B. Kol and M. Smolkin, *Classical Effective Field Theory and Caged Black Holes*, *Phys. Rev. D* **77** (2008) 064033, [arXiv:0712.2822].

[17] B. Kol and M. Smolkin, *Non-Relativistic Gravitation: From Newton to Einstein and Back*, *Class. Quant. Grav.* **25** (2008) 145011, [arXiv:0712.4116].

[18] J. B. Gilmore and A. Ross, *Effective field theory calculation of second post-Newtonian binary dynamics*, *Phys. Rev. D* **78** (2008) 124021, [arXiv:0810.1328].

[19] S. Foffa and R. Sturani, *Effective field theory calculation of conservative binary dynamics at third post-Newtonian order*, *Phys. Rev. D* **84** (2011) 044031, [arXiv:1104.1122].

[20] S. Foffa, P. Mastrolia, R. Sturani, and C. Sturm, *Effective field theory approach to the gravitational two-body dynamics, at fourth post-Newtonian order and quintic in the Newton constant*, *Phys. Rev. D* **95** (2017), no. 10 104009, [arXiv:1612.00482].

[21] R. A. Porto and I. Z. Rothstein, *Apparent ambiguities in the post-Newtonian expansion for binary systems*, *Phys. Rev. D* **96** (2017), no. 2 024062, [arXiv:1703.06433].

[22] S. Foffa, P. Mastrolia, R. Sturani, C. Sturm, and W. J. Torres Bobadilla, *Static two-body potential at fifth post-Newtonian order*, *Phys. Rev. Lett.* **122** (2019), no. 24 241605, [arXiv:1902.10571].

[23] J. Blümlein, A. Maier, and P. Marquard, *Five-Loop Static Contribution to the Gravitational Interaction Potential of Two Point Masses*, *Phys. Lett. B* **800** (2020) 135100, [arXiv:1902.11180].

[24] S. Foffa and R. Sturani, *Conservative dynamics of binary systems to fourth Post-Newtonian order in the EFT approach I: Regularized Lagrangian*, *Phys. Rev. D* **100** (2019), no. 2 024047, [arXiv:1903.05113].

[25] S. Foffa, R. A. Porto, I. Rothstein, and R. Sturani, *Conservative dynamics of binary systems to fourth Post-Newtonian order in the EFT approach II: Renormalized Lagrangian*, *Phys. Rev. D* **100** (2019), no. 2 024048, [arXiv:1903.05118].

[26] J. Blümlein, A. Maier, P. Marquard, and G. Schäfer, *Fourth post-Newtonian Hamiltonian dynamics of two-body systems from an effective field theory approach*, *Nucl. Phys. B* **955** (2020) 115041, [arXiv:2003.01692].

[27] B. Bertotti, *On gravitational motion*, *Nuovo Cimento* **4** (1956) 898–906.

[28] R. P. Kerr, *The Lorentz-covariant approximation method in general relativity I*, *Nuovo Cim.* **13** (1959), no. 3 469–491.

[29] B. Bertotti and J. Plebanski, *Theory of gravitational perturbations in the fast motion approximation*, *Annals Phys.* **11** (1960), no. 2 169–200.

[30] M. Portilla, *Momentum and angular momentum of two gravitating particles*, *J. Phys. A* **12** (1979) 1075–1090.

[31] K. Westpfahl and M. Goller, *Gravitational scattering of two relativistic particles in postlinear approximation*, *Lett. Nuovo Cim.* **26** (1979) 573–576.

[32] L. Bel, T. Damour, N. Deruelle, J. Ibanez, and J. Martin, *Poincaré-invariant gravitational field and equations of motion of two pointlike objects: The postlinear approximation of general relativity*, *Gen. Rel. Grav.* **13** (1981) 963–1004.

[33] K. Westpfahl, *High-Speed Scattering of Charged and Uncharged Particles in General Relativity*, *Fortsch. Phys.* **33** (1985), no. 8 417–493.

[34] T. Ledvinka, G. Schaefer, and J. Bicak, *Relativistic Closed-Form Hamiltonian for Many-Body Gravitating Systems in the Post-Minkowskian Approximation*, *Phys. Rev. Lett.* **100** (2008) 251101, [arXiv:0807.0214].

[35] T. Damour, *High-energy gravitational scattering and the general relativistic two-body problem*, *Phys. Rev. D* **97** (2018), no. 4 044038, [arXiv:1710.10599].

[36] N. E. J. Bjerrum-Bohr, J. F. Donoghue, and P. Vanhove, *On-shell Techniques and Universal Results in Quantum Gravity*, *JHEP* **02** (2014) 111, [arXiv:1309.0804].

[37] N. E. J. Bjerrum-Bohr, P. H. Damgaard, G. Festuccia, L. Planté, and P. Vanhove, *General Relativity from Scattering Amplitudes*, *Phys. Rev. Lett.* **121** (2018), no. 17 171601, [arXiv:1806.04920].

[38] C. Cheung, I. Z. Rothstein, and M. P. Solon, *From Scattering Amplitudes to Classical Potentials in the Post-Minkowskian Expansion*, *Phys. Rev. Lett.* **121** (2018), no. 25 251101, [arXiv:1808.02489].

[39] D. A. Kosower, B. Maybee, and D. O'Connell, *Amplitudes, Observables, and Classical Scattering*, *JHEP* **02** (2019) 137, [arXiv:1811.10950].

[40] B. Maybee, D. O'Connell, and J. Vines, *Observables and amplitudes for spinning particles and black holes*, *JHEP* **12** (2019) 156, [arXiv:1906.09260].

[41] Z. Bern, C. Cheung, R. Roiban, C.-H. Shen, M. P. Solon, and M. Zeng, *Scattering Amplitudes and the Conservative Hamiltonian for Binary Systems at Third Post-Minkowskian Order*, *Phys. Rev. Lett.* **122** (2019), no. 20 201603, [arXiv:1901.04424].

[42] Z. Bern, C. Cheung, R. Roiban, C.-H. Shen, M. P. Solon, and M. Zeng, *Black Hole Binary Dynamics from the Double Copy and Effective Theory*, *JHEP* **10** (2019) 206, [arXiv:1908.01493].

[43] A. Antonelli, A. Buonanno, J. Steinhoff, M. van de Meent, and J. Vines, *Energetics of two-body Hamiltonians in post-Minkowskian gravity*, *Phys. Rev. D* **99** (2019), no. 10 104004, [arXiv:1901.07102].

[44] A. Koemans Collado, P. Di Vecchia, and R. Russo, *Revisiting the second post-Minkowskian eikonal and the dynamics of binary black holes*, *Phys. Rev. D* **100** (2019), no. 6 066028, [arXiv:1904.02667].

[45] A. Cristofoli, P. H. Damgaard, P. Di Vecchia, and C. Heissenberg, *Second-order Post-Minkowskian scattering in arbitrary dimensions*, *JHEP* **07** (2020) 122, [arXiv:2003.10274].

[46] E. Herrmann, J. Parra-Martinez, M. S. Ruf, and M. Zeng, *Gravitational Bremsstrahlung from Reverse Unitarity*, *Phys. Rev. Lett.* **126** (2021), no. 20 201602, [arXiv:2101.07255].

[47] E. Herrmann, J. Parra-Martinez, M. S. Ruf, and M. Zeng, *Radiative classical gravitational observables at $\mathcal{O}(G^3)$ from scattering amplitudes*, *JHEP* **10** (2021) 148, [arXiv:2104.03957].

[48] A. Cristofoli, R. Gonzo, D. A. Kosower, and D. O'Connell, *Waveforms from amplitudes*, *Phys. Rev. D* **106** (2022), no. 5 056007, [arXiv:2107.10193].

[49] L. de la Cruz, A. Luna, and T. Scheopner, *Yang-Mills observables: from KMOC to eikonal through EFT*, arXiv:2108.02178.

[50] A. Cristofoli, R. Gonzo, N. Moynihan, D. O'Connell, A. Ross, M. Sergola, and C. D. White, *The Uncertainty Principle and Classical Amplitudes*, arXiv:2112.07556.

[51] Y. F. Bautista and A. Laddha, *Soft Constraints on KMOC Formalism*, arXiv:2111.11642.

[52] J. Blümlein, A. Maier, P. Marquard, and G. Schäfer, *Testing binary dynamics in gravity at the sixth post-Newtonian level*, *Phys. Lett. B* **807** (2020) 135496, [arXiv:2003.07145].

[53] C. Cheung and M. P. Solon, *Classical gravitational scattering at $\mathcal{O}(G^3)$ from Feynman diagrams*, *JHEP* **06** (2020) 144, [arXiv:2003.08351].

[54] D. Bini, T. Damour, and A. Geralico, *Binary dynamics at the fifth and fifth-and-a-half post-Newtonian orders*, *Phys. Rev. D* **102** (2020), no. 2 024062, [arXiv:2003.11891].

[55] D. Bini, T. Damour, and A. Geralico, *Sixth post-Newtonian local-in-time dynamics of binary systems*, *Phys. Rev. D* **102** (2020), no. 2 024061, [arXiv:2004.05407].

[56] D. Bini, T. Damour, and A. Geralico, *Novel approach to binary dynamics: application to the fifth post-Newtonian level*, *Phys. Rev. Lett.* **123** (2019), no. 23 231104, [arXiv:1909.02375].

[57] N. Siemonsen and J. Vines, *Test black holes, scattering amplitudes and perturbations of Kerr spacetime*, *Phys. Rev. D* **101** (2020), no. 6 064066, [arXiv:1909.07361].

[58] A. Antonelli, C. Kavanagh, M. Khalil, J. Steinhoff, and J. Vines, *Gravitational spin-orbit coupling through third-subleading post-Newtonian order: from first-order self-force to arbitrary mass ratios*, *Phys. Rev. Lett.* **125** (2020), no. 1 011103, [arXiv:2003.11391].

[59] Z. Bern, J. Parra-Martinez, R. Roiban, M. S. Ruf, C.-H. Shen, M. P. Solon, and M. Zeng, *Scattering Amplitudes and Conservative Binary Dynamics at $\mathcal{O}(G^4)$*, *Phys. Rev. Lett.* **126** (2021), no. 17 171601, [arXiv:2101.07254].

[60] D. Bini, T. Damour, and A. Geralico, *Radiative contributions to gravitational scattering*, *Phys. Rev. D* **104** (2021), no. 8 084031, [arXiv:2107.08896].

[61] J. Blümlein, A. Maier, P. Marquard, and G. Schäfer, *The fifth-order post-Newtonian Hamiltonian dynamics of two-body systems from an effective field theory approach*, arXiv:2110.13822.

[62] Z. Bern, J. Parra-Martinez, R. Roiban, M. S. Ruf, C.-H. Shen, M. P. Solon, and M. Zeng, *Scattering Amplitudes, the Tail Effect, and Conservative Binary Dynamics at O(G4)*, *Phys. Rev. Lett.* **128** (2022), no. 16 161103, [arXiv:2112.10750].

[63] G. Kälin, Z. Liu, and R. A. Porto, *Conservative Dynamics of Binary Systems to Third Post-Minkowskian Order from the Effective Field Theory Approach*, *Phys. Rev. Lett.* **125** (2020), no. 26 261103, [arXiv:2007.04977].

[64] G. Cho, B. Pardo, and R. A. Porto, *Gravitational radiation from inspiralling compact objects: Spin-spin effects completed at the next-to-leading post-Newtonian order*, *Phys. Rev. D* **104** (2021), no. 2 024037, [arXiv:2103.14612].

[65] C. Dlapa, G. Kälin, Z. Liu, and R. A. Porto, *Dynamics of binary systems to fourth Post-Minkowskian order from the effective field theory approach*, *Phys. Lett. B* **831** (2022) 137203, [arXiv:2106.08276].

[66] C. Dlapa, G. Kälin, Z. Liu, and R. A. Porto, *Conservative Dynamics of Binary Systems at Fourth Post-Minkowskian Order in the Large-eccentricity Expansion*, arXiv:2112.11296.

[67] D. Neill and I. Z. Rothstein, *Classical Space-Times from the S Matrix*, *Nucl. Phys. B* **877** (2013) 177–189, [arXiv:1304.7263].

[68] Z. Bern, L. J. Dixon, D. C. Dunbar, and D. A. Kosower, *One loop n point gauge theory amplitudes, unitarity and collinear limits*, *Nucl. Phys. B* **425** (1994) 217–260, [hep-ph/9403226].

[69] Z. Bern, L. J. Dixon, D. C. Dunbar, and D. A. Kosower, *Fusing gauge theory tree amplitudes into loop amplitudes*, *Nucl. Phys. B* **435** (1995) 59–101, [hep-ph/9409265].

[70] R. Britto, F. Cachazo, and B. Feng, *Generalized unitarity and one-loop amplitudes in N=4 super-Yang-Mills*, *Nucl. Phys. B* **725** (2005) 275–305, [hep-th/0412103].

[71] H. Kawai, D. C. Lewellen, and S. H. H. Tye, *A Relation Between Tree Amplitudes of Closed and Open Strings*, *Nucl. Phys. B* **269** (1986) 1–23.

[72] Z. Bern, J. Carrasco, and H. Johansson, *New Relations for Gauge-Theory Amplitudes*, *Phys. Rev. D* **78** (2008) 085011, [arXiv:0805.3993].

[73] Z. Bern, J. J. M. Carrasco, and H. Johansson, *Perturbative Quantum Gravity as a Double Copy of Gauge Theory*, *Phys. Rev. Lett.* **105** (2010) 061602, [arXiv:1004.0476].

[74] Z. Bern, J. Carrasco, L. Dixon, H. Johansson, and R. Roiban, *Simplifying Multiloop Integrands and Ultraviolet Divergences of Gauge Theory and Gravity Amplitudes*, *Phys. Rev. D* **85** (2012) 105014, [arXiv:1201.5366].

[75] Z. Bern, J. J. Carrasco, M. Chiodaroli, H. Johansson, and R. Roiban, *The Duality Between Color and Kinematics and its Applications*, arXiv:1909.01358.

[76] J. Parra-Martinez, M. S. Ruf, and M. Zeng, *Extremal black hole scattering at $\mathcal{O}(G^3)$: graviton dominance, eikonal exponentiation, and differential equations*, *JHEP* **11** (2020) 023, [arXiv:2005.04236].

[77] F. V. Tkachov, *A Theorem on Analytical Calculability of Four Loop Renormalization Group Functions*, *Phys. Lett. B* **100** (1981) 65–68.

[78] K. Chetyrkin and F. Tkachov, *Integration by Parts: The Algorithm to Calculate beta Functions in 4 Loops*, *Nucl. Phys. B* **192** (1981) 159–204.

[79] S. Laporta, *High precision calculation of multiloop Feynman integrals by difference equations*, *Int. J. Mod. Phys. A* **15** (2000) 5087–5159, [hep-ph/0102033].

[80] A. Kotikov, *Differential equations method: New technique for massive Feynman diagrams calculation*, *Phys. Lett. B* **254** (1991) 158–164.

[81] Z. Bern, L. J. Dixon, and D. A. Kosower, *Dimensionally regulated one loop integrals*, *Phys. Lett. B* **302** (1993) 299–308, [hep-ph/9212308]. [Erratum: Phys.Lett.B 318, 649 (1993)].

[82] E. Remiddi, *Differential equations for Feynman graph amplitudes*, *Nuovo Cim. A* **110** (1997) 1435–1452, [hep-th/9711188].

[83] T. Gehrmann and E. Remiddi, *Differential equations for two loop four point functions*, *Nucl. Phys. B* **580** (2000) 485–518, [hep-ph/9912329].

[84] J. M. Henn, *Multiloop integrals in dimensional regularization made simple*, *Phys. Rev. Lett.* **110** (2013) 251601, [arXiv:1304.1806].

[85] J. M. Henn, *Lectures on differential equations for Feynman integrals*, *J. Phys. A* **48** (2015) 153001, [arXiv:1412.2296].

[86] C. Anastasiou and K. Melnikov, *Higgs boson production at hadron colliders in NNLO QCD*, *Nucl. Phys. B* **646** (2002) 220–256, [hep-ph/0207004].

[87] C. Anastasiou, L. J. Dixon, and K. Melnikov, *NLO Higgs boson rapidity distributions at hadron colliders*, *Nucl. Phys. B Proc. Suppl.* **116** (2003) 193–197, [hep-ph/0211141].

[88] C. Anastasiou, L. J. Dixon, K. Melnikov, and F. Petriello, *Dilepton rapidity distribution in the Drell-Yan process at NNLO in QCD*, *Phys. Rev. Lett.* **91** (2003) 182002, [hep-ph/0306192].

[89] C. Anastasiou, C. Duhr, F. Dulat, E. Furlan, F. Herzog, and B. Mistlberger, *Soft expansion of double-real-virtual corrections to Higgs production at N^3LO*, *JHEP* **08** (2015) 051, [arXiv:1505.04110].

[90] W. Bonnor, *Spherical gravitational waves*, *Philos. Trans. R. Soc. London* **A 251** (1959) 233.

[91] W. Bonnor and M. Rotenberg, *Gravitational waves from isolated sources*, *Proc. R. Soc. London* **Ser A 289** (1966) 247.

[92] K. S. Thorne, *Multipole Expansions of Gravitational Radiation*, *Rev. Mod. Phys.* **52** (1980) 299–339.

[93] L. Blanchet and T. Damour, *Tail Transported Temporal Correlations in the Dynamics of a Gravitating System*, *Phys. Rev. D* **37** (1988) 1410.

[94] L. Blanchet and T. Damour, *Hereditary effects in gravitational radiation*, *Phys. Rev. D* **46** (1992) 4304–4319.

[95] L. Blanchet and G. Schaefer, *Gravitational wave tails and binary star systems*, *Class. Quant. Grav.* **10** (1993) 2699–2721.

[96] G. Kälin and R. A. Porto, *From Boundary Data to Bound States*, *JHEP* **01** (2020) 072, [arXiv:1910.03008].

[97] G. Kälin and R. A. Porto, *From boundary data to bound states. Part II. Scattering angle to dynamical invariants (with twist)*, *JHEP* **02** (2020) 120, [arXiv:1911.09130].

[98] D. Bini, T. Damour, and A. Geralico, *Sixth post-Newtonian nonlocal-in-time dynamics of binary systems*, *Phys. Rev. D* **102** (2020), no. 8 084047, [arXiv:2007.11239].

[99] M. V. S. Saketh, J. Vines, J. Steinhoff, and A. Buonanno, *Conservative and radiative dynamics in classical relativistic scattering and bound systems*, *Phys. Rev. Res.* **4** (2022), no. 1 013127, [arXiv:2109.05994].

[100] D. Bini and T. Damour, *Gravitational scattering of two black holes at the fourth post-Newtonian approximation*, *Phys. Rev. D* **96** (2017), no. 6 064021, [arXiv:1706.06877].

[101] G. Cho, G. Kälin, and R. A. Porto, *From Boundary Data to Bound States III: Radiative Effects*, arXiv:2112.03976.

[102] P. H. Damgaard, L. Plante, and P. Vanhove, *On an exponential representation of the gravitational S-matrix*, *JHEP* **11** (2021) 213, [arXiv:2107.12891].

[103] U. Kol, D. O'Connell, and O. Telem, *The Radial Action from Probe Amplitudes to All Orders*, arXiv:2109.12092.

[104] R. J. Glauber, *Lectures in theoretical physics, Interscience Publishers Inc., New York* **I** (1959) 315.

[105] D. Amati, M. Ciafaloni, and G. Veneziano, *Higher Order Gravitational Deflection and Soft Bremsstrahlung in Planckian Energy Superstring Collisions*, *Nucl. Phys. B* **347** (1990) 550–580.

[106] E. Laenen, G. Stavenga, and C. D. White, *Path integral approach to eikonal and next-to-eikonal exponentiation*, *JHEP* **03** (2009) 054, [arXiv:0811.2067].

[107] R. Akhoury, R. Saotome, and G. Sterman, *High Energy Scattering in Perturbative Quantum Gravity at Next to Leading Power*, *Phys. Rev. D* **103** (2021), no. 6 064036, [arXiv:1308.5204].

[108] Z. Bern, H. Ita, J. Parra-Martinez, and M. S. Ruf, *Universality in the classical limit of massless gravitational scattering*, *Phys. Rev. Lett.* **125** (2020), no. 3 031601, [arXiv:2002.02459].

[109] T. Adamo, A. Cristofoli, and P. Tourkine, *Eikonal amplitudes from curved backgrounds*, arXiv:2112.09113.

[110] J. Blümlein, A. Maier, P. Marquard, and G. Schäfer, *The 6th post-Newtonian potential terms at $O(G_N^4)$*, *Phys. Lett. B* **816** (2021) 136260, [arXiv:2101.08630].

[111] V. Vaidya, *Gravitational spin Hamiltonians from the S matrix*, *Phys. Rev. D* **91** (2015), no. 2 024017, [arXiv:1410.5348].

[112] J. Vines, *Scattering of two spinning black holes in post-Minkowskian gravity, to all orders in spin, and effective-one-body mappings*, *Class. Quant. Grav.* **35** (2018), no. 8 084002, [arXiv:1709.06016].

[113] A. Guevara, *Holomorphic Classical Limit for Spin Effects in Gravitational and Electromagnetic Scattering*, *JHEP* **04** (2019) 033, [arXiv:1706.02314].

[114] J. Vines, J. Steinhoff, and A. Buonanno, *Spinning-black-hole scattering and the test-black-hole limit at second post-Minkowskian order*, *Phys. Rev. D* **99** (2019), no. 6 064054, [arXiv:1812.00956].

[115] A. Guevara, A. Ochirov, and J. Vines, *Scattering of Spinning Black Holes from Exponentiated Soft Factors*, *JHEP* **09** (2019) 056, [arXiv:1812.06895].

[116] M.-Z. Chung, Y.-T. Huang, J.-W. Kim, and S. Lee, *The simplest massive S-matrix: from minimal coupling to Black Holes*, *JHEP* **04** (2019) 156, [arXiv:1812.08752].

[117] A. Guevara, A. Ochirov, and J. Vines, *Black-hole scattering with general spin directions from minimal-coupling amplitudes*, *Phys. Rev. D* **100** (2019), no. 10 104024, [arXiv:1906.10071].

[118] M.-Z. Chung, Y.-T. Huang, and J.-W. Kim, *Classical potential for general spinning bodies*, *JHEP* **09** (2020) 074, [arXiv:1908.08463].

[119] P. H. Damgaard, K. Haddad, and A. Helset, *Heavy Black Hole Effective Theory*, *JHEP* **11** (2019) 070, [arXiv:1908.10308].

[120] R. Aoude, K. Haddad, and A. Helset, *On-shell heavy particle effective theories*, *JHEP* **05** (2020) 051, [arXiv:2001.09164].

[121] Z. Bern, A. Luna, R. Roiban, C.-H. Shen, and M. Zeng, *Spinning black hole binary dynamics, scattering amplitudes, and effective field theory*, *Phys. Rev. D* **104** (2021), no. 6 065014, [arXiv:2005.03071].

[122] D. Kosmopoulos and A. Luna, *Quadratic-in-spin Hamiltonian at $\mathcal{O}(G^2)$ from scattering amplitudes*, *JHEP* **07** (2021) 037, [arXiv:2102.10137].

[123] A. Guevara, B. Maybee, A. Ochirov, D. O'connell, and J. Vines, *A worldsheet for Kerr*, *JHEP* **03** (2021) 201, [arXiv:2012.11570].

[124] M. Levi, A. J. Mcleod, and M. Von Hippel, *N^3LO gravitational quadratic-in-spin interactions at G^4*, *JHEP* **07** (2021) 116, [arXiv:2003.07890].

[125] M. Levi, A. J. Mcleod, and M. Von Hippel, *N^3LO gravitational spin-orbit coupling at order G^4*, *JHEP* **07** (2021) 115, [arXiv:2003.02827].

[126] W.-M. Chen, M.-Z. Chung, Y.-t. Huang, and J.-W. Kim, *The 2PM Hamiltonian for binary Kerr to quartic in spin*, arXiv:2111.13639.

[127] Z. Liu, R. A. Porto, and Z. Yang, *Spin Effects in the Effective Field Theory Approach to Post-Minkowskian Conservative Dynamics*, *JHEP* **06** (2021) 012, [arXiv:2102.10059].

[128] A. Brandhuber and G. Travaglini, *On higher-derivative effects on the gravitational potential and particle bending*, *JHEP* **01** (2020) 010, [arXiv:1905.05657].

[129] M. Accettulli Huber, A. Brandhuber, S. De Angelis, and G. Travaglini, *Note on the absence of R^2 corrections to Newton's potential*, *Phys. Rev. D* **101** (2020), no. 4 046011, [arXiv:1911.10108].

[130] C. Cheung and M. P. Solon, *Tidal Effects in the Post-Minkowskian Expansion*, *Phys. Rev. Lett.* **125** (2020), no. 19 191601, [arXiv:2006.06665].

[131] G. Kälin, Z. Liu, and R. A. Porto, *Conservative Tidal Effects in Compact Binary Systems to Next-to-Leading Post-Minkowskian Order*, *Phys. Rev. D* **102** (2020) 124025, [arXiv:2008.06047].

[132] K. Haddad and A. Helset, *Tidal effects in quantum field theory*, *JHEP* **12** (2020) 024, [arXiv:2008.04920].

[133] R. Aoude, K. Haddad, and A. Helset, *Tidal effects for spinning particles*, *JHEP* **03** (2021) 097, [arXiv:2012.05256].

[134] M. Accettulli Huber, A. Brandhuber, S. De Angelis, and G. Travaglini, *Eikonal phase matrix, deflection angle and time delay in effective field theories of gravity*, *Phys. Rev. D* **102** (2020), no. 4 046014, [arXiv:2006.02375].

[135] M. Accettulli Huber, A. Brandhuber, S. De Angelis, and G. Travaglini, *From amplitudes to gravitational radiation with cubic interactions and tidal effects*, arXiv:2012.06548.

[136] C. Cheung, N. Shah, and M. P. Solon, *Mining the Geodesic Equation for Scattering Data*, *Phys. Rev. D* **103** (2021), no. 2 024030, [arXiv:2010.08568].

[137] Z. Bern, J. Parra-Martinez, R. Roiban, E. Sawyer, and C.-H. Shen, *Leading Nonlinear Tidal Effects and Scattering Amplitudes*, *JHEP* **05** (2021) 188, [arXiv:2010.08559].

[138] P. Di Vecchia, C. Heissenberg, R. Russo, and G. Veneziano, *Universality of ultra-relativistic gravitational scattering*, *Phys. Lett. B* **811** (2020) 135924, [arXiv:2008.12743].

[139] T. Damour, *Radiative contribution to classical gravitational scattering at the third order in G*, *Phys. Rev. D* **102** (2020), no. 12 124008, [arXiv:2010.01641].

[140] A. Buonanno, *Reduction of the two-body dynamics to a one-body description in classical electrodynamics*, *Phys. Rev. D* **62** (2000) 104022, [hep-th/0004042].

[141] H. A. Lorentz, *La théorie électromagnétique de Maxwell et son application aux corps mouvants*, vol. 25. EJ Brill, 1892.

[142] M. Abraham, *Theorie der Elektrizität*. BG Teubner, 1912.

[143] P. A. M. Dirac, *Classical theory of radiating electrons*, *Proceedings of the Royal Society of London. Series A. Mathematical and Physical Sciences* **167** (1938), no. 929 148–169, [https://royalsocietypublishing.org/doi/pdf/10.1098/rspa.1938.0124].

[144] P. Di Vecchia, C. Heissenberg, R. Russo, and G. Veneziano, *The eikonal approach to gravitational scattering and radiation at $\mathcal{O}(G^3)$*, *JHEP* **07** (2021) 169, [arXiv:2104.03256].

[145] M. Beneke and V. A. Smirnov, *Asymptotic expansion of Feynman integrals near threshold*, *Nucl. Phys. B* **522** (1998) 321–344, [hep-ph/9711391].

[146] D. Kosmopoulos, *Simplifying D-Dimensional Physical-State Sums in Gauge Theory and Gravity*, arXiv:2009.00141.

[147] J. L. Bourjaily, E. Herrmann, and J. Trnka, *Prescriptive Unitarity*, *JHEP* **06** (2017) 059, [arXiv:1704.05460].

[148] L. D. Landau and E. M. Lifshitz, *Mechanics, Third Edition: Volume 1 (Course of Theoretical Physics)*. Butterworth-Heinemann, 3 ed., Jan., 1976.

[149] N. E. J. Bjerrum-Bohr, L. Plante, and P. Vanhove, *Post-Minkowskian Radial Action from Soft Limits and Velocity Cuts*, arXiv:2111.02976.

[150] A. Brandhuber, G. Chen, G. Travaglini, and C. Wen, *Classical gravitational scattering from a gauge-invariant double copy*, *JHEP* **10** (2021) 118, [arXiv:2108.04216].

[151] L. D. Landau and E. M. Lifshitz, *The Classical Theory of Fields*. Butterworth-Heinemann, 4 ed., Jan., 1980.

[152] C. R. Galley, A. K. Leibovich, and I. Z. Rothstein, *Finite size corrections to the radiation reaction force in classical electrodynamics*, *Phys. Rev. Lett.* **105** (2010) 094802, [arXiv:1005.2617].

[153] P. Forgacs, T. Herpay, and P. Kovacs, *Comment on 'Finite Size Corrections to the Radiation Reaction Force in Classical Electrodynamics'*, *Phys. Rev. Lett.* **109** (2012) 029501, [arXiv:1202.6289].

[154] O. Birnholtz, S. Hadar, and B. Kol, *Theory of post-Newtonian radiation and reaction*, *Phys. Rev. D* **88** (2013), no. 10 104037, [arXiv:1305.6930].

[155] D. Bini and T. Damour, *Gravitational radiation reaction along general orbits in the effective one-body formalism*, *Phys. Rev. D* **86** (2012) 124012, [arXiv:1210.2834].

[156] R. Aoude and A. Ochirov, *Classical observables from coherent-spin amplitudes*, *JHEP* **10** (2021) 008, [arXiv:2108.01649].

[157] F. Febres Cordero, M. Kraus, G. Lin, M. S. Ruf, and M. Zeng, *Conservative Binary Dynamics with a Spinning Black Hole at O(G3) from Scattering Amplitudes*, *Phys. Rev. Lett.* **130** (2023), no. 2 021601, [arXiv:2205.07357].

[158] G. Menezes and M. Sergola, *NLO deflections for spinning particles and Kerr black holes*, *JHEP* **10** (2022) 105, [arXiv:2205.11701].

[159] G. U. Jakobsen, G. Mogull, J. Plefka, and J. Steinhoff, *SUSY in the sky with gravitons*, *JHEP* **01** (2022) 027, [arXiv:2109.04465].

[160] G. U. Jakobsen and G. Mogull, *Conservative and Radiative Dynamics of Spinning Bodies at Third Post-Minkowskian Order Using Worldline Quantum Field Theory*, *Phys. Rev. Lett.* **128** (2022), no. 14 141102, [arXiv:2201.07778].

[161] G. U. Jakobsen and G. Mogull, *Linear response, Hamiltonian, and radiative spinning two-body dynamics*, *Phys. Rev. D* **107** (2023), no. 4 044033, [arXiv:2210.06451].

[162] G. U. Jakobsen, G. Mogull, J. Plefka, B. Sauer, and Y. Xu, *Conservative Scattering of Spinning Black Holes at Fourth Post-Minkowskian Order*, *Phys. Rev. Lett.* **131** (2023), no. 15 151401, [arXiv:2306.01714].

[163] G. U. Jakobsen, G. Mogull, J. Plefka, and B. Sauer, *Dissipative scattering of spinning black holes at fourth post-Minkowskian order*, arXiv:2308.11514.

[164] G. U. Jakobsen, G. Mogull, J. Plefka, and J. Steinhoff, *Gravitational Bremsstrahlung and Hidden Supersymmetry of Spinning Bodies*, *Phys. Rev. Lett.* **128** (2022), no. 1 011101, [arXiv:2106.10256].

[165] D. Bini, A. Geralico, and P. Rettegno, *Spin-orbit contribution to radiative losses for spinning binaries with aligned spins*, *Phys. Rev. D* **108** (2023), no. 6 064049, [arXiv:2307.12670].

[166] R. Aoude, K. Haddad, C. Heissenberg, and A. Helset, *Leading-order gravitational radiation to all spin orders*, arXiv:2310.05832.

[167] A. Brandhuber, G. R. Brown, G. Chen, J. Gowdy, and G. Travaglini, *Resummed spinning waveforms from five-point amplitudes*, arXiv:2310.04405.

[168] S. De Angelis, R. Gonzo, and P. P. Novichkov, *Spinning waveforms from KMOC at leading order*, arXiv:2309.17429.

[169] C. Heissenberg, *Angular Momentum Loss Due to Spin-Orbit Effects in the Post-Minkowskian Expansion*, arXiv:2308.11470.

[170] Z. Bern, D. Kosmopoulos, A. Luna, R. Roiban, T. Scheopner, F. Teng, and J. Vines, *Quantum Field Theory, Worldline Theory, and Spin Magnitude Change in Orbital Evolution*, arXiv:2308.14176.

[171] L. P. S. Singh and C. R. Hagen, *Lagrangian formulation for arbitrary spin. 1. The boson case*, *Phys. Rev. D* **9** (1974) 898–909.

[172] L. W. Lindwasser, *Consistent actions for massive particles interacting with electromagnetism and gravity*, arXiv:2309.03901.

[173] L. W. Lindwasser, *Covariant actions and propagators for all spins, masses, and dimensions*, arXiv:2307.11750.

[174] L. Cangemi and P. Pichini, *Classical limit of higher-spin string amplitudes*, *JHEP* **06** (2023) 167, [arXiv:2207.03947].

[175] N. Arkani-Hamed, T.-C. Huang, and Y. tin Huang, *Scattering amplitudes for all masses and spins*, 2021.

[176] H. Johansson and A. Ochirov, *Double copy for massive quantum particles with spin*, *JHEP* **09** (2019) 040, [arXiv:1906.12292].

[177] Z. Bern, D. Kosmopoulos, A. Luna, R. Roiban, and F. Teng, *Binary Dynamics through the Fifth Power of Spin at* $O(G^2)$, *Phys. Rev. Lett.* **130** (2023), no. 20 201402, [arXiv:2203.06202].

[178] Z. Bern, J. P. Gatica, E. Herrmann, A. Luna, and M. Zeng, *Scalar QED as a toy model for higher-order effects in classical gravitational scattering*, *JHEP* **08** (2022) 131, [arXiv:2112.12243].

[179] M. Levi and J. Steinhoff, *Spinning gravitating objects in the effective field theory in the post-Newtonian scheme*, *JHEP* **09** (2015) 219, [arXiv:1501.04956].

[180] J. Steinhoff, *Spin and quadrupole contributions to the motion of astrophysical binaries*, *Fund. Theor. Phys.* **179** (2015) 615–649, [arXiv:1412.3251].

[181] J. Steinhoff, *Spin gauge symmetry in the action principle for classical relativistic particles*, arXiv:1501.04951.

[182] J. Vines, D. Kunst, J. Steinhoff, and T. Hinderer, *Canonical Hamiltonian for an extended test body in curved spacetime: To quadratic order in spin*, *Phys. Rev. D* **93** (2016), no. 10 103008, [arXiv:1601.07529]. [Erratum: Phys.Rev.D 104, 029902 (2021)].

[183] J. Ehlers and E. Rudolph, *Dynamics of extended bodies in general relativity center-of-mass description and quasirigidity*, *General Relativity and Gravitation* **8** (1977), no. 3 197–217.

[184] D. Forde, *Direct extraction of one-loop integral coefficients*, *Phys. Rev. D* **75** (2007) 125019, [arXiv:0704.1835].

[185] P. Di Vecchia, C. Heissenberg, R. Russo, and G. Veneziano, *Classical gravitational observables from the Eikonal operator*, *Phys. Lett. B* **843** (2023) 138049, [arXiv:2210.12118].

[186] P. Di Vecchia, C. Heissenberg, R. Russo, and G. Veneziano, *The gravitational eikonal: from particle, string and brane collisions to black-hole encounters*, arXiv:2306.16488.

[187] A. Herderschee, R. Roiban, and F. Teng, *The sub-leading scattering waveform from amplitudes*, *JHEP* **06** (2023) 004, [arXiv:2303.06112].

[188] T. Adamo, A. Cristofoli, A. Ilderton, and S. Klisch, *All Order Gravitational Waveforms from Scattering Amplitudes*, *Phys. Rev. Lett.* **131** (2023), no. 1 011601, [arXiv:2210.04696].

[189] C. R. T. Jones and M. S. Ruf, *Absorptive Effects and Classical Black Hole Scattering*, arXiv:2310.00069.

[190] C. R. T. Jones and M. Solon, *Scattering amplitudes and N-body post-Minkowskian Hamiltonians in general relativity and beyond*, *JHEP* **02** (2023) 105, [arXiv:2208.02281].

[191] N. Arkani-Hamed, T.-C. Huang, and Y.-t. Huang, *Scattering amplitudes for all masses and spins*, *JHEP* **11** (2021) 070, [arXiv:1709.04891].

[192] Y. F. Bautista, A. Guevara, C. Kavanagh, and J. Vines, *Scattering in black hole backgrounds and higher-spin amplitudes. Part II*, *JHEP* **05** (2023) 211, [arXiv:2212.07965].

[193] Y. F. Bautista, M. Khalil, M. Sergola, C. Kavanagh, and J. Vines, *Post-Newtonian observables for aligned-spin binaries to sixth order in spin from gravitational self-force and Compton amplitudes*, arXiv:2408.01871.

[194] Y. F. Bautista, G. Bonelli, C. Iossa, A. Tanzini, and Z. Zhou, *Black hole perturbation theory meets CFT2: Kerr-Compton amplitudes from Nekrasov-Shatashvili functions*, *Phys. Rev. D* **109** (2024), no. 8 084071, [arXiv:2312.05965].

[195] A. Luna, N. Moynihan, D. O'Connell, and A. Ross, *Observables from the Spinning Eikonal*, arXiv:2312.09960.

[196] M. Alaverdian, Z. Bern, D. Kosmopoulos, A. Luna, R. Roiban, T. Scheopner, and F. Teng, *Conservative Spin Magnitude Change in Orbital Evolution in General Relativity*, arXiv:2407.10928.

[197] J. P. Gatica, *The Eikonal Phase and Spinning Observables*, arXiv:2312.04680.

[198] D. Akpinar, F. Febres Cordero, M. Kraus, M. S. Ruf, and M. Zeng, *Spinning Black Hole Scattering at $\mathcal{O}(G^3S^2)$: Casimir Terms, Radial Action and Hidden Symmetry*, arXiv:2407.19005.

[199] Z. Bern, E. Herrmann, R. Roiban, M. S. Ruf, A. V. Smirnov, V. A. Smirnov, and M. Zeng, *Amplitudes, supersymmetric black hole scattering at $\mathcal{O}\left(G^5\right)$, and loop integration*, *JHEP* **10** (2024) 023, [arXiv:2406.01554].

[200] R. Gonzo and C. Shi, *Scattering and bound observables for spinning particles in Kerr spacetime with generic spin orientations*, arXiv:2405.09687.

[201] C. Dlapa, G. Kälin, Z. Liu, and R. A. Porto, *Local in Time Conservative Binary Dynamics at Fourth Post-Minkowskian Order*, *Phys. Rev. Lett.* **132** (2024), no. 22 221401, [arXiv:2403.04853].

[202] J. Wilson-Gerow, *Conservative scattering of Reissner-Nordström black holes at third post-Minkowskian order*, *JHEP* **05** (2024) 265, [arXiv:2310.17731].

[203] F. Alessio and P. Di Vecchia, *2PM waveform from loop corrected soft theorems*, *J. Phys. A* **57** (2024), no. 47 475402, [arXiv:2402.06533].

[204] M. Bianchi, C. Gambino, and F. Riccioni, *A Rutherford-like formula for scattering off Kerr-Newman BHs and subleading corrections*, *JHEP* **08** (2023) 188, [arXiv:2306.08969].

[205] P. Di Vecchia, C. Heissenberg, R. Russo, and G. Veneziano, *The eikonal operator at arbitrary velocities I: the soft-radiation limit*, *JHEP* **07** (2022) 039, [arXiv:2204.02378].

[206] B. Bellazzini, G. Isabella, and M. M. Riva, *Classical vs quantum eikonal scattering and its causal structure*, *JHEP* **04** (2023) 023, [arXiv:2211.00085].

[207] M. Correia and G. Isabella, *The Born regime of gravitational amplitudes*, arXiv:2406.13737.

[208] F. Costa, C. A. R. Herdeiro, J. Natario, and M. Zilhao, *Mathisson's helical motions for a spinning particle: Are they unphysical?*, *Phys. Rev. D* **85** (2012) 024001, [arXiv:1109.1019].

[209] L. F. O. Costa and J. Natário, *Center of mass, spin supplementary conditions, and the momentum of spinning particles*, *Fund. Theor. Phys.* **179** (2015) 215–258, [arXiv:1410.6443].

[210] S. Ajith, Y. Du, R. Rajagopal, and D. Vaman, *Worldline Formalism, Eikonal Expansion and the Classical Limit of Scattering Amplitudes*, arXiv:2409.17866.

[211] L. Bohnenblust, L. Cangemi, H. Johansson, and P. Pichini, *Binary Kerr black-hole scattering at 2PM from quantum higher-spin Compton*, arXiv:2410.23271.

[212] R. Aoude, A. Cristofoli, A. Elkhidir, and M. Sergola, *Inelastic Coupled-Channel Eikonal Scattering*, arXiv:2411.02294.

[213] Y. F. Bautista, Y.-T. Huang, and J.-W. Kim, *Absorptive Effects in Black Hole Scattering*, arXiv:2411.03382.

[214] W. D. Goldberger and I. Z. Rothstein, *Dissipative effects in the worldline approach to black hole dynamics*, *Phys. Rev. D* **73** (2006) 104030, [hep-th/0511133].

[215] R. A. Porto, *Absorption effects due to spin in the worldline approach to black hole dynamics*, *Phys. Rev. D* **77** (2008) 064026, [arXiv:0710.5150].

[216] W. D. Goldberger and I. Z. Rothstein, *An Effective Field Theory of Quantum Mechanical Black Hole Horizons*, *JHEP* **04** (2020) 056, [arXiv:1912.13435].

[217] W. D. Goldberger and I. Z. Rothstein, *Horizon radiation reaction forces*, *JHEP* **10** (2020) 026, [arXiv:2007.00731].

[218] W. D. Goldberger, J. Li, and I. Z. Rothstein, *Non-conservative effects on spinning black holes from world-line effective field theory*, *JHEP* **06** (2021) 053, [arXiv:2012.14869].

[219] E. Poisson and M. Sasaki, *Gravitational radiation from a particle in circular orbit around a black hole. 5: Black hole absorption and tail corrections*, *Phys. Rev. D* **51** (1995) 5753–5767, [gr-qc/9412027].

[220] A. Nagar and S. Akcay, *Horizon-absorbed energy flux in circularized, nonspinning black-hole binaries and its effective-one-body representation*, *Phys. Rev. D* **85** (2012) 044025, [arXiv:1112.2840].

[221] A. Taracchini, A. Buonanno, S. A. Hughes, and G. Khanna, *Modeling the horizon-absorbed gravitational flux for equatorial-circular orbits in Kerr spacetime*, *Phys. Rev. D* **88** (2013) 044001, [arXiv:1305.2184]. [Erratum: Phys.Rev.D 88, 109903 (2013)].

[222] S. Endlich and R. Penco, *A Modern Approach to Superradiance*, *JHEP* **05** (2017) 052, [arXiv:1609.06723].

[223] M. V. S. Saketh, J. Steinhoff, J. Vines, and A. Buonanno, *Modeling horizon absorption in spinning binary black holes using effective worldline theory*, *Phys. Rev. D* **107** (2023), no. 8 084006, [arXiv:2212.13095].

[224] R. Aoude and A. Ochirov, *Gravitational partial-wave absorption from scattering amplitudes*, arXiv:2307.07504.

[225] H. Tagoshi, S. Mano, and E. Takasugi, *PostNewtonian expansion of gravitational waves from a particle in circular orbits around a rotating black hole: Effects of black hole absorption*, *Prog. Theor. Phys.* **98** (1997) 829–850, [gr-qc/9711072].

[226] K. Chatziioannou, E. Poisson, and N. Yunes, *Improved next-to-leading order tidal heating and torquing of a Kerr black hole*, *Phys. Rev. D* **94** (2016), no. 8 084043, [arXiv:1608.02899].

[227] H. S. Chia, *Tidal deformation and dissipation of rotating black holes*, *Phys. Rev. D* **104** (2021), no. 2 024013, [arXiv:2010.07300].

[228] M. V. S. Saketh, Z. Zhou, and M. M. Ivanov, *Dynamical tidal response of Kerr black

holes from scattering amplitudes, *Phys. Rev. D* **109** (2024), no. 6 064058, [arXiv:2307.10391].

[229] Y. F. Bautista, *Dynamics for super-extremal Kerr binary systems at O(G2)*, *Phys. Rev. D* **108** (2023), no. 8 084036, [arXiv:2304.04287].

[230] R. Brito, V. Cardoso, and P. Pani, *Superradiance: New Frontiers in Black Hole Physics*, *Lect. Notes Phys.* **906** (2015) pp.1–237, [arXiv:1501.06570].

[231] R. J. Eden, P. V. Landshoff, D. I. Olive, and J. C. Polkinghorne, *The analytic S-matrix*. Cambridge Univ. Press, Cambridge, 1966.

[232] D. N. Page, *Particle Emission Rates from a Black Hole: Massless Particles from an Uncharged, Nonrotating Hole*, *Phys. Rev. D* **13** (1976) 198–206.

[233] J. P. Gatica, *One-Loop Observables to Higher Order in Spin*, arXiv:2412.02034.

[234] D. Akpinar, F. Febres Cordero, M. Kraus, A. Smirnov, and M. Zeng, *First Look at Quartic-in-Spin Binary Dynamics at Third Post-Minkowskian Order*, *Phys. Rev. Lett.* **135** (2025), no. 4 041602, [arXiv:2502.08961].

[235] M. Alaverdian, Z. Bern, D. Kosmopoulos, A. Luna, R. Roiban, T. Scheopner, and F. Teng, *Observables and Unconstrained Spin Tensor Dynamics in General Relativity from Scattering Amplitudes*, arXiv:2503.03739.

[236] S. Weinberg, *The Quantum theory of fields. Vol. 1: Foundations.* Cambridge University Press, 6, 2005.

[237] S. M. Wagh and N. Dadhich, *ABSENCE OF SUPERRADIANCE OF THE DIRAC PARTICLES IN THE KERR-NEWMAN GEOMETRY AND THE WEAK POSITIVE ENERGY CONDITION*, *Phys. Rev. D* **32** (1985) 1863–1865.